Bioremediation of brewery sludge and hydrogen production using combined approaches

ITZCOATL RAFAEL GARDUNO IBARRA

Thesis submitted to the University of Ottawa
in partial fulfillment of the requirements for the
Degree of Doctor of Philosophy in Environmental Engineering

Department of Civil Engineering
Faculty of Engineering
University of Ottawa

Abstract

Hydrogen is re-emerging as a serious alternative to fossil fuels. It is a clean gas with high energy density and its combustion only generates water vapour. Nevertheless, the hydrogen industry has a significant carbon footprint since this gas is mostly derived from fossil fuels reforming processes. This project focusses on the development of sustainable alternatives to conventional hydrogen production, in which approaches based on dark fermentation (DF) using an inexpensive residue from the brewery industry as primary feedstock are presented. Firstly, a fungal pre-treatment (FT) was proposed to degrade a high-strength brewery waste slurry (BWS) to obtain an effluent with a lower concentration of chemical oxygen demand (COD) but rich in readily fermentable sugars for the ensuing DF, thus improving hydrogen yields (HY). Secondly, microbial electrolysis and fuel cells (MECs and MFCs) were proposed to assist DF, generating electricity in MFCs while improving HY by MECs. Coupling both microbial electrochemical technologies sequentially after DF did not show any advantage. However, promising results were obtained for electricity and hydrogen production when taking a single-staged approach. Treating BWS directly by MFCs produced 2.0 watts/g COD consumed, while the DF process assisted simultaneously by MECs (DF/MEC) produced 1.6 times more hydrogen than DF alone. An average HY of 2.32 ± 0.06 mol H_2/mol glucose was attained between both DF/MEC and DF after FT, hence approaching the theoretical value of 2.4 mol H_2/mol glucose, representing roughly a 50% improvement compared to DF alone. With an overall COD reduction above 76%, the DF after FT exhibited the highest energy conversion rate per substrate consumed (6.3 kJ/g COD). As valuable by-products obtained, up to 31 g/L of fungal biomass, which is appreciated in many state-of-the-art biomaterials applications, was produced by using BWS. While in the DF/MEC process, 18 g/L of butyric acid were generated, which is three times more than with DF alone. Butyric acid being the precursor to butanol and building block of biodegradable thermoplastics, this result is not without significance. The proposed approaches not only valorize BWS but also validate their economic and environmental attractiveness as promising alternative hydrogen production methods.

Résumé

L'hydrogène est de nouveau considéré comme solution de rechange aux combustibles fossiles. Il s'agit d'un gaz propre à haute densité énergétique et sa combustion ne génère que de la vapeur d'eau. Néanmoins, l'industrie de l'hydrogène a une empreinte carbone considérable puisque sa production provient principalement des combustibles fossiles. Face à ce problème, ce projet présente différentes approches basées sur la fermentation sombre (FS), utilisant les boues de brasserie (BRB) comme principale matière première. Premièrement, un prétraitement fongique (TF) a été proposé pour dégrader le composant organique des BRB pour obtenir un effluent à faible concentration de demande chimique en oxygène (DCO), mais riche en sucres simples dans une FS subséquente, améliorant ainsi le rendement en hydrogène (HY). Deuxièmement, l'utilisation des cellules d'électrolyse et des piles à combustible microbiennes (CEM et PCM) a été proposée pour assister la FS. Le couplage séquentiel des procédés électrochimiques microbiens effectué après la FS n'a pas démontré d'avantages. Cependant, en adoptant une approche en une seule étape, des résultats prometteurs ont été obtenus en matière de production d'électricité et d'hydrogène. Le traitement direct des BRB par les PCM a généré 2,0 watts/g de DCO consommée, tandis que la combinaison simultanée de la FS avec les CEM (FS/CEM) a produit 1,6 fois plus d'hydrogène que la FS seule. Un HY moyen de 2,32 ± 0,06 mol H_2/mol glucose a été obtenu entre la FS/CEM et la FS après le TF, approchant ainsi la valeur théorique de 2,4 mol H_2/mol glucose, ce qui représente une amélioration d'environ 50 % par rapport à la FS seule. Ayant réduit la DCO de plus de 76 %, la FS après le TF a présenté le meilleur taux de conversion énergétique par substrat consommé (6,3 kJ/g DCO). Soulignons que la biomasse fongique, utilisée dans plusieurs biomatériaux, a été produite jusqu'à 31 g/L. Dans la FS/CEM, 18 g/L d'acide butyrique ont été générés, soit trois fois plus qu'avec la FS seule. Il s'agit d'un résultat significatif considérant l'importance du butyrate comme précurseur des biocarburants et bioplastiques. Ces approches valorisent donc les BRB en tant que méthodes alternatives de production d'hydrogène.

Statement of Contributions of Collaborators

I hereby declare that I am the sole author of this thesis. I conducted all of the experimental work, performed all of the data analysis, and wrote all the chapters presented in this work.

Sequencing analysis of the 16s rRNA gene performed was kindly conducted by Alexandra Tsitouras and Shruti Sharad Tanga.

Dr. Elena Baranova and Dr. Chris Kinsley supervised this thesis project. Since I was her student, Dr. Baranova provided guidance on the electrochemical part of the project, especially on the design of the microbial electrochemical cells here presented. Dr. Kinsley has supported me immensely since he took over the direction of this project, guiding me mainly in the field of anaerobic fermentations. He also contributed substantially to the written work of this thesis.

Acknowledgements

This thesis is a personal achievement, but it is far from being an individual effort. Throughout this 7-year journey, there is plenty to be grateful for and many to whom I owe recognition. I was only the main character of a story backed up by many people whom I name hereunder trying to do them justice as best as I can:

Firstly, I want to note my humble gratitude to **Dr. Kathlyn Kirkwood** (1972 – 2019), in posthumous thanks for the opportunity she offered to me seven years ago, and for all the support I received from her. This story began with her. Unfortunately, the course of events took a tragic turn one day. Although the project is no longer the same, some of the original proposals I devised with her remained in the work presented here.

Anima eius requiescat in pace.

* * *

I am profoundly thankful to **Dr. Chris Kinsley** for having agreed to pick up the baton of a challenging project that started abruptly from scratch. We struggled with many obstacles besides the obvious amid the difficult times that have come upon all of us. But he was patient, gave his all for this project until the last moment, and I must say that he trusted me so much that he even supported me financially more than once, for which I will be always grateful.

Likewise, I owe my deep gratitude to **Dr. Elena Baranova** for believing in me and my project to no smaller extent, always supporting me thoughtfully with the best advice as well as kindly facilitating the best equipment at her disposal, even before she became part of this project.

I thank you both for your continued support in spite of the odds… Sometimes words are insufficient to fully convey an emotion, and sometimes they run the risk of becoming meaningless through repetition. I humbly hope though, that it is not an understatement to say that, as many others before me and surely many to come, I am truly grateful to you both for your commitment, your goodwill, and the thoughtfulness with which you selflessly welcomed me under your unparalleled supervision.

I would like to thank the examiners **Dr. Christopher Lan** and **Dr. Majid Sartaj**, from the University of Ottawa, **Dr. Banu Ormeci** from Carleton University, and **Dr. Youri Gendel**, from the Israel Institute of Technology, first of all, for agreeing to review my research, and of course for their valuable comments and suggestions.

Special thanks to **Dr. Myron Smith** from Carleton University, who generously allowed me to work in his lab where I carried out the experiments related to the white-rot fungi.

I also express my profound gratitude to **CONACYT** (the Mexican National Council for Science and Technology), for the enormous financial support during the first four years of my doctorate program. Likewise, this scholarship and the beginning of the great adventure this doctorate has been, would not have been possible if it had not been for the intercession of my master's mentors: **Dr. Juan Carlos Serratos**, **Dr. Ricardo Manríquez**, and **Dr. Juan Carlos Meza**… Eight years later, I am still grateful to you.

* * *

Continuing with an important core of the research work, I thank the technicians from the Department of Chemical and Biological Engineering, **Franco Ziroldo**, **Gérard Nina**, and especially **James Macdermid**, who machined all the cells I designed for this project. Special thanks to **Patrick D'Aoust** as well, who, beyond being the Environmental Engineering Technician, he has been a good friend and a great colleague in the lab.

From the administrative staff, I thank **Philippe Jolette** and **Francine Petrin**. For his commitment and extraordinary labour beyond his duties, **Luc Cloutier** should receive more recognition. All my gratitude to him. Moreover, special thanks to the director of my program, **Dr. Robert Delatolla**, through whose hands all sorts of critical documents pass, and who stoically carries out this important job. I am particularly grateful because thanks to his intercession I could receive an important grant during a rough time.

I don't want to let go of the chance to mention the professors with whom I took classes, **Dr. Boguslaw Kruczek** and **Dr. Roberto Narbaitz**; and some of those whom I worked with, like **Dr. Oleksiy Krupin** and **Dr. Jean-Philippe St-Pierre**. I learned many interesting things with them and had great academic experiences that I won't forget.

I want to mention all my friends and colleagues from the lab. I profoundly thank **Shruti Tanga**, so as to **Afrida** and **Richard** from the EVG lab. At the CCRI I thank **Mohammed Houache** and remember here all the good talks and moments we spent together side by side. I also thank in particular **Ju Wang**, **Chris Panaritis**, **Arash Jahromi**, **Emily Cossar** and **Najmeh Ahledel**, all of whom very kindly helped me when I needed something in the lab. I also want to mention **Sijia Li**, **Sydney Vanderburg** and **Justin Brown**, young undergrads who assisted me during the last phase of my experiments.

Looking back to the times before the beginning of this final project presented here, I remember my good friend and former lab partner **Jessica Johnson**; for a while we were side by side, accompanying each other on a lonely and eventful road. I also remember here the sparkling company of a young **Emma Moreside** and the long talks with my Yugoslavian friend, **Maja Mujcin**. After many years, I made it. Thank you, girls.

* * *

I continue with the good friends I met in Canada, starting with the dearest Mexican gang **Gerardo**, **Mayté**, **Francisco** and **Negmi**, **Luis** and **Karen**, with whom I spent many happy moments. It is also worth remembering here and to genuinely thank the people who consistently showed me which way to go, even if at first I did not want to see it. I thank new friends like **Gabriela Jiménez**, and surely my plants are more grateful to her. Thanks to **Raúl Castañeda**, a good friend and colleague in the field of Chemistry. To **Connor Grant**, from whom I have learned a lot about Canada. To my litter sister **Subi Kalanje**, the two unique **Olympe Tegba** and **Christoph Désormeaux** —the latter who kindly helped me with the abstracts—, and to my good friend **Maximiliano González** and his sweet wife **Carolina**; all amazing characters who, in their own way, shared with me numerous meaningful experiences.

Immense gratitude to **Sylvie Larouche** who was very supportive, and her family too. A warm, kind-hearted friendship which is like belonging to a family in Montréal.

To my dear friend **Ata Babakhani**, a highly respectable character. In addition to having been my classmate since the very beginning, we were also co-workers in the grocery

store owned by his compatriots **Mr. Arash** and his wife **Mojgan**, amazing people to whom I am also grateful and honoured to have been their employee.

Special thanks to my good brethren from the Eddy Lodge #41, in particular to **Victor Karkaji**, **Hady Tabbal**, **Adel Ghié** and **Toni Mechalani**. They always trusted and believed in me as well, and I have been welcomed as one of them every time.

And of course, many thanks to my dear, extraordinary friend **Mario Valencia** and his lovely wife **Jessica Pérez**. An unconditional friendship in which I have been warmly welcomed with open arms… so much to catch up with you guys.

* * *

Finally, to my family. Thank you to my all cousins and relatives from both families **Garduño Montaño** and **Ibarra Ibarra**, especially those who have been close all this time, the **Najera Ibarra** family.

Heartfelt thanks to my brothers **Braulio** and **Vladimir Garduño Ibarra**. The simple fact that you are my brothers is already a source of strength, a motivation to be proud of and to be thankful. But even more so with all your support throughout these years, and especially at the end of the road. I am indebted to you my brothers.

And to my parents, **Xóchitl Ibarra,** and **Rafael Garduño**. As your son, I am at a loss for words to express my eternal gratitude, not only on this occasion but for so much more that lies behind being my parents. If I never fell, in spite of myself, it was because of you. In all honesty, if it were not for you, this whole endeavour would not exist for I could not have been able to cope with it alone. This is for all we are, for you, my parents, my brothers, and for our beloved pets who have left us. Thank you, mother. Thank you, father. This work is also yours, my dear family.

Thank you, God. Thank you for everything.

In the end, we always arrive at the place where we are expected

José Saramago

To my parents.

To my brothers.

In loving memory of Sissi, Tanque and Gatito.

Table of Contents

Abstract ..... *ii*

Résumé ..... *iii*

Statement of Contributions of Collaborators ..... *iv*

Acknowledgments ..... *v*

List of Tables ..... *xiv*

List of Figures ..... *xv*

Chapter 1. Introduction 1

1.1 General Hypothesis 3

1.2 General Objectives 3

1.3 Dark fermentation 4

1.4 Fungal pre-treatment 5

1.5 Microbial electrochemical technologies 7

1.6 Novelty and contributions 10

References 10

Chapter 2. Literature review 12

2.1 Climate change: the ongoing public health, humanitarian, and economical crisis 12

2.2 Fossil fuels substitute: why hydrogen? 14

2.3 Biohydrogen 17

2.3.1 Biotechnologies for hydrogen production 18

Biophotolysis 18

Photofermentation 19

Dark fermentation 20

Bio-catalyzed electrolysis 21

2.3.2 Advantages and disadvantages of these biotechnologies 22

2.4 Fundaments and challenges of dark fermentation 22

2.4.1 Operational parameters 27

2.4.2 Hydrogen yield and process limitations 28

2.4.3 Bioreactor Configuration and Operational Mode 30
2.4.4 Organic wastes as feedstock for biohydrogen production 31
2.5 Microbial Electrochemical Technologies (METs) 32
2.5.1 Working principle 32
2.5.2 Effect of electrode potentials 36
2.5.3 Bacteria as catalysts in METs 37
2.5.4 Electron transfer mechanisms in METs 38
2.5.5 METs configuration and materials 39
Anode materials 40
Cathode materials 41
Carbon-based modified electrodes 42
Ion exchange membranes 42
2.5.6 Technological challenges 42
2.5.7 Efficiency of the electrochemical processes 44
2.5.8 Coupled systems for hydrogen and electricity production: DF/MEC–MFC 46
2.6 Valorisation of brewery residues 50
2.6.1 Brewery wastewaters as potential substrate for white-rot fungi 54
2.6.2 Role of white-rot fungi to produce biofuels from brewery residues 57
2.6.3 Brewery residues as substrate for energy conversion biotechnologies 60
2.7 Conclusions 62
References 64
Chapter 3. Valorization of brewery waste slurry and glycerol co-substrate for hydrogen and butyrate production using dark fermentation 78
3.1 Introduction 78
3.2 Materials and methods 82
3.2.1 Feedstocks, chemicals, and reagents 82
3.2.2 Inoculum selection 83
3.2.3 Optimization of organic loading 84
3.2.4 Effect of glycerol addition with uncontrolled pH 85
3.2.5 Optimization of pH 85

3.2.6 Dark fermentation trial at optimal conditions 85
3.2.7 Chemical analysis 86
3.2.8 Mathematical model for hydrogen production 87
3.3 Results and discussion 87
3.3.1 Inoculum selection 87
3.3.2 Effect of organic loading 88
3.3.3 Effect of glycerol addition with uncontrolled pH 89
3.3.4 Effect of pH 91
3.3.5 Dark fermentation at optimum conditions with and without glycerol addition 92
3.4 Proposed two-staged Dark Fermentation-Anaerobic Digestion System 96
3.5 Conclusions 97
References 98
Chapter 4. Hydrogen production potential in dark fermentation of a brewery waste slurry pre-treated with white-rot fungi in submerged culture 103
4.1 Introduction 103
4.2 Materials and Methods 107
4.2.1 Feedstocks, chemicals, and reagents 107
4.2.2 Fungal strains selection 108
4.2.3 Submerged fermentation 109
4.2.4 Dark fermentation 110
4.2.5 Physicochemical analysis 111
4.3 Results and discussion 113
4.3.1 Screening test of fungal growth inhibition in BWS 113
4.3.2 Fungal growth in submerged fermentation 114
4.3.3 Bioremediation of BWS with *P. ostreatus* 117
4.3.4 Total sugars and crude exopolysaccharides 119
4.3.5 Hydrogen production in dark fermentation 121
4.4 Conclusions 124
References 125

Chapter 5. Hydrogen and electricity generation from brewery sludge as primary feedstock using microbial-electrochemical technologies 131
5.1 Introduction 131
5.2 Materials and Methods 134
5.2.1 Feedstocks, chemicals, and reagents 134
5.2.2 METs configuration 135
5.2.3 Deposition of polyaniline in carbon-based electrode 136
5.2.4 Ruthenium dioxide nanoparticles 136
5.2.5 Modified carbon-based electrodes performance 136
5.2.6 Dark fermentation 137
5.2.7 Chemical analysis 137
5.2.8 Electrochemical measurements 138
5.2.9 Hydrogen yield and energy recovery analysis 138
5.3 Results and discussion 140
5.3.1 Enhancement of the carbon felt electrode 140
5.3.2 Microbial fuel cells 143
5.3.3 Hydrogen production 147
5.3.4 Microbial population analysis 150
5.3.5 Hydrogen yield and energy efficiency 153
5.4 Conclusions 156
References 158
Chapter 6. Conclusions 163
6.1 Summary 163
6.2 Recommendations for future research 170
6.2.1 Dark fermentation and anaerobic digestion 170
6.2.2 Dark fermentation and microbial electrochemical technologies 171
6.2.3 Fungal treatment 172
Appendix 174

List of Tables

Table 1.1 Energy recovery efficiencies commonly reported in methane generation from brewery wastewaters 2

Table 2.1 Comparison properties of hydrogen and hydrocarbon fuels 14

Table 2.2 Size of bioreactor required to power PEM fuel cells (modified) 21

Table 2.3 Hydrogen produced from different organic wastes in dark fermentation 31

Table 2.4 Common biological redox reactions 35

Table 2.5 By-products from MECs at different applied potentials 36

Table 2.6 Operating features and performance of combined systems Dark Fermentation-Microbial Fuel Cells..... 48

Table 2.7 Operating features and performance of combined systems Dark Fermentation-Microbial Electrolysis Cells 49

Table 2.8 Physicochemical characteristics of brewery wastewater 52

Table 2.9 Characteristics of wastewater generated during each step of the brewing process 53

Table 3.1 Characteristics of the brewery sludge after filtration 83

Table 3.2 Organic acids concentration in g/L after 24 hours of fermentation in two different anaerobic sludges, cultured in two different defined media: Reinforced clostridial medium (RCM), and modified minimal M9 medium (M9M) 88

Table 3.3 Optimum dilution of brewery waste slurry (BWS) for gas production 89

Table 3.4 COD removed, fermentation gases produced, maximum CO_2 detected, and final pH of the dark fermentation process of BWS (50 – 55 g/L COD) at 35°C with and without 5 g/L glycerol (BWS + Gro) 90

Table 3.5 Hydrogen production during dark fermentation of 75% BWS at 35°C with and without 5 g/L glycerol. Performance comparison with similar residues 95

Table 4.1 Characteristics of the brewery sludge after filtration 108

Table 4.2 Fungal growth of *F. velutipes*, *P. ostreatus*, and *P. eryngii* after 9 days in three different semisolid media in Petri dishes: 1) Maltose extract agar (MEA), 2) brewery slurry-agar (BSA), 3) potato-dextrose-agar (PDA) 113

Table 4.3 Comparative analysis of studies on the culture of Pleurotus ostreatus in submerged fermentation for biomass production 118

Table 4.4 Total sugars content (g/L, glucose equivalent) in the raw brewery waste slurry (100% BWS), and in the BWS-based media before and after the fungal treatment, before and after being autoclaved (121°C, 15 psia for 20 min) 120

Table 5.1 Comparative analysis of studies on energy conversion in MFCs from brewery wastewaters 146

Table 6.1 COD reduction and energy conversion efficiencies exhibited by each treatment studied in the present research work 164

List of Figures

Figure 1.1 Schematic of the proposed fungal pre-treatment of brewery waste slurry prior to dark fermentation, obtaining fungal biomass and butyric acid as by-products 6

Figure 1.2 Schematic of the two proposed DF-METs systems. A) Two-staged integrated system for dark fermentation of BWS followed by MECs and MFCs. B) Direct treatment of BWS in MFCs (1b) and dark fermentation assisted by MECs (1a) for hydrogen production and butyric acid recovery 9

Figure 2.1 Hydrogen production platforms (left), and hydrogen demand and applications (right) 16

Figure 2.2 Anaerobic Digestion schematic process 23

Figure 2.3 Hydrogen production pathways during dark fermentation: A) enteric bacteria; B) clostridia 24

Figure 2.4 Microbial Fuel Cells (MFCs) and Microbial Electrolysis Cells (MECs) working principles 32

Figure 2.5 Cell configurations. Double and single chambered MFCs, and single chamber MECs 40

Figure 2.6 Emeraldine general composition from chemical polymerization of aniline in HCl, catalyzed by ammonium persulfate. Self-secreted mediators like phenazines and pyocyanin by *Pseudomonas*, and flavins by *Shewanella* spp. are also presented 41

Figure 2.7 Potential losses during electron transfer in microbial electrochemical cells 43

Figure 2.8 Brewing process with its residues (own figure) 50

Figure 2.9 Oyster mushroom (*Pleurotus ostreatus*), by Michel Langeveld, licensed under (CC-BY-SA 4.0) Retrieved from https://www.inaturalist.org/photos/173512182 55

Figure 2.10 The schematic diagram of biological processes for biofuel production employing white-rot fungi. Modified from Tri *et al*. (2020) 58

Figure 3.1 Proposed two-staged system Dark Fermentation/Anaerobic Digestion for hydrogen-enriched biogas from brewery waste slurry treatment. 82

Figure 3.2 Cumulative gas produced, COD concentration and pH drop throughout the dark fermentation process in capped bottles during 48 hours of A) brewery waste slurry alone, B) supplemented with 5 g/L of glycerol 90

Figure 3.3 Fermentation gases produced per gram of COD consumed (mL/g) at each different buffered pH 91

Figure 3.4 Production rate (mL/min) of hydrogen (•), carbon dioxide (•), and methane (•) during the treatment of A), 50 – 60 g/L COD brewery waste slurry alone; B), with the addition of glycerol (5 g/L). C), Gompertz Model of gas production (mL) of hydrogen and the percentage of COD reduced in brewery waste slurry alone and with the addition of glycerol (5 g/L) 92

Figure 3.5 Main organic acids produced and final composition after 30 h of dark fermentation at initial buffered pH 6.4 in A), brewery waste slurry alone (BWS); and B), with 5 g/L of glycerol (BWS + Gro). Hac, acetic acid; HFc, formic acid; HPc, propionic acid, HLc, lactic acid; HBu, butyric acid 94

Figure 4.1 Fungal biomass yield of *P. ostreatus* and *P. eryngii* after 12 days in BWS under different conditions. The combined effect of the addition of two different concentrations of ammonium chloride (1 and 2 g/L) as a nitrogen source (NS), and the addition of 10 g/L glucose as a carbon source, in contrast to BWS without the addition of nutrients and the control medium (Czapek). All the experiments contained 50% BWS, except for the control medium 115

Figure 4.2 Moisture, dry-weight total biomass, and ashes relative content from the wet biomass of *P. ostreatus* and *P. eryngii* produced in each fermentation condition 116

Figure 4.3 Summary of the bioremediation parameters obtained from the small- and large-scale fermentation with *P. ostreatus* in 60 g COD/L BWS (1 g/L N). Modelled fungal biomass growth (g/L dw) and COD consumption (g/L) from experimental data fitted into the Logistic-Monod model 117

Figure 4.4 Dark fermentation of the fungal-treated BWS: A) Production rate (mL/min) of hydrogen, carbon dioxide, and methane; B) Hydrogen and carbon dioxide cumulative production, and %COD reduced. Gas production modelled data presented from to the modified Gompertz equation 122

Figure 5.1 A) Chronoamperometry of PANI-coated carbon felt and bare carbon felt. B) SEM image of bare carbon felt C) SEM PANI-coated carbon felt after. D) SEM image of bacterial colonies in PANI-coated carbon felt after 24 h of fermentation under anaerobic conditions 141

Figure 5.2 Cyclic voltammetry (50 mV/s, pH 6.4). A) Plain carbon felt in M9 medium from t = 0 h to t = 18 h. B) Effect of polyaniline deposition on the carbon felt, with and without RuOx nanoparticles in M9 medium (no inoculum). C) Maximum peak of electrocatalytic activity by each electrode in inoculated M9 medium. D) Electrochemical activity over time of polyaniline modified carbon felt in inoculated brewery waste slurry and 5 g/L glycerol (pH 6.4, adjusted with 0.03 M potassium phosphate buffer) 142

Figure 5.3 A) Polarization curves of each MFC at the highest activity. B) Power density for each MFC expressed in mW/m^3 147

Figure 5.4 **A)** Production rate (mL/min) of hydrogen (•), carbon dioxide (•), and methane (•) during dark fermentative microbial electrolysis process (DF/MEC); B), Modelled cumulative hydrogen volume from DF/MEC versus dark fermentation alone 150

Figure 5.5 Microbial population analysis of A) the heat-treated inoculum; B) after the MFC process; and C) after the dark fermentative MEC assisted processes (DF/MEC) 152

Figure 5.6 Energy balance of the two proposed systems to produce hydrogen from a medium based on high strength brewery waste slurry: 1. Two-staged combined system showing DF process followed by MEC; 2. Simultaneous DF/MEC treatment 155

Figure A.1 Radial mycelial growth in Petri dishes on different semisolid media after 9 days of incubation at 30°C. 1) PDA – Potato-dextrose-agar; 2) BSA, medium prepared with brewery waste slurry, diluted 1:2, and agar (18 g/L); 3) MEA – Maltose extract-agar 177

Figure A.2 Preliminary growth tests of the three fungal strains in submerged fermentation. Effect of the addition of 10 g/L glucose as a carbon source (CS) alone and combined with two different concentrations of ammonium chloride (1 and 2 g/L) as a nitrogen source (NS) to the brewery waste slurry, in contrast to the control medium (Czapek). 1) CS+2 g/L NS; 2) CS+1 g/L NS; 3) CS alone; 4) Czapek medium 178

Figure A.3 Spectrophotogram of brewery waste slurry based medium (80% BWS + 1 g/L NH4Cl, autoclaved: 121°C, 15 psia, 20 min), before any treatment (••••), against (—) the BWS-based medium after dark Fermentation (no fungal pre-treatment), and (—) BWS-based medium after the fungal treatment inoculated with *P. ostreatus* (12 days). Area under the curve within the visible spectrum wavelengths (380 nm – 700 nm), and at the punctual wavelength of 475 nm, calculated for each treatment 179

Figure A.4 Production rate (mL/min) of hydrogen (•), carbon dioxide (•), and methane (•) during the dark fermentation treatment of non autoclaved and autoclaved fungal-treated BWS effluent 180

Figure A.5 Polarization and power density curves of the MFCs fed with fresh BWS compared to the MFCs fed with the effluent from the dark fermentation process. Both devices used PANI/CF electrodes 180

Figure A.6 Gas production rates using the same substrate conditions (BWS+5 g/L glycerol) in different treatments, comparing: **A** – DF alone, and **B** – simultaneous DF and MEC using PANI-modified carbon felt electrode, against **C** – simultaneous DF and MEC using a PANI/RuOx composite carbon felt electrode, and **D** – subsequent MEC after DF, using PANI-modified carbon felt electrode 181

Figure A.7 Reactor used for dark fermentation with continuous measurement of hydrogen production 182

Figure A.8 Double chamber cylindrical cell design 182

Figure A.9 Membraneless, single-chambered microbial electrolysis cell used in this project 183

Figure A.10 Single chamber tubular cell design 184

Figure A.11 Single-chambered microbial fuel cell used in this project 184

Chapter 1. Introduction

The central objective of this research is the valorization of brewery waste slurry to produce hydrogen by dark fermentation supported by microbial biotechnologies while producing value-added by-products and bioremediating the waste.

Firstly, Brewery wastewater (BWW) is an interesting feedstock, rich in carbohydrates and nutrients for microbial growth[1]. Its chemically stored energy has been estimated at around 14 kJ per g of COD[2]. Conversion of only ~22% of the chemical energy stored in BWW into methane is enough to cover the necessary energy input to operate feed pumps, mixing and heating of the reactor contents during the anaerobic digestion process, in which, in addition, a 99% COD removal can be attained[3]. However, in biotechnological processes, a great deal of the energy contained in the substrates is used to sustain the growth of the microorganisms, so only a fraction of this energy is recovered. Thus, the conversion potential into methane of the total energy contained in BWW is normally low (**Table 1.1**). Yet, anaerobic digestion is still the most common method applied to manage brewery sludge and wastewaters[4].

The purpose of producing hydrogen from brewery wastewaters instead of streamlining methane yields adheres to the fact that hydrogen is a clean gas with the highest energy-to-weight ratio of all fuels (122−142 kJ/g)[5], and whose combustion generates only water vapour[6]. Moreover, although hydrogen's heating value per mole is ~3 times lower than that of methane (890 kJ/mol CH_4 vs 286 kJ/mol H_2), the latter is a greenhouse gas, which combusted generates CO_2, and if it is not used as a fuel, can remain in the atmosphere for several years, being 20 times more effective in trapping heat than CO_2[7]. However, the application of hydrogen as a fuel on large scale is hindered by the substantial carbon footprint behind the conventional ways to obtain it. In this vein, this project stems from the need to find cleaner technologies for hydrogen production that can rival current fossil fuel-based techniques.

Table 1.1 Energy recovery efficiencies commonly reported in methane generation from brewery wastewaters

Reactor type	COD (g/L)	HRT (days)	Methane yield (L/g COD)	COD removal eff. (%)	Energy conversion per g COD* (%)	Ref.
EGSB-AF	4.52	97 - 133	0.28	82.1	20.8	[8]
AnMBR	10	68	0.53	>98.0	13.4	[9]
CSTR	4.2	1 – 10	0.25 – 0.32	95.4 – 98.5	15.4	[10]
AnMBR	28.5	4.2	0.28 – 0.35	99.0	21.8	[3]

* Efficiency relative to substrate added, calculated assuming a total energy content in BWW of 14 kJ per g COD
EGSB-AF: Expanded granular sludge bed-anaerobic filter; AnMBR: Anaerobic mixed bed reactor
CSTR: Completely stirred tank reactor

Fermentative hydrogen production processes are more environmentally friendly, and a wide variety of substrates can be used, of which many are wastes. The use of agro-industrial residues is attractive because they can reduce costs, and although biotechnological processes are highly limited by metabolic constraints, these can lead to the generation of many by-products with commercial interests, thus increasing the attractiveness of these alternative technologies. In this sense, brewery wastewater can be an ideal feedstock for fermentative hydrogen production because, in addition to being abundantly generated worldwide, its composition rich in organic matter can also be exploited for the obtention of value-added by-products.

With all the above in mind, the essence of this research is to improve energy conversion rates through the incorporation of other biotechnologies in synergy with dark fermentation, which combined could contribute to extracting more energy from wastes like brewery wastewater, while also looking to harness value-added by-products from the process. Two different strategies are proposed: 1) a pre-treatment with white-rot fungi, and 2) microbial electrochemical technologies (MFCs and MECs); both techniques assist dark fermentation separately. In this study, only a few by-products were addressed from each proposed treatment, described in detail below. Little has been reported regarding the use of brewery wastewater as a substrate to produce hydrogen biologically, hence, the present work contributes to the lack of published information in that regard, in addition to presenting initial considerations for future research.

1.1 General Hypothesis

Increased hydrogen production can be attained from dark fermentation in synergy with other biotechnologies using brewery waste slurry as primary feedstock while producing high value by-products and degrading the waste slurry.

1.2 General Objectives

1. Optimize the dark fermentative hydrogen production process using a high-strength brewery waste slurry, evaluating the effect of adding glycerol.

2. Pre-treat brewery waste slurry with white-rot fungi to obtain a biodegraded sugar-enriched effluent for hydrogen production in dark fermentation while producing fungal biomass as the main by-product.

3. Optimize microbial electrochemical devices by the modification of carbon felt electrodes with chemical deposition of conductive polymer polyaniline.

4. Determine operational parameters and overall efficiencies of the dark fermentation alone, assisted by microbial electrochemical process, and after the fungal treatment.

1.3 Dark fermentation

The first phase of the research study is to determine the potential of brewery waste slurry as a substrate for hydrogen production in dark fermentation with and without glycerol as a co-substrate.

The addition of glycerol has been shown to enhance biogas production in anaerobic digestion[11,12]. Since dark fermentation is the acidogenic part of the anaerobic digestion process, it is expected that the addition of glycerol will also have a positive effect on increased hydrogen production. Moreover, there are limited studies on the use of brewery wastewater in dark fermentation, let alone with other co-substrates, and so far, there is no literature reporting the co-mixture with glycerol. Another compelling reason to use this substrate is that it is available in large surplus quantities as a by-product of biodiesel production and obtainable at low cost[13]. As the worldwide biodiesel industry has been growing, glycerol disposal problems have arisen accordingly[13].

Hypothesis

A metabolic pathway can be selected using an appropriate inoculum to optimize hydrogen and butyric acid production with dark fermentation of brewery waste slurry. The addition of glycerol as a co-substrate can increase hydrogen production.

General objective

Optimize conditions for the valorization of high organic-loaded brewery wastewater as a substrate for hydrogen production in dark fermentation using an adapted inoculum and evaluate the effect of glycerol as a co-substrate on hydrogen yield.

Particular objectives

- Select an appropriate inoculum to carry out the dark fermentation of brewery waste slurry.
- Determine the maximum COD concentration in the brewery waste slurry at which the dark fermentation can be carried out.

- Determine the optimum pH as a function of COD degradation and total gas production in batch fermentations.
- Evaluate the effect on hydrogen production of glycerol addition to the brewery waste slurry, fermented under optimum pH and initial COD conditions in batch fermentation.
- Model the fermentative hydrogen production process to determine operational parameters.
- Study the relationships between organic acids production, reduction in COD and metabolic pathways.

1.4 Fungal pre-treatment

Although numerous strategies integrating a white-rot fungi (WRF) treatment with other microbial fermentations have been explored in the search for a sustainable biofuel production process from lignocellulosic biomass, little has been reported in the use of liquid residues like brewery wastewaters. The high energy content in these residues can be exploited after a WRF saccharifying pre-treatment while producing fungal biomass, one of the many valued by-products than can be obtained from WRF.

Hypothesis

White-rot fungal biomass can be substantially produced while significantly treating a high-strength brewery waste slurry leading to the generation of an effluent rich in fermentable sugars which will enhance a subsequent dark fermentative process.

General objective

To bioremediate brewery waste slurry with white-rot fungi including the conversion of recalcitrant molecules to produce a substrate rich in simple sugars and potentially exploitable by-products.

Particular objectives

- Evaluate the growth of three white-rot fungi strains (*Flammulina velutipes*, *Pleurotus eryngii* and *Pleurotus ostreatus*), in submerged fermentation using brewery waste slurry-based media in order to select the strain that generates the highest biomass production.
- Bioremediation assessment of the brewery waste slurry by the selected strain determining COD reduction, as well as colour and turbidity removal.
- Determine fermentable sugars in solution after the fungal treatment.
- Assess the potential of the fungal treatment effluent as a substrate for hydrogen production in dark fermentation.

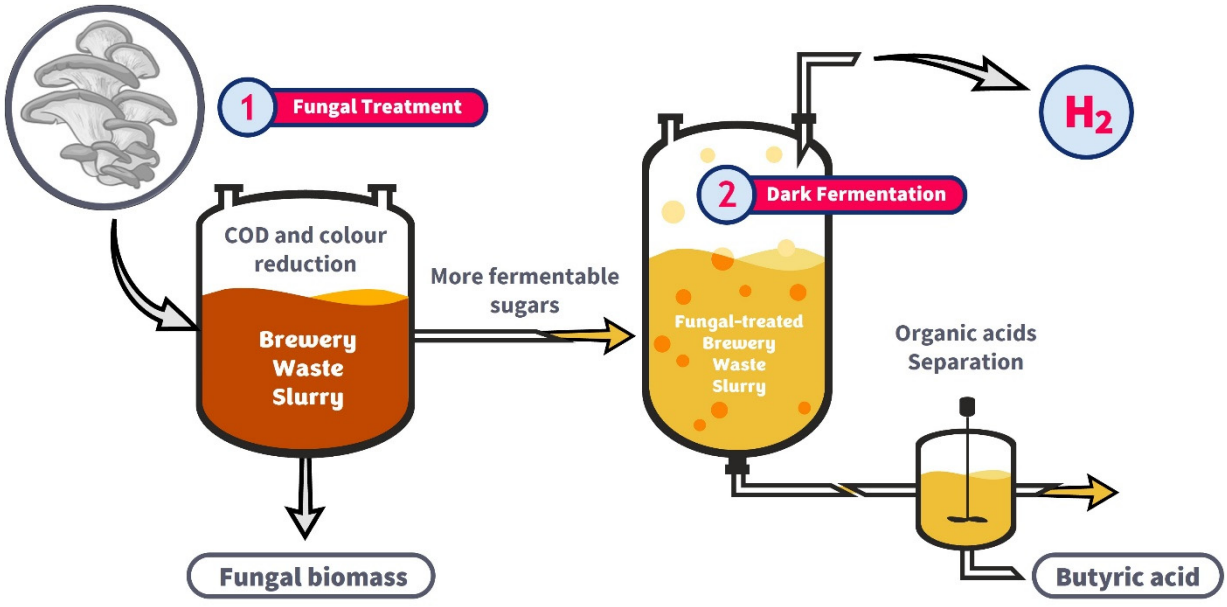

Figure 1.1 *Schematic diagram of the proposed fungal pre-treatment of brewery waste slurry prior to dark fermentation, obtaining fungal biomass and butyric acid as by-products.*

1.5 Microbial electrochemical technologies

Firstly, it is intended to use a carbon-felt modified electrode with polyaniline (PANI) to enhance not only the conductivity of the electrode, but its capacitance, and promote the electron transfer between the living cells and the surface of the electrode, given the well-documented biocompatibility of polyaniline[14]. This is to improve the catalytic activity throughout the process in galvanic (MFC) and electrolysis mode (MEC). On the other hand, the use of metal oxides such as ruthenium (RuOx) have been employed to confer extra capacitance to carbon-based electrodes, and in MFC, RuOx nanoparticles have shown to improve power output by 17 times, while the anode performed as a biocapacitor[15,16]. Therefore, it is also intended to evaluate the effect of adding RuOx nanoparticles to the PANI-modified carbon felt electrode. Finally, both MFCs and MECs were configured to work as a single chamber to reduce internal resistance.

Hypothesis

Combining dark fermentation and bioelectrochemical systems can increase hydrogen production using brewery waste slurry as primary feedstock.

General objective

Evaluate and compare the use of MFCs following dark fermentation, hydrogen production from dark fermentation assisted by MECs, and MECs following dark fermentation utilizing a brewery waste slurry as the primary feedstock.

Particular objectives

- Modifying an inexpensive carbon felt electrode for both MFCs and MECs by depositing polyaniline obtained by chemical polymerization of aniline, as well as the addition of ruthenium oxide nanoparticles.
- Characterizing the performance of the modified polyaniline/carbon felt electrodes, with and without ruthenium oxide nanoparticles, compared to the bare carbon felt electrode, by simple electrochemical methods (*e.g.*, cyclic voltammetry).

- Assess the performance of MFCs, in terms of power output and COD reduction, set with the polyaniline-modified electrodes (with and without ruthenium oxide), fed with fresh brewery waste slurry and dark fermentation effluent.
- Assess the hydrogen production, COD removal, and organic acids produced in MECs, poised with a potential of 0.4 V, set with the polyaniline-modified electrodes (with and without ruthenium oxide), fed with fresh brewery waste slurry and dark fermentation effluent.
- Determine the feasibility of the use of MFCs and MECs assisting a dark fermentative process based on the efficiency parameters calculated for each technology: coulombic efficiency, COD reduction, power output in MFCs; efficiency based on electric input, substrate input, hydrogen recovery, in MECs.

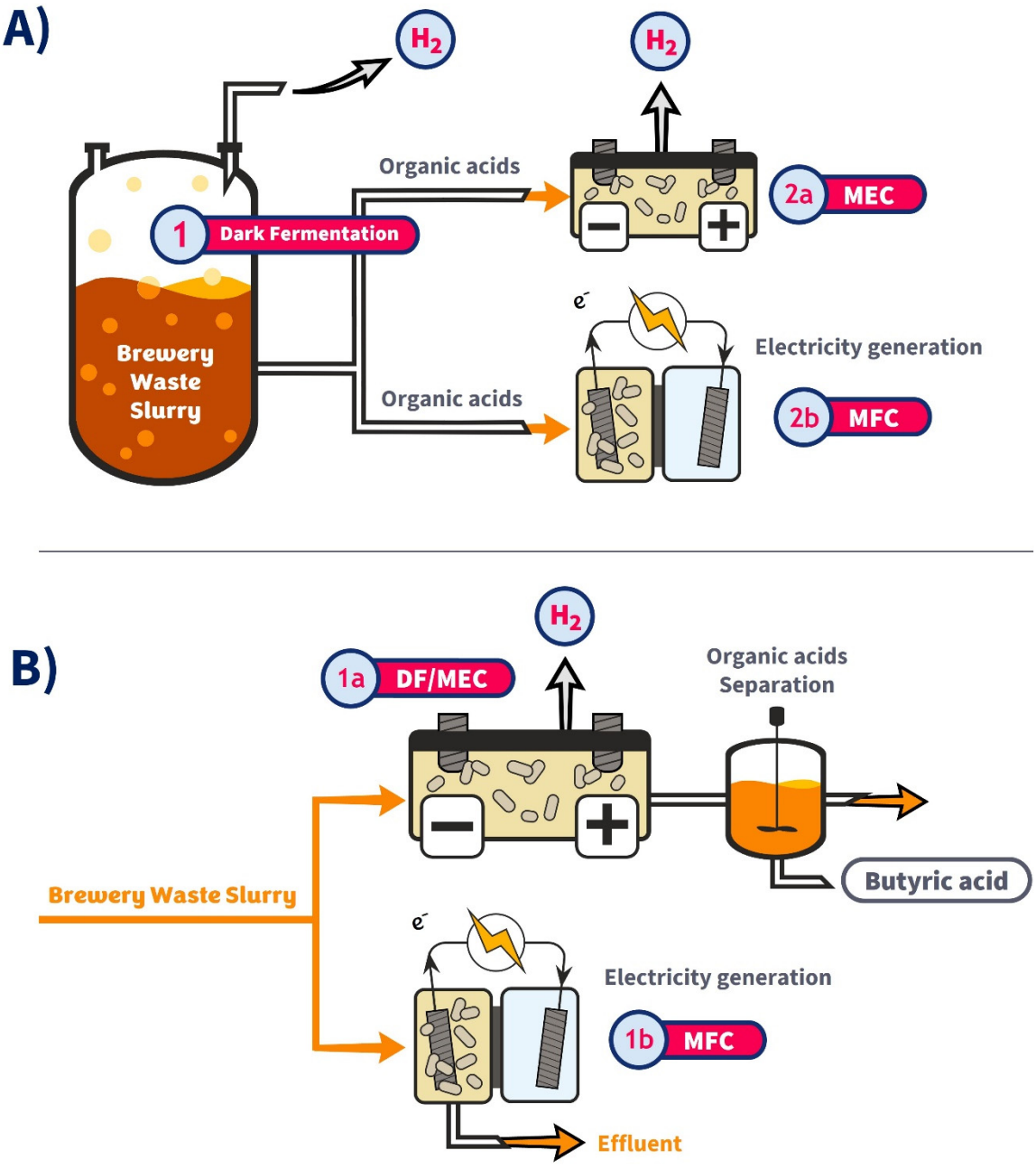

Figure 1.2 *Schematic diagram of the two proposed DF-METs systems. A) Two-staged integrated system for dark fermentation of BWS followed by MECs and MFCs. B) Direct treatment of BWS in MFCs (1b) and dark fermentation assisted by MECs (1a) for hydrogen production and butyric acid recovery.*

1.6 Novelty and contributions

Microbial electrochemical technologies are a relatively new field of biotechnology, and the application of microbial electrolysis is a novel and expanding field, as it is a technology that has emerged only in the last 15 years. While the use of this technology to assist dark fermentation to produce hydrogen has been explored in recent years, to the authors' knowledge nothing has been reported with respect to the treatment of brewing industry wastes, which represents large volumes of waste generated annually. Finally, combining a white-rot fungal pre-treatment with dark fermentation is a strategy with high potential for treatment and valorization of high strength liquid wastes such as brewery waste slurry, however, there is little to no reported literature on this topic. It is in these two main aspects where the relevance and novelty of this project lie.

References

1 Schneider, T.; Graeff-Hönninger, S.; French, W. T.; Hernandez, R.; Merkt, N.; Claupein, W.; Hetrick, M.; Pham, P. Lipid and Carotenoid Production by Oleaginous Red Yeast Rhodotorula Glutinis Cultivated on Brewery Effluents. *Energy* **2013**, *61*, 34–43.

2 Ojong, E. T.; Brunschweiger, S.; Glas, K.; Haseneder, R. Brewery Wastewater as Source of Raw Material for Electrical Energy Generation and Hydrogen Production. *Chemie Ing. Tech.* **2020**, *92* (9), 1278–1278.

3 Ince, B. K.; Ince, O.; Anderson, G. K.; Arayici, S. Assessment of Biogas Use As an Energy Source From Anaerobic Digestion of Brewery Wastewater. *Water. Air. Soil Pollut.* **2001**, *126*, 239–251.

4 Brito, A. G.; Peixoto, J.; Oliveira, J. M.; Oliveira, J. A.; Costa, C.; Nogueira, R.; Rodrigues, A. Brewery and Winery Wastewater Treatment: Some Focal Points of Design and Operation. In *Utilization of By-Products and Treatment of Waste in the Food Industry*; Oreopoulou, V., Russ, W., Eds., **2007**; pp 109–131.

5 Mohamedali, M.; Henni, A.; Ibrahim, H. Hydrogen Production from Oxygenated Hydrocarbons: Review of Catalyst Development, Reaction Mechanism and Reactor Modeling. In *Hydrogen Production Technologies*; Sankir, M., Sankir, N. D., Eds.; Scrivener Publishing LLC, **2017**; pp 3–76.

6 Krupp, M. *Biohydrogen Production from Organic Waste and Wastewater by Dark Fermentation - a Promising Module for Renewable Energy Production*; Shaker Verlag: Aachen, **2007**.

7 Banerji, S. K.; Surampalli, R. Y.; Kao, C. M.; Zhang, T. C.; Tyagi, R. D. High Strength Wastewater to Bioenergy. In *Bioenergy and Biofuel from Biowastes and Biomass*; Khanal, S. K., Surampalli, R. Y., Zhang, T. C., Lamsal, B. P., Tyagi, R. D., Kao, C. M., Eds.; American Society of Civil Engineers, **2010**; pp 23–42.

8 Connaughton, S.; Collins, G.; O'Flaherty, V. Psychrophilic and Mesophilic Anaerobic Digestion of Brewery Effluent: A Comparative Study. *Water Res.* **2006**, *40* (13), 2503–2510.

9 Chen, R.; Chang, S.; Hong, Y.; Wu, P. Brewery Wastewater Treatment by Anaerobic Membrane Bioreactor. *Proceedings, Annu. Conf. - Can. Soc. Civ. Eng.* **2015**, *1_2015*, 390–399.

10 Borja, R.; Martín, A.; Durán, M. M.; Luque, M.; Alonso, V. Kinetic Study of Anaerobic Digestion of Brewery Wastewater. *Process Biochem.* **1994**, *29* (8), 645–650.

11 Athanasoulia, E.; Melidis, P.; Aivasidis, A. Co-Digestion of Sewage Sludge and Crude Glycerol from Biodiesel Production. *Renew. Energy* **2014**, *62*, 73–78.

12 Chow, W. L.; Chong, S.; Lim, J. W.; Chan, Y. J.; Chong, M. F. Anaerobic Co-Digestion of Wastewater Sludge : A Review of Potential Co-Substrates and Operating. *Processes* **2020**, *8(1)* (39), 1–21.

13 He, Q. (Sophia); McNutt, J.; Yang, J. Utilization of the Residual Glycerol from Biodiesel Production for Renewable Energy Generation. *Renew. Sustain. Energy Rev.* **2017**, *71*, 63–76.

14 Hidalgo, D.; Tommasi, T.; Bocchini, S.; Chiolerio, A.; Chiodoni, A.; Mazzarino, I.; Ruggeri, B. Surface Modification of Commercial Carbon Felt Used as Anode for Microbial Fuel Cells. *Energy* **2016**, *99*, 193–201.

15 Lv, Z.; Xie, D.; Yue, X.; Feng, C.; Wei, C. Ruthenium Oxide-Coated Carbon Felt Electrode : A Highly Active Anode for Microbial Fuel Cell Applications C1s. *J. Power Sources* **2012**, *210*, 26–31.

16 Lv, Z.; Xie, D.; Li, F.; Hu, Y.; Wei, C. Microbial Fuel Cell as a Biocapacitor by Using Pseudo-Capacitive Anode Materials. *J. Power Sources* **2014**, *246*, 642–649.

Chapter 2. Literature review

2.1 Climate change: the ongoing public health, humanitarian, and economical crisis

Amid the continuing threat to public health posed by several diseases around the globe, and the dire ongoing humanitarian crisis, the world is facing not only the urgent need to overcome the economic downturn after the COVID-19 pandemic[1], but also the grave consequences from all the absurd geopolitical conflicts of present days. This grim panorama worsens when we put it all into the perspective of the ever-present, life-threatening climate crisis. Undeniable is the evidence of global warming and its deleterious effects. From an economic perspective, weather-related disasters cause financial instabilities in estimated losses between 1%–7% of the affected country's GDP (more than $340 billion USD in losses per year globally), without taking into account the implications to the economy in the longterm[2–4]. The latter poses a greater impact on developing countries, intensifying social inequality and hampering human development[5]. While there is yet no direct evidence to correlate the recent pandemic with climate change, the link between global warming and human displacement is indisputable. In 2020 alone, an estimated 30 million people were internally displaced due to weather-related disasters, an increasingly frequent occurrence engendering human suffering, especially in regions with scarce resources[6].

Before the COVID-19 outbreak, according to the IRENA, the energy-related CO_2 emissions in 2019 were 34 Gt, and barely decreasing to 33 Gt by 2050, far from the 9.5 Gt Paris Agreement's goals[7]. We have seen encouraging sings when greenhouse gas (GHG) emissions were reduced during the great lockdown in 2020, although the effects of climate change will not recoil just for a temporary respite[2]. To put into perspective, a reduction in emissions of 17% was observed in April 2020 compared to the same period in 2019, and the sector that contributed the most to this change was surface transportation (-43%)[8], and by the end of 2020, it was estimated that global emissions will be 8% lower[9]. Nevertheless, even though traffic and transportation significantly reduced the carbon footprint during the pandemic, this change is negligible compared

to the accumulated emissions from past years. In the same month of April 2020 an average CO_2 concentration in the atmosphere of ~416 ppm was measured, the highest since 1958[10]. Furthermore, the experience of previous crises demonstrates that while carbon footprint temporally drops during a crisis (e.g. GFC in 2009), a dramatic increase in emissions follows throughout the years after re-establishing economic activity[2]. In this vein, many experts and international organizations view this current situation as a critical turning point toward a low-carbon-based economy[11]. To prevent a disproportionate upsurge of CO_2 emissions and to provide a sustainable, resilient economic recovery, many countries are implementing more fiscal stimulus and finance packages to accelerate the transition to low-carbon economies in the short-term. Similarly, some organizations (The World Bank, the OECD, the UNEP, and the WTO, among others) recommend several policies to achieve a low-carbon recovery, some of them related to energy and carbon emissions[2].

In this context, it is necessary to address climate change, investing more in clean technology and green jobs, otherwise, there is the risk we will continue in a fossil-based economy with implications nearly impossible to escape[11]. Among many other promising clean energy sources, hydrogen re-emerges as a fossil fuel substitute. The European Union's strategy to overcome the economic crisis in 2020 included a plan to invest €470 billion by 2050 in green hydrogen, although to secure EU´s energy independence, the targeted production planned by 2030 was increased by 250%, and recently, the European Commission unveiled in 2022 a €300 million public-private program to fund hydrogen research[12,13]. For their part, the governments of the UK and France have approved the release of an investment of £4 billion and €30 billion, respectively, to strengthen their hydrogen sector by 2030[14,15]. In the case of Canada, the Federal government aims to be among the top ten hydrogen producers, investing $1.5 billion “in a Low-carbon and Zero-Emissions Fuels Fund to increase the production and use of low-carbon fuels, including hydrogen”[16]. With all of the above, why hydrogen now?

Table 2.1. Comparison properties of hydrogen and hydrocarbon fuels[17]

Property	Hydrogen	Methane	Gasoline	Propane	Ethanol	Methanol
	H_2	CH_4	C_8H_8	C_3H_8	C_2H_5OH	CH_3OH
Molecular weight	2.02	16.04	102	44.10	46.07	32.04
Molar carbon to hydrogen ratio	0.000	0.250	0.444	0.375	0.333	0.250
Stoichiometric air/fuel ratio, mass	34.32	17.20	15.11	15.67	9.00	6.45
Latent heat of vaporization (kJ/kg)	446	509	348	449	921	1176
Lower heating value (MJ/kg)	119.93	50.02	44.50	46.40	26.86	19.93
Flammability limits (% by volume)	4.1 – 74.0	5.3 – 15.0	1.4 – 6.7	2.2 – 9.5	4.3 – 19.0	7.3 – 36.0
Self-ignition temperature (K)	855	813	530	755	696	737
Combustion speed in air (m/s)	2.933	0.355	0.356	0.432	0.455	0.455
Octane number (R+M)/2	130+(R)	120+	86 – 94	104	100	100

2.2 Fossil fuels substitute: why hydrogen?

The enormous energy potential of hydrogen as an alternative to fossil fuels is not new to the scientific community or industry. In fact, the practical use of hydrogen as a fuel at a large scale can be placed, at least, at the dawn of the space race in the 1950's[18], and the first internal combustion automobile invented was powered not with conventional hydrocarbons fuels, but with hydrogen, back in 1806[19]. Hydrogen gas (H_2) has a high energy density (122–142 kJ/g)[20], however, it is not an energy source, rather it has to be produced from another feedstock, therefore it is referred to as a potential secondary energy carrier (like electricity)[21]. It is nonpolluting; virtually the only exhaust product of its conversion into energy is water. Nonetheless, despite the historical background and the fact that it is the most abundant element in the universe (nearly 75% accounts for hydrogen), this molecule is rarely present on Earth in its elementary form. Besides, due to its lightness and diffusivity, hydrogen gas can easily escape to outer space, and so it barely constitutes 0.5–1.0 ppm of the atmosphere[22,23]. Therefore, to exploit all its potential, hydrogen must be obtained from various sources, such as fossil fuels and water, which are abundant resources on our planet.

Sources of hydrogen is not the challenge to be met; in fact, it is used globally on a massive scale (**Figure 2.1**). Currently, hydrogen demand is 70 million tons annually, mostly destined to synthesize ammonia and petroleum refining[23,24]. It is used as well to produce methanol and has found application in several chemical syntheses in food, metal formation, plastics, and electronic industries[25]. While the capacity to produce hydrogen is not a problem, the challenges for its application as an energy carrier on a large scale are rather related to *sustainability*. Some experts even claim that hydrogen is too valuable to be burned[26]. On the one hand, storage, transport, and distribution are one side of the problem. As the lightest molecule, H_2 diffuses easily through most materials containing it. Also, at normal ambient conditions, H_2 is a gas, making it difficult to condense to a liquid due to its low critical point ($Tc = -240.01$ °C, $Pc = 12.96$ bar)[27]. The latter not only poses a safety problem regarding storage and transportation, given its flammability but also represents less volumetric energy, compared to other liquid fuels. Despite having a high energy density (~4 times higher than gasoline), in terms of volumetric energy (kJ/volume), H_2 presents a much lower value than that of gasoline (~10^3 times lower)[28]. Notwithstanding, H_2 still could be used as a secondary energy carrier, and mixed with other gases, like methane or ammonia, it considerably increases the gas mixture's energy potential[29,30].

More importantly, lies the environmental impact of the conventional platforms of H_2 production, which are based mainly on the thermochemical decomposition of hydrocarbons. As mentioned above, H_2 is obtained from several abundant resources, however, more than 90% of the H_2 produced is linked to the fossil fuels industry. Natural gas and oil reforming are the most widespread methods, accounting for 78% of the world's H_2 production, followed by coal gasification (18%) and water conversion (4%)[28,31]. Moreover, around 45–60% of energy input is lost to produce synthetic carbons or ammonia from hydrogen[24]. In this sense, to distinguish the hydrogen production platform in terms of GHG emissions, a colour classification system is commonly used. Generally, a three-colour system is widely accepted[32], although one or more colours could be added, depending on the literature source.

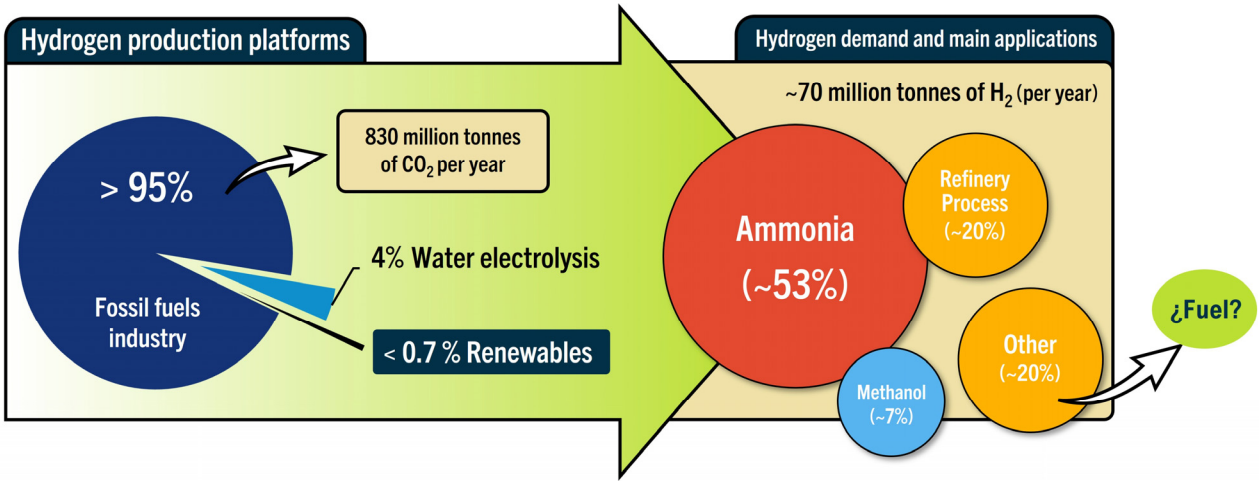

Figure 2.1. *Hydrogen production platforms (left), and hydrogen demand and applications (right)*[23,24]

Firstly, most of the hydrogen currently used industrially and produced through the gasification/steam reforming of fossil fuels is referred to as ***'Gray'*** hydrogen; sometimes ***'Brown'*** is to classify fossil fuels gasification, and *Gray* refers to steam reforming of methane only. Either way, these two are the platforms with the highest environmental impact. Then, comes ***'Blue'*** hydrogen, which is the gas obtained from steam reforming of natural gas with the addition of a carbon capture technology. ***'Green'*** hydrogen is the most environment-friendly group, in which water electrolysis is comprised, provided that the energy employed comes from a renewable source, given the high power requirement (~4.5 kW*h/Nm^3 per mol of H_2)[33,34]. Therefore, even though hydrogen combustion does not generate GHG emissions, water electrolysis could pose a significant impact on the environment, thus compromising the character of hydrogen as a clean energy[25,35].

Hydrocarbon reforming has proven to be a low-cost and more efficient process than other methods, although it is not a clean process and not based on a renewable source[36,37]. Among the reforming routes of methane, steam reforming (SMR) is the least expensive and most accepted to generate hydrogen from natural gas. SMR catalytic process undergoes a series of reactions between methane and steam[38]:

$$CH_4 + H_2O \xrightarrow{\text{catalytic}} CO + 3H_2 \qquad \textbf{Eq. (2.1a)}$$

$$CH_4 + 2H_2O \xrightarrow{\text{catalytic}} CO_2 + 4H_2 \qquad \textbf{Eq. (2.1b)}$$

$$CO + H_2O \xrightarrow{\text{catalytic}} CO_2 + H_2 \qquad \textbf{Eq. (2.2)}$$

Methane can also be pyrolyzed, from which no CO nor CO_2 is generated since oxygen is not involved in the decomposition reaction[38]:

$$CH_4 \xrightarrow{\Delta} C + 2H_2 \qquad \textbf{Eq. (2.3)}$$

Hydrogen from oil reforming also relies on the same reforming routes as natural gas, *i.e.*, steam reforming, partial oxidation, as well as pyrolysis. The process undergoes the same four stages as methane reforming (desulfurization, reforming (with steam and/or oxygen), water–gas shift, and purification). Hence, the general reactions for hydrogen from any given hydrocarbon are the following[38]:

$$\text{Steam reforming: } C_nH_m + nH_2O \xrightarrow{\text{catalytic}} nCO + (n + 0.5m)H_2 \qquad \textbf{Eq. (2.4)}$$

$$\text{Partial oxidation: } C_nH_m + 0.5nO_2 \xrightarrow{\text{catalytic}} nCO + 0.5mH_2 \qquad \textbf{Eq. (2.5)}$$

$$\text{Pyrolysis: } C_nH_m \xrightarrow{\Delta} nCO + 0.5mH_2 \qquad \textbf{Eq. (2.6)}$$

Other alternatives to conventional production processes are biomass-based methods in which hydrogen is obtained either thermochemically or biologically from different renewable sources, and as in the case of water electrolysis, they could be classified as ***'Green'*** hydrogen.

2.3 Biohydrogen

By convention, hydrogen obtained from biomass conversion is referred to as *biohydrogen*[39]. Wood, whether as raw material or waste, is since the dawn of time, the largest biomass source that is still used to produce energy, and in the same vein, biohydrogen is also mainly obtained through the pyrolysis of lignocellulosic

materials[31,40]. Other thermochemical technologies are merely an extension of the conventional processes mentioned above (*i.e.*, steam reforming and gasification of biomass-derived chemicals[41–43]), which represents the same environmental impact.

On the other hand, several biological technologies offer some unique opportunities using raw biomass as well as biowastes as feedstocks. *But could these biotechnologies be considered among those 'Green hydrogen' production platforms?* In the following section, the main biological processes extensively researched and exploited to produce hydrogen will be presented in a broad manner presenting their advantages and disadvantages.

2.3.1 Biotechnologies for hydrogen production.

Biophotolysis

Biologically, hydrogen can be obtained from photoautotrophic microorganisms and their sunlight-to-chemical-energy enzymatic conversion process under anaerobic conditions, fueled by the low potential reducing agents released from water splitting, and from which it can be distinguished by two different pathways[44].

$$2H_2O \xrightarrow{\text{Light energy}} O_2 + 4H^+ + 4e^- \qquad \textbf{Eq. (2.7)}$$

$$6H_2O + 2CO_2 \xrightarrow{\text{Light energy}} C_6H_{12}O_6 + 6O_2 \qquad \textbf{Eq. (2.8)}$$

$$C_6H_{12}O_6 + 2H_2O \xrightarrow{\text{Dark fermentation}} 4H_2 + 2CH_3COOH + 2CO_2 \qquad \textbf{Eq. (2.9)}$$

$$2CH_3COOH + 4H_2O \xrightarrow{\text{Light energy}} 8H_2 + 4CO_2 \qquad \textbf{Eq. (2.10)}$$

In the first pathway, as described in **Eq. 2.7,** a carbon-independent pathway known as *direct biophotolysis*, the solar energy is captured by two light-harvesting protein complexes (LHPC) in the cell wall of green algae and cyanobacteria[45]. These complexes mediate the light-dependent oxidation of water, splitting it into protons, and yielding electrons and oxygen[46]. The energy harvested from the water-splitting reaction leads to an electron transport chain from the LHPC mediated by several enzymes embedded in

the cell wall until reaching the terminal electron acceptor ferredoxin (Fd)[44]. Finally, the energy transferred to Fd is stored in molecular hydrogen by the enzymatic action of *hydrogenases*, while the remaining energy is stored in lipids and carbohydrates within the cell (i.e., starch and glycogen), by the reduction of CO_2 via the Calvin cycle[44,45].

In the second pathway, as described in **Eq. 2.8**–**2.10**, named *indirect biophotolysis*, the reducing agents (electrons) do not come directly from the splitting of water, but from the oxidation of intracellular carbohydrate reserves formed in the fermentative metabolism (Calvin cycle), thus serving as chemical energy carriers between the water-splitting photosynthetic process and the hydrogen-producing reaction[47,48]. Therefore, this process is essentially comprised of two stages: 1) accumulation of carbohydrates via fermentative metabolism; 2) dark fermentation of the reserved carbon sources to generate ATP and further production of hydrogen. This pathway has been observed in many organisms such as *Chlamydomonas*, *Platymonas*, and *Chlorella*[49].

Photofermentation

Similarly, as in the indirect photosynthetic pathway occurring in biophotolysis, certain bacteria can evolve H_2 via *nitrogenases* under anaerobic conditions[50]. However, if in indirect biophotolysis the reducing agents were accumulating carbon-based reserves in the inner cell, in *photofermentation*, an external carbon source is necessary for bacterial growth. Photoheterotrophs such as purple non-sulphur bacteria (e.g., *Rhodobacter, Rhodopseudomonas, Rhodovulum*) are capable to produce H_2 from sunlight energy and reduced organic compounds, mainly organic acids (i.e., lactate, malate, succinate, butyrate), although other carbon sources are also employed, like simple sugars, amino acids, alcohols, inter alia[46,51].

Through the photosynthetic activity, ATP and electrons are generated from the breakdown of organic sources, rather than from water splitting, and hydrogen evolution occurs as a means to create the necessary redox balance for the metabolic route, in which electrons are finally transferred to *nitrogenases* via Fd, where nitrogen gas is reduced into ammonia. Therefore, in these microorganisms, H_2 is a by-product of nitrogen

fixation, following the principle in **Eq. 2.11**[45,52,53]. Photofermentation is definitely a more efficient process for H_2 production than biophotolysis. Some works have reported an overall efficiency of around 80% of conversion, despite common setbacks like low solar energy conversion[51]. This is mainly because *nitrogenases* are fundamentally the sole entity in which H_2 is produced, and since O_2 is not generated during the metabolic process, their activity is not inhibited[53].

$$N_2 + 8H^+ + 8e^+ + 16\ ATP \longrightarrow 2NH_3 + H_2 + 16\ ATP + 16\ Pi \qquad \textbf{Eq. (2.11)}$$

Dark fermentation

Anaerobic digestion comprises the anaerobic degradation of organic matter by heterotrophic bacteria and microalgae. The process known as *dark fermentation* (DF), naturally occurs in the first two phases of the anaerobic digestion process where these microorganisms hydrolyze and partially oxidize complex organic substrates producing organic acids (*i.e.*, acetate and butyrate) while releasing H_2 and CO_2. The hydrogen-producing microbes involved in this anaerobic fermentation are facultative anaerobes and strict anaerobes. Theoretically, 12 mol of H_2 can be obtained from 1 mol of glucose, although this reaction is energetically unfavourable concerning biomass growth, and the real conversion is usually lower[54]. Low acidic environments and high H_2 partial pressure are important factors that have a direct impact on H_2 yield as well. Additionally, enteric bacteria produce other fermentation products (lactate, acetate, etc.) which can inhibit H_2 production if allowed to accumulate[55]. In consequence, the maximum H_2 yield is 4 moles of H_2 per mole of glucose[56]. In fact, H_2 yield in DF hardly achieves over 33% of the theoretical 12:1 ratio[57]. Notwithstanding, DF's greatest potential lies in its versatility and lower reaction volumes when compared to the aforementioned technologies. Only a 1/50 of the photofermentation reaction volume is needed, and more than 20 times smaller than indirect biophotolysis to produce the same amount of volumetric energy (**Table 2.2**).

Table 2.2. Size of bioreactor required to power PEM fuel cells (modified)[58]

System	Size of bioreactor required (m^3) to power PEM fuel cell of:			
	1.0 KW	1.5 KW	2.5 KW	5.0 KW
Direct biophotolysis	341	512	856	1710
Indirect biophotolysis	67.3	101	169	337
Photofermentation	149	224	374	758
Dark fermentation	2.91	4.38	7.31	14.62

Bio-catalyzed electrolysis

Finally, in the past two decades, ***Microbial Electrochemical Cells*** (MECs) have been studied to produce H_2 from the electrolysis of water and oxidation of organic matter, as it would be performed in a conventional electrolysis cell. In these devices, the organic matter is oxidized by bacteria in the anode to yield protons and electrons, and the electrons transferred to the cathode reduce H_2O to produce H_2 and OH^- (**Eq. 2.12, 2.13**). However, this coupled redox reaction is thermodynamically unfavourable, therefore, an external potential must be applied.

Anodic reaction (for any given carbon source)

$$C_xH_yO_z + (2x - z)H_2O \longrightarrow (y + 4x - 2z)H^+ + (y + 4x - 2z)e^- + xCO_2 \qquad \textbf{Eq. (2.12)}$$

Cathodic reaction

$$2H^+ + 2e^- \longrightarrow H_2 \qquad E^o = -0.420\ \text{V}\ vs\ \text{SHE} \qquad \textbf{Eq. (2.13)}$$

Notwithstanding, it has been observed that MECs are capable of generating H_2 at greater efficiencies since the theoretical energy input required could be around one-tenth of that of conventional water electrolysis[59]. Moreover, besides H_2, so as in the case of DF, other compounds can be obtained from MECs by poising the anode at a given potential to produce methane or H_2O_2. As an emerging technology, MECs are in the process of consolidation, although so far, they have proven to be a robust technology

able to deal with a wide range of organic substrates with direct application in wastewater treatment[60].

2.3.2 Advantages and disadvantages of these biotechnologies.

The aforementioned biotechnologies have attracted more attention in recent years since they pose a more environmentally friendly platform: they operate at mild temperatures and low pressures (25°C–40°C, and standard pressure), implying a lower energy impact compared to conventional thermochemical processes, which operate in the range of 600°C–1200°C[61], representing considerable high GHG emissions over 15 times more than renewable sources[62]. Furthermore, there is an important feature to consider, as these biotechnologies do not represent competition for feedstock production lands, since they can be fed with agroindustry and municipal wastes, and unlike other biofuels (*e.g*. biogas, biodiesel, etc.), with which CO_2 is emitted when they are combusted, the CO_2 generated during the fermentation processes can be easily captured or sequestrated *in situ*[52]. However, in this review, we will pay close attention to dark fermentation and microbial electrolysis cells only, given their advantages over biophotolysis and photofermentation. Firstly, H_2 can be produced all day long since the process is light-independent, and it is not restricted by reactor dimensions, secondly, a wider variety of renewable carbon sources can be used as a substrate, both in DF and MECs, producing several valuable end products in the process[36,63,64].

2.4 Fundaments and challenges of dark fermentation

To fully understand the fundaments of DF it is important to first refer to the Anaerobic Digestion process (AD), which is the natural process where certain microorganisms, in the absence of air, decompose complex organic matter at mild temperatures, releasing a gas, mainly composed by methane. The remaining material, known as digestate, is rich in nutrients (nitrogen, potassium, and phosphate) and it is a good quality, soil conditioner. The biogas generated is normally used as a fuel to generate heat and/or electricity, and in its refined state, it is very similar in composition to natural gas[65].

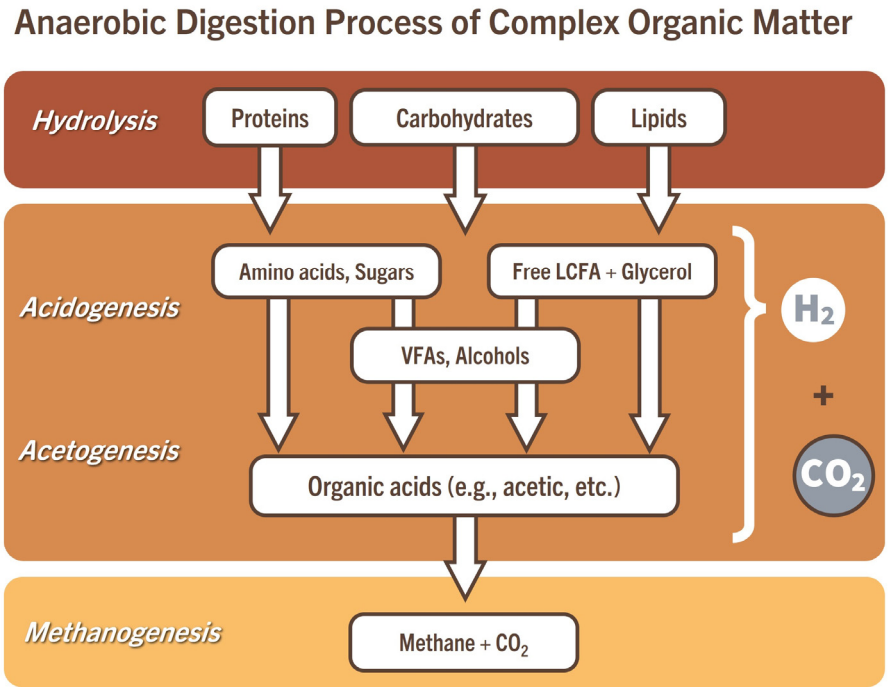

Figure 2.2. *Anaerobic Digestion schematic process*

In the AD treatment process, broadly speaking, several groups of microorganisms are involved in a series of four steps: *Hydrolysis*, *Acidogenesis*, *Acetogenesis* and *Methanogenesis* (**Figure 2.2**). In the first stages (hydrolysis and acidogenesis), the species commonly found are *Butyrivibrio*, *Propionibacterium*, *Clostridium*, *Bacteroides*, *Ruminococcus*, *Acetovibrio*, *Bifidobacterium*, *Eubacterium*, *Selenomonas*, *Lactobacillus*, and members of the *Streptococcaceae* and *Enterobacteriaceae* families[66]. In dark fermentation, enteric bacteria are the most studied facultative anaerobes (e.g., *E. coli* and other *Enterobacter*), whereas *Clostridium* spp. is one of the most important strict anaerobes; these genera can reach up to 70%–80% of the total population in a hydrogen-producing bacteria consortium[67].

Hydrogen in DF is produced mainly through two metabolic pathways (**Figure 2.3**). Firstly, the complex substrates are hydrolyzed into smaller molecules, mainly soluble saccharides, amino acids, and glycerol. In the following step, simple sugars, like glucose, are metabolized to pyruvate via glycolysis. In enteric bacteria, pyruvate is broken down to acetyl-CoA, simultaneously producing formate, a reaction catalyzed by

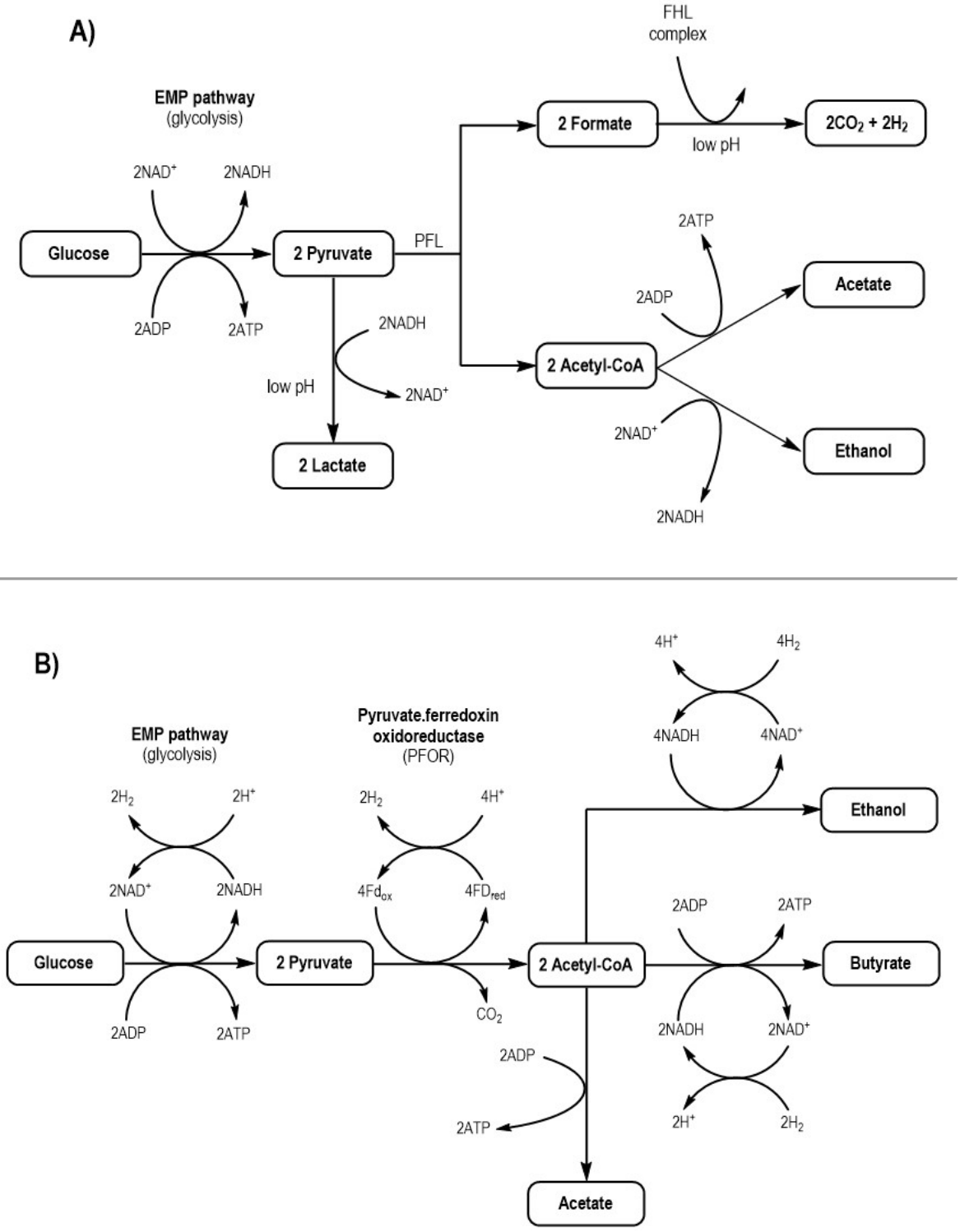

Figure 2.3. *Hydrogen production pathways during dark fermentation: A) enteric bacteria; B) clostridia*[68].

the activity of pyruvate formate lyase (PFL). Hydrogen is then derived from formic acid oxidation by a formate hydrogen lyase complex (FHL), (**Eq. 2.14** and **Eq. 2.15**)[69]. The functionality of PFL is regulated by the level of oxygen in the environment[70]. In strict anaerobes, pyruvate is metabolized to acetyl-CoA involving a pyruvate-ferredoxin oxidoreductases complex (PFOR), producing hydrogen from the reduction of protons by the action of hydrogenases in the presence of $Fe_{(red)}$[52,55] (**Eq. 2.16**).

$$\text{pyruvate} + \text{CoA} \xleftarrow{\text{PFL}} \text{acetylCoA} + \text{HCOO}^- \qquad \Delta G^\circ = -16.3 \text{ kJ/mol} \qquad \textbf{Eq. (2.14)}$$

$$\text{HCOO}^- + \text{H}_2\text{O} \xleftarrow{\text{FHL}} \text{HCO}_3^- + \text{H}_2 \qquad \Delta G^\circ = +1.3 \text{ kJ/mol} \qquad \textbf{Eq. (2.15)}$$

$$\text{pyruvate} + \text{CoA} + \text{Fd}_{(ox)} \xleftarrow{\text{PFOR}} \text{acetyl-CoA} + \text{Fd}_{(red)} + \text{CO}_2 \qquad \Delta G^\circ = -19.2 \text{ kJ/mol} \qquad \textbf{Eq. (2.16)}$$

$$\text{NADH} + \text{H}^+ \longrightarrow \text{NAD}^+ + \text{H}_2 \qquad \Delta G^\circ = +81.1 \text{ kJ/mol} \qquad \textbf{Eq. (2.17)}$$

$$2\text{Fd}_{(red)} + 2\text{H}^+ \longrightarrow 2\text{Fd}_{(ox)} + \text{H}_2 \qquad \Delta G^\circ = +3.1 \text{ kJ/mol} \qquad \textbf{Eq. (2.18)}$$

Hydrogen formation occurs before acetyl-CoA derivation into acetate or butyrate, since the reduction reaction H^+ into H_2 gas is thermodynamically more favourable via Ferredoxin ($Fd_{(red)}/Fd_{(ox)}$) than NAD^+/NADH (**Eq. 2.17, 2.18**)[71]. Thus, acetyl-CoA is the key substance for hydrogen production in DF, because its fate will define whether the process is governed by the acetate or butyrate route.

Several end products can be derived from acetyl-CoA, mainly volatile fatty acids (VFAs), including acetate, butyrate, propionate, lactate; and alcohols, such as ethanol. However, to produce hydrogen, at normal conditions only butyrate and acetate favour the release of hydrogen. In theory, 4 mol H_2/mol of glucose can be produced from acetate fermentation, and a maximum of 2 mol H_2/mol of glucose from butyrate fermentation[72]. Nevertheless, the latter is more energetically favourable (**Eq. 2.20**), and, considering that a very low partial pressure of hydrogen is necessary to promote more hydrogen production from acetate ($<10^{-3}$ atm), the butyrate route by *Clostridium* spp. is often sought[50,56]. Several studies suggest that butyric acid appears to be the most toxic of organic acids generated in dark fermentation for hydrogen-producing

bacteria[73,74], notwithstanding, energetically wise, microorganisms in anaerobic conditions prefer to produce the less acidic butyric acid[75]. Hence, in the pH range of 5.5–7.0, butyrate is commonly found as the main end-product[76,77]. Below pH 5 in DF, acetogenesis shifts to solventogenesis, leading to the sporulation phase of strict anaerobes or death[40]. Moreover, at lower pH, ethanol and lactic acid begin to accumulate, with the latter's metabolism impeding hydrogen production[55,71].

$$C_6H_{12}O_6 + 2H_2O \longrightarrow 2CH_3COOH + 2CO_2 + 4H_2 \qquad \Delta G^\circ = -206 \text{ kJ/mol} \qquad \textbf{Eq. (2.19)}$$

$$C_6H_{12}O_6 + 2H_2O \longrightarrow CH_3CH_2CH_2OOH + 2CO_2 + 2H_2 \qquad \Delta G^\circ = -255 \text{ kJ/mol} \qquad \textbf{Eq. (2.20)}$$

In the acetogenic step, VFAs and alcohols are decomposed by obligately hydrogen-producing bacteria (including homoacetogens), forming more acetate, H_2 and CO_2. Homoacetogens are found in *Acetobacterium*, *Clostridium*, and *Butyribacterium* genera, inter alia, whereas obligate proton-reducing acetogens have been found in *Syntrophobacter* and *Syntrophomonas* genera, to mention a few[66]. Hydrolyzed long-chain fatty acids (LCFA) and glycerol can also be oxidized in the presence of an electron acceptor during this phase[78]. In this way, acetogenesis normally occurs in concomitance with the acidogenic stage.

Finally, the production of methane from the oxidized carbon sources formed in the previous stages is carried out by certain archaea from the order *Methanobacteriales*, *Methanococcales*, *Methanomicrobiales*, *Methanosarcinales*, and *Methanopyrales*, through three metabolic pathways: 1) hydrogenotrophic, 2) acetoclastic, and 3) methylotrophic pathways[79]. Approximately, one-third of the methane produced worldwide comes from the hydrogenotrophic pathway, exhibited by *Methanococcales*, *Methanobacteriales*, *Methanomicrobiales*, and *Methanopyrales*, in which methane is derived from carbon dioxide reduction using H_2 as an electron donor (although formate is also used as a source of electrons, except for *Methanopyrus*)[80]. Hence, to efficiently obtain H_2 in dark fermentative processes, it is important to suppress the growth of hydrogen-consuming methanogens.

2.4.1 Operational parameters

To ensure the desired hydrogenic metabolic routes, proper treatment of the seed sludge is applied, which normally includes heat treatment, looking not only to suppress the activity of methanogens but also to reduce at the minimum the activity of some other species known to hinder hydrogen production, like lactic acid bacteria. After pre-treatments, the seed sludge is mostly comprised of *Clostridiales*; about 70%–80% of the hydrogen producers belong to this genus, coexisting with several other species of the genera *Enterobacter*, *Bacillus*, and *Enterococcus*[56,81]. It is known that a proper heat treatment selectively eliminates hydrogen-consuming microbes and facilitates the activation of hydrogen-producing spores. Enriched cultures of hydrogen-producing microbes can be attained by treating the seed sludge for at least 10–20 min at temperatures between 70–104°C, although after a few days of operation, H_2 production in the bioreactor might drop by as much as 80%[56]. Electric treatment has also been proposed, or the combination of both heat/electric treatments, in which the seed culture is subjected to a discharge, applying voltages in the range of 3 V–20 V, suppressing methanogens and other hydrogen-consuming bacteria[56,82]. An appropriate hydraulic retention time (HRT) can also help to control bacterial community by washing out undesirable hydrogen-consuming species. Specific growth rates of methanogens are very low (0.0167–0.020 h^{-1}), in comparison to those of hydrogen-producing bacteria (0.172 h^{-1})[71]. Methanogens can be fully suppressed by maintaining short retention times (2–10 h), without affecting hydrogen production, since the optimum HRT has been reported between 8–14 hours[83].

Controlling the pH is arguably the most important factor to control. The role of hydrogenases in biohydrogen production systems is vital, since these are the enzymes responsible for H_2 formation from the excess of electrons and protons in the fermentation broth, and like many other enzymes, they are strongly pH dependant[84]. Standard H^+/H_2 reduction potentials observed for hydrogenases *in vitro* are found between pH 5.5–7.0, and the optimal condition has been found at pH 6.0[85]. The suitable pH for hydrogenases activity *in vivo* ranges between 5.0–6.5, with optimal

conditions at 5.5 in many strains, including *Escherichia coli*[86], and below pH 5.0 the activity of hydrogenases begins to fail[87]. Moreover, methanogenesis optimally occurs in pH conditions close to neutrality, and when the pH drops below 6.5, methanogens are inhibited[79,88], whereas the optimal pH for H_2 production has been reported to be between 5.0–6.0[46,83]. Thus, maintaining a low pH can help to control the population in the dark fermentative reactor. However, many studies have reported maximum hydrogen production rates at pH between 6.0 and 6.5[89–91].

Another challenge in DF is the partial pressure of H_2. If it is too high, the formation of organic acids is favoured, which lowers the pH of the medium, turning the H_2 production process thermodynamically unfavourable. Therefore removal of produced hydrogen from the system is necessary to maintain the process in optimum conditions[71]. Stirring can decrease the partial pressure, although the most effective strategy is to sparge the culture medium with an inert gas, like N_2. An increase of 68% to 88% in hydrogen production has been reported by sparging nitrogen gas[92].

2.4.2 Hydrogen yield and process limitations

The main challenges of dark fermentation are associated with low substrate conversion rates. Theoretically, 12 moles of H_2 can be obtained from 1 mol of glucose, however, this reaction will never occur[71]:

$$C_6H_{12}O_6 + 12H_2O \longrightarrow 6HCO_3^- + 6H^+ + 12H_2 \qquad \Delta G^\circ = 32\ \text{kJ/mol} \qquad \textbf{Eq. (2.21)}$$

As discussed earlier, hydrogen is obtained spontaneously only when acetate or butyrate are derived from glucose: Gibbs's free energy is -206 kJ/mol and -255 kJ/mol, respectively (**Eq. 2.19, 2.20**). Dark fermentations are the most spontaneous microbial hydrogen-producing processes; water biophotolysis' Gibbs free energy is highly endergonic ($\Delta G^\circ = +237$ kJ/mol)[46], for example. Yet, the maximum theoretical hydrogen yield (HY) that can be achieved in dark fermentation is 4 moles per mol of glucose, derived from the acetate route. Some authors refer that this is 33% of the maximum theoretical (4 mol/12 mol from **Eq. 2.21**)[93], although in reality is even lower.

Empirically, it has been observed that butyrate governed most of dark fermentations, because from an energy conservation point of view, producing butyric acid generates fewer proton equivalents than acetate, whose formation releases twice as many H^+ as butyrate, thus acidifying the medium more rapidly and disrupting NADH reoxidation as pH drops[75], impeding not only H_2 formation, but also pyruvate, and so on. Excess of acetate, therefore, can be recycled to acetyl-CoA, by butyryl-CoA:acetate CoA transferase, producing more butyrate[76], and then, the theoretical HY of 4 moles per mol of glucose from the acetate fermentation, in reality, becomes no more than 2 moles[56]. Contrarily, acetate is the major VFA observed at pH above 7 (pH 8–10), due to the acetoclastic methanogenic activity triggered by CO_2 and CH_4 accumulation, favoured by the alkaline conditions[94].

Moreover, to produce the other 2 moles of hydrogen to achieve the maximum of 4 moles per mol of glucose from the acetate route, additional hydrogen must be derived from the NADH route[52]. However, as mentioned above, hydrogen production through NADH is thermodynamically unfavourable (**Eq. 2.17**), unless H_2 partial pressure is extremely low ($<10^{-3}$ atm)[56]. Therefore, under normal conditions (1 atm H_2), dark fermentations normally are found between 2 and 4 mol H_2/mol glucose, governed mostly by the more thermodynamically favourable butyrate route. Thus, all hydrogen yields reported are normally based on that maximum of 4 moles from acetate, and not on the 33% aforementioned. Furthermore, as normally butyrate is the major end product, the empirically observed HY, between 2.4–2.6 mol H_2/mol glucose[46,95], can be a baseline to evaluate the substrate conversion efficiency.

Regarding bioremediation, bacteria in DF partially oxidize the organic matter in the medium, accumulating end products in the culture broth. Ironically, hydrogen accumulation is the main issue affecting the entire fermentative process. Thus, normally 60%–70% of organic load remains in the DF effluent, and it requires further treatment before disposal[93], although under certain conditions, COD removal above 40% has been observed[96]. Notwithstanding, in the same way, there is the maximum molar yield per mass of substrate, the performance of the fermentation can also be

evaluated in terms of COD consumption, and theoretically, the maximum attainable volume of hydrogen is 0.47 L H_2/g COD, based on glucose as substrate model[56].

Finally, the performance of the dark fermentative process is generally evaluated according to the following ratios[97]:

Volumetric hydrogen production rate (HPR)

$$\frac{\text{Total amount of hydrogen produced (mL)}}{\text{Reactor volume (mL)} \times \text{Time duration}}$$

Specific hydrogen production rate (SPR)

$$\frac{\text{Total amount of hydrogen produced (mL)}}{\text{Mass of substrate used} \times \text{Time duration}}$$

Hydrogen production yield (HY)

$$\frac{\text{Amount of hydrogen produced (mol)}}{\text{Amount of substrate consumed (mol)}}$$

To make dark fermentation more cost-effective, different alternatives have been explored, from optimizing operational conditions to the use of inexpensive wastes, as well as coupling the process with other techniques. In addition to the natural option of anaerobic digestion, photofermentation and METs have also been studied. The case of the latter will be discussed further below.

2.4.3 Bioreactor Configuration and Operational Mode

Dark fermentation can be operated in batch or continuous mode. In lab-scale studies, batch tests are more often documented because of their simplicity and flexibility, whereas continuous processes are recommended considering industrial applications, mainly because of their economic feasibility and their practical engineering design when treating large amounts of substrates[98].

Different kinds of bioreactor configurations have been used for continuous hydrogen production, although CSTRs are more common[71,99]. Generally, it is associated with a relatively short start-up phase when compared to other configurations due to better

mass transfer, but it also needs rigorous supervision due to the disposition of cells to be washed out. The fed-batch operation also reported high HY. Several studies have reported maximum hydrogen produced between 2.1 to 3.1 mol per mole of glucose, using cellulosic wastes (waste powder, starch, etc.)[97].

2.4.4 Organic wastes as feedstock for biohydrogen production

Simple sugars, (*i.e.*, glucose, fructose, xylose, sucrose, and lactose), have been generally used as model substrates in DF, however, the costs of using them can be high in large-scale application[61]. On the other hand, the limitations of hydrogen production via dark fermentative processes mentioned above can lead to a negative net energy balance[43]. Therefore, among the strategies to overcome those limitations and make DF more cost-effective, is the use of inexpensive substrates, like food industry organic wastes. Some of the residues from different industries exploited in DF are shown in **Table 2.3**:

Table 2.3. Hydrogen produced from different organic wastes in dark fermentation[71]

Seed sludge	Substrate	Operational mode	Hydrogen yield
Mixed culture	Food waste	Continuous	3.5 L H_2/L-day
Mixed culture	Olive pulp wastewater	Continuous	2.8 mol H_2/mol hexose
Sludge compost	Sugary wastewater	Continuous	2.5 mol H_2/mol hexose
Klebsiella pneumoniae	Cane molasses	Continuous	11.2 mmol H_2/g COD
Mixed culture	Dairy waste	Continuous	1.6 mmol H_2/L-day
C. saccharoperbutylacetonicum ATCC27021	Cheese whey	Continuous	2.7 mol H_2/mol lactose
Thermoanaerobacterium-rich sludge	POME	Batch	6.3 L H_2/L substrate
C. freundii 01, *E. aerogenes* E10, and *R. palustric* P2	Distillery wastewater	Batch	2.7 mol H_2/mol hexose
Mixed culture	Brewery wastewater	Batch	6.1 mmol H_2/g COD
Mixed culture	Vinasse wastewater	Batch	24.9mmol H_2/g COD

2.5 Microbial Electrochemical Technologies (METs)

2.5.1 Working principle

MECs were developed in two different laboratories simultaneously back in 2005 by electrochemically assisting Microbial Fuel Cells (MFCs) to produce hydrogen from acetate[100,101]. MFCs are devices that can convert chemical energy stored in organic matter into electrical energy through electrochemical reactions involving bacteria as catalysts. MFCs and MECs are in principle the same technology, although the difference lies in whether the system is operating in electrolytic mode (MECs), or galvanic mode (MFCs) (**Figure 2.4**). In both systems, organic matter is oxidized by microorganisms in the anode chamber through anaerobic respiration, yielding protons and electrons. From here the similarities end, and to understand the working principle of MECs, it must be understood how MFCs work. Firstly, there is the maximum energy available for bacterial growth from the oxidation of organic matter, governed to some extent by the anodic potential.

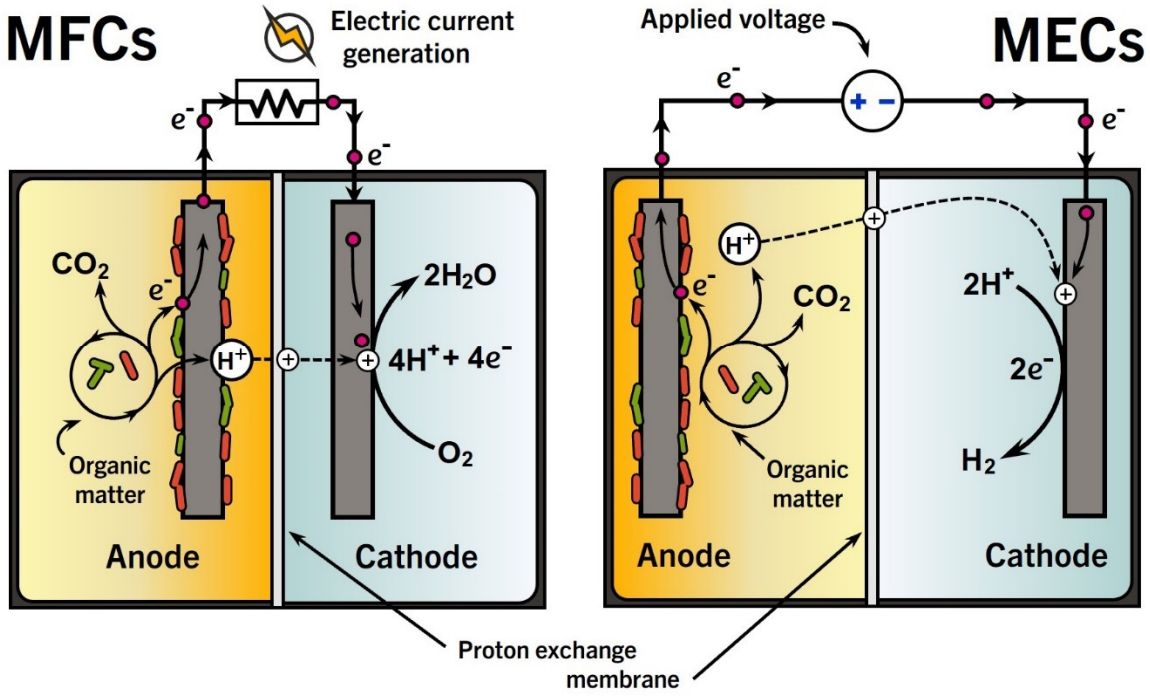

***Figure 2.4**. Microbial Fuel Cells (MFCs) and Microbial Electrolysis Cells (MECs) working principles.*

$$\Delta G^{o\prime} = -nFE^{o\prime} = -nF\left(E^{o\prime}_{\text{donor}} - E^{o\prime}_{\text{acceptor}}\right) \qquad \textbf{Eq. (2.22)}$$

Theoretically, the energy that can be harnessed by microorganisms per mol of acetate, for example, ranges from −74 to −859 kJ, calculated from **Eq. 2.22**, since the standard biological potential of acetate is −0.289 V vs SHE, and the potential of any anode as the electron acceptor in MFCs ranges between −0.195 V to +0.822 V vs SHE[102]. It is evident, therefore, that lower anode potentials furnish less energy per electron transferred for bacterial growth. Normally, bacterial activity in the anode chamber results in a negative anode potential around −0.2 V vs SHE[103], which is slightly more positive than the half-cell reaction potential for acetate. Thus, the potential of the terminal electron acceptor (TEA) in the cathode is also as important as the anode potential.

Anodic reaction

$$CH_3COO^- + 4H_2O \longrightarrow 2HCO_3^- + 9H^+ + 8e^- \qquad E^o = -0.289\ \text{V}\ vs\ \text{SHE} \qquad \textbf{Eq. (2.23)}$$

Cathodic reaction in MFC

$$O_2(g) + 4H^+(aq) + 4e^- \longrightarrow 2H_2O(l) \qquad E^o = +0.840\ \text{V}\ vs\ \text{SHE} \qquad \textbf{Eq. (2.24)}$$

$$E_{\text{emf}} = E_{\text{cathode}} - E_{\text{anode}} \qquad \textbf{Eq. (2.25)}$$

The theoretical electromotive force E_{emf} from the coupled redox reactions above is + 1.129 V (**Eq. 2.23**, **2.24**, reversible potential corrected to standard biological conditions at pH 7.0), indicating that the oxidation of organic matter in the anode is spontaneous (ΔG° is negative) and that the excess of energy can be harvested in the form of electricity. This is the working principle of MFCs. The reduction reaction in the cathode is always carried at a higher electrochemical potential than that at the anode, leading to a spontaneous generation of electrical current. Typically, oxygen is the preferred TEA given the high reduction potential of the oxygen reduction reaction (ORR) (**Eq. 2.24**)[104]. Experimentally, however, cathode potentials are considerably lower than the theoretical value; +0.3 V to +0.5 V, even with Pt catalyzing the ORR[103].

While oxygen is reduced in the cathode chamber of MFCs, the transferred electrons from the anode to the cathode in MECs can further reduce water leading to the formation of H_2 and OH^-. This coupled redox reaction (**Eq. 2.26**, **2.27**) is thermodynamically unfavourable since the theoretical cell potential is $E°' = -1.23$ V ($\Delta G°'$ is positive, regardless of the pH)[105], hence, an external potential must be applied:

Water electrolysis half-reactions

Anodic reaction

$$2H_2O(l) \longrightarrow O_2(g) + 4H^+(aq) + 4e^- \qquad E°' = +1.23 \text{ V } vs \text{ SHE} \qquad \textbf{Eq. (2.26)}$$

Cathodic reaction in MEC

$$2H^+(aq) + 2e^- \longrightarrow H_2(g) \qquad E°' = 0.00 \text{ V } vs \text{ SHE} \qquad \textbf{Eq. (2.27)}$$

$$E°_{\text{cell}} = E°_{\text{cathode}} - E°_{\text{anode}} \qquad \textbf{Eq. (2.28)}$$

In MECs, the energy input is lower than in conventional water electrolysis since the organic carbon degradation supplies part of the required energy. This is partly due to the standard redox potential of biological redox reactions (**Table 2.4**), and also to the decrease in the overpotential of the microbial electrolysis system, which helps to reduce the energy input by greater than 50% (0.2 V–0.8 V in MECs vs 1.23 V–1.8 V in conventional electrolysis)[104,106,107]. Continuing with the use of acetate as a model, under standard conditions ($[H^+] = 1.0$ M, 25 °C, 1 atm) and neutral pH (7.0), hydrogen can be produced at the cathode at a theoretical potential of –0.420 V vs SHE, therefore, the standard cell potential, calculated from redox standard potentials in **Eq. 2.13** and **Eq. 2.23** is $E° = -0.131$ V vs SHE:

Anodic reaction

$$CH_3COO^- + 4H_2O \longrightarrow 2HCO_3^- + 9H^+ + 8e^- \qquad E^o = -0.289 \text{ V } vs \text{ SHE} \qquad \textbf{Eq. (2.23)}$$

Cathodic reaction in MEC

$$2H^+ + 2e^- \longrightarrow H_2 \qquad E^o = -0.420 \text{ V } vs \text{ SHE} \qquad \textbf{Eq. (2.13)}$$

Table 2.4. Common biological redox reactions[108].

Redox reaction	E° (V) vs SHE
$2H^+ + 2e^- \rightarrow 2H_2$	−0.420
$\text{Ferredoxin}(Fe^{3+}) + e^- \rightarrow \text{Ferredoxin}(Fe^{2+})$	−0.420
$NAD^+ + H^+ + 2e^- \rightarrow NADH$	−0.320
$S + 2H^+ + 2e^- \rightarrow H_2S$	−0.274
$SO_4^{2-} + 10H^+ + 8e^- \rightarrow H_2S + 4H_2O$	−0.220
$\text{Pyruvate}^{2-} + 2H^+ + 2e^- \rightarrow \text{Lactate}^{2-}$	−0.185
$FAD^+ + 2H^+ + 2e^- \rightarrow FADH_2$	−0.180
$\text{Fumarate}^{2-} + 2H^+ + 2e^- \rightarrow \text{Succinate}^{2-}$	+0.031
$\text{Cytochrome } b(Fe^{3+}) + e^- \rightarrow \text{Cytochrome } b(Fe^{2+})$	+0.075
$\text{Ubiquinone} + 2H^+ + 2e^- \rightarrow \text{Ubiquinone}H_2$	+0.113
$\text{Cytochrome } c(Fe^{3+}) + e^- \rightarrow \text{Cytochrome } c(Fe^{2+})$	+0.254
$NO_3^- + 2H^+ + 2e^- \rightarrow NO_2^- + H_2O$	+0.421
$NO_2^- + 8H^+ + 6e^- \rightarrow NH_4^+ + 2H_2O$	+0.440
$Fe^{3+} + e^- \rightarrow Fe^{2+}$	+0.771
$O_2 + 4H^+ + 4e^- \rightarrow 2H_2O$	+0.840

All values are valid for pH=7

The latter indicates that to produce hydrogen in the cathode from the biological oxidation of acetate, it will be required to apply 0.131 V, which is 9.3 times less energy than the theoretical voltage supply to a conventional water electrolysis process. Therefore, due to the favourable thermodynamics of organic matter degradations, typically, more negative potentials are applied to increase gas production[103]. Moreover, besides H_2, other compounds can be obtained from MECs. Microbial electrolysis is also used to assist methanogenesis in anaerobic digestion. In this case, the potential applied accelerates the synthesis of end products in each stage of the AD process, and it has been found that above a poised potential of 0.6 V, hydrogen-consuming bacterial communities increased their population in the vicinity of the anode, accelerating acetogenesis and reducing HRTs[109,110]. In **Table 2.5** some reported values of applied potentials are shown, as well as the respective value-added products obtained.

Table 2.5. By-products from MECs at different applied potentials[104].

Product	Applied potential (V)	Recovery rate (*L/L-day*)	Energy efficiency (%)
H_2	0.6	0.53	204
	0.4	0.2	267
CH_4	0.8	0.17 – 0.75	240 – 84
	0.9	0.12	67
H_2O_2	0.5	1.25	83.1

2.5.2 Effect of electrode potentials

As discussed above, the higher the anode potential the more energy is gained by bacteria, but to improve the performance of MFCs, the anode potential must be as low and the cathode potential as high as possible to increase the electromotive force of the cell[102]. Metabolic routes can be affected dramatically only based on the anode potential. High cell potentials elicit higher redox oxidative metabolic pathways in the anodic chamber, improving energy efficiencies, while when the potential decreases, bacteria deliver electrons to electron acceptors with higher potential, (*e.g.*, sulphate or nitrates), and in the absence of such compounds, fermentative pathways become the main processes (acetate and butyrate fermentation routes)[108]. It is important to note, that MFCs must be devised to sustain a constant or intermittent replenishment of oxidized substrate at the anode to keep high cell potentials over time, otherwise the system would perform as a biobattery[111].

The latter also applies to MECs. High cell potentials trigger higher reduction currents, stimulate colonization on the surface of electrodes, and it has been observed that bacteria regulate their respiratory pathway to maximize their energy efficiency[112]. Furthermore, the anode potential has a significant effect on the growth and distribution of anode-respiring bacteria. High diversity is observed when a low anode potential is applied while increasing the anode potential selectively reduces microbial diversity[113].

This have a significant impact in hydrogen production. According to reported data, in general, methanogenesis is favoured at higher applied potentials (0.6 V–1.8 V), specifically, the activity of hydrogenotrophic methanogens is relieved by the hydrogen diffusion rate restrictions in the system[109]. Hydrogenesis is favoured between 0.4 V–0.6 V[103,104], however, there is always the risk of hydrogen-consuming archaea growing in the cathode, reducing the MEC system hydrogen yield[112].

Notwithstanding, as catalysts, bacteria play a vital role in these technologies, and the contribution to current and hydrogen production is far more complex than just changing the potential of a certain electrode. Either with single strain or mixed cultures, regardless of the phylogenetic diversity, only the microorganisms capable of complete oxidation of organic compounds are the most significant direct contributors to power production[114]. The materials and the cell design are determinants as well. Several strategies can be taken to improve the performance of these technologies based only on the use of certain materials as an electrode. Some of the most important electrochemically active bacteria, as the materials and cell configurations, are discussed in the following sections.

2.5.3 Bacteria as catalysts in METs

The microorganisms capable of completely oxidizing organic matter to CO_2 in the presence of an electrode serving as the sole electron acceptor, are often referred as to *electrogenic bacteria*[115]. Only a few species are known to exhibit this feature. The metal-reducing bacteria *Geobacter sulfurreducens* and *Shewanella oneidensis* can use a conductive material as the sole electron acceptor[116–118]. Such is also the case of the Gram-positive bacteria *Therminocola potens* among other *Clostridiales*[119]. Nonetheless, there are non-electrogenic bacteria that exhibit electrogenic activity by the means of mediators. *Pseudomonadaceae*, *Geobacteraceae* and *Enterobacteriaceae* interact with the surface of electrodes via exogenous or self-secreted mediating compounds[120]. Therefore, provided favourable conditions, several non-electrogenic species can be electrocatalytically active, both in microbial electrolysis and fuel cells.

2.5.4 Electron transfer mechanisms in METs

Basically, there are two types of extracellular electron transfer (EET) mechanisms: *Direct Electron Transfer* and *Mediated Electron Transfer*. In the first case, direct contact between the cell wall and the solid electron acceptor is established through outer membrane redox proteins or even by cell appendages. Outer membrane *c*-type cytochrome complexes are responsible to establish direct interaction with electron acceptors in *Geobacter* spp. and *Shewanella* spp.[121]. *G. sulfurreducens* can deploy long pili, called *nanowires*, establishing electrically active contact with the electrode surface[122]. Nanowires show the presence of aligned cytochromes along the structure in which electron hopping occurs[123]. *S. oneidensis* interact with the electron acceptor surface by extended protuberances from the periplasmic membrane[124].

Mediated electron transfer is driven by electron shuttles. These mediator compounds could be either self-produced or artificially added. There is also the specific case for direct electron transfer in which mediator molecules are attached to the cell wall[125]. The self-produced metabolites widely reported as mediators are flavins produced by *Shewanella* spp.[126], where riboflavin is dominant in biofilms[127]; and phenazines by *Pseudomonas*[128]. These mediators could be secreted in the biofilm (microbial formation on the surface of the electrode), as well as in the planktonic phase. The most common exogenous mediators are potassium ferricyanide; colourants such as methylene blue, methyl viologen, and neutral red; and quinoid-like compounds, like anthraquinones and resazurin[125]. However, the toxicity of artificial mediators is an important drawback[129]. Natural organic mediators like flavins have been tested to enhance electron transfer and current generation in non-electrogenic microbes such as yeasts and Gram-positive, like the order of *Clostridiales* and *Bacillales*[130].

Finally, there is the complex cross-feeding interaction between species in which microbes from a community interact with each other to gain energy. Ubiquitous humic acids and analogue molecules (*i.e.*, quinones, anthraquinones, *inter alia*) can mediate interspecies electron transfer in several environments[131]. Small electron acceptors like formate also play an important role as electron mediators[132]. Interspecies direct

electron transfer has also been observed through extensive nets of connections deployed, facilitating cytoplasmic exchange between bacteria. These structures have been referred to tentatively as interspecies nanotubes[133]. In other cases, the addition of a conductive material, like activated carbon, may elicit interspecies electron transfer, substituting natural appendages interactions[134].

2.5.5 METs configuration and materials

Oxygen is a major subject in METs configuration. Since it is a good electron acceptor, it will compete with the anode. Therefore a suitable MET system must be designed to keep the anode isolated from oxygen[120]. The basic MET configuration is a double chamber device, in which an ion exchange membrane separates both compartments. In the case of MFCs, several double-chambered versions have emerged with variations in the electrodes, surface-to-volume ratios, and reactor configurations[135]. There are also single-chambered MFCs in which the anode and the cathode are located in the same compartment. In this case, the cathode is placed in direct contact with air either in the presence or absence of a membrane (**Figure 2.5**). The simplicity associated with single-chamber air-cathode MFCs also provides another significant advantage compared to a double-chamber configuration, as it does not require aeration, boosting the overall efficiency of the system. Also, according to some reports, larger power densities have been achieved when aqueous-cathodes are replaced by air-cathodes[135,136]. Nevertheless, the absence of a separator increases oxygen cross over and substrate diffusion, affecting conversion efficiency and electrocatalytic activity of the biofilm at the anode[120,137]. Therefore, a selective separator is still necessary for MFCs.

In the case of MECs, since O_2 is not required to be introduced in the system, there is no need to prevent the gas produced from entering the anodic chamber[104]. The typical double chamber with anolyte and catholyte separated with a membrane, help to prevent substrate crossover. However, a single chamber configuration is attractive to reduce costs, although the H_2 productivity has shown to be low since this compound could be employed by the anaerobic bacteria to produce methane[106].

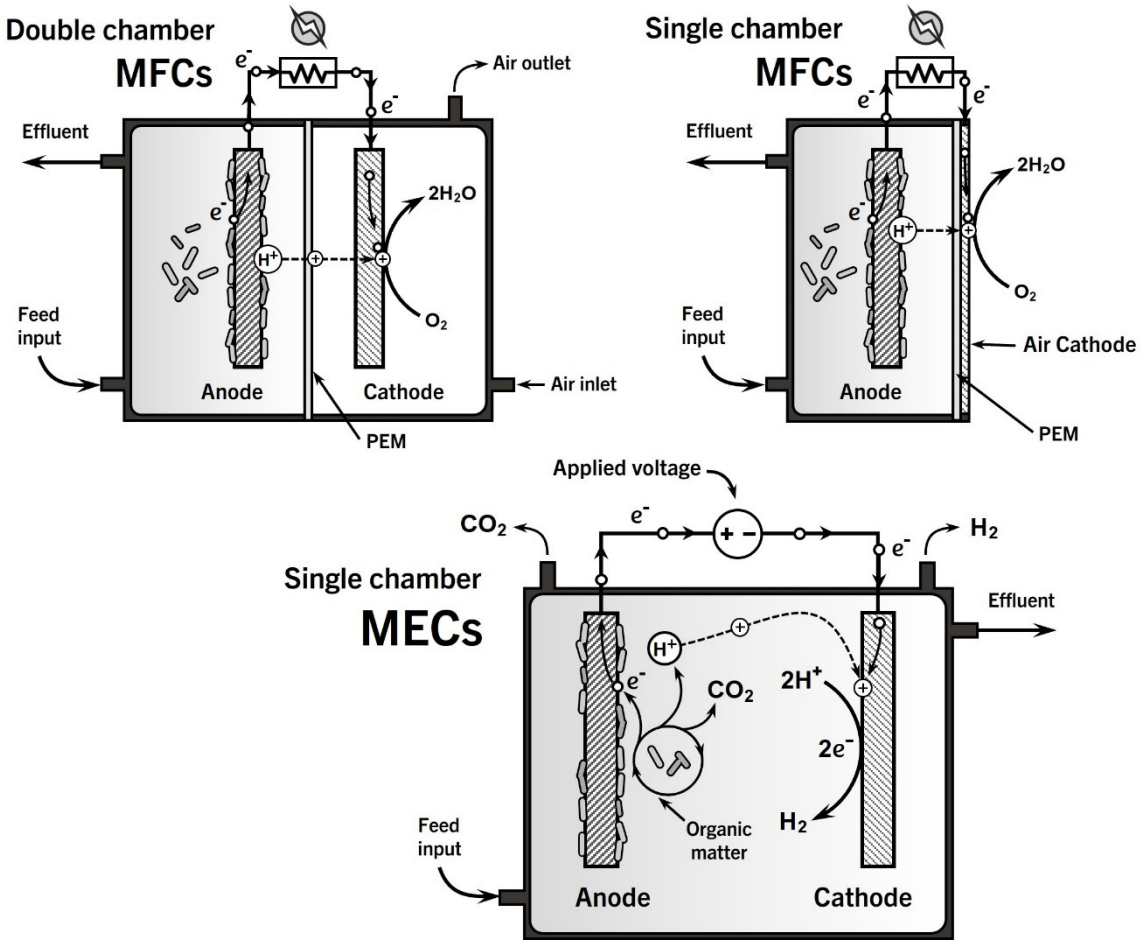

Figure 2.5. *Cell configurations. Double and single-chambered MFCs, and single-chamber MECs*

Anode materials

The anodic performance is strongly limited by the EET between the anode and electrogenic bacteria, so the material for the anode must be highly conductive, biocompatible and stable within the bulk solution[138]. The most versatile material is carbon, due to its high surface area and good conductivity[111]. Graphite electrodes with large surface areas, like foams or fabrics, feature higher conductivity than simple graphite rods, for instance[139]. Carbon nanotubes (CNT) and graphene have higher surface areas and excellent electronic conductivity with good chemical stability[140], nevertheless, their high costs are prohibitive, and other inexpensive carbon-based materials (*i.e.*, cloth, felts, paper) are preferred as electrodes.

Cathode materials

Oxygen reduction reaction in the cathode is one of the most important hindrances in fuel cells' performance. ORR is a slow reaction, hence a catalyst must be used to improve the rates in any given type of fuel cell, where Pt is considered the reference[141]. However, the excessive costs associated with Pt-based catalysts and other precious metals (*e.g.*, palladium, rhodium, or gold) impede large-scale applications. The large specific surface area of carbon-based materials is important when choosing a catalyst for the cathodic reaction. High power densities as obtained with Pt as the catalyst can be achieved with inexpensive chemical activated carbon fibres, for instance[142].

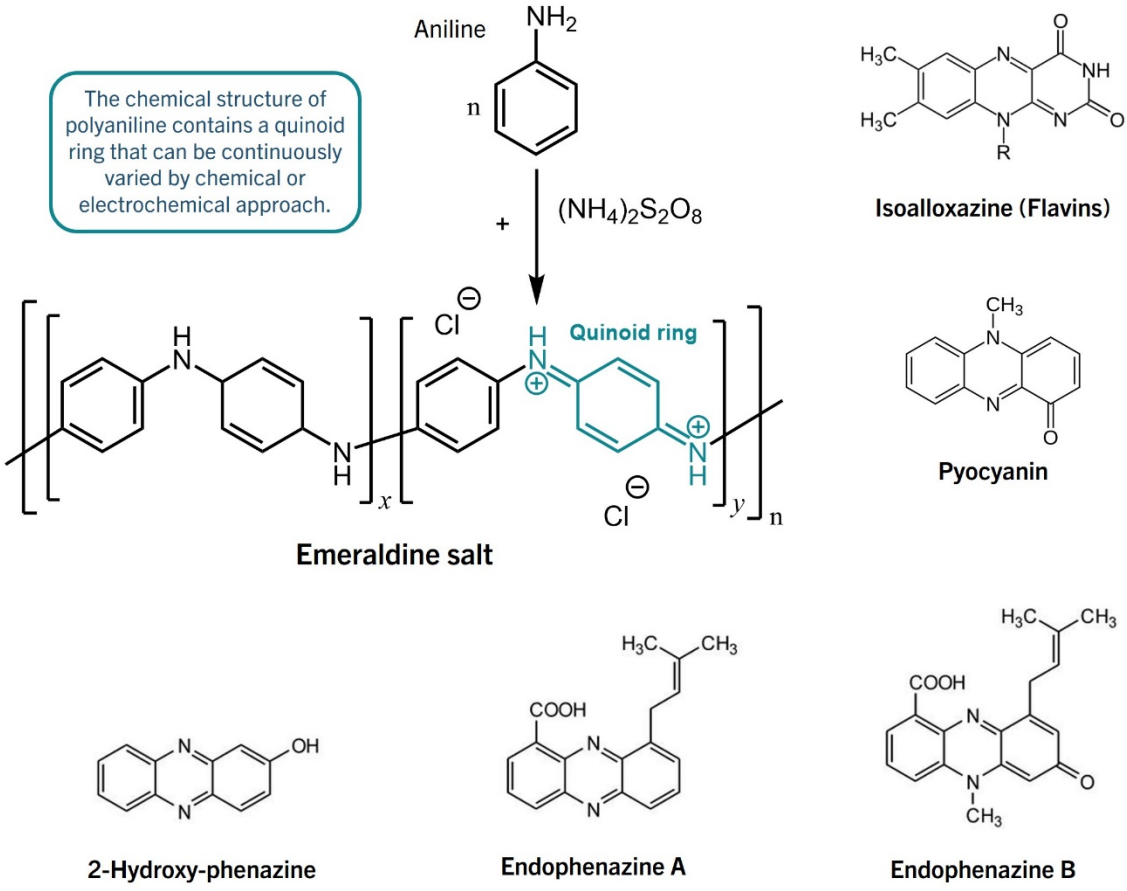

Figure 2.6. *Emeraldine general composition from chemical polymerization of aniline in HCl, catalyzed by ammonium persulfate. Self-secreted mediators like phenazines and pyocyanin by* Pseudomonas *and flavins by* Shewanella *spp. are also presented.*

Carbon-based modified electrodes

Modifying carbon-based materials with polyaniline (PANI) is an attractive option given its easy preparation procedure, low cost, ability to easily form various nanostructures and excellent environmental stability[143]. The partially protonated form, named emeraldine, is the most conductive species, which can be easily synthesized by chemical or electrochemical polymerization of aniline[144]. PANI-modified electrodes have shown great potential in METs, by virtue of their good electrical conductivity, high biocompatibility and stability in biological conditions[145]. This is due to PANI's chemical structure (**Figure 2.6**), consisting of quinoid rings, closely related not only to most of the bacterial self-secreted electron transfer mediators but also to molecules that form part of the electron transfer chain complexes in the respiratory pathway of microorganisms, in which ubiquinone is on of the electron shuttles in the cell wall[146].

Ion exchange membranes

Membranes play a major role in METs' design, as they directly affect the overall performance and the final cost, estimated at 38% of the total cost of a conventional dual chamber device, for instance[147]. Proton exchange membranes (PEM) are currently the most widely used separators for METs operations, being Nafion® (DuPontTM) the most commonly used membrane of its kind, due to its high proton conductivity and excellent mechanical and thermal stability[148]. When using a membrane, the performance of the cells is related to the size of the PEM, rather than the projected surface area of the electrodes. The power output in MFCs increases with larger PEMs, regardless of the surface area of the anode, as demonstrated by Oh & Logan[149].

2.5.6 Technological challenges

Several factors affect the performance of METs. The major problem with both MFCs and MECs is the energy losses due to the internal resistances (**Figure 2.7**), which leads to energy inputs higher than theoretically necessary in MECs and low energy recovery efficiencies in MFCs. As a matter of fact, the strategies to improve the performance of MFCs and MECs are in the same vein, listed below[112,150]:

1. Optimizing architecture and cells design, to reduce internal resistances allowing the increase of the current density.
2. Enhancing the performance of electrodes, using low-cost materials, modifying the surface of electrodes, developing high-performance catalysts, etc.
3. Selection of better acclimated electrochemically active biofilms in both systems, in addition to better selective inhibition of methanogens in MECs.
4. Optimizing the separator, even remove it, if possible.
5. Evaluate the mechanisms of extracellular electron transfer processes between microorganisms and electrodes to improve the kinetics of the process.
6. Scale-up challenges, including voltage reversal in MFCs stacks, energy losses and low hydrogen recovery in MECs.

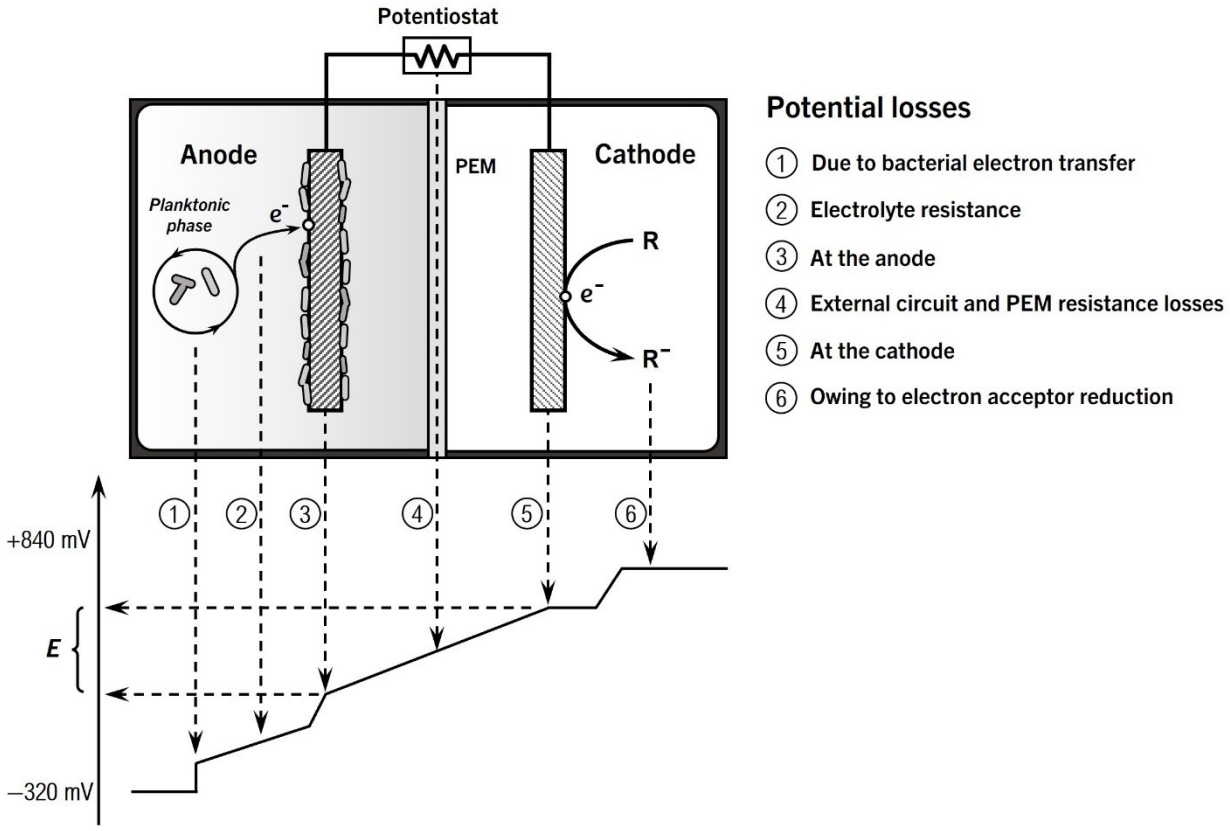

Figure 2.7. *Potential losses during electron transfer in microbial electrochemical cells.*

In the case of MFCs, the main barrier is the low power output in addition to the capital required to set up this technology, which can be 30 times higher when compared to conventional activated sludge treatment[151]. Additionally, the average power density in MFCs is lower than 100 mW/m^2, five orders of magnitude less than in conventional fuel cells[152]. Notwithstanding, the direct electricity generation associated with low operational costs (around 10 times lower than activated sludge treatment), and high COD removal efficiencies, are two major advantages of MFCs difficult to overloook[153]. Furthermore, integrated systems with MFCs are gaining attention, whether they are applied as a pre-treatment or post-treatment stage, or even in parallel with other technologies, specially MECs and DF. A lab-scale integrated MFC-MEC system, for instance, showed an increase in hydrogen production rates of 38% when a capacitor system is employed to transfer almost 90% of the energy produced in the MFCs to the MECs, improving the efficiency up to 60%[154]. Another strategy is the development of efficient harvesting energy technologies to boost the low current densities delivered. Santoro *et al.*[155], demonstrated to obtain an outstanding power output of 84 W/m^2 with the help of a super capacitive air-breathing system, enhancing cathodic performance with bilirubin oxidase electrodes, demonstrated in addition the proof-of-concept of a self-powered supercapacitor connected to each electrode of the MFC.

2.5.7 Efficiency of the electrochemical processes.

The most important key factor for evaluating the performance of MFCs is energy recovery. The overall energetic efficiency, η_{E}, is defined as the ratio of power produced to the heat of combustion of the organic substrate added, calculated as follows[111]:

$$\eta_{\mathrm{E}} = \frac{\int_0^t E_{cell} I \mathrm{d}t}{\Delta \mathrm{H_S} m_{\mathrm{S}}} \qquad \textbf{Eq. (2.29)}$$

Where $\Delta \mathrm{H_S}$ is the heat of combustion (J/mol) of the substrate, and m_{S} is the mass of substrate added (mol). **Eq. 2.29** is usually used when the composition of the substrate is known. However, when wastewater with unknown substrate composition are employed, there is another parameter to evaluate the efficiency of the process.

The Coulombic efficiency, (%CE), defined as the ratio of total Coulombs actually transferred to the anode from the substrate to the maximum possible Coulombs if all substrate removal produced current, is a useful parameter to evaluate the microbial electrocatalytic activity[111]. Moreover, %CE can be calculated based on COD consumption:

$$\%\mathrm{CE} = \frac{8\int_0^t I\mathrm{d}t}{FV_{an}\Delta\mathrm{COD}} \qquad \textbf{Eq. (2.30)}$$

Where V_{an} is the volume of the anodic chamber, and 8 is a constant used for COD based on M_{O_2} (32 g/mol) and 4 electrons exchanged per mole of O_2. If the %CE is low, it means that bacteria are using alternate electron acceptors or that the process is governed by fermentative pathways. In the case of MECs, coulombic efficiency is defined as the ratio of moles of H_2 that can be recovered based on the measured current to the maximum theoretical hydrogen that can be produced from the substrate.

$$\%\mathrm{CE} = \frac{\eta_{\mathrm{CE}}}{\eta_{\mathrm{th}}} \qquad \textbf{Eq. (2.31)}$$

This ratio can also be based on COD removal:

$$\eta_{\mathrm{CE}} = \frac{\int_0^t I\mathrm{d}t}{2F} \qquad \textbf{Eq. (2.32)}$$

$$\eta_{\mathrm{th}} = \frac{b_{\mathrm{H_2/S}}\, V_{\mathrm{L}}\, \Delta\mathrm{S}}{M_{\mathrm{S}}} \qquad \textbf{Eq. (2.33)}$$

Where F is Faraday's constant (96,485 C/mol e^-) $b_{\mathrm{H_2/S}}$ is the maximum theoretical stoichiometric hydrogen production from the substrate (4 mol H_2 per mol of glucose[70] versus 2.4 mol H_2 per mol of glucose when butyrate is the main end product[95]), V_{L} is the fermentation volume, $\Delta\mathrm{S}$ is the change in substrate concentration, and M_{S} is the substrate molecular weight. $\Delta\mathrm{S}$ can be substituted by $\Delta\mathrm{COD}$, with a conversion factor (*e.g.*, 1.07 g COD/g glucose)[156].

Finally, the energy efficiency related to the electrical input η_E, and that related to the substrate added η_S, are the most common parameters to evaluate the performance of hydrogen production in a MEC process:

$$\eta_E = \frac{W_{H_2}}{W_E} = \frac{\eta_{H_2} \Delta H_{H_2}}{W_E} \quad \text{Eq. (2.34)}$$

$$\eta_S = \frac{W_{H_2}}{W_S} = \frac{W_{H_2}}{\Delta H_S \eta_S} \quad \text{Eq. (2.35)}$$

where is $\Delta H_{H_2} = 285.83$ kJ/mol, η_{H_2} is the amount of H_2 moles obtained during the process. The efficiency η_S is calculated based on the heat of combustion of each component added as substrate. The electrical energy input W_E is defined by the following equation:

$$W_E = \sum_1^n \left(I E_{ap} \Delta t - I^2 R_{ex} \Delta t \right) \quad \text{Eq. (2.36)}$$

Where E_{ap} is the voltage applied, I and R_{ex} are the current measured and the external resistor closing the MEC circuit.

2.5.8 Coupled systems for hydrogen and electricity production: DF/MEC–MFC

As has been mentioned above, biohydrogen production systems on their own are limited in many ways. DF exhibits higher H_2 evolution rates in comparison to photofermentation or biophotolysis, but the maximum yield is restricted by metabolic and thermodynamic fundamentals. In order to achieve a more practical, energy-efficient DF-based hydrogen production process, various attempts have been studied, such as sequential anaerobic digestion (AD) post-treatment, and two-staged processes to generate more hydrogen, like photofermentation or METs[110,157].

As opposed to photofermentation, in which feeds normally are greatly diluted substrates, METs usually accept feeds with a higher organic load within the typical DF discharge range (2–40 g COD/L). Besides, DF effluents are rich in volatile fatty acids

(VFAs), which can serve as a suitable carbon source for microorganisms in METs[158]. Another advantage is that the dark-fermentative process can be assisted by METs in a single-staged process[159]. The integration of METs can improve COD reduction to levels lower than 1 g /L, performing as an effluent polishing process while generating electricity in MFCs, and further conversion of residuals to H_2 in MECs[158]. In this sense, there is the potential to convert more energy through METs from the fermented organic wastes, overcoming the biological and thermodynamic limitations of the DF process alone.

Some studies on DF coupled with MFCs reported stabilization of the DF effluent by the increase of COD removal while electrical energy is produced. VFAs served as a readily biodegradable substrate for the MFCs process rendering a final COD removal between 79%–99%[160,161]. Nevertheless, even though several studies have reported the potential of MFCs as part of an integrated system with DF and AD[162], the general reported data for MFCs fed with DF effluents shows a reduction in power output with an increase in OLR, a situation that limits its application at a large scale (**Table 2.6**). On the contrary, as seen in **Table 2.7**, in the case of DF coupled with MECs, several recent studies reported the successful integration of both systems, demonstrating an enhanced H_2 production rate (HPR) at the end of the process, and in some cases, reporting remarkable higher H_2 yields per g of COD consumed.

Finally, as seen in **Tables 2.6-2.7**, there is a wide variety of organic wastes used as substrates for both DF/MFC and DF/MEC coupled systems. Nevertheless, little work has been reported on the use of residues from beer production processes. The use of brewery wastewater (BWW) has been extensively studied on each technology separately. In the course of the last decade, for instance, widely varied power outputs (7–670 mW/m^2) have been reported from MFCs fed with BWW[163,164]. However, there is scarce literature reporting the use of BWW in DF/METs systems, despite the great potential of these organic residues, as discussed further below.

Table 2.6. Operating features and performance of combined systems Dark Fermentation-Microbial Fuel Cells.

MFC Configuration	Substrate (H_2 production effluent)	Inoculum	OLR (g COD/L-d)	Max. Power density (W/m^3)	ξ_{COD} (%)	SDR (g COD_R/L-d)	SPY (W-h/g COD_R)	CE (%)	Energy conversion (%)	Ref.
Single chamber	Vegetable waste (DFE)	Biohydrogen fermentation bacteria	1.51	21.8	99.5	1.5	0.346	52.6	8.40	165
			3.07	23.4	98.0	3.0	0.187	31.6	4.53	165
			6.17	17.9	96.7	5.97	0.047	14.1	1.74	165
Double chamber	DFE	Pretreated manure sludge	0.19	12.5	72.0	0.14	0.331	47.8	11.00	166
Single chamber	Vegetable waste (DFE)	Anaerobic sludge from a DF reactor	0.93	1.56	80.0	0.74	0.264	12.6	—	161
Single chamber	Spent molasses (DFE)	Anaerobic mixed consortia	1.50	3.01	85.4	1.28	—	3.63	2.2	161
Double chamber	Crude glycerol (DFE)	Anaerobic sludge	>0.08	2.58	50.2	—	—	27.2	—	167
Double chamber (3 stacks in series)	DFE	Pretreated manure sludge	1.92	3.2	82.0	—	—	—	—	168

DFE, dark fermentation effluent; ξ_{COD} COD removal efficiency; SDR, substrate degradation rate; SPY, specific power yield; CE, Coulombic efficiency; OLR, Organic load rate

Table 2.7. Operating features and performance of combined systems Dark Fermentation-Microbial Electrolysis Cells[169].

Dark fermentation (first stage)					Microbial Electrolysis Cells (second stage)		
Inoculum/seed source	Starting material	H_2 yield	HPR ($L\ H_2/L\text{-}d$)	Major compounds in DF effluent (MECs substrate)	Inoculum	H_2 yield	HPR ($L\ H_2/L\text{-}d$)
Anaerobic consortia	glucose	0.25 L H_2/g COD	0.28	acetate, propionate, butyrate	Anaerobic consortia	0.05 L H_2/g VFA	0.07
Cow dung compost	Corn stalk	0.13 L H_2/g corn stalk	1.73	acetate, butyrate, ethanol, propionate	H_2 fermentation effluent	0.26 L H_2/g corn stalk	3.43
Anaerobic digestion sludge	Sugar beet juice	0.16 L H_2/g COD_{added}	1.88	acetate, butyrate, propionate	Acetate-fed MEC effluent	0.19 L H_2/g COD_{added}	—
Mixed microbial community	Molasses wastewater	0.19 L H_2/g COD	0.7	ethanol, acetate, propionate, butyrate, valerate	Domestic wastewater	1.15 L H_2/g COD	1.41
Sediment microbial consortium	Crude glycerol	0.55 mol H_2/mol glycerol	0.17	acetate, propionate, valerate, butyrate	Anaerobic sludge	0.05 L H_2/g COD	0.02
Cow dung compost	Pretreated corn stalk	0.13 L H_2/g corn stalk	1.73	acetate, butyrate, propionate, ethanol	Cow dung compost	0.87 L H_2/g COD	4.52
Anaerobic digestion sludge	Cheese whey	0.12 L H_2/g COD	0.093	ethanol, butyrate, acetate, succinate	Anaerobic sediment	0.72 L H_2/g COD	0.023

HPR, Hydrogen production rate

2.6 Valorisation of brewery residues

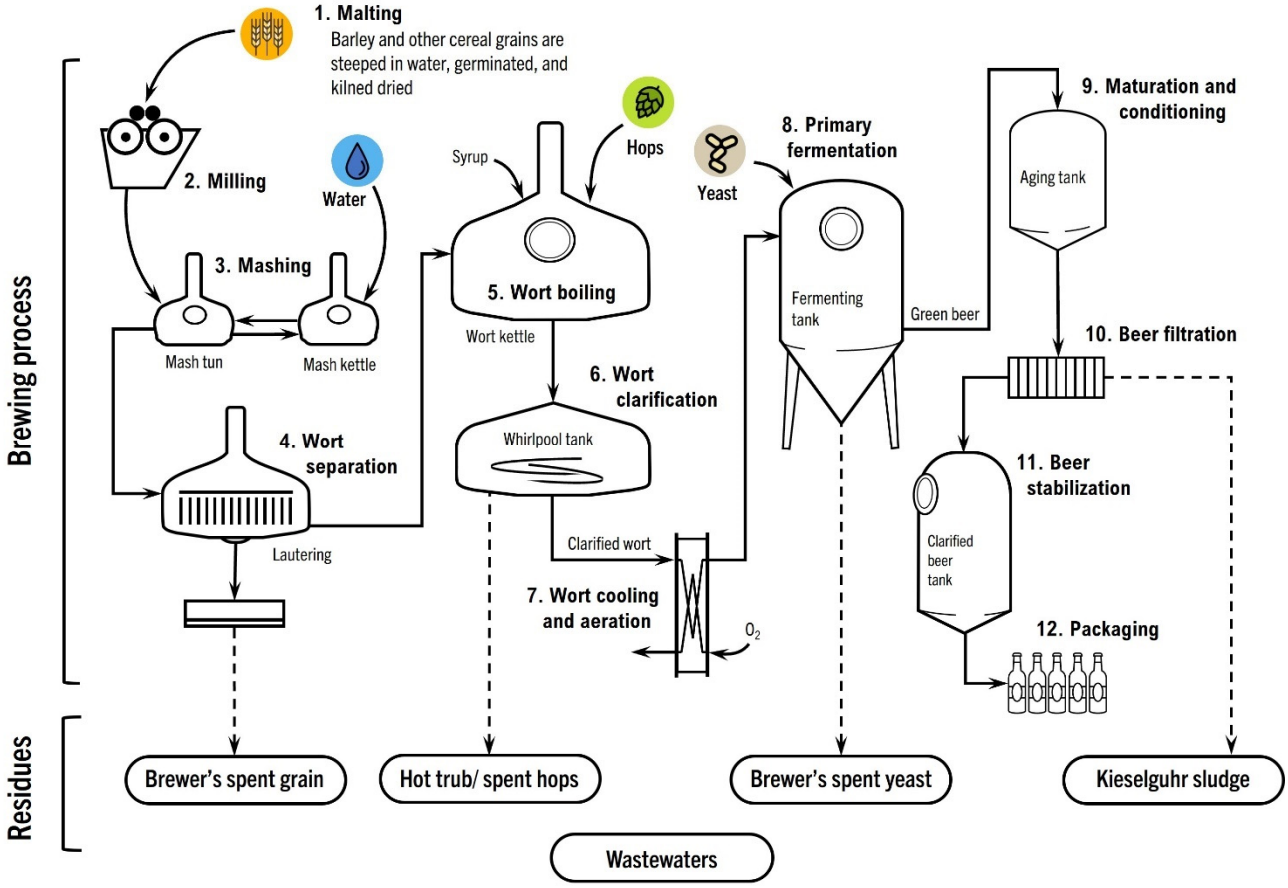

Figure 2.8. *Brewing process with its residues (own figure).*

Beer is the most popular alcoholic beverage worldwide, despite the decline in its consumption in the last decades[170]. The global significance of the brewing industry is reflected in its market size, ~744 billion USD in 2020[171]; and in its impact on the economy with 1 in every 110 jobs in the world related directly or indirectly to the beer sector[172]. Notwithstanding the commercial relevance, the environmental footprint of the brewing process is also of considerable significance due to the large proportion of high-strength organic waste residues generated[173,174]. There are four main solid wastes identified, and the wastewater from the brewing process.

The fundamental ingredients to produce beer are water, malted barley, hops, and yeast. Broadly speaking, the brewing process comprises the stages of 1) malting, 2) milling, 3) mashing, 4) wort separation, 5) wort boiling, 6) wort clarification, 7) wort cooling and aeration, 8) fermentation, 9) maturing, 10) beer filtration, 11) stabilization and 12) packaging[170] (**Figure 2.8**). The most abundant waste is the brewers' spent grain (BSG), which comes at the end of every mash, and it constitutes about 85% of all waste generated during the entire process[175]. This residue is destined mainly as livestock feed, especially for ruminants. BSG can contain 27% protein, 6%–7% fat, crude fibre 15%, and N-free extract 45%[176]. However, managing the sheer volumes is often a problem, so BSG ends up being disposed of in landfills[176]. Then, there is the spent yeast (BSY), which is collected by sedimentation from the fermenters. It is mostly comprised of water (85%–90%), and it represents 10%–15% of the total brewery waste[174]. The yeast (from the *Saccharomyces* genera), can be reused, although only up to a maximum of six times[177], after that, the surplus yeast is often disposed directly to the sewage system[178]. The hot trub is a precipitate coming from the wort boiling process. With a high content of water (80%–90%), the dry matter content consists predominantly of complexes formed from the coagulation of high molecular weight proteins and polyphenols from the wort, and it can contain a high sugar content (up to 20%)[177]. Another important solid residue is the kieselguhr sludge, containing the diatomaceous earths used to clarify the beer. This is a waste with considerable disposal costs, and while there are methods to regenerate recovered diatomaceous earths, they never substitute the filtration quality of fresh ones[173], hence, kieselguhr sludge is often separated, neutralized with lime, and disposed of in landfills[176]. Finally, there is wastewater. The production of beer is a very water-intensive process. The water to beer volume ratio is estimated between 5–15, from which roughly 70% of the water supply is discharged; that is a wastewater to beer volume ratio of 3–10[173,179]. Moreover, these residues typically contain an organic load of 11–13 g/L soluble COD[180], although it can be as high as 200 g/L[181]. In general, BWW are pre-treated onsite prior to discharge to the sewer system. Anaerobic digestion is the most common method applied to manage brewery sludge and wastewaters[179,182].

Table 2.8. Physicochemical characteristics of brewery wastewater[183,184]

Parameter	Value
pH	3.0 – 12.0
Temperature (°C)	18 – 40
COD (mg/L)	2,000 – 32,500
BOD (mg/L)	1,200 – 19,500
BOD/COD ratio	1.67
Total Kjeldahl N (mg/L)	25 – 450
$N\text{-}NH_4$ (mg/L)	5.0 – 21.6
PO_4 (mg/L)	<1 – 216
TS (mg/L)	5,100 – 8,750
TSS (mg/L)	620 – 3,000
VSS (mg/L)	380 – 4,800

Given their composition, BSG and BSY are exploited in a myriad of applications. As lignocellulosic biomass, BSG contains a considerable amount of sugars embedded in the complex matrix of lignin, hemicellulose and cellulose; almost 45% of the dry weight of BSG is conformed by simple sugars, predominately glucose and xylose, among many others[185]. Proteins for human consumption are isolated from BSG through diverse physicochemical methodologies, while bioactive peptides are generally obtained by enzymatic hydrolysis[186]. Additionally, BSG is an inexpensive raw material rich in phenolic compounds, mainly ferulic, vanillic, syringic and coumaric acids, and other common flavonoids derived from the flavan-3-ol skeleton (*e.g.*, catechin)[187]. These compounds are highly appreciated for their antioxidant activity and normally are extracted from the BGS through various conventional chemical methods[188]. The BSY is also an interesting substrate. The high protein content (45%–60% dw), of which about 40% are essential amino acids, in addition to the high level of non-soluble polysaccharides (85% of total carbohydrates), make BSY a highly appreciated substrate [189]. As with BSG, the main destination of surplus yeast is as livestock feed[178], although it can also find commercial applications in the food industry, as a flavour enhancer[190], as a supplement for human consumption, and inexpensive nitrogen source for several biotechnological processes[191].

Although BSG and BSY attract researchers' attention the most, brewery wastewaters (BWW) are an interesting substrate too. The composition of BWW, consisting mainly of sugars, soluble starch, ethanol, and volatile fatty acids[192,193], makes them an attractive, suitable fermentable substrate for the activity of a wide spectrum of microorganisms as well. There is the use of MFCs fed with BWW, which has been extensively studied in the last decade[183,194], so as the growth of microalgae for different purposes (lipids in *Chlorella vulgaris* as feedstock for biofuels production[195,196], and proteins extraction from *Spirulina platensis*[197]). Moreover, similarly to the case of the lignocellulosic materials like BSG, wood-decaying fungi have been studied in submerged fermentation (SmF) of different effluents, including BWW[198,199].

Table 2.9. Characteristics of wastewater generated during each step of the brewing process[200]

Source	Operation	Characteristics
Mash tun	Rinsing	Cellulose, sugars, amino acids ~3,000 ppm BOD
Lauter tun	Rinsing	Cellulose, sugars, spent grain SS ~3,000 ppm, BOD ~10,000 ppm
Spent grain	Last running and washing	Cellulose, nitrogenous material. Extremely high in SS (~30,000 ppm). Up to 100,000 ppm BOD
Boil kettle	Dewatering	Nitrogenous residue. BOD ~2,000 ppm
Whirlpool	Rinsing spent hops and hot trub	Proteins, sludge, and wort. High in SS (~35,000 ppm). BOD ~85,000 ppm
Fermenters	Rinsing	Yeast SS ~6,000 ppm, BOD up to 100,000 ppm
Storage tanks	Rinsing	Beer, yeast, protein. High SS (~4,000 ppm). BOD ~80,000 ppm
Filtration	Cleaning, start-up, end of filtration, leaks during filtration	Excessive SS (up to 60,000 ppm). Beer, yeast, proteins. BOD up to 135,000 ppm
Beer spills	Waste, flushing, etc.	1,000 ppm BOD
Bottle washer	Discharges from washer operation	High pH due to the chemical used. Also, high SS and BOD, especially thru a load of paper pulp.
Keg washer	Discharges from washing operations	Low in SS (~400 ppm). Higher BOD.
Miscellaneous	Discharged cleaning and sanitation materials	Relatively low on SS and BOD. The problem is pH due to chemicals being used.

2.6.1 Brewery wastewaters as potential substrate for white-rot fungi

Three groups of wood-decaying fungi (also known as xylophagous), are recognized from the type of decomposition they exhibit in woody materials: brown, soft, and white rots[201]. The case of white-rot fungi (WRF) is particularly noteworthy. These are mostly basidiomycetes well known for degrading and mineralizing lignin into CO_2 and H_2O more efficiently than any other microorganism[202]. Furthermore, besides lignin, the extracellular enzymatic system of these fungi is capable of oxidizing a wide variety of structures (halogenated and non-halogenated aromatic compounds as well as some non-aromatic organopollutants)[203]. In WRF, laccases (*Lac*), and the lignin (*LiP*) and manganese (*MnP*) peroxidases, are the three main secreted enzymes involved in lignin mineralization by the action of their non-specific, yet broad spectrum catalysis of dihydroxy and diamino aromatic compounds oxidation[204]. These ligninolytic enzymes are known to cleave the carbon–carbon and carbon–oxygen bonds of lignin, regardless of the chiral conformations of the molecule, generating radicals which may serve as secondary oxidants, acting as mediators away from the enzymatic active sites[203].

Despite the extensive research over the decades, the mediated decomposition of lignin by WRF is still a subject of discussion, as it is not clear exactly how the ligninolytic enzyme complex acts over every different structure due to its unspecific nature[205]. In *Lac*-mediated reactions, there is a tendency for re-polymerization of free aryl radicals, whereas *LiP* and *MnP* cleaving activities are affected by several conditions (*e.g.*, the limited lifespan of redox mediators, the necessity of H_2O_2, which presence is also dependent on environmental conditions, etc.)[204]. Moreover, some WRF secrete all three ligninolytic enzymes while LiP, for example, is expressed only by 40% of the species[206]. Although lignin can be fully degraded, WRF cannot utilize it as a source of energy for growth, but the substrates embedded in the ligneous material instead; sugars from the cellulose and hemicellulose, or other carbon sources[203].

Hence, many other enzymes are also involved indirectly as auxiliaries during the lignin decomposition process (*e.g.*, glucose and aryl alcohol oxidase, glucanases, xylanases, cellobiose dehydrogenases, *inter alia*)[207,208]. Among the most studied WRFs, there are the

Figure 2.9. *Oyster mushroom* (Pleurotus ostreatus)*, by Michel Langeveld, licensed under (CC-BY-SA 4.0) Retrieved from https://www.inaturalist.org/photos/173512182*

well-known genera of *Trametes* spp. and *Bjerkandera* spp.; species such as *Pycnoporus cinnabarinus, Phanerochaete chrysosporium*, and *Ganoderma lucidum*; as well as the edible mushrooms *Flammulina velutipes* (enoki mushroom), *Lentinula edodes* (shiitake mushroom), and the genus *Pleurotus* spp., which includes the edible common oyster mushroom (**Figure 2.9**), and king oyster mushroom[209].

One of the attractive features of WRFs is their ability to degrade xenobiotic pollutants, like simple aromatic compounds, polychlorinated biphenyls, and polyaromatic hydrocarbons[204]. Among the studied applications there is the bioremediation of pulp and paper mill sludge[210], decolouration of dyes in industry effluents[211,212], olive mill residues[213,214]; and other wastes similar to BWW, like those from the ethanol industry and distillery wastewaters[215,216]. In the case of BWW, the type and concentration of organopollutants will depend on the brewing process and which stage of it they come from. Furfuryl alcohol, for instance, is generated mostly during the wort boiling, and significantly more in darker beers than in lagers[217]. Furan and furfural-derived

molecules are Maillard reaction end-products, mainly formed when sugars and amino acids from the cellulosic material in the BSG are subjected to heating. They are known to inhibit the central carbon metabolism of microorganisms, in fact, the presence of these compounds demands more resistant strains in the production of ethanol from lignocellulosic materials[218,219].

Other Maillard condensation products are melanoidins, partly responsible for the colour and taste of beverages like beer and coffee[220]. Due to the randomness of sugar-amine reactions in Maillard condensation, the structure of melanoidins is hard to predict, although there are some generally accepted skeleton structures proposed in the literature[221]. The release of melanoidins in wastewaters, however, given their structural complexity, poses a potential threat to ecosystems by the increased load of recalcitrant organic material, especially to natural water bodies[222]. They can inhibit microbial growth in biological treatment processes[223]. Physical treatments to remove melanoidins include coagulation, flocculation, adsorption, membrane processes, electrocoagulation and oxidation[224], nonetheless, the problem of disposal persists, as the melanoidins are not destroyed. According to some researchers, notwithstanding the high COD removal yields, conventional aerobic-anaerobic treatment can reduce up to 6%–7% of melanoidins; consequently, the brown colour remains practically untouched after the treatment[225]. Besides chemical degradation and adsorption methods, some acetogenic bacteria can reduce melanoidins in waste streams by up to 76% under optimal conditions[226]. However, the WRF *P. chrysosporium* and *T. versicolor* can degrade melanoidins above 80%[224].

Fungal treatment of residues like BWW is attractive for several reasons. Besides the aforementioned enzymatic system meant to break down complex lignin-like molecules such as melanoidins, there is the adsorption of pollutants by the mycelium and exopolysaccharides produced. Some studies on residues like BWW indicate that ~17% of the brown colour of molasses and distillery effluents is removed by adsorption of the mycelium[222]. Moreover, the fungal strains generate by-products that can be utilized in animal feedstuff[224] and several other potential applications. Among the by-products of

commercial interest, the predominant application exploited is related to ligninolytic enzyme production with the aim, chiefly, to bioremediate diverse coloured effluents[227,228]. Although not as extensively reported as the enzymatic production, there are other interesting compounds produced as well, such as organic alcohols, like coniferyl alcohol from ferulic acid[229]; vanillin[230] and benzaldehyde (almond scent)[231]; bioactive compounds and organic acids like auxin (indole acetic acid), with antioxidant activities[232]; and functional peptides for medical purposes[233]. And in recent years, interest in biomaterials from fungal mycelium has blossomed.

Although the natural choice to grow WRFs is in solid state fermentation (SSF), there are other advantages of fungal growth in submerged fermentation in this field. While the availability of oxygen is not a limitation in SSF, important parameters like pH and temperature are easier to control in SmF, as the purification of metabolites produced by the fungi during the process[234]. The intrinsic conditions in SmF allow the production of pure mycelium, while in SSF, the biomaterial obtained is a rigid composite made out of the mycelium and the lignocellulosic matrix that supported the fungal growth. These lignocellulosic composites have gained attention as an alternative to expanded polystyrene packaging, while pure mycelium exhibits more flexible properties with a wider range of applications: from skincare and meat alternative products to substitutes for conventional leather and textiles. In the case of the latter, WRF of the genera *Ganoderma* spp., *Trametes* spp., *Pleurotus* spp., and *Pycnoporus* spp., have been used to produce what it is called 'myco-leather'[235]. In this regard, BWW offers an inexpensive, suitable choice of substrate for WRF biomass production, as has been reported recently for the growth of the edible species *Pleurotus ostreatus* and *Lentinula edodes*, so as *Trametes versicolor*[198].

2.6.2 Role of white-rot fungi to produce biofuels from brewery residues.

Brewer's spent grain and yeast have been studied for methane production in anaerobic digestion, albeit with modest yields, between 70–105 mL CH_4 per gram of COD consumed[175,236]. Low yields of biofuels from ligneous biomass are associated with the recalcitrancy of lignocellulose structure against microbial fermentation processes[237].

To overcome these hindrances, BSG must undergo various treatments, to obtain the fermentable sugars embedded in the ligneous structure and reduce the impact of the recalcitrant lignin-derived compounds. These procedures can be physical treatment, chemical or enzymatic hydrolysis, or all of them combined[237]. There is another biological strategy, which is the use of wood-decaying fungi. As seen in **Figure 2.10**, there are four strategies to incorporate white-rot fungal treatment of lignocellulosic biomass to produce biofuels. The role of WRF goes from an auxiliary step, as part of an integrated system using physicochemical pre-treatments, enzymatic saccharification and hydrolysis; to the central role to carry out the entire delignifying/saccharifying treatments simultaneously, while co-fermenting the biomass along with other microorganisms to produce butanol, ethanol, and also hydrogen[237,238].

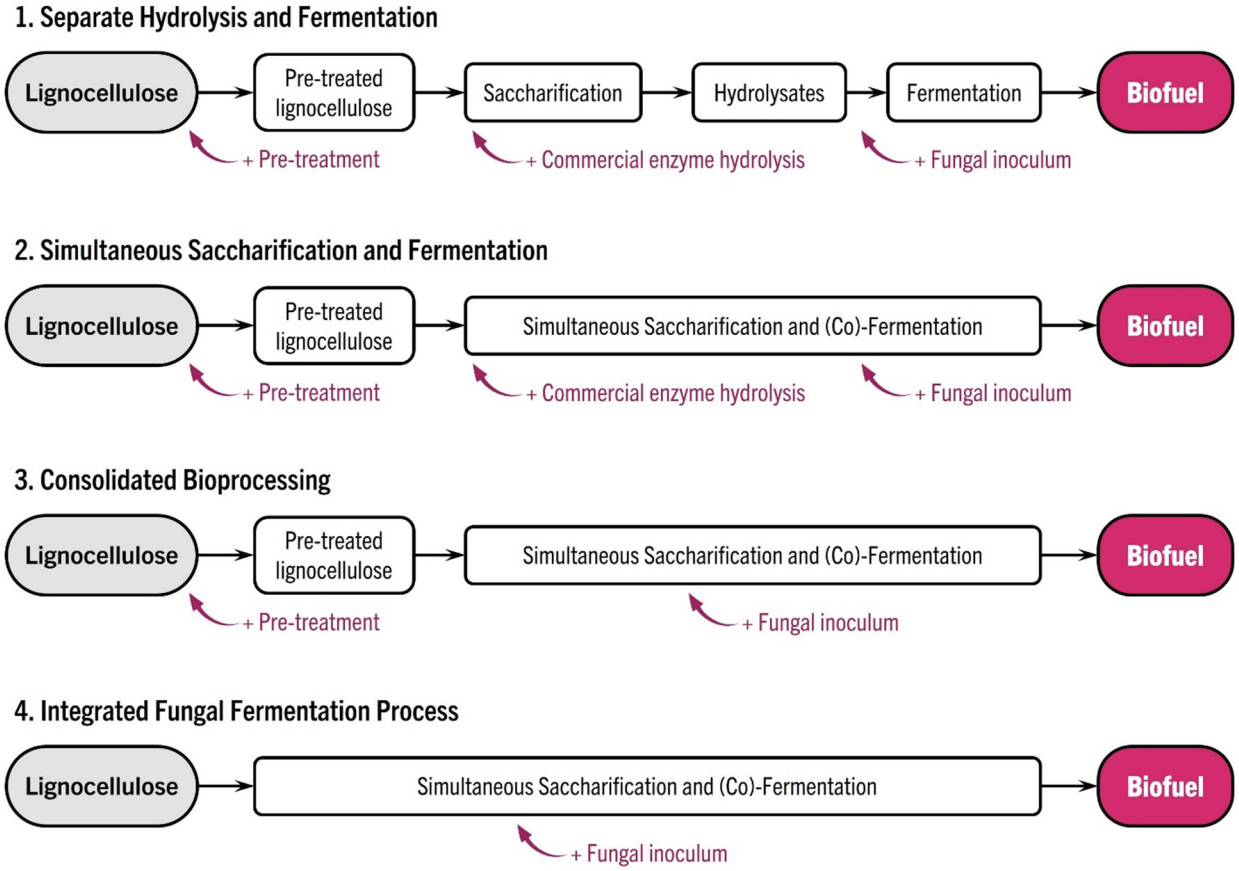

Figure 2.10. *The schematic diagram of biological processes for biofuel production employing white-rot fungi. Modified from Tri* et al.,[237]

Cellulose, composed of β-(1→4) D-glucopyranose chains, is the most abundant material in the biosphere, followed by lignin[239]. Hemicellulose comprises 24%–40% of woody materials[206]. It is a more complex biopolymer made of linear polysaccharides composed of different sugars (i.e., xylose, galactose, mannose, and arabinose)[239]. The function of hemicellulose is to bind cellulose and lignin together. Lignin is a highly branched three-dimensional heteropolymer comprised of intertwined phenolic and non-phenolic compounds, arranged in a random manner which confers rigidity to the plants' stems but also makes it one of the most recalcitrant molecules[240,241]. Therefore, to obtain the carbohydrates from cellulose and hemicellulose and exploit them as raw materials for biofuel production, lignin must be destroyed first. To release as many sugars as possible, lignocellulosic biomass undergoes various treatments, the most common are physicochemical methods (steam-explosion, hydrothermal processes, ammonia fibre explosion, alkali hydrolysis, organosolvents), which require high energy, or expensive reactants with toxic waste disposals, besides destroying some fermentable carbohydrates in the process[206]. Enzymatic hydrolysis is very selective and efficient, although the cost of the enzymes is prohibitive in large-scale applications, hence the method is often combined with other physicochemical techniques[188]. Among several microorganisms, WRFs are an attractive option for bio-delignifying ligneous materials before being processed for biofuel production. Thus, there is ethanol being produced after wheat straw pre-treated with *Pleurotus eryngii* and *Irpex lacteus*[242], or even direct ethanol production from different carbon sources by *Trametes hirsuta*[243]. Biogas production was doubled after fungal pre-treatment of wheat straw with *Pleurotus florida*[244]. Methane and hydrogen production from pre-treated beech and cedar wood with different WRF strains was markedly improved; the pre-treatment with *Phanerochaete sordida* YK-624 being suitable for methane, while *P. chrysosporium*-based treatment showed better results in hydrogen production by the pure strain *Clostridium thermocellum*[245]. Other studies reported enhanced hydrogen production after the fungal treatment of wheat straw[246], and from the decomposition of volatile bitumen coal in SmF[247], both with the WRF *P. chrysosporium*.

2.6.3 Brewery residues as substrate for energy conversion biotechnologies

As seen above, what makes BWW an interesting substrate is the content of sugars, proteins, and other nutrients for the growth of a wide variety of microbial species. However, recalcitrant compounds derived from lignin can be found in these residues, which are known to have inhibitory effects over bacteria[237,248,249], which hinders the application of BWW as a substrate to convert their chemically stored energy into biofuels and secondary energy carriers like hydrogen. Some of these toxic substances occur naturally in the raw materials used to produce beer, like the lignin-derived aromatic molecules, and humic and fulvic acids[250,251]. Other, as have been mentioned above, are generated during the brewing process, such as simple and highly branched Maillard condensation products (i.e., melanoidins, furans, etc.). However, WRF have the advantage over other microorganisms to thrive in toxic environments, under their ability to degrade xenobiotic compounds and complex organic matter derived from lignin better than other organisms. BWW, although not a solid waste, is characterized by the high content of solids in suspension (**Table 2.9**), which comes from residual lignocellulosic biomass of the cereals and hops processed. Hence, according to the model presented by Tri *et al*.[237] in **Figure 2.10**, WRF can be part of a 4th-level integrated fermentation process, since BWW are already a residue coming from a pre-treatment, delignifying and saccharification of lignocellulosic biomass (that is the mash, lauter and boiling of grains and hops). However, little has been reported in this vein, although the use of similar residues can provide the sought insight regarding BWW as substrate for energy conversion technologies.

Such is the case of molasses and distillery wastewater. Fungal treatment of these wastes is mainly focused on colour degradation and purifying the effluent under aerobic conditions[252–254], although a few research works have ventured into the study of fungal treatment as a preliminary step to energy conversion from these wastes, with different degrees of success. Strong[255] concluded that fungal treatment of winery wastewaters before methanogenic digestion (AD) was not beneficial in terms of COD removal, hence economically not feasible in that sense. Contrarily, as an example of combining METs

with a fungal pre-treatment step, there is the report of MFCs attaining a final COD degradation of 99% after the fungal pre-treatment of distillery wastewaters. The maximum power output exhibited was 2.6 W/m^3 (~130 mW/m^2) from the organic load of 1.5 kg COD/m^3 of vinasses[256]. Notwithstanding, the use of WRF as part of biofuel production systems is normally reported in solid-state fermentation of lignocellulosic biomass, as has been discussed above.

Brewery wastewaters are customarily treated using anaerobic digestion producing methane, and microbial electrochemical technologies have been widely explored, although individually. Nevertheless, little has been documented in the case of dark fermentation, let alone DF/METs combined systems to produce hydrogen from these residues. In this regard, a recent review paper of bio-hydrogen production from brewery industrial wastewater[257] describes methane production, glucose, sucrose, and lactose as substrates to produce hydrogen, even about Hippocrates and healthy food; in short, everything but the actual production of hydrogen from brewery wastewaters… In the same manner, the documented studies using similar residues can provide a snapshot of the current state of DF combined with METs to produce hydrogen and electricity.

Dark fermented distillery wastewaters with COD content ranging from 3.9–24.5 g/L exhibited cumulative volumes of 86 to 305 mL H_2/L substrate, and the COD was reduced between 27.4%–44.3%. The maximum hydrogen yield was obtained with the highest COD concentration fed removal efficiency of 35.7%[96]. In another study, the maximum hydrogen production from dark fermented sugar cane molasses was 276 mL H_2/g COD removed. The DF effluent was used to feed MFCs, attaining a power output of 3.02 W/m^3 and a final COD reduction of 88%[258]. Furthermore, a combined system DF/MEC-MFC not only demonstrated to greatly improve H_2 production compared to DF alone (340.5 mL H_2/g cellulose, 41% higher vs DF alone) but also that MECs can be powered by the MFCs' power output, obtained simultaneously[259].

2.7 Conclusions

Dark fermentation is an interesting hydrogen-producing biotechnology without the need for sunlight, and it is a robust process that can be fed with higher organic loads in comparison with photofermentation or biophotolysis. Yet, dark fermentation is constrained by metabolic thermodynamics, and H_2 molar yields are low compared to conventional technologies, which are based on fossil-fuels thermochemical reforming. Although these platforms pose a large environmental footprint, their hydrogen production rates are still unrivalled by dark fermentative hydrogen production rates. Nevertheless, the advantages to DF are the mild operating conditions, and the organic substrates that can be used, including several food and industry wastes; enabling the production of hydrogen while addressing an environmental issue associated with the waste used as substrate. Furthermore, this process can be enhanced by other robust biological technologies. Anaerobic digestion is commonly used as a secondary phase of treatment after DF, but microbial electrochemical technologies hold great potential as well. Microbial fuel cells and microbial electrolysis cells can convert the chemically stored energy in organic substrates by the means of electrochemical reactions catalyzed by bacteria. MECs are novel technologies, which have grown faster in the last decade. Hydrogen can be produced in these devices more efficiently than in conventional water electrolysis, by their intrinsic biological overpotentials, which can reduce more than 50% of the energy required to split water. On the other hand, MFCs are devices that can convert chemically stored energy into electricity while reducing the organic content in several wastes. Combined with DF, these technologies can greatly improve not only hydrogen production rates but also COD removal efficiencies. Furthermore, a wide variety of organic wastes can be employed to feed these combined systems. One of them is brewery wastewater. These residues are intensively generated by the steady, global beer industry. BWW high generation rates pose a huge environmental impact.

These residues are usually biotreated under anaerobic digestion before being disposed. However, BWW biological methane potentials are low. Other strategies have been

widely documented in the field of METs, in particular in MFCs. In the field of bioenergy derived from organic residues, little has been documented in the use of BWW besides methane. On the contrary, similar residues are commonly found in the literature (distillery and molasses wastewater). The composition of BWW is particularly attractive given the high content of fermentable carbonaceous substances and nutrients to sustain microbial growth in processes to produce biofuels, or to obtain secondary energy carriers, like hydrogen and electricity. Nevertheless, these residues also contain inhibitory substances for a wide variety of microorganisms, which can limit their potential. In this regard, white-rot fungi can be part of a BWW co-fermentation process for hydrogen production, since these filamentous basidiomycetes are able to degrade lignin-like xenobiotic compounds in liquid wastes, thriving in media rich in lignin-derived substances, like BWW. In general, WRF-based treatment, as well as DF and METs technologies fed with BWW-like substrates, are strategies studied separately, or as part of other systems. The combination of all treatments, despite their well-documented potential, is barely studied. Regarding the production processes to obtain different biofuels and in particular, environmentally friendly energy carriers like hydrogen, the combination of these biotechnologies is attractive to overcome the intrinsic limitations that each technique exhibits individually. The development of these biotechnologies combined could represent a solid alternative among others in search of robust sustainable processes to bridge the gap between the conventional hydrogen production technologies, thus contributing their bit to turning the table on the global humanitarian crisis posed by the life-threatening climate change of our times.

References

1 Gopinath, G. *The Great Lockdown: Worst Economic Downturn Since the Great Depression*. Available from: https://blogs.imf.org/2020/04/14/the-great-lockdown-worst-economic-downturn-since-the-great-depression/ (accessed Sep 24, 2020).

2 OECD. COVID−19 and the Low-Carbon Transition Impacts and Possible Policy Responses. **2020**, No. June.

3 Botzen, W. J. W.; Deschenes, O.; Sanders, M. The Economic Impacts of Natural Disasters: A Review of Models and Empirical Studies. *Rev. Environ. Econ. Policy* **2019**, *13* (2), 167−188.

4 Wahlstrom, M.; Guha-Sapir, D. *The Human Cost of Weather Related Disasters*; **2015**.

5 Tol, R. S. J. The Economic Impacts of Climate Change. *Rev. Environ. Econ. Policy* **2018**, *12* (1), 4−25.

6 *Displacement in a Changing Climate*; Geneva, **2021**.

7 IRENA. *Global Renewables Outlook: Energy Transformation 2050*; **2020**.

8 Le Quéré, C.; Jackson, R. B.; Jones, M. W.; Smith, A. J. P.; Abernethy, S.; Andrew, R. M.; De-Gol, A. J.; Willis, D. R.; Shan, Y.; Canadell, J. G.; Friedlingstein, P.; Creutzig, F.; Peters, G. P. Temporary Reduction in Daily Global CO2 Emissions during the COVID-19 Forced Confinement. *Nat. Clim. Chang.* **2020**, *10* (7), 647−653.

9 IEA. *Global Energy Review 2020: The Impacts of the Covid-19 Crisis on Global Energy Demand and CO2 Emissions*; **2020**.

10 UNEP. *Record global carbon dioxide concentrations despite COVID-19 crisis*. Available from: https://www.unenvironment.org/news-and-stories/story/record-global-carbon-dioxide-concentrations-despite-covid-19-crisis. (accessed Sep 24, 2020)

11 Hepburn, C.; O'Callaghan, B.; Stern, N.; Stiglitz, J.; Zenghelis, D. Will COVID-19 Fiscal Recovery Packages Accelerate or Retard Progress on Climate Change? *Oxford Rev. Econ. Policy* **2020**, *36* (20), 1−48.

12 Kurmayer, N. J. *EU unveils €300 million plan to fund hydrogen research*. Available from: https://www.euractiv.com/section/energy/news/eu-unveils-e300-million-hydrogen-research-priorities/ (accessed May 15, 2022).

13 Naujokaitytė, G. *Hydrogen to get a boost as EU looks to secure energy independence*. Available from: https://sciencebusiness.net/climate-news/news/hydrogen-get-boost-eu-looks-secure-energy-independence (accessed Mar 23, 2022).

14 France 2030 : présentation du plan. Avalable from: https://www.youtube.com/watch?v=v9mQlu-EQ-I (accessed May 23, 2022).

15 UK government launches plan for a world-leading hydrogen economy Available from: https://www.gov.uk/government/news/uk-government-launches-plan-for-a-world-leading-hydrogen-economy (accessed Mar 23, 2022).

16 Canada Launches Hydrogen Strategy Steering Committee. Available: https://www.canada.ca/en/natural-resources-canada/news/2021/04/canada-launches-hydrogen-strategy-steering-committee.html (accessed May 23, 2022).

17 Al-Baghdadi, M. Green Hydrogen and the Beginning of a New Energy Era. *Int. J. Energy Environ.* **2021**, *12* (1), 1−18.

18 Nasa (n.d.). *Hydrogen and Fuel Cells*. Available from: https://www.nasa.gov/content/space-applications-of-hydrogen-and-fuel-cells (accessed Jun 29, 2021).

19 De Miranda, P. E. V. *Hydrogen Energy: Sustainable and Perennial*; **2018**.

20 Mohamedali, M.; Henni, A.; Ibrahim, H. Hydrogen Production from Oxygenated Hydrocarbons: Review of Catalyst Development, Reaction Mechanism and Reactor Modeling. In *Hydrogen Production Technologies*; Sankir, M., Sankir, N. D., Eds.; Scrivener Publishing LLC, **2017**; pp 3–76.

21 Manzardo, A.; Ren, J.; Toniolo, S.; Scipioni, A. *Critical Factors and Cause-Effect Analysis for Enhancing the Sustainability of Hydrogen Supply Chain*; Elsevier Ltd, **2017**.

22 American Chemical Society (n.d.). *Hydrogen.* Available from: https://www.acs.org/content/acs/en/molecule-of-the-week/archive/h/hydrogen.html (accessed Sep 8, 2020).

23 Zohuri, B. The Chemical Element Hydrogen. In *Hydrogen Energy*, **2019**; pp 1–35.

24 IEA. *The Future of Hydrogen*; **2019**. Available from: https://doi.org/10.1016/S1464-2859(12)70027-5.

25 Dell, R. M.; Rand, D. A. J. Hydrogen Energy. In *Clean Energy*; **2004**; pp 198–241.

26 Robb, D. PowerGen EU Shifts Emphasis from Fossil Fuels to Renewables. *Turbomachinery International: Can Natural Gas Generation Survive?*. **2020**, pp 24–27.

27 Møller, K. T.; Jensen, T. R.; Akiba, E.; Li, H. wen. Hydrogen - A Sustainable Energy Carrier. *Prog. Nat. Sci. Mater. Int.* **2017**, *27* (1), 34–40.

28 Capocelli, M.; De Falco, M. Enriched Methane: A Ready Solution for the Transition Towards the Hydrogen Economy. In *Enriched Methane: The First Step Towards the Hydrogen Economy*; De Falco, M., Basile, A., Eds.; Springer Cham Heidelberg New York Dordrecht London, 2016; pp 1–21.

29 Middha, P. Explosion Risks of Hydrogen/Methane Blends. In *Enriched Methane: The First Step Towards the Hydrogen Economy*; De Falco, M., Basile, A., Eds.; **2016**; pp 235–257.

30 He, X.; Shu, B.; Nascimento, D.; Moshammer, K.; Costa, M.; Fernandes, R. X. Auto-Ignition Kinetics of Ammonia and Ammonia/Hydrogen Mixtures at Intermediate Temperatures and High Pressures. *Combust. Flame* **2019**, *206*, 189–200.

31 Kanna, I. V.; Paturu, P. A Study of Hydrogen as an Alternative Fuel. *Int. J. Ambient Energy* **2020**, *41* (12), 1433–1436.

32 Leachman, J. *The colors of hydrogen* Available from: https://hydrogen.wsu.edu/2015/12/22/the-colors-of-hydrogen/ (accessed Jun 18, 2021).

33 Deign, J. So, *What Exactly Is Green Hydrogen?* Available from: https://www.world-energy.org/article/10310.html (accessed Jun 18, 2021).

34 Grigoriev, S. A.; Fateev, V. N. Hydrogen Production by Water Electrolysis. In *Hydrogen Production Technologies*; Sankir, M., Sankir, N. D., Eds.; **2017**; pp 231–276.

35 Lubitz, W.; Tumas, B. Hydrogen : An Overview. *Chem. Rev.* **2007**, *107*, 3900–3903.

36 Demirbas, A. Biohydrogen. In *Biohydrogen: For Future Engine Fuel Demands*, **2009**; pp 163–219.

37 Dimitriou, P.; Tsujimura, T. A Review of Hydrogen as a Compression Ignition Engine Fuel. *Int. J. Hydrogen Energy* **2017**, *42* (38), 24470–24486.

38 Xu, D.; Dong, L.; Ren, J. Introduction of Hydrogen Routines. *Hydrog. Econ. Supply Chain. Life Cycle Anal. Energy Transit. Sustain.* **2017**, 35–54.

39 Demirbas, A. Introduction. In *Biohydrogen*; Springer-Verlag London Limited, **2009**; pp 1–42.

40 Das, D.; Khanna, N.; Dasgupta, C. N. *Biohydrogen Production*; **2014**.

41 He, L.; Yang, J.; Chen, D. Hydrogen from Biomass: Advances in Thermochemical Processes. In *Renewable Hydrogen Technologies: Production, Purification, Storage, Applications and Safety*; Gandía, L. M.,

Arzamendi, G., Diéguez, P. M., Eds.; **2013**; pp 111–133.

42 Kaur, R.; Gera, P.; Jha, M. K.; Bhaskar, T. *Thermochemical Route for Biohydrogen Production*; **2020**.

43 Martínez-Merino, V.; Gil, M. J.; Cornejo, A. Biomass Sources for Hydrogen Production. *Renew. Hydrog. Technol. Prod. Purification, Storage, Appl. Saf.* **2013**, 87–110.

44 Ghirardi, M. L.; King, P. W.; Mulder, D. W.; Eckert, C.; Dubini, A.; Maness, P.-C.; Yu, J. Microbial BioEnergy: Hydrogen Production. In *Microbial BioEnergy: Hydrogen Production*; Zannoni, D., De Philippis, R., Eds.; Springer Dordrecht Heidelberg New York London, **2014**; pp 101–135.

45 Das, D.; Khanna, N.; Dasgupta, C. N. Hydrogen Production Processes. In *Biohydrogen Production*; Veziroğlu, T. N., Ed.; Taylor & Francis Group, **2014**; pp 55–109.

46 Martínez-Merino, V.; Gil, M. J.; Cornejo, A. Biological Hydrogen Production. In *Renewable Hydrogen Technologies: Production, Purification, Storage, Applications and Safety*; Gandía, L. M., Arzamendi, G., Diéguez, P. M., Eds.; Elsevier B.V., **2013**; pp 171–199.

47 Das, D.; Khanna, N.; Dasgupta, C. N. Hydrogen Production Processes. In *Biohydrogen Production*; Veziroğlu, T. N., Ed.; Taylor & Francis Group, **2014**; pp 55–109.

48 Nagarajan, D.; Dong, C. Di; Chen, C. Y.; Lee, D. J.; Chang, J. S. Biohydrogen Production from Microalgae—Major Bottlenecks and Future Research Perspectives. *Biotechnol. J.* **2021**, *16* (5), 1–12.

49 Lam, M. K.; Chun, A.; Loy, M.; Yusup, S.; Lee, K. T. *Biohydrogen Production From Algae*; Elsevier B.V., **2019**.

50 Levin, D. B.; Pitt, L.; Love, M. Biohydrogen Production: Prospects and Limitations to Practical Application. *Int. J. Hydrogen Energy* **2004**, *29* (2).

51 Balat, M. Production of Hydrogen via Biological Processes. *Energy Sources, Part A Recover. Util. Environ. Eff.* **2009**, *31* (20), 1802–1812.

52 Hallenbeck, P. C. Bioenergy from Microorganisms: An Overview. In *Microbial BioEnergy: Hydrogen Production*; 2014; Vol. 38, pp 3–21.

53 Higuchi-Takeuchi, M.; Numata, K. Marine Purple Photosynthetic Bacteria as Sustainable Microbial Production Hosts. *Front. Bioeng. Biotechnol.* **2019**, *7* (October), 1–8.

54 Cavinato, C.; Bolzonella, D.; Pavan, P.; Cecchi, F. Two-Phase Anaerobic Digestion of Food Wastes for Hydrogen and Methane Production. In *Enriched Methane: The First Step Towards the Hydrogen Economy*; De Falco, M., Basile, A., Eds.; Springer Cham Heidelberg New York Dordrecht London, 2016; pp 75–90.

55 Redwood, M. D.; Paterson-Beedle, M.; MacAskie, L. E. Integrating Dark and Light Bio-Hydrogen Production Strategies: Towards the Hydrogen Economy. *Rev. Environ. Sci. Biotechnol.* **2009**, *8* (2), 149–185.

56 Khanal, S. K. Biohydrogen Production: Fundamentals, Challenges, and Operation Strategies for Enhanced Yield. In *Anaerobic biotechnology for bioenergy production: principles and applications*; Khanal, S. K., Ed.; Wiley-Blackwell, **2008**; pp 189–219.

57 Wang, J.; Yin, Y. Fermentative Hydrogen Production Using Various Biomass-Based Materials as Feedstock. **2018**, *92* (March), 284–306.

58 Krupp, M. *Biohydrogen Production from Organic Waste and Wastewater by Dark Fermentation - a Promising Module for Renewable Energy Production*; Shaker Verlag: Aachen, **2007**.

59 Cotterill, S.; Heidrich, E.; Curtis, T. *Microbial Electrolysis Cells for Hydrogen Production*; Elsevier Ltd., **2016**.

60 Escapa, A.; Mateos, R.; Martínez, E. J.; Blanes, J. Microbial Electrolysis Cells: An Emerging Technology for Wastewater Treatment and Energy Recovery. from Laboratory to Pilot Plant and Beyond. *Renew. Sustain.*

Energy Rev. **2016**, *55*, 942–956.

61 Tapia-Venegas, E.; Ramirez-Morales, J. E.; Silva-Illanes, F.; Toledo-Alarcón, J.; Paillet, F.; Escudie, R.; Lay, C. H.; Chu, C. Y.; Leu, H. J.; Marone, A.; Lin, C. Y.; Kim, D. H.; Trably, E.; Ruiz-Filippi, G. Biohydrogen Production by Dark Fermentation: Scaling-up and Technologies Integration for a Sustainable System. *Rev. Environ. Sci. Biotechnol.* **2015**, *14* (4), 761–785.

62 Galera, S.; Ortiz, F. J. G. Life Cycle Assessment of Hydrogen and Power Production by Supercritical Water Reforming of Glycerol. *Energy Convers. Manag.* **2015**, *96*, 637–645.

63 Wang, J.; Yin, Y. Introduction. In *Biohydrogen Production from Organic Wastes*; Wang, J., Yin, Y., Eds.; Springer Nature Singapore Pte Ltd: Singapore, **2017**; pp 1–17.

64 Imam, J.; Singh, P. K.; Shukla, P. Biohydrogen as Biofuel: Future Prospects and Avenues for Improvements. In *Biofuel Technologies: Recent Developments*; Gupta, V. K., Tuohy, M. G., Eds.; Springer Berlin Heidelberg: Berlin, Heidelberg, 2014; pp 301–315.

65 Pullen, T. *Anaerobic Digestion - Making Biogas - Making Energy*; 2015.

66 Archer, D. B.; Kirsop, B. H. The Microbiology and Control of Anaerobic Digestion. In *Anaerobic Digestion: a Waste Treatment Technology*; Wheatley, A., Ed.; Elsevier Science Publishing Co., Inc, **1990**; pp 43–91.

67 Khanal, S. K. *Anaerobic Biotechnology for Bioenergy Production Anaerobic Biotechnology for Bioenergy Production*; **2008**.

68 Khanal, S. K. Microbiology and Biochemistry of Anaerobic Biotechnology. In *Anaerobic biotechnology for bioenergy production: principles and applications*; Khanal, S. K., Ed.; Wiley-Blackwell, **2008**; pp 29–41.

69 Burger, Y.; Schwarz, F. M.; Müller, V. Formate-Driven H2 Production by Whole Cells of Thermoanaerobacter Kivui. *Biotechnol. Biofuels Bioprod.* **2022**, *15* (1), 1–12.

70 Ntaikou, I.; Antonopoulou, G.; Lyberatos, G. Biohydrogen Production from Biomass and Wastes via Dark Fermentation: A Review. *Waste and Biomass Valorization* **2010**, *1* (1), 21–39.

71 Gopalakrishnan, B.; Khanna, N.; Das, D. *Dark-Fermentative Biohydrogen Production*; **2019**.

72 Baeyens, J.; Zhang, H.; Nie, J.; Appels, L.; Dewil, R.; Ansart, R.; Deng, Y. Reviewing the Potential of Bio-Hydrogen Production by Fermentation. *Renew. Sustain. Energy Rev.* **2020**, *131*.

73 Bundhoo, M. A. Z.; Mohee, R. Inhibition of Dark Fermentative Bio-Hydrogen Production: A Review. *Int. J. Hydrogen Energy* **2016**, *41* (16), 6713–6733.

74 Chen, Y.; Yin, Y.; Wang, J. Influence of Butyrate on Fermentative Hydrogen Production and Microbial Community Analysis. *Int. J. Hydrogen Energy* **2021**, *46* (53), 26825–26833.

75 Doelle, H. W. Fermentation. In *Bacterial Metabolism (Second Edition)*; **1975**; pp 559–692.

76 Detman, A.; Mielecki, D.; Chojnacka, A.; Salamon, A.; Błaszczyk, M. K. Cell Factories Converting Lactate and Acetate to Butyrate : Clostridium Butyricum and Microbial Communities from Dark Fermentation Bioreactors. *Microb. Cell Fact.* **2019**, 1–12.

77 Guo-qing, H. E.; Qing, K.; Qi-he, C.; Hui, R. Batch and Fed-Batch Production of Butyric Acid by Clostridium Butyricum ZJUCB. **2005**, No. 11, 1076–1080.

78 Costa, J. C.; Souza, D. Z.; Pereira, M. A.; Stams, A. J. M.; Alves, M. M. Biomethanation Potential of Biological and Other Wastes. In *Biofuel Technologies: Recent Developments*; Gupta, V. K., Tuohy, M. G., Eds.; Springer - Verlag Berlin Heidelberg New York: Heidelberg New York Dordrecht London, **2013**; pp 369–396.

79 Lyu, Z.; Shao, N.; Akinyemi, T.; Whitman, W. B. Methanogenesis. *Curr. Biol.* **2018**, *28* (13), R727–R732.

80 Ferry, J. G.; Kastead, K. A. Methanogenesis. In *Archaea*; John Wiley & Sons, Ltd, **2007**; pp 288–314.

81 Wang, J.; Yin, Y. Principle and Application of Different Pretreatment Methods for Enriching Hydrogen-Producing Bacteria from Mixed Cultures. *Int. J. Hydrogen Energy* **2017**, *42* (8), 4804–4823.

82 Jeong, D. Y.; Cho, S. K.; Shin, H. S.; Jung, K. W. Application of an Electric Field for Pretreatment of a Seeding Source for Dark Fermentative Hydrogen Production. *Bioresour. Technol.* **2013**, *139*, 393–396.

83 Mohan, S. V.; Rohit, M. V; Amulya, K.; Kumar, A. N.; Modestra, J. A.; Sravan, J. S.; Hemalatha, M.; Chatterjee, S.; Ranadheer, P.; Swathi, K. *Acidogenic Biohydrogen Production Integrated With Biorefinery Approach*; Elsevier B.V., **2019**.

84 Ren, Y.; Si, B.; Liu, Z.; Jiang, W. Promoting Dark Fermentation for Biohydrogen Production : Potential Roles of Iron-Based Additives. *Int. J. Hydrogen Energy* **2021**, *47* (3), 1499–1515.

85 Lubitz, W.; Ogata, H.; Rüdiger, O.; Reijerse, E. Hydrogenases. *Chem. Rev.* **2014**, *114* (8), 4081–4148.

86 Noguchi, K.; Riggins, D. P.; Eldahan, K. C.; Kitko, R. D.; Slonczewski, J. L. Hydrogenase-3 Contributes to Anaerobic Acid Resistance of Escherichia Coli. **2010**, *5* (4), 27–29.

87 Patriarca, C.; De Luca, E.; Felici, C.; Lona, L.; Mazzurco Miritana, V.; Massini, G. Bio-Production of Hydrogen and Methane Through Anaerobic Digestion Stages. In *Enriched Methane: The First Step Towards the Hydrogen Economy*; De Falco, M., Basile, A., Eds.; Springer Cham Heidelberg New York Dordrecht London, **2016**; pp 91–109.

88 David, B.; Federico, B.; Cristina, C.; Marco, G.; Federico, M.; Paolo, P. Biohythane Production From Food Wastes. In *Biohydrogen*; 2019; pp 347–368.

89 Wongthanate, J.; Chinnacotpong, K. Impacts of PH , Temperature and Pretreatment Method on Biohydrogen Production from Organic Wastes by Sewage Microflora. **2014**.

90 Vijaya Krishna, S.; Kiran Kumar, P.; Chaitanya, N.; Bhagawan, D.; Himabindu, V.; Lakshmi Narasu, M. Biohydrogen Production from Brewery Effluent in a Batch and Continuous Reactor with Anaerobic Mixed Microbial Consortia. *Biofuels* **2017**, *8* (6), 701–707.

91 Veeramalini, J. B.; Selvakumari, I. A. E.; Park, S.; Jayamuthunagai, J.; Bharathiraja, B. Continuous Production of Biohydrogen from Brewery Effluent Using Co-Culture of Mutated Rhodobacter M 19 and Enterobacter Aerogenes. *Bioresour. Technol.* **2019**, *286*.

92 Das, D.; Khanna, N.; Dasgupta, C. N. Process and Culture Parameters. In *Biohydrogen Production: Fundamentals and Technology Advances*; 2014; pp 219–265.

93 Mohan, S. V.; Chiranjeevi, P.; Chandrasekhar, K.; Babu, P. S.; Sarkar, O. *Acidogenic Biohydrogen Production From Wastewater*; Elsevier B.V., 2019.

94 Dahiya, S.; Sarkar, O.; Swamy, Y. V; Mohan, S. V. Bioresource Technology Acidogenic Fermentation of Food Waste for Volatile Fatty Acid Production with Co-Generation of Biohydrogen. *Bioresour. Technol.* **2015**, *182*, 103–113.

95 Zhang, C.; Yang, H.; Yang, F.; Ma, Y. Current Progress on Butyric Acid Production by Fermentation. *Curr. Microbiol.* **2009**, *59* (6), 656–663.

96 Venkata Mohan, S.; Agarwal, L.; Mohanakrishna, G.; Srikanth, S.; Kapley, A.; Purohit, H. J.; Sarma, P. N. Firmicutes with Iron Dependent Hydrogenase Drive Hydrogen Production in Anaerobic Bioreactor Using Distillery Wastewater. *Int. J. Hydrogen Energy* **2011**, *36* (14), 8234–8242.

97 Singh, R. Fermentative Biohydrogen Production Using Microbial Consortia. In *Biofuel Technologies: Recent*

Developments; Gupta, V. K., Tuohy, M. G., Eds.; 2013; pp 273–299.

98 Toledo-Alarcón, J.; Capson-Tojo, G.; Marone, A.; Paillet, F.; Júnior, A. D. N. F.; Chatellard, L.; Bernet, N.; Trably, E. Basics of Bio-Hydrogen Production by Dark Fermentation. In *Bioreactors for Microbial Biomass and Energy Conversion*; 2018; pp 199–220.

99 Wang, J.; Yin, Y. Influencing Factors for Biohydrogen Production. In *Biohydrogen Production from Organic Wastes*; 2017; pp 197–268.

100 Rozendal, R. A.; Buisman, C. J. N. Bio-electrochemical process for producing hydrogen. WO 2005005981, **2005**.

101 Liu, H.; Grot, S. Electrochemically Assisted Microbial Production of Hydrogen from Acetate. **2005**, *39* (11), 4317–4320.

102 Aelterman, P.; Freguia, S.; Keller, J.; Verstraete, W.; Rabaey, K. The Anode Potential Regulates Bacterial Activity in Microbial Fuel Cells. *Appl. Microbiol. Biotechnol.* **2008**, *78* (3), 409–418.

103 Logan, B. E.; Rabaey, K. Conversion of Wastes into Bioelectricity and Chemicals by Using Microbial Electrochemical Technologies. *Science (80-.).* **2012**, *337* (6095), 686–690.

104 Zhou, M.; Wang, H.; Hassett, D. J.; Gu, T. Recent Advances in Microbial Fuel Cells (MFCs) and Microbial Electrolysis Cells (MECs) for Wastewater Treatment, Bioenergy and Bioproducts. *J. Chem. Technol. Biotechnol.* **2013**, *88* (4), 508–518.

105 Millet, P. Fundamentals of Water Electrolysis. In *Hydrogen Production*; **2015**; pp 33–62.

106 Kadier, A.; Simayi, Y.; Abdeshahian, P.; Azman, N. F.; Chandrasekhar, K.; Kalil, M. S. A Comprehensive Review of Microbial Electrolysis Cells (MEC) Reactor Designs and Configurations for Sustainable Hydrogen Gas Production. *Alexandria Eng. J.* **2014**, *55* (1), 427–443.

107 Logan, B. E. 8 - MECs for Hydrogen Production. In *Microbial Fuel Cells*; **2007**; pp 125–145.

108 Rabaey, K.; Verstraete, W. Microbial Fuel Cells: Novel Biotechnology for Energy Generation. *Trends Biotechnol.* **2005**, *23* (6), 291–298.

109 Wang, X. T.; Zhang, Y. F.; Wang, B.; Wang, S.; Xing, X.; Xu, X. J.; Liu, W. Z.; Ren, N. Q.; Lee, D. J.; Chen, C. Enhancement of Methane Production from Waste Activated Sludge Using Hybrid Microbial Electrolysis Cells-Anaerobic Digestion (MEC-AD) Process – A Review. *Bioresour. Technol.* **2022**, *346*, 126641.

110 Premier, G. C.; Kim, J. R.; Massanet-nicolau, J.; Kyazze, G.; Esteves, S. R. R. Integration of Biohydrogen , Biomethane and Bioelectrochemical Systems. *Renew. Energy* **2013**, *49*, 188–192.

111 Logan, B. E.; Hamelers, B.; Rozendal, R.; Schröder, U.; Keller, J.; Freguia, S.; Aelterman, P.; Verstraete, W.; Rabaey, K. Microbial Fuel Cells: Methodology and Technology. *Environ. Sci. Technol.* **2006**, *40* (17), 5181–5192.

112 Cardeña, R.; Cercado, B.; Buitrón, G. *Microbial Electrolysis Cell for Biohydrogen Production*; Elsevier B.V., **2019**.

113 Hasany, M.; Mardanpour, M. M.; Yaghmaei, S. Biocatalysts in Microbial Electrolysis Cells: A Review. *Int. J. Hydrogen Energy* **2016**, *41* (3), 1477–1493. https://doi.org/10.1016/j.ijhydene.2015.10.097.

114 Lovley, D. R. The Microbe Electric: Conversion of Organic Matter to Electricity. *Curr. Opin. Biotechnol.* **2008**, *19* (6), 564–571.

115 Debabov, V. G. Electricity from Microorganisms. *Mikrobiologiia* **2008**, *77* (2), 149–157.

116 Nevin, K. P.; Lovley, D. R. Mechanisms for Fe(III) Oxide Reduction in Sedimentary Environments. *Geomicrobiol. J.* **2002**, *19* (2), 141–159.

117 Gregory, K. B.; Bond, D. R.; Lovley, D. R. Graphite Electrodes as Electron Donors for Anaerobic Respiration. *Environ. Microbiol.* **2004**, *6* (6), 596–604.

118 Bond, D. R.; Holmes, D. E.; Tender, L. M.; Lovley, D. R. Bond et Al 2002 - Electrode-Reducing Microorganisms That Harvest Energy from Marine Sediments..PDF. 2001, pp 293–296.

119 Wrighton, K. C.; Thrash, J. C.; Melnyk, R. A.; Bigi, J. P.; Byrne-Bailey, K. G.; Remis, J. P.; Schichnes, D.; Auer, M.; Chang, C. J.; Coates, J. D. Evidence for Direct Electron Transfer by a Gram-Positive Bacterium Isolated from a Microbial Fuel Cell. *Appl. Environ. Microbiol.* **2011**, *77* (21), 7633–7639.

120 Logan, E. B. Microbial Fuel Cells. **2008**.

121 Shi, L.; Richardson, D. J.; Wang, Z.; Kerisit, S. N.; Rosso, K. M.; Zachara, J. M.; Fredrickson, J. K. The Roles of Outer Membrane Cytochromes of Shewanella and Geobacter in Extracellular Electron Transfer. *Environ. Microbiol. Rep.* **2009**, *1* (4), 220–227.

122 Reguera, G.; McCarthy, K. D.; Mehta, T.; Nicoll, J. S.; Tuominen, M. T.; Lovley, D. R. Extracellular Electron Transfer via Microbial Nanowires. *Nature* **2005**, *435* (7045), 1098–1101.

123 Leang, C.; Qian, X.; Mester, T.; Lovley, D. R. Alignment of the C-Type Cytochrome OmcS along Pili of Geobacter Sulfurreducens. *Appl. Environ. Microbiol.* **2010**, *76* (12), 4080–4084.

124 Pirbadian, S.; Barchinger, S. E.; Leung, K. M.; Byun, H. S.; Jangir, Y.; Bouhenni, R. A.; Reed, S. B.; Romine, M. F.; Saffarini, D. A.; Shi, L.; Gorby, Y. A.; Golbeck, J. H.; El-Naggar, M. Y. Shewanella Oneidensis MR-1 Nanowires Are Outer Membrane and Periplasmic Extensions of the Extracellular Electron Transport Components. *Proc. Natl. Acad. Sci. U. S. A.* **2014**, *111* (35), 12883–12888.

125 Philips, J.; Verbeeck, K.; Rabaey, K.; Arends, J. B. A. *Electron Transfer Mechanisms in Biofilms*; Elsevier Ltd., **2016**.

126 Von Canstein, H.; Ogawa, J.; Shimizu, S.; Lloyd, J. R. Secretion of Flavins by Shewanella Species and Their Role in Extracellular Electron Transfer. *Appl. Environ. Microbiol.* **2008**, *74* (3), 615–623.

127 Marsili, E.; Baron, D. B.; Shikhare, I. D.; Coursolle, D.; Gralnick, J. a; Bond, D. R. Shewanella Secretes Flavins That Mediate Extracellular Electron Transfer. *Proc. Natl. Acad. Sci. U. S. A.* **2008**, *105* (10), 3968–3973.

128 Rabaey, K.; Boon, N.; Siciliano, S. D.; Verstraete, W.; Verhaege, M. Biofuel Cells Select for Microbial Consortia That Self-Mediate Electron Transfer Biofuel Cells Select for Microbial Consortia That Self-Mediate Electron Transfer. *Appl. Environ. Microbiol.* **2004**, *70* (9), 5373–5382.

129 Rinaldi, A.; Mecheri, B.; Garavaglia, V.; Licoccia, S.; Di Nardo, P.; Traversa, E. Engineering Materials and Biology to Boost Performance of Microbial Fuel Cells: A Critical Review. *Energy Environ. Sci.* **2008**, *1* (4), 417.

130 Wu, S.; Xiao, Y.; Wang, L.; Zheng, Y.; Chang, K.; Zheng, Z.; Yang, Z.; Varcoe, J. R.; Zhao, F. Extracellular Electron Transfer Mediated by Flavins in Gram-Positive Bacillus Sp. WS-XY1 and Yeast Pichia Stipitis. *Electrochim. Acta* **2014**, *146*, 564–567.

131 Hernandez, M. E.; Newman, D. K. Cellular and Molecular Life Sciences Extracellular Electron Transfer. **2001**, *58*, 1562–1571.

132 Yeun, N.; Su, K.; Kim, N.; Bin, O. Long - Term Adaptation of Escherichia Coli to Methanogenic Co - Culture Enhanced Succinate Production from Crude Glycerol. *J. Ind. Microbiol. Biotechnol.* **2018**, *45* (1), 71–76.

133 Lovley, D. R. Reach out and Touch Someone: Potential Impact of DIET (Direct Interspecies Energy Transfer) on Anaerobic Biogeochemistry, Bioremediation, and Bioenergy. *Rev. Environ. Sci. Biotechnol.* **2011**, *10* (2), 101–105.

134 Liu, F.; Rotaru, A.-E.; Shrestha, P. M.; Malvankar, N. S.; Nevin, K. P.; Lovley, D. R. Promoting Direct Interspecies Electron Transfer with Activated Carbon. *Energy Environ. Sci.* **2012**, *5* (10), 8982.

135 Gadhamshetty, V.; Nirmalakhandan, N.; Khanal, S. K.; & Johnson, G. R. Bioreactor Systems for

Biofuel/Bioelectricity Production. In *Bioenergy and Biofuel from Biowastes and Biomass*; **2010**; pp 275–312.

136 Premier, G. C.; Michie, I. S.; Boghani, H. C.; Fradler, K. R.; Kim, J. R. *Reactor Design and Scale-Up*; Elsevier Ltd., **2016**.

137 Li, W.-W.; Sheng, G.-P.; Liu, X.-W.; Yu, H.-Q. Recent Advances in the Separators for Microbial Fuel Cells. *Spec. Issue Biofuels - II Algal Biofuels Microb. Fuel Cells* **2011**, *102* (1), 244–252.

138 Antolini, E. Composite Materials for Polymer Electrolyte Membrane Microbial Fuel Cells. *Biosens. Bioelectron.* **2015**, *69*, 54–70.

139 Chaudhuri, S. K.; Lovley, D. R. Electricity Generation by Direct Oxidation of Glucose in Mediatorless Microbial Fuel Cells. *Nat. Biotechnol.* **2003**, *21* (10), 1229–1232.

140 Antolini, E.; Gonzalez, E. R. Polymer Supports for Low-Temperature Fuel Cell Catalysts. *Appl. Catal. A Gen.* **2009**, *365* (1), 1–19.

141 Bajracharya, S.; ElMekawy, A.; Srikanth, S.; Pant, D. *Cathodes for Microbial Fuel Cells*; Elsevier Ltd., **2016**.

142 Ghasemi, M.; Shahgaldi, S.; Ismail, M.; Kim, B. H.; Yaakob, Z.; Wan Daud, W. R. Activated Carbon Nanofibers as an Alternative Cathode Catalyst to Platinum in a Two-Chamber Microbial Fuel Cell. *Int. J. Hydrogen Energy* **2011**, *36* (21), 13746–13752.

143 Dumitru, A.; Scott, K. *Anode Materials for Microbial Fuel Cells*; Elsevier Ltd., **2016**.

144 MacDiarmid, A. G. "Synthetic Metals": A Novel Role for Organic Polymers (Nobel Lecture) Copyright((c)) The Nobel Foundation 2001. We Thank the Nobel Foundation, Stockholm, for Permission to Print This Lecture. *Angew Chem Int Ed Engl* **2001**, *40* (14), 2581–2590.

145 Hidalgo, D.; Tommasi, T.; Bocchini, S.; Chiolerio, A.; Chiodoni, A.; Mazzarino, I.; Ruggeri, B. Surface Modification of Commercial Carbon Felt Used as Anode for Microbial Fuel Cells. *Energy* **2016**, *99*, 193–201.

146 Cohen, G. N. *Microbial Biochemistry: Second Edition*; **2011**.

147 Ghasemi, M.; Shahgaldi, S.; Ismail, M.; Yaakob, Z.; Daud, W. R. W. New Generation of Carbon Nanocomposite Proton Exchange Membranes in Microbial Fuel Cell Systems. *Chem. Eng. J.* **2012**, *184*, 82–89.

148 Hernández-Fernández, F. J.; Pérez De Los Ríos, A.; Salar-García, M. J.; Ortiz-Martínez, V. M.; Lozano-Blanco, L. J.; Godínez, C.; Tomás-Alonso, F.; Quesada-Medina, J. Recent Progress and Perspectives in Microbial Fuel Cells for Bioenergy Generation and Wastewater Treatment. *Fuel Process. Technol.* **2015**, *138*, 284–297.

149 Oh, S. E.; Logan, B. E. Proton Exchange Membrane and Electrode Surface Areas as Factors That Affect Power Generation in Microbial Fuel Cells. *Appl. Microbiol. Biotechnol.* **2006**, *70* (2), 162–169.

150 Chen, S.; Patil, S. A.; Keith, R.; Schröder, U. Strategies for Optimizing the Power Output of Microbial Fuel Cells : Transitioning from Fundamental Studies to Practical Implementation. **2019**, *234*, 15–28.

151 Do, M. H.; Ngo, H. H.; Guo, W. S.; Liu, Y.; Chang, S. W.; Nguyen, D. D.; Nghiem, L. D.; Ni, B. J. Challenges in the Application of Microbial Fuel Cells to Wastewater Treatment and Energy Production: A Mini Review. *Sci. Total Environ.* **2018**, *639*, 910–920.

152 Zhang, Q.; Hu, J.; Lee, D. Bioresource Technology Microbial Fuel Cells as Pollutant Treatment Units : Research Updates. *Bioresour. Technol.* **2016**, *217*, 121–128.

153 Gude, V. G. Wastewater Treatment in Microbial Fuel Cells e an Overview. *J. Clean. Prod.* **2016**, *122*, 287–307.

154 Hatzell, M. C.; Kim, Y.; Logan, B. E. Powering Microbial Electrolysis Cells by Capacitor Circuits Charged Using Microbial Fuel Cell. *J. Power Sources* **2013**, *229*, 198–202.

155 Santoro, C.; Soavi, F.; Serov, A.; Arbizzani, C.; Atanassov, P. Self-Powered Supercapacitive Microbial Fuel

Cell: The Ultimate Way of Boosting and Harvesting Power. *Biosens. Bioelectron.* **2016**, *78*, 229–235.

156 Call, D.; Logan, B. E. Hydrogen Production in a Single Chamber Microbial Electrolysis Cell Lacking a Membrane. *Environ. Sci. Technol.* **2008**, *42* (9), 3401–3406. https://doi.org/10.1021/es8001822.

157 Bakonyi, P.; Kumar, G.; Koók, L.; Tóth, G.; Rózsenberszki, T. Bioresource Technology Microbial Electrohydrogenesis Linked to Dark Fermentation as Integrated Application for Enhanced Biohydrogen Production : A Review on Process Characteristics , Experiences and Lessons. **2018**, *251*, 381–389.

158 Guwy, A. J.; Dinsdale, R. M.; Kim, J. R.; Massanet-nicolau, J.; Premier, G. Bioresource Technology Fermentative Biohydrogen Production Systems Integration. *Bioresour. Technol.* **2011**, *102* (18), 8534–8542.

159 Sadhukhan, J.; Lloyd, J. R.; Scott, K.; Premier, G. C.; Yu, E. H.; Curtis, T.; Head, I. M. A Critical Review of Integration Analysis of Microbial Electrosynthesis (MES) Systems with Waste Biore Fi Neries for the Production of Biofuel and Chemical from Reuse of CO 2. **2016**, *56*, 116–132.

160 Pandit, S.; Balachandar, G.; Das, D. Improved Energy Recovery from Dark Fermented Cane Molasses Using Microbial Fuel Cells. **2014**, *8* (1), 43–54.

161 Mohanakrishna, G.; Mohan, S. V.; Sarma, P. N. Utilizing Acid-Rich Effluents of Fermentative Hydrogen Production Process as Substrate for Harnessing Bioelectricity : An Integrative Approach. *Int. J. Hydrogen Energy.* **2010**, *35* (8), 3440–3449.

162 Schievano, A.; Pepè, T.; Chang, Y.; Scaglia, B.; Salati, S.; Zanardo, M.; Quiao, W.; Dong, R.; Adani, F. Dark Fermentation , Anaerobic Digestion and Microbial Fuel Cells : An Integrated System to Valorize Swine Manure and Rice Bran. **2016**, *56*, 519–529.

163 Wen, Q.; Wu, Y.; Zhao, L. X.; Sun, Q.; Kong, F. Y. Electricity Generation and Brewery Wastewater Treatment from Sequential Anode-Cathode Microbial Fuel Cell. *J. Zhejiang Univ. Sci. B.* **2010**, *11* (2), 87–93.

164 Wen, Q.; Wu, Y.; Zhao, L.; Sun, Q. Production of Electricity from the Treatment of Continuous Brewery Wastewater Using a Microbial Fuel Cell. *Fuel.* **2010**, *89* (7), 1381–1385.

165 Choi, J.; Ahn, Y. Bioresource Technology Enhanced Bioelectricity Harvesting in Microbial Fuel Cells Treating Food Waste Leachate Produced from Biohydrogen Fermentation. *Bioresour. Technol.* **2015**, *183*, 53–60.

166 Elmekawy, A.; Srikanth, S.; Vanbroekhoven, K.; Wever, H. De; Pant, D. Bioelectro-Catalytic Valorization of Dark Fermentation Ef Fl Uents by Acetate Oxidizing Bacteria in Bioelectrochemical System (BES). *J. Power Sources.* **2014**, *262*, 183–191.

167 Chookaew, T.; Prasertsan, P.; Ren, Z. J. Two-Stage Conversion of Crude Glycerol to Energy Using Dark Fermentation Linked with Microbial Fuel Cell or Microbial Electrolysis Cell. *N. Biotechnol.* **2014**, *31* (2), 179–184.

168 Babu, S.; Srikanth, S.; Mohan, S. V. ScienceDirect Continuous Mode Operation of Microbial Fuel Cell (MFC) Stack with Dual Gas Diffusion Cathode Design for the Treatment of Dark Fermentation Effluent. *Int. J. Hydrogen Energy* **2015**, *40* (36), 12424–12435.

169 Bakonyi, P.; Kumar, G.; Koók, L.; Tóth, G.; Rózsenberszki, T. Bioresource Technology Microbial Electrohydrogenesis Linked to Dark Fermentation as Integrated Application for Enhanced Biohydrogen Production : A Review on Process Characteristics , Experiences and Lessons. **2018**, *251* (December 2017), 381–389.

170 Willaert, R. The Beer Brewing Process: Wort Production and Beer Fermentation. In *Handbook of Food Products Manufacturing*; Hui, Y. H., Ed.; John Wiley & Sons, Inc., 2007; pp 443–506.

171 Fortune Business Insights. *Beer Market* Available from: https://www.fortunebusinessinsights.com/beer-

market-102489 (accessed Jun 4, 2022).

172 Lindenberger, H. *New Report On Beer's Global Economic Footprint Highlights The Impact The Industry Makes* Available from: https://www.forbes.com/sites/hudsonlindenberger/2022/02/10/new-report-highlights-the-global-economic-impact-the-beer-industry-makes/?sh=2e748c6b4241 (accessed Jul 29, 2022).

173 Olajire, A. A. The Brewing Industry and Environmental Challenges. *J. Clean. Prod.* **2020**, *256*, 102817.

174 Olivares-Galván, S.; Marina, M. L.; García, M. C. Extraction of Valuable Compounds from Brewing Residues: Malt Rootlets, Spent Hops, and Spent Yeast. *Trends Food Sci. Technol.* **2022**.

175 Panji, M.; Drago, G.; Zeli, B. Anaerobic Biodegradation of Raw and Pre-Treated Brewery Spent Grain Utilizing Solid State Anaerobic Digestion. **2015**, 818–827.

176 Briggs, D. E.; Boulton, C. A.; Brookes, P. A.; Stevens, R. Water, Effluents and Wastes. In *Brewing Science and practice*; **2004**; pp 52–84.

177 Rachwał, K.; Waśko, A.; Gustaw, K.; Polak-Berecka, M. Utilization of Brewery Wastes in Food Industry. *PeerJ* **2020**, *8*, 1–28.

178 Kerby, C.; Vriesekoop, F. An Overview of the Utilisation of Brewery By-Products as Generated by British Craft Breweries. *Beverages* **2017**, *3* (2).

179 Brito, A. G.; Peixoto, J.; Oliveira, J. M.; Oliveira, J. A.; Costa, C.; Nogueira, R.; Rodrigues, A. Brewery and Winery Wastewater Treatment: Some Focal Points of Design and Operation. In *Utilization of By-Products and Treatment of Waste in the Food Industry*; Oreopoulou, V., Russ, W., Eds., **2007**; pp 109–131.

180 Simate, G. S.; Cluett, J.; Iyuke, S. E.; Musapatika, E. T.; Ndlovu, S.; Walubita, L. F.; Alvarez, A. E. The Treatment of Brewery Wastewater for Reuse : State of the Art. *DES* **2011**, *273* (2–3), 235–247.

181 Sinbuathong, N.; Somjit, C.; Leungprasert, S. Feasibility Study for Biohydrogen Production from Raw Brewery Wastewater. **2015**, No. March, 1769–1777.

182 Keenan, J. D.; Kormi, I. Anaerobic Digestion of Brewery By-Products. *Water Pollut. Control Fed.* **1981**, *53* (1), 66–77.

183 Simate, G. S. *Water Treatment and Reuse in Breweries*; Elsevier Ltd, **2015**.

184 Arantes, M. K.; Alves, H. J.; Sequinel, R.; da Silva, E. A. Treatment of Brewery Wastewater and Its Use for Biological Production of Methane and Hydrogen. **2017**, *42*, 26243–26256.

185 Ravindran, R.; Jaiswal, S.; Abu-Ghannam, N.; Jaiswal, A. K. A Comparative Analysis of Pretreatment Strategies on the Properties and Hydrolysis of Brewers' Spent Grain. *Bioresour. Technol.* **2018**, *248*, 272–279.

186 Wen, C.; Zhang, J.; Duan, Y.; Zhang, H.; Ma, H. A Mini-Review on Brewer's Spent Grain Protein: Isolation, Physicochemical Properties, Application of Protein, and Functional Properties of Hydrolysates. *J. Food Sci.* **2019**, *84* (12), 3330–3340.

187 Briggs, D. E.; Boulton, C. A.; Brookes, P. A.; Stevens, R. The Science of Mashing. In *Brewing Science and practice*; **2004**; pp 87–170.

188 Bonifácio-Lopes, T.; Teixeira, J. A.; Pintado, M. Current Extraction Techniques towards Bioactive Compounds from Brewer's Spent Grain–A Review. *Crit. Rev. Food Sci. Nutr.* **2020**, *60* (16), 2730–2741.

189 Jaeger, A.; Arendt, E. K.; Zannini, E.; Sahin, A. W. Brewer's Spent Yeast (BSY), an Underutilized Brewing By-Product. *Fermentation* **2020**, *6* (4), 1–23.

190 Rakowska, R.; Sadowska, A.; Dybkowska, E.; Świderski, F. Spent Yeast as Natural Source of Functional Food Additives. *Rocz. Panstw. Zakl. Hig.* **2017**, *68* (2), 115–121.

191 Marson, G. V.; de Castro, R. J. S.; Belleville, M. P.; Hubinger, M. D. Spent Brewer's Yeast as a Source of High

Added Value Molecules: A Systematic Review on Its Characteristics, Processing and Potential Applications. *World J. Microbiol. Biotechnol.* **2020**, *36* (7).

192 Schneider, T.; Graeff-Hönninger, S.; French, W. T.; Hernandez, R.; Merkt, N.; Claupein, W.; Hetrick, M.; Pham, P. Lipid and Carotenoid Production by Oleaginous Red Yeast Rhodotorula Glutinis Cultivated on Brewery Effluents. *Energy* **2013**, *61*, 34–43.

193 Jia, R.; Sun, D.; Dang, Y.; Meier, D.; Holmes, D. E.; Smith, J. A. Carbon Cloth Enhances Treatment of High-Strength Brewery Wastewater in Anaerobic Dynamic Membrane Bioreactors. *Bioresour. Technol.* **2020**, *298* (December 2019), 122547.

194 Dannys, E.; Green, T.; Wettlaufer, A.; Madhurnathakam, C. M. R.; Elkamel, A. Wastewater Treatment with Microbial Fuel Cells: A Design and Feasibility Study for Scale-up in Microbreweries. *J. Bioprocess. Biotech.* **2016**, *6* (1), 1–6.

195 Amenorfenyo, D. K.; Huang, X.; Zhang, Y.; Zeng, Q.; Zhang, N.; Ren, J.; Huang, Q. Microalgae Brewery Wastewater Treatment: Potentials, Benefits and the Challenges. *Int. J. Environ. Res. Public Health* **2019**, *16* (11).

196 Choi, H. J. Parametric Study of Brewery Wastewater Effluent Treatment Using Chlorella Vulgaris Microalgae. *Environ. Eng. Res.* **2016**, *21* (4), 401–408.

197 Pereira, L. T.; Lisboa, C. R.; Costa, J. A. V.; da Rosa, L. M.; de Carvalho, L. F. Evaluation of Protein Content and Antimicrobial Activity of Biomass from Spirulina Cultivated with Residues from the Brewing Process. *J. Chem. Technol. Biotechnol.* **2022**, *97* (1), 160–166.

198 Bodin, H.; Hultberg, M. Fungi-based Treatment of Real Brewery Waste Streams and Its Effects on Water Quality. *Bioprocess Biosyst. Eng.* **2019**, *42* (8), 1317–1324.

199 Łebkowska, M.; Załeska-Radziwiłł, M. Application of White-Rot Fungi for Biodegradation of Refractory Organic Compounds-a Review. *Desalin. Water Treat.* **2014**, *52* (19–21), 3708–3713.

200 Brewer's Association. Water and Wastewater: Treatment/Volume Reduction Manual. *Brew. Assoc.* **2011**, 1–47.

201 Schwarze, F. W. M. R. Wood Decay under the Microscope. *Fungal Biol. Rev.* **2007**, *21* (4), 133–170.

202 Kirk, T. K.; Farrell, R. L. Enzymatic "Combustion": The Microbial Degradation of Lignin. *Annu. Rev. Microbiol.* **1987**, 465–505.

203 Reddy, C. A.; Mathew, Z. Bioremediation Potential of White Rot Fungi. *Fungi in Bioremediation* **2009**, 52–78.

204 Harvey, P. J.; Thurston, C. F. The Biochemistry of Ligninolytic Fungi. *Fungi in Bioremediation* **2009**, 27–51.

205 del Cerro, C.; Erickson, E.; Dong, T.; Wong, A. R.; Eder, E. K.; Purvine, S. O.; Mitchell, H. D.; Weitz, K. K.; Markillie, L. M.; Burnet, M. C.; Hoyt, D. W.; Chu, R. K.; Cheng, J. F.; Ramirez, K. J.; Katahira, R.; Xiong, W.; Himmel, M. E.; Subramanian, V.; Linger, J. G.; Salvachúa, D. Intracellular Pathways for Lignin Catabolism in White-Rot Fungi. *Proc. Natl. Acad. Sci. U. S. A.* **2021**, *118* (9), 1–10.

206 Suryadi, H.; Judono, J. J.; Putri, M. R.; Eclessia, A. D.; Ulhaq, J. M.; Agustina, D. N.; Sumiati, T. Biodelignification of Lignocellulose Using Ligninolytic Enzymes from White-Rot Fungi. *Heliyon* **2022**, *8* (2), e08865.

207 Pointing, S. B. Feasibility of Bioremediation by White-Rot Fungi. **2001**, 20–33.

208 Leonowicz, A.; Matuszewska, A.; Luterek, J.; Ziegenhagen, D.; Wojtaś-Wasilewska, M.; Cho, N. S.; Hofrichter, M.; Rogalski, J. Biodegradation of Lignin by White Rot Fungi. *Fungal Genet. Biol.* **1999**, *27* (2–3), 175–185.

209 Knapp, J. S.; Vantoch-Wood, E. J.; Zhang, F. *Use of Wood-Rotting Fungi for the Decolorization of Dyes and Industrial Effluents*; **2009**.

210 Mehdi Dashtban, Y. H. Lignin in Paper Mill Sludge Is Degraded by White-Rot Fungi in Submerged

Fermentation. *J. Microb. Biochem. Technol.* **2015**, *07* (04), 177–181.

211 Cardona, M.; Osorio, J.; Quintero, J. Degradación de Colorantes Industriales Con Hongos Ligninolíticos. *Rev. Fac. Ing.* **2009**, No. 48, 27–37.

212 Rodríguez, E.; Pickard, M. A.; Vazquez-Duhalt, R. Industrial Dye Decolorization by Laccases from Ligninolytic Fungi. *Curr. Microbiol.* **1999**, *38* (1), 27–32.

213 D'Annibale, A.; Quaratino, D.; Federici, F.; Fenice, M. Effect of Agitation and Aeration on the Reduction of Pollutant Load of Olive Mill Wastewater by the White-Rot Fungus Panus Tigrinus. *Biochem. Eng. J.* **2006**, *29* (3), 243–249.

214 Atila, F. Cultivation of Pleurotus Spp., as an Alternative Solution to Dispose Olive Waste. *J. Agric. Ecol. Res. Int.* **2017**, *12* (4), 1–10.

215 FitzGibbon, F.; Singh, D.; McMullan, G.; Marchant, R. The Effect of Phenolic Acids and Molasses Spent Wash Concentration on Distillery Wastewater Remediation by Fungi. *Process Biochem.* **1998**, *33* (8), 799–803.

216 Strong, P. J. Fungal Remediation of Amarula Distillery Wastewater. *World J. Microbiol. Biotechnol.* **2010**, *26* (1), 133–144.

217 Hernandes, K. C.; Souza-Silva, É. A.; Assumpção, C. F.; Zini, C. A.; Welke, J. E. Carbonyl Compounds and Furan Derivatives with Toxic Potential Evaluated in the Brewing Stages of Craft Beer. *Food Addit. Contam. - Part A Chem. Anal. Control. Expo. Risk Assess.* **2020**, *37* (1), 61–68.

218 Rosatella, A. A.; Simeonov, S. P.; Frade, R. F. M.; Afonso, C. A. M. 5-Hydroxymethylfurfural (HMF) as a Building Block Platform: Biological Properties, Synthesis and Synthetic Applications. *Green Chem.* **2011**, *13* (4), 754–793.

219 Heer, D.; Sauer, U. Identification of Furfural as a Key Toxin in Lignocellulosic Hydrolysates and Evolution of a Tolerant Yeast Strain. *Microb. Biotechnol.* **2008**, *1* (6), 497–506.

220 Langner, E.; Rzeski, W. Biological Properties of Melanoidins: A Review. *Int. J. Food Prop.* **2014**, *17* (2), 344–353.

221 Cämmerer, B.; Jalyschko, W.; Kroh, L. W. Intact Carbohydrate Structures as Part of the Melanoidin Skeleton. *J. Agric. Food Chem.* **2002**, *50* (7), 2083–2087.

222 Chandra, R.; Bharagava, R. N.; Rai, V. Melanoidins as Major Colourant in Sugarcane Molasses Based Distillery Effluent and Its Degradation. *Bioresour. Technol.* **2008**, *99* (11), 4648–4660.

223 Kumar, V.; Chandra, R. Bioremediation of Melanoidins Containing Distillery Waste for Environmental Safety. In *Bioremediation of Industrial Waste for Environmental Safety*; **2020**; pp 495–529.

224 Rizvi, S.; Singh, A.; Kushwaha, A.; Gupta, S. K. Recent Advances in Melanoidin Removal from Wastewater: Sources, Properties, Toxicity, and Remediation Strategies. In *Emerging trends to Approaching Zero Waste*, **2022**; pp 361–386.

225 Liakos, T. I.; Lazaridis, N. K. Melanoidin Removal from Molasses Effluents by Adsorption. *J. Water Process Eng.* **2016**, *10*, 156–164.

226 Sirianuntapiboon, S.; Phothilangka, P.; Ohmomo, S. Decolorization of Molasses Wastewater by a Strain No . BP103 of Acetogenic Bacteria. *Bioresour. Technol.* **2004**, *92*, 31–39.

227 Sen, S. K.; Raut, S.; Bandyopadhyay, P.; Raut, S. Fungal Decolouration and Degradation of Azo Dyes: A Review. *Fungal Biol. Rev.* **2016**, *30* (3), 112–133.

228 Gao, D.; Du, L.; Yang, J.; Wu, W. M.; Liang, H. A Critical Review of the Application of White Rot Fungus to Environmental Pollution Control. *Crit. Rev. Biotechnol.* **2010**, *30* (1), 70–77.

229 Nishida, A.; Fukuzumi, T. Formation of Coniferyl Alcohol from Ferulic Acid by the White Rot Fungus Trametes. *Phytochemistry* **1978**, *17* (3), 417–419.

230 Falconnier, B.; Lapierre, C.; Lesage-Meessen, L.; Yonnet, G.; Brunerie, P.; Colonna-Ceccaldi, B.; Corrieu, G.; Asther, M. Vanillin as a Product of Ferulic Acid Biotransformation by the White-Rot Fungus Pycnoporus Cinnabarinus I-937: Identification of Metabolic Pathways. *J. Biotechnol.* **1994**, *37* (2), 123–132.

231 Lapadatescu, C.; Bonnarme, P. Production of Aryl Metabolites in Solid-State Fermentations of the White-Rot Fungus Bjerkandera Adusta. *Biotechnol. Lett.* **1999**, *21* (9), 763–769.

232 Chandra, P.; Arora, D. S.; Pal, M.; Sharma, R. K. Antioxidant Potential and Extracellular Auxin Production by White Rot Fungi. *Appl. Biochem. Biotechnol.* **2019**, *187* (2), 531–539.

233 Okamoto, K.; Ito, R.; Hayashi, J.; Tagawa, M. Production of the Antihypertensive Peptide Tyr-Pro from Milk Using the White-Rot Fungus Peniophora Sp. in Submerged Fermentation and a Jar Fermentor. *Dairy* **2021**, *2* (3), 452–461.

234 Subramaniyam, R.; Vimala, R. Solid State and Submerged Fermentation for the Production of Bioactive Substances : A Comparative Study. *Int. J. Sci. Nat.* **2012**, *3* (3), 480–486.

235 Vandelook, S.; Elsacker, E.; Van Wylick, A.; De Laet, L.; Peeters, E. Current State and Future Prospects of Pure Mycelium Materials. *Fungal Biol. Biotechnol.* **2021**, *8* (1), 1–10.

236 Sosa-Hernández, O.; Parameswaran, P.; Alemán-Nava, G. S.; Torres, C. I.; Parra-Saldívar, R. Evaluating Biochemical Methane Production from Brewer's Spent Yeast. *J. Ind. Microbiol. Biotechnol.* **2016**, *43* (9), 1195–1204.

237 Tri, C. L.; Khuong, L. D.; Kamei, I. Wood Rot Fungi in the Advanced Biofuel Production. *Fungal Biotechnol. Prospect. Ave.* **2022**, 367–382.

238 Kumar, S.; Dheeran, P.; Taherzadeh, M.; Khanal, S. *Fungal Biorefineries*; **2018**.

239 Taiz, L.; Zeiger, E. *Plant Physiology*; Sinauer Associates Inc, **2010**.

240 Niladevi, K. N. Ligninolytic Enzymes. In *Biotechnology for Agro-Industrial Residues Utilisation*; Nigam, P., Pandey, A., Eds.; Springer Netherlands, **2009**; pp 397–414.

241 Singh Nee Nigam, P.; Gupta, N.; Anthwal, A. Pre-Treatment of Agro-Industrial Residues. In *Biotechnology for Agro-Industrial Residues Utilisation*; Nigam, P., Pandey, A., Eds.; Springer Netherlands, **2009**; pp 13–33.

242 López-Abelairas, M.; Álvarez Pallín, M.; Salvachúa, D.; Lú-Chau, T.; Martínez, M. J.; Lema, J. M. Optimisation of the Biological Pretreatment of Wheat Straw with White-Rot Fungi for Ethanol Production. *Bioprocess Biosyst. Eng.* **2013**, *36* (9), 1251–1260.

243 Okamoto, K.; Nitta, Y.; Maekawa, N.; Yanase, H. Direct Ethanol Production from Starch, Wheat Bran and Rice Straw by the White Rot Fungus Trametes Hirsuta. *Enzyme Microb. Technol.* **2011**, *48* (3), 273–277.

244 Müller, H. W.; Trösch, W. Screening of White-Rot Fungi for Biological Pretreatment of Wheat Straw for Biogas Production. *Appl. Microbiol. Biotechnol.* **1986**, *24* (2), 180–185.

245 Mori, T.; Iwata, M.; Kimura, H.; Kawagishi, H.; Hirai, H.; Science, G. 木質バイオマスからのメタン発酵前処理に適した 白色腐朽菌の選抜. **2020**, *28* (2), 56–61.

246 Zhi, Z.; Wang, H. White-Rot Fungal Pretreatment of Wheat Straw with Phanerochaete Chrysosporium for Biohydrogen Production: Simultaneous Saccharification and Fermentation. *Bioprocess Biosyst. Eng.* **2014**, *37* (7), 1447–1458.

247 Zhang, H.; Yao, Y.; Deng, J.; Zhang, J. L.; Qiu, Y.; Li, G.; Liu, J. Hydrogen Production via Anaerobic Digestion

of Coal Modified by White-Rot Fungi and Its Application Benefits Analysis. *Renew. Sustain. Energy Rev.* **2022**, *157* (February), 112091.

248 Akunna, J. C. *Anaerobic Treatment of Brewery Wastes*; Elsevier Ltd, **2015**.

249 Elbeshbishy, E.; Dhar, B. R.; Nakhla, G.; Lee, H. S. A Critical Review on Inhibition of Dark Biohydrogen Fermentation. *Renew. Sustain. Energy Rev.* **2017**, *79* (May), 656–668.

250 Barbosa-Pereira, L.; Bilbao, A.; Vilches, P.; Angulo, I.; Lluis, J.; Fité, B.; Paseiro-Losada, P.; Cruz, J. M. Brewery Waste as a Potential Source of Phenolic Compounds: Optimisation of the Extraction Process and Evaluation of Antioxidant and Antimicrobial Activities. *Food Chem.* **2014**, *145*.

251 Janhom, T.; Wattanachira, S.; Pavasant, P. Characterization of Brewery Wastewater with Spectrofluorometry Analysis. *J. Environ. Manage.* **2009**, *90* (2), 1184–1190.

252 Dahiya, J.; Singh, D.; Nigam, P. Decolourisation of Synthetic and Spentwash Melanoidins Using the White-Rot Fungus Phanerochaete Chrysosporium JAG-40. *Bioresour. Technol.* **2001**, *78* (1), 95–98.

253 Pant, D.; Adholeya, A. Enhanced Production of Ligninolytic Enzymes and Decolorization of Molasses Distillery Wastewater by Fungi under Solid State Fermentation. *Biodegradation* **2007**, *18* (5), 647–659.

254 Mohana, S.; Acharya, B. K.; Madamwar, D. Distillery Spent Wash: Treatment Technologies and Potential Applications. *J. Hazard. Mater.* **2009**, *163* (1), 12–25.

255 Strong, P. J. Fungal Remediation and Subsequent Methanogenic Digestion of Sixteen Winery Wastewaters. *South African J. Enol. Vitic.* **2008**, *29* (2), 85–93.

256 Ray, S. G.; Ghangrekar, M. M. Bioresource Technology Enhancing Organic Matter Removal , Biopolymer Recovery and Electricity Generation from Distillery Wastewater by Combining Fungal Fermentation and Microbial Fuel Cell. *Bioresour. Technol.* **2015**, *176*, 8–14.

257 Aravind Kumar, J.; Sathish, S.; Krithiga, T.; Praveenkumar, T. R.; Lokesh, S.; Prabu, D.; Annam Renita, A.; Prakash, P.; Rajasimman, M. A Comprehensive Review on Bio-Hydrogen Production from Brewery Industrial Wastewater and Its Treatment Methodologies. *Fuel* **2022**, *319* (February), 123594.

258 Pandit, S.; Balachandar, G.; Das, D. Improved Energy Recovery from Dark Fermented Cane Molasses Using Microbial Fuel Cells. *Front. Chem. Sci. Eng.* **2014**, *8* (1), 43–54.

259 Wang, A.; Sun, D.; Cao, G.; Wang, H.; Ren, N.; Wu, W. M.; Logan, B. E. Integrated Hydrogen Production Process from Cellulose by Combining Dark Fermentation, Microbial Fuel Cells, and a Microbial Electrolysis Cell. *Bioresour. Technol.* **2011**, *102* (5), 4137–4143.

Chapter 3. Valorization of brewery waste slurry with glycerol as co-substrate for hydrogen and butyrate production using dark fermentation

Abstract

Among the methods to produce hydrogen biologically, dark fermentation stands out mainly due to its low operating requirements. However, hydrogen yields are lower compared to conventional technologies. Inexpensive organic wastes, such as brewing industry waste slurries and glycerol, can provide a cost-effective feedstock with the additional potential of generating value-added by-products, while addressing a wastewater treatment issue. The hydrogen production potential in dark fermentation of a high strength brewery waste slurry inoculated with a selected seed sludge, was assessed. The optimum conditions for hydrogen production included an initial COD concentration of 50 – 60 g/L, 6.4 pH and 30h HRT. The main end product was butyric acid, accounting for over 50% of the analysed carboxylic acids. The efficiency of the process on the basis of volume of H_2 obtained per gram of COD converted into organic acids was 393 ± 5 and 430 ± 6 mL without and with glycerol, respectively, and the molar ratio of H_2 per mol of substrate was 71% of the theoretical molar yield when the fermentation is dominated by butyrate as the end product. A proposed brewery sludge treatment system comprising dark fermentation followed by anaerobic digestion is promising and can be more advantageous than anaerobic digestion alone with recovery of valuable butyrate, a reduction in 4.3 kg of CO_2 emissions per cubic meter of sludge treated, with only a 24% net loss in energy potential.

3.1 Introduction

Beer is the third most popular beverage worldwide, a market worth 605 – 744 billion USD in 2020[1,2], although this industry has a large environmental footprint due to the high water use and production of high-strength organic waste. The brewing process requires 3 to 10 L of water per liter of beer produced with a typical wastewater to beer ratio of between 1.2 – 2.0[3,4]. Moreover, these residues typically contain an organic load

of 11 – 13 g/L soluble COD[5], although it can be as high as 200 g/L[6]. This becomes a problem when considering that all brewery wastewaters must be properly treated to meet regulatory discharge criteria, either to a municipal sewer system or to the environment. Nonetheless, the rich content of organic load can be exploited to valorise these residues.

The most common method applied to manage brewery sludge and wastewaters is treatment through anaerobic digestion[4,7], in which biogas is produced from the organic matter decomposition through a series of metabolic interactions between different groups of microorganisms. During the first stages, certain groups of bacteria hydrolyze complex macromolecules into simpler organic compounds (e.g., volatile fatty acids and alcohols), by obligately hydrogen-producing bacteria (including homoacetogens), generating H_2 and CO_2. These gases are consumed by acetogenic bacteria, producing acetate, and ultimately methane by methanogenic archaea. At the end of the process, depending on the nature of the digested substrate (dry or wet digestion), the methane composition can range between 0.4 – 0.8 L per g of volatile solids processed, with a methane to carbon dioxide ratio of 2:1, and small amounts of H_2S, N_2, H_2, water vapor, and other residual gases[8,9]. However, methanogenic archaea can be inhibited, either by physical or chemical pre-treatment, leading to a partial oxidation of the organic matter, but also to the accumulation of hydrogen[10]. This partial anaerobic digestion process is known as dark fermentation (DF), a process that has been gaining interest in recent years amid the development of low-carbon energy sources.

Hydrogen in DF is produced mainly through two metabolic pathways. Firstly, simple sugars, like glucose, are metabolized to pyruvate via glycolysis. In enteric bacteria, after pyruvate has been broken down to acetyl coenzyme, hydrogen is derived from formic acid by a formate hydrogen lyase complex, or FHL. In strict anaerobes, pyruvate is metabolized to acetyl coenzyme involving a pyruvate-ferredoxin oxireductases complex, or PFOR, producing hydrogen in the process from the reduction of protons by the action of hydrogenases in the presence of $Fe_{(red)}$[11,12]. Several end products can be metabolized from acetyl coenzyme, although only butyrate and acetate favour the

release of hydrogen. Theoretically, 4 mol H_2/mol of glucose can be produced via the acetate fermentation, and a maximum of 2 mol H_2/mol of glucose through the butyrate fermentation[13]. Nevertheless, the latter is more energetically favorable (**Eq. 3.1**), and, considering that a very low partial pressure of hydrogen is necessary to promote more hydrogen production from acetate ($<10^{-3}$ atm), the butyrate route by *Clostridium* spp. is often sought[14,15]. Although butyric acid appears to be the most toxic of organic acids in dark fermentation for hydrogen-producing bacteria[16,17], what it is certain is that energetically wise, in strict anaerobes like Clostridia, microorganisms prefer to produce the less acidic butyric acid[18]. Hence, in the pH range 5.5 – 7.0, butyrate is commonly seen as the main end-product[19,20], and below that, these microorganisms shift to solventogenesis, sporulate or die[21]. Moreover, at lower pH, ethanol and lactic acid begin to accumulate, with the latter's metabolism impeding hydrogen production[12,22]. Thus, to achieve the desired metabolic pathway, a proper treatment of the seed sludge is applied, which normally includes heat treatment, looking not only to supress the activity of methanogens, but also to reduce at the minimum the activity of the ubiquitous lactic acid bacteria. Hence, after pre-treatment, the seed sludge is mostly comprised of Clostridia species; about 70% – 80% of the hydrogen producers belong to this genus, coexisting with several other species of the genera *Enterobacter* spp., *Bacillus* spp., and *Enterococcus* spp.[14,23].

$$C_6H_{12}O_6 + 2H_2O \longrightarrow CH_3CH_2CH_2OOH + 2CO_2 + 2H_2 \qquad \Delta G^\circ = -255 \text{ kJ/mol} \qquad \textbf{(Eq. 3.1)}$$

$$C_6H_{12}O_6 + 2H_2O \longrightarrow 2CH_3COOH + 2CO_2 + 4H_2 \qquad \Delta G^\circ = -184 \text{ kJ/mol} \qquad \textbf{(Eq. 3.2)}$$

Among the methods to produce hydrogen biologically, DF is generally agreed to be more effective in comparison to other biocatalytic processes (*i.e.*, biophotolysis and photofermentation)[24–26]. Perhaps its most promising feature lies in two factors: 1), it is the natural process occurring in the first stages of anaerobic digestion as mentioned above; and 2), it requires low energy inputs, since the optimal conditions are mostly carried out at mesophilic conditions (25 – 45°C), and hydrogen yields are higher at low pressures[27,28]. In other words, DF is more environmentally friendly than other hydrogen production platforms. Some of the by-products can be recovered, valorising the

process even more. Butyric acid, for instance, (the major carboxylic acid produced as mentioned above), is widely used in several applications, from chemical, food, and pharmaceutical industries[29]. It is commonly obtained from the synthesis of petroleum-based propylene and represents a growing global market above $175 million USD (2020), sold at a unitary price of ~$1.8 USD per kg[30,31]. Nevertheless, hydrogen yields in dark fermentation are low (2 – 4 mol of H_2 per mol of glucose) compared to other conventional technologies, hence, currently DF continues to be relegated to small-scale applications[32,33], although inexpensive organic residues, with the additional potential of generating value-added by-products, can provide a cost-effective feedstock for hydrogen production while addressing a wastewater treatment issue.

Brewery wastewaters are an appropriate substrate for DF as demonstrated from previous studies, although at organic loading of COD <10 g/L and mostly supplemented with synthetic media (e.g., glucose, fructose, or xylose, plus micronutrients)[34–38]. Moreover, there are limited studies with the use of brewery wastewater and other co-substrates, while the mixture of municipal wastewaters supplemented with brewery residues as a co-substrate is commonly reported[8]. Some co-substrates investigated with brewery wastewater include cheese whey[39], corn[40], liquid swine manure[41], and brewer´s spent grain[42]. To the author's knowledge there is no literature reporting the co-mixture with glycerol, a substrate available in large surplus quantities as a by-product of biodiesel production and obtainable at low cost[43]. Theoretically, hydrogen can be obtained at a ratio of 3 moles per mol of glycerol[44] However, when it has been used as the sole carbon source in DF, this substrate has demonstrated low yields at mesophilic conditions (less than 0.1 mol H_2/mol glycerol at temperatures between 30 – 40°C)[45]. On the other hand, it is well documented that it can boost biogas production in anaerobic digestion[46]. Depending on factors such as mixing ratio, temperature, and HRT, the addition of glycerol to sewer sludge can improve methane yield (volume of CH_4 per g of VS added) in AD up to 115% – 176%[47]. Recent research has also reported that in the co-mixture of food waste and sewer sludge with glycerol at 1% and 3% v/v, in a two staged system DF/AD, glycerol improved hydrogen production by 48% and 87%, respectively, mainly due to the synergetic effect of the substrates' composition[48].

In view of the above, in addition to treating brewery wastewaters to produce hydrogen with butyrate as the principle by-product in DF, the use of a readily available co-substrate like glycerol, could serve to further increase hydrogen production.

Therefore, it is the aim of this work to optimize conditions for the valorization of high organic-loaded brewery wastewater for hydrogen and butyric acid production using an adapted inoculum and to evaluate the effect of glycerol as co-substrate on hydrogen yield. Furthermore, a proposed complete low-carbon solution for brewery sludge is described in **Figure 3.1** and consists of applying DF as a pre-treatment followed by anaerobic digestion to complete the conversion of residual organics, with hydrogen from the DF enriching the methane produced.

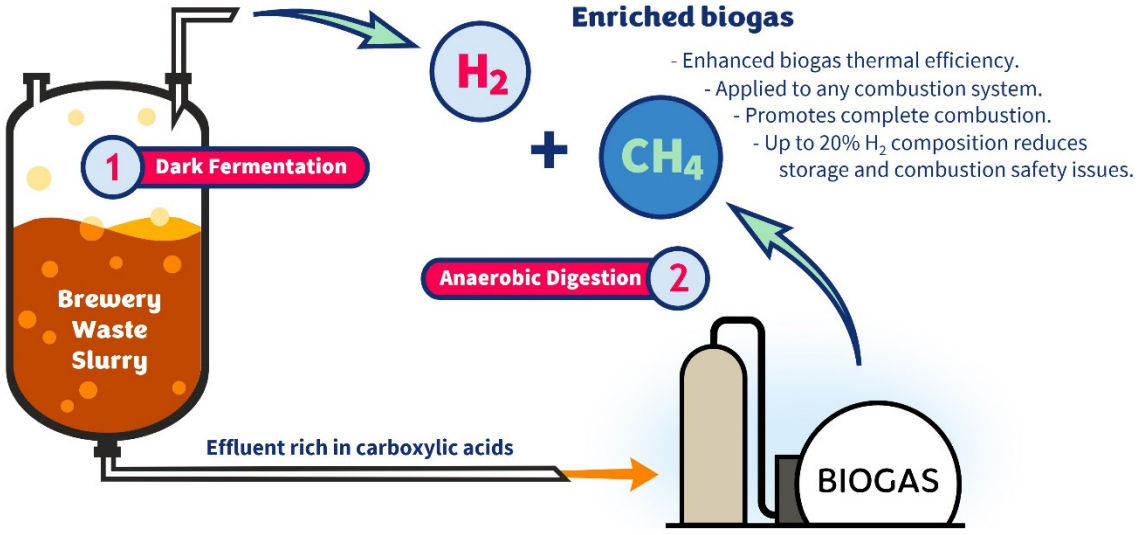

***Figure 3.1**. Proposed two-staged system Dark Fermentation/Anaerobic Digestion for hydrogen-enriched biogas from brewery waste slurry treatment.*

3.2 Materials and methods

3.2.1 Feedstocks, chemicals, and reagents

Two defined media were employed: Reinforced Clostridial Medium (RCM) (Oxoid™), and modified M9 medium (M9M). The salts and nutrients employed to prepare the latter were: KH_2PO_4 (Fisher Chemical™), $Na_2HPO_4{\cdot}7H_2O$ (EMD Millipore™), NaCl (Fisher BioReagents™), NH_4Cl (Sigma-Aldrich™), yeast extract (Thermo Scientific™), glycerol ≥99.5 % (Fisher Chemical™), and the trace salts $MgSO_4$ (Sigma-Aldrich™) and $CaCl_2$

(Fisher Chemical™). Besides KH_2PO_4, other buffer salts include K_2HPO_4 (Fisher Chemical™) and sodium acetate (Alfa Aesar™). This synthetic M9 medium was prepared according to the standard procedure shown elsewhere in[49], using a concentration of 5 g/L both of yeast extract and glycerol.

The standard solutions for the chromatography analysis were prepared using glacial acetic acid ≥99.5% (Fisher Scientific™), *n*-butyric acid ≥99.0 % (Sigma-Aldrich™), lactic acid 98.0% (Sigma-Aldrich™), formic acid 99.0 % (Thermo Scientific™), propionic acid ≥99.5% (Sigma-Aldrich™), and the mobile phase was prepared with H_2SO_4 0.5 N (LabChem®). The gases to obtain the calibration curves for spectrometric analysis (H_2, CO_2, CH_4), as well as argon as the carrier, were compressed, pure gases (≥99.9%), all provided by Linde® Canada.

3.2.2 Inoculum selection

The residue employed was a brewery waste slurry (BWS) obtained from a regional brewery in eastern Ontario, Canada (see **Table 1**). It contains slurry from the brewing process in addition to waste beer and does not include spent yeast. The BWS was first filtered through a conventional strainer with a gauze to remove gross solids, and then stored at 4°C for further experiments. Total suspended solids and soluble COD analysis were conducted after this coarse filtration.

Table 3.1. Characteristics of the brewery sludge after filtration.

COD	71.5 g/L
pH	4.2 – 4.5
Alkalinity	—
Total solids	24.8 – 30.1 g/L
Volatile solids	23.4 – 28.1 g/L
Total suspended solids	983 mg/L
Ammonia	17.3 – 24.7 mg/L

Two different sources of seed sludge were tested to obtain a suitable inoculum for the DF process. The first was obtained from an anaerobic digestor at a dairy farm located near the city of Ottawa. The second was obtained from the anaerobic digestor of the City of Ottawa's wastewater treatment plant (ROPEC WWTP). The two sludge samples were heat-treated (boiling for 2 h) to supress methanogens and activate the H_2-producing spores, as has been reported[14,50]. After heat treatment, a set of fermentations in two different defined media, RCM and M9M, were conducted with the aim of obtaining a suitable inoculum capable of producing butyric acid while suppressing the production of lactic acid. M9M is a minimal medium use to grow bacterial strains, particularly, *Escherichia coli*, although not limited to it, while RCM is formulated for the cultivation of *Clostridium* species, microorganisms responsible for butyric acid production in DF.

The fermentations were performed with a 30 mL working volume of each defined media in 120 mL serum bottles, inoculated with 1.3% v/v of each heat-treated sludge, then sparged with nitrogen (~3 min) to provide suitable anaerobic conditions, properly sealed with split stoppers and aluminium open-top seals, finally incubated in orbital agitation (120 rpm) at 35°C for 24 h. The bacterial culture that met the requirements was selected and cultured in a 50% BWS (same operational conditions), a provisional concentration of BWS before defining the desired BWS concentration for the ensuing DF experiments.

3.2.3 Optimization of organic loading

The effect of BWS organic strength on gas production was evaluated with the objective of maximizing % BWS. Three COD concentrations were evaluated: 1) 73.1 ± 1.6 g/L (100% BWS), 2) 59.8 ± 1.3 g/L (75% BWS), and 3) 46.9 ± 0.8 g/L (63% BWS). All were supplemented with 1 g/L of NH_4Cl. Triplicates were conducted with 120 mL working volume in 250 mL KIMEX medium bottles, sparged with nitrogen, then closed tightly with a hollow cap and self-sealing rubber stopper which allows inserting syringes to measure the gas volume in the headspace (water displacement method) and taking samples from the medium without opening the bottle to measure COD concentration.

Likewise, the bottles were incubated in orbital agitation (100 rpm) at 35°C for 24 h, or until no more gas was measured. The bottles were inoculated with the selected inoculum from the heat-treated sludge, at a ratio of 1.3% v/v of the total working volume. The pH throughout the first tests was left uncontrolled, but the initial pH of each treatment was set at 7.1 by increasing the alkalinity (addition of 100 mg/L of $CaCO_3$), and then adjusting with a 1M NaOH solution. All media and bottles were autoclaved (121°C, 15 psia for 20 min) before inoculation.

3.2.4 Effect of glycerol addition with uncontrolled pH

After finding the optimum COD concentration, the effect of adding 5 g/L glycerol was evaluated, following the same methodology: triplicates of 120 mL substrate in KIMEX bottles capped with self-sealing rubber stopper, inoculated after sterilization). Gas production and the change of COD were measured. The initial pH was 7.1 and left uncontrolled throughout the tests, conducted under anaerobic conditions during 48 h.

3.2.5 Optimization of pH

The effect of pH on gas production was evaluated at three pH values. In addition of alkalinity (100 mg/L of $CaCO_3$), the pH was adjusted to 6.4 with 0.03 M potassium phosphate buffer (8.9 mM K_2HPO_4 and 21.1 mM KH_2PO_4), pH 5.8 with 0.03 M potassium phosphate buffer (1.8 mM K_2HPO_4 and 28.3 mM KH_2PO_4), and pH 5.3 with 0.025 M acetate buffer solution (20.1 mM sodium acetate and 48.2 mM acetic acid). The pH 6.4 was selected after the optimization experiment and utilized in further experiments. As previous tests, triplicates were conducted with 120 mL working volume in 250 mL KIMEX medium bottles, autoclaved and under anaerobic conditions. Gas production, COD concentration and change in pH were measured.

3.2.6 Dark fermentation trial at optimal conditions

The experiments described above maintained the gas in the headspace of the serum bottles, which is appropriate for optimizing operational parameters, however, the hydrogen yield tends be lower due to the growth of its own partial pressure inside the

sealed bottles, pushing the gas into the liquid phase and to its own oxidation, thus reducing hydrogen collection[15].

Therefore, to accurately determine the hydrogen production, a different bottle setup was used. This consisted of a small glass reactor (max volume of 250 mL) properly sealed but provided with an inlet and outlet for the gas carrier inflow (Argon) to a mass spectrometer to detect the gases of fermentation, and with a sampling port, allowing to collect liquid samples without disrupting the system to determine pH, COD and organic acids produced. Optimal pH was adjusted at 6.4 as mentioned above. The temperature was kept at 35°C by submerging the reactor in a water bath. The small reactor, so as the medium were autoclaved (121°C, 15 psia for 20 min) before inoculation. Duplicate batches were conducted during 30 h.

3.2.7 Chemical analysis

The production of organic acids was determined by chromatography in an Agilent® HPLC Series 1200, using a Bio-Rad Aminex HPX-87H column, both Reflective Index and UV at 210 nm. The column was kept at 60°C and the RID at 50°C. Samples from the bottles were taken periodically, centrifuged (10,000 rpm, 10 min), and the supernatant was filtered with a hydrophobic PTFE syringe filter (0.22 µm). Finally, 20 µL of each sample was injected and diluted in H_2SO_4 5 mM as the mobile phase. The elution time of each sample was 25 min. The fermentation gases accumulated in the headspace of the bottles were analyzed by gas chromatography using a GOW-MAC series 350 Gas Chromatograph using a column mole sieve 5X column, setting the column at 35 °C, and the detector and injector at 180 °C and 50 °C, respectively. The flow rate was adjusted to 30 cm^3/min using helium as the gas carrier. Samples were taken periodically with a 1000 µL syringe. In the final trials, the gases were monitored continuously through mass spectroscopy during 30 h in a Dycor Proline Process Mass Spectrometer (Ametek® Instruments), carried by a stream of argon at 100 mL/min, flow rate monitored and controlled by a Horiba® VIA-510 Gas Analyzer. Finally, the COD was determined by the HACH® 8000 Reactor Digestion Method using high range vials (20 – 1,500 mg/L), in which 2 mL of diluted samples (50 – 10 times) were digested in a

HACH® DRB200 Dry Thermostat Reactor for 2 hours at 150°C. After cooling, the vials were read in a HACH® DR6000 UV-VIS Laboratory Spectrophotometer to obtain the COD value in mg/L.

3.2.8 Mathematical model for hydrogen production

The hydrogen production data was processed and modelled using a modified Gompertz function. Although this equation is not a predictive model, it is commonly used to model the parameters determining the hydrogen production yield, (as well as methane in the case of anaerobic digestion)[51,52].

$$H(t) = P \times \exp\left\{-\exp\left[\frac{2.71828 \cdot R_m}{P}(\lambda - t) + 1\right]\right\} \quad \textbf{(Eq. 3.3)}$$

Where $\boldsymbol{H(t)}$ is the cumulative hydrogen (mL) at a given time $\boldsymbol{t}$, $\boldsymbol{P}$ is the hydrogen production potential, also referred to ultimate hydrogen production (mL), λ is the lag phase (h), and $\boldsymbol{R_m}$ is the hydrogen production rate (mL/h). Data processing was carried out in Excel, fitting the RSE of the model versus the data obtained from the Mass-Spectrometer.

3.3 Results and discussion

3.3.1 Inoculum selection

The inoculum selection from two sludge sources and two growth media was determined primarily by the chromatographic analysis of the end products of each treatment. The organic acids produced from the two anaerobic sludge sources are presented in **Table 3.2**. The sludge from the dairy farm anaerobic reactor was inappropriate for hydrogen production with both growth media as butyric acid was barely produced, and lactic acid was the major end product. The sludge from the ROPEC WWTP cultivated in M9M yielded promising results with butyric acid as the main end product, while ROPEC WWTP sludge cultivated in RCM exhibited high lactic and low butyric acid production.

Table 3.2. Organic acids concentration in g/L after 24 hours of fermentation in two different anaerobic sludges, cultured in two different defined media: Reinforced clostridial medium (RCM), and modified minimal M9 medium (M9M)

	Dairy farm anaerobic sludge		WWTP anaerobic sludge	
Organic acids	RCM	M9M	RCM	M9M
Formic	0.5 ± 0.0	0.5 ± 0.1	0.4 ± 0.0	0.5 ± 0.1
Acetic	4.3 ± 0.4	3.7 ± 0.2	3.4 ± 0.4	0.3 ± 0.0
Lactic	10.9 ± 0.2	7.9 ± 1.1	5.7 ± 0.1	1.5 ± 0.1
Propionic	7.9 ± 0.5	1.9 ± 0.1	1.8 ± 0.2	0.6 ± 0.0
Butyric	1.0 ± 0.4	0.5 ± 0.0	0.4 ± 0.1	4.8 ± 0.3
Final pH (24 h)	3.7 ± 0.0	4.5 ± 0.1	4.3 ± 0.1	4.9 ± 0.1
Gas produced (mL)	12.1 ± 0.2	12.2 ± 0.3	10.9 ± 0.3	16.4 ± 0.5

It appears that RCM, rich in glucose and nitrogen sources, provided a better combination of nutrients for lactic acid producer development in both sludge sources. Furthermore, the optimum combination of ROPEC WWTP sludge and M9M produced the largest gas volume during the fermentation along with the highest final pH. Several studies observed that when the butyrate concentration is higher than that of acetate, there is more hydrogen produced[28,53,54]. Therefore, in all following experiments, the inoculum was always obtained from the heat-treated AD sludge from the ROPEC WWTP, cultured in minimal M9M, then transferred after 24 hours to a BWS medium before any DF experiment, at a certain concentration of BWS, discussed below.

3.3.2 Effect of organic loading

The impact of organic loading (g/L of COD) on the DF process was evaluated with the objective of maximizing the percent of brewery slurry in the fermentation (**Table 3.3**). Complete process inhibition was observed at 100% BWS (73 g/L COD), with no change in the initial pH and no gas produced. Therefore, with the particular seed sludge used, COD should be adjusted to a maximum of 60 g/L, corresponding to the highest gas production observed in this screening trial. In a similar experiment, Balachandar *et al.*[55]

Table 3.3. Optimum dilution of brewery waste slurry (BWS) for gas production.

	COD concentration (g/L)		pH[a]		Cumulative Gas
	Initial	Final	18 h	30 h	(mL/g of **COD consumed**)
100% BWS	73.1 ± 1.6	65.7 ± 2.0	7.1 ± 0.0	—	—
75% BWS	59.8 ± 1.3	43.2 ± 1.2	5.4 ± 0.2	4.7 ± 0.1	7.1 ± 0.1[b]
63% BWS	46.9 ± 0.8	30.9 ± 0.6	5.1 ± 0.1	4.7 ± 0.1	6.8 ± 0.2[b]

[a] initial pH = 7.1 (uncontrolled); [b] gas accumulated after 30 hours of fermentation

found the maximum hydrogen production, in batch mode, was attained by feeding a distillery effluent with 50 to 60 g/L of COD with no more hydrogen obtained by increasing the COD beyond that limit. Given the surprising complete inhibition observed at 100% BWS and no significant difference in gas produces between 65 and 75% BWS, the cause of the inhibition is unlikely directly related to the organic load or to the C:N ratio, which was the same for the three loading rates.

The complete inhibition at 100% BWS (73 g/L COD) suggests a toxicity toward the acid producers in the inoculum. The toxicity could be due to the presence of a diverse group of molecules commonly found in this type of slurry including humic and fulvic like compounds[56], diatomaceous earths employed in the clarification process of beers[57], melanoidins[58], and polyphenols[59]; all of which are known to have a certain degree of inhibitory effect[60,61]. At higher concentrations of brewery effluents the bacterial growth could be inhibited, particularly acidogens; bacteria directly involved in hydrogen production, which cannot absorb complex organic matter directly into the cell wall[62].

3.3.3 Effect of glycerol addition with uncontrolled pH

The addition of 5 g/L of glycerol increased gas production by 45% (**Figure 3.2**). This represents a 40% increase in gas volume per g COD removed (**Table 3.4**); which is similar to what has been reported with anaerobic digestion[46]. However, only 31% of the glycerol was consumed in the fermentation, possibly due to the choice of inoculum or to the drop in pH. Analysis of the gasses found no methane detected in both cases and 11.4% ± 1.3% CO_2 in the BWS with glycerol and 7.2% ± 0.9% without, indicating the presence of hydrogen in substantial quantities.

Table 3.4. COD removed, fermentation gases produced, maximum CO_2 detected, and final pH of the dark fermentation process of BWS (50 – 55 g/L COD) at 35°C with and without 5 g/L glycerol (BWS + Gro).

Treatment	COD (g/L)			Gas in the head space (mL)		Gas per grams of COD consumed (mL/g)	pH
	Initial	Final	%rem.	$\%CO_2$[†]	Cumulative	Total	Final
BWS	50.1 ± 0.2	31.5 ± 1.9	37.1	7.2 ± 0.9	94.3 ± 4.5	5.1 ± 0.7	5.1 ± 0.18
BWS + Gro	54.2 ± 1.5	35.2 ± 1.4	35.1	11.4 ± 1.3	136.6 ± 7.3	7.2 ± 0.3	5.0 ± 0.15

[†] maximum peak of gas, measured at 30 h.

A strong decline in COD was observed during the first 6 hrs of fermentation, both with and without glycerol, and coinciding with limited gas production. This suggests that the initial COD removed was due to the hydrolysis of more complex molecules in the medium. The initial rate of COD reduction was lower with the addition of glycerol suggesting either an inhibition of the hydrolyzing bacteria or a competition between substrates. Peak gas production was observed between the 18th and the 30th hour, with the subsequent decline likely due to a combination of substrate limitation and low pH, as the pH declined from 7.1 to approximately 5.0 at 48 hrs.

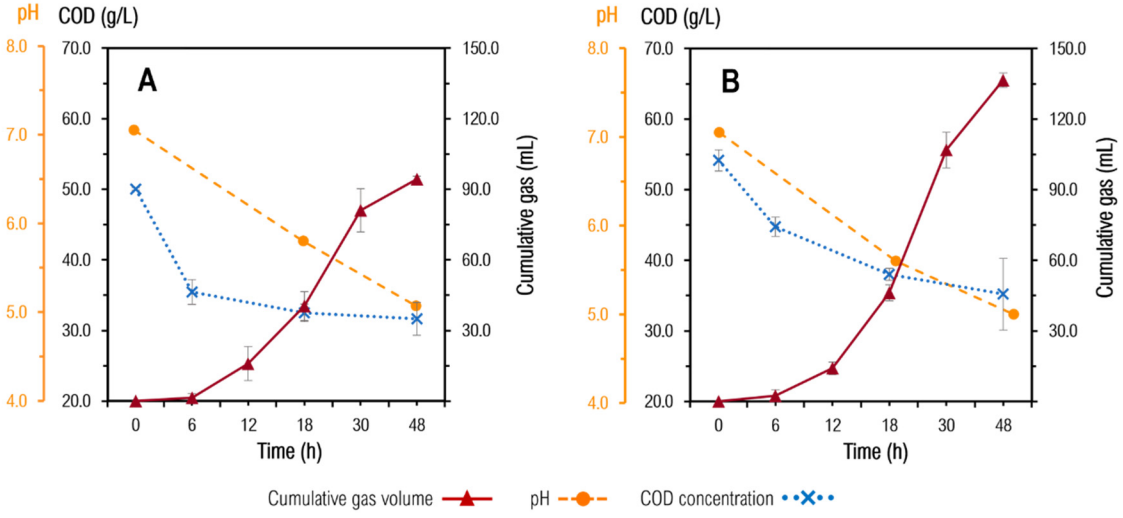

***Figure 3.2**. Cumulative gas produced, COD concentration and pH drop throughout the dark fermentation process in capped bottles during 48 hours of A) brewery waste slurry alone, B) supplemented with 5 g/L of glycerol.*

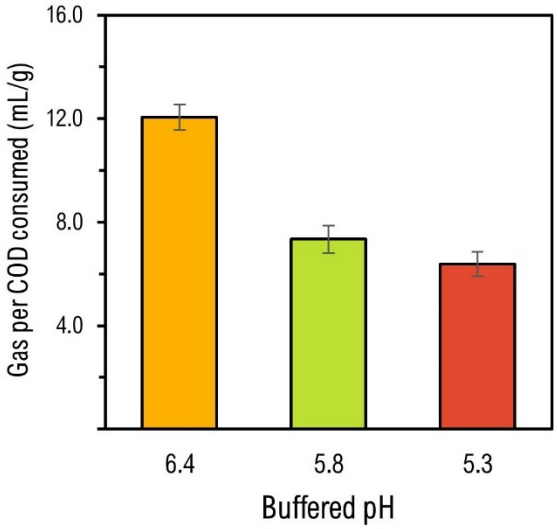

***Figure 3.3**. Fermentation gases produced per gram of COD consumed (mL/g) at each different buffered pH.*

3.3.4 Effect of pH

BWS fermentations were conducted at controlled pH conditions spanning the potential optimum range for hydrogen production while remaining below pH 6.5, the lower limit for effective methanogenesis[63]. The highest gas production was observed at pH 6.4 (12.1 ± 0.2 mL/g COD), with significantly lower volumes recorded at both pH 5.8 and 5.3 (**Figure 3.3**). COD reductions were similar at pH 6.4 and 5.8 with 38% and 39% reduction, respectively, while only 28% COD reduction was observed at pH 5.3. The role of hydrogenases in biohydrogen production systems is vital, since these are the enzymes responsible of H_2 formation from the excess of electrons and protons in the fermentation broth, and like many other enzymes, they are strongly pH dependant[64]. It is well known that at pH lower than 5.0 the activity of hydrogenases begins to fail, in addition to the observed behaviour below this pH value, where the lactic acid route is favoured, and the butyric fermentation route shifts into solventogenesis, leading to an irretrievable cessation of gas production[65]. Standard H^+/H_2 reduction potentials observed for hydrogenases *in vitro* are found between pH 5.5 – 7.0, and the optimal condition at pH 6.0[66]. The suitable pH for hydrogenases activity *in vivo* ranges between 5.0 – 6.5, with optimal conditions at 6.0[67], and in in many strains, including *Escherichia coli*, 5.5 is the optimum[68]. The optimum pH of 6.4 identified in this study corresponds to other reports using food wastes in DF, where the best performance was found at pH 6.0 – 6.5[69–71], in contrast to pH 5.5, referred to as the optimum in some reviews[14,22].

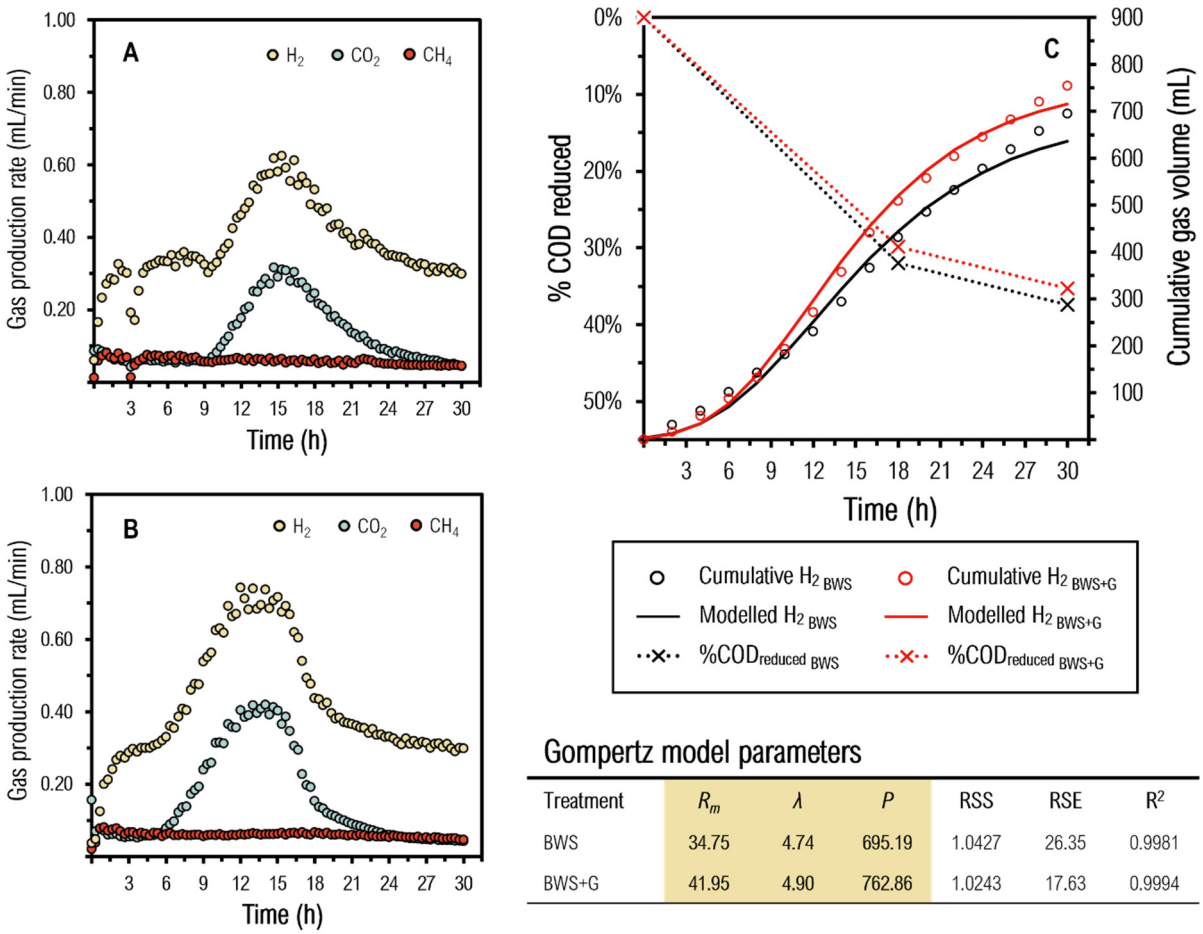

Gompertz model parameters

Treatment	R_m	λ	P	RSS	RSE	R^2
BWS	34.75	4.74	695.19	1.0427	26.35	0.9981
BWS+G	41.95	4.90	762.86	1.0243	17.63	0.9994

Figure 3.4*. Production rate (mL/min) of hydrogen (○), carbon dioxide (○), and methane (●) during the treatment of A), 50 – 60 g/L COD waste slurry alone; B), with the addition of glycerol (5 g/L). C), Gompertz Model of gas production (mL) of hydrogen and the percentage of COD reduced in brewery waste slurry alone and with the addition of glycerol (5 g/L).*

3.3.5 Dark fermentation at optimum conditions with and without glycerol addition

A final set of fermentation experiments were conducted at the optimum conditions of 50 – 60 g/L COD and pH buffered to 6.4, although the pH declined to between pH 5.7-5.9 after 30 h of fermentation. Hydrogen was produced from the beginning of the batch fermentations and attained a maximum average flow rate of 35.2 ± 0.7 mL H_2/h after 15 hrs without glycerol and 42.0 ± 0.8 mL H_2/h after 12 hrs with glycerol, similar to what has been reported in the literature[72]. Beyond the maximum peak of activity, the gas production substantially dropped in both treatments (**Figure 3.4 A,B**). This pattern is also observed with the COD consumption rate after the 18th hour. The total cumulative

volume of hydrogen produced in the BWS with glycerol was 762 mL H_2/L BWS, which is 9.7% more than in BWS alone (694 mL H_2/L BWS), corresponding to a 10.0% increase in H_2 produced per gram of COD consumed with the addition of glycerol (**Table 3.5**).

The content of H_2 in the biogas was approximately two thirds of the total gas volume both with and without glycerol, which is similar to that reported by Wicher *et al.*[73] with a lower strength distillery wastewater. The Gompertz model (**Figure 3.4 C**) fit the data very well with maximum modelled flow rates (R_m) of 42.0 mL H_2/h and 34.8 mL H_2/h, with and without the addition of glycerol, respectively. In both cases, the lag phase was between 4.5 and 5.0 hours. In order to maximize hydrogen production, methanogenesis must be suppressed as hydrogen is consumed in the formation of methane. Methane was detected, but in low quantities, with a steady rate of approximately 0.045–0.046 mL CH_4/min and a total cumulative volume of 15% of the H_2 produced from both treatments.

Regarding the end products of the fermentation, the primary organic acid detected was butyric acid in both treatments, followed by lactic acid and propionic acid. A rapid acidification can be related to the profile of carboxylic acids produced during the first half of the fermentation (**Figure 3.5 A, B**). It appears that the process approached a stationary phase at the 18th hour, given the cessation of carboxylic acids production, which coincides, again, with a decline in the rate of COD reduction (**Figure 3.4 C**). It is to be noted that the concentration of acetic acid was the lowest volatile acid in both treatments, clearly indicating that the preferred metabolic pathway is the butyrate-type fermentation. In both cases, from the 18th hour to the 30th hour, the concentration of acetic, and butyric acid remained fairly constant, indicating that COD converted into formate is largely responsible for the remaining hydrogen produced. As seen before, only 31%– 32% glycerol was consumed.

With the additional glycerol, hydrogen production increased by 10% mL per g of COD consumed. This represents half of the theoretical molar yield of the depleted glycerol (47.9% on the basis of the difference of volume produced per L of BWS). The yield here presented (1.44 mol H_2/mol of glycerol) falls within the expected yield in mesophilic conditions in the reported literature[74].

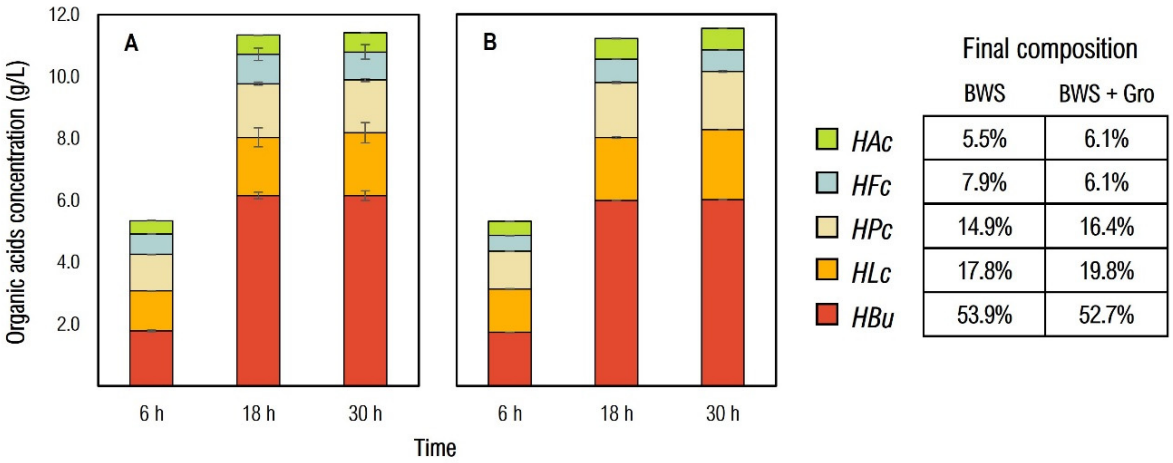

***Figure 3.5**. Main organic acids produced and final composition after 30 h of dark fermentation at initial buffered pH 6.4 in A), brewery waste slurry alone (BWS); and B), with 5 g/L of glycerol (BWS + Gro). HAc, acetic acid; HFc, formic acid; HPc, propionic acid, HLc, lactic acid; HBu, butyric acid.*

Experimental hydrogen production yield in the BWS (without glycerol), based on the stoichiometry of the reported primary metabolic pathways for the formation of butyric, acetic, and formic acids from glucose, was 1.7 mol H_2/mol of glucose, or 71% of the theoretical maximum yield defined by Zhang *et al.*[29] when butyrate is the predominant end product.

Hydrogen yield on the basis of COD consumed is typically reported around 100 mL H_2/g COD[75]. In this study, 331.3 ± 7.1 mL H_2/g COD consumed with glycerol added, and 299.7 ± 11.0 mL H_2/g COD without was attained (**Table 3.5**). There is scarce literature regarding hydrogen production from brewery wastewaters, and the existing literature is difficult to compare as the brewery wastewaters were largely diluted and supplemented, normally with glucose, to attain a certain COD concentration (2 – 10 g/L COD initial)[36,37,70], whereas in other cases, hydrogen production is overlooked by the methane potential instead[6]. In a study using distillery effluent with the same initial COD as this study, 1,156 ± 25 mL H_2/L was reported, which is 5 to 6 times lower than the present work[55]. On the other hand, a continuous UASB reactor fed with 34 g COD/L rice winery wastewater produced similar results to this study with a maximum yield of 1.74 mol H_2/mol of hexose, 4% less than the molar ratio estimated for the BWS without glycerol in this study, but at a pH of 5.5[76].

Table 3.5. Hydrogen production during dark fermentation of BWS at 35°C with and without 5 g/L glycerol. Performance comparison with similar residues.

Substrate	Inoculum	Reactor type	Temp. (°C)	pH	COD initial (g/L)	H_2 yield				Ref.
						mL H_2/L	mL H_2/g COD†	mL H_2/g COD‡	mL H_2/g VS‡	
Brewery waste slurry	Anaerobic sludge	Batch	35	6.4	50.1	5,785 ± 72	299.7 ± 11.0	112.1 ± 4.1	226.5 ± 20.7	This study
Brewery waste slurry + glycerol (5 g/L)	Anaerobic sludge	Batch	35	6.4	54.2	6,351 ± 89	331.3 ± 7.1	117.0 ± 2.5	248.7 ± 22.7	This study
Distillery effluent	*Enterobacter cloacae*	Batch	37	6.5*	50.0	1,156 ± 25	23.1 ± 0.5	—	—	55
Brewery effluent	Mutated *E. aerogenes* and *Rhodobacter* M 19	Batch	31	6.9	—	2,877	—	—	—	71
Brewery effluent	Anaerobic sewer sludge	UASB	55	6.5	>3.6	17 ± 0.3	—	—	—	70
Brewery wastewater	*Klebsiella pneumoniae*	ASBBR	35	5.5	~10.0	455 ± 15	—	45.9 ± 1.1	—	38
Brewery wastewater + glucose-based synthetic medium	Anaerobic sludge	Batch	35.9	5.95	6.1	—	—	147	—	37
Distillery wastewater	Activated sludge	Batch	37	5.5	5.6	1,030 ± 25	185.0 ± 5.0	64.4 ± 1.6	—	73
Tequila vinasses	Anaerobic sludge	CSTR	35	6.5 – 5.8	~86.0	2,600 ± 100	—	31.2 ± 1.8	—	77
Vinasses	Anaerobic sludge	Batch	25	5.5	0.25	—	—	579	—	78
Food waste + sewage sludge + glycerol	Anaerobic sludge	Batch	35	5.5	—	212.4	—	—	177	48
Food waste + primary sludge + waste activated sludge	Anaerobic digested sludge	Batch	37	5.5	~90.0	6,800 ± 430	—	76 ± 4.3	165 ± 13	79

† COD consumed; ‡ COD and VS initial; * Unregulated pH

Another study explored tequila vinasses (57.7 g COD/L) in a CSTR at 35°C and controlled pH between 5.8 – 6.5, although with a particular inoculum (ATCC PTA-124566), comprised by lactic acid bacteria, *Acetobacter* and *Clostridium*. The authors obtained a yield of 124 ± 9.0 mL H_2/g VS added[80], which is approximately half of the yield obtained in the present study. Other similar works are summarized in **Table 3.5**.

3.4 Proposed two-staged Dark Fermentation-Anaerobic Digestion System

Dark fermentation of BWS can be applied as a first stage of treatment to produce hydrogen and butyric acid, followed by a second stage anaerobic digestion process to remove remaining COD, and produce methane, as shown in **Figure 3.1**. The dark fermentation (without glycerol) reduced the initial COD by 37% (18.5 g/L), produced organic acids representing 34% of the initial COD (17 g/L) leaving a residual 29% COD (14.5 g/L) consisting of more complex organic matter.

The amount of butyric acid produced represents more than 50% of the total carboxylic acids in the medium, and if it is separated from the fermentation effluent prior to anaerobic digestion (considering a 88% recovery efficiency as described in[31]), it would represent a reduction of 4.3 kg of CO_2 emissions per cubic meter of BWS treated, with a potential value of $9.54 USD/$m^3$ BWS. However, more studies need to be done to determine the feasibility of this approach.

The energy value from anaerobic digestion can be estimated from literature to compare with anaerobic digestion in a second stage. The biochemical methane potential (BMP) from anaerobically treated brewery wastewaters, typically reported in the range from 150 to 360 mL of methane per COD removed[81–84], with bioremediation efficiencies between 78% – 98%[8]. Therefore, considering a 90% COD removal efficiency, an average conversion rate of 283 mL CH_4/g COD removed, and NTP values of both CH_4 and H_2[85], the BMP of the effluent from the dark fermentation would account for roughly 290 kJ/L BWS, which in addition to the 70 kJ/L BWS from the energy content of hydrogen produced in DF, represents 78% of the gross bioconversion into methane if the BWS were to be fully digested. The hydrogen/methane ratio corresponds to 24% hydrogen in the mixture. It is known that 10% – 30% hydrogen in the biogas mixture

positively impacts the energy input and the efficiency of machines already working on methane, bringing more complete combustion, thus reducing CO and NOx emission in lean conditions[86,87].

In view of the above, therefore, it is an attractive approach to apply a two-staged treatment strategy for brewery wastewaters to extract a valuable chemical compound such as butyric acid, which can be also used to obtain other biofuels (*e.g.*, butanol) derived from it[88], reducing CO_2 emission while maintaining 78% of the biogas potential energy content. Or a simpler approach would be to convert all the organic acids into methane and enhanced energy production with the addition of hydrogen. With this approach a 24% increased in energy output could be achieved compared to single-stage anaerobic digestion.

3.5 Conclusions

In summary, high strength slurry from the beer industry is a suitable substrate for hydrogen production in dark fermentation. The optimum conditions determined by this study include a heat-treated inoculum from a municipal sludge anaerobic digester, an initial COD between 50 – 60 g/L, and controlled pH of 6.4, in 30 h batch reactions at 35°C. Adding 10% w/w of glycerol as COD generated only 10% more hydrogen, however, only 31% of the glycerol was consumed. A total of 331 mL H_2/g COD consumed was observed versus 300 mL H_2/g COD consumed without glycerol, with both results higher than comparable reported literature using brewery wastewaters and other similar wastes. The optimal pH of 6.4 was higher than what is generally reported. The organic acids generated accounted for 67% – 71% of the remaining COD with butyric acid as the main by-product. A brewery sludge treatment system comprising dark fermentation followed by anaerobic digestion shows great promise with the recovery of valuable butyrate, a reduction in 4.3 kg of CO_2 emissions per cubic meter of BWS treated, and only a 24% net loss in energy potential.

References

1 Chouhan, N.; Vig, H.; Deshmukh, R. *Beer Market*, Available at: https://www.alliedmarketresearch.com/beer-market (accessed Jun 4, 2022).

2 Fortune Business Insights. *Beer Market*, Available at: https://www.fortunebusinessinsights.com/beer-market-102489 (accessed Jun 4, 2022).

3 Ashraf, A.; Ramamurthy, R.; Rene, E. R. Wastewater Treatment and Resource Recovery Technologies in the Brewery Industry : Current Trends and Emerging Practices. *Sustain. Energy Technol. Assessments* **2021**, *47* (June), 101432.

4 Brito, A. G.; Peixoto, J.; Oliveira, J. M.; Oliveira, J. A.; Costa, C.; Nogueira, R.; Rodrigues, A. Brewery and Winery Wastewater Treatment: Some Focal Points of Design and Operation. In *Utilization of By-Products and Treatment of Waste in the Food Industry*; Oreopoulou, V., Russ, W., Eds., **2007**; pp 109–131.

5 Simate, G. S.; Cluett, J.; Iyuke, S. E.; Musapatika, E. T.; Ndlovu, S.; Walubita, L. F.; Alvarez, A. E. The Treatment of Brewery Wastewater for Reuse : State of the Art. *DES* **2011**, *273* (2–3), 235–247.

6 Sinbuathong, N.; Somjit, C.; Leungprasert, S. Feasibility Study for Biohydrogen Production from Raw Brewery Wastewater. **2015**, No. March, 1769–1777.

7 Keenan, J. D.; Kormi, I. Anaerobic Digestion of Brewery By-Products. *Water Pollut. Control Fed.* **1981**, *53* (1), 66–77.

8 Arantes, M. K.; Alves, H. J.; Sequinel, R.; da Silva, E. A. Treatment of Brewery Wastewater and Its Use for Biological Production of Methane and Hydrogen. **2017**, *42*, 26243–26256.

9 Komilis, D.; Barrena, R.; Grando, R. L.; Vogiatzi, V.; Sánchez, A.; Font, X. A State of the Art Literature Review on Anaerobic Digestion of Food Waste: Influential Operating Parameters on Methane Yield. *Rev. Environ. Sci. Biotechnol.* **2017**, *16* (2), 347–360.

10 Torquato, L. D. de M.; de Almeida, S.; de Oliveira, J. E.; Crespi, M. S.; Maintinguer, S. I. Thermal Characterization of Anaerobic Sludges from Wastewater Treatments Applied to Biological Generation of H2. *J. Therm. Anal. Calorim.* **2017**, *127* (2).

11 Hallenbeck, P. C. Bioenergy from Microorganisms: An Overview. In *Microbial BioEnergy: Hydrogen Production*; **2014**; Vol. 38, pp 3–21.

12 Redwood, M. D.; Paterson-Beedle, M.; MacAskie, L. E. Integrating Dark and Light Bio-Hydrogen Production Strategies: Towards the Hydrogen Economy. *Rev. Environ. Sci. Biotechnol.* **2009**, *8* (2), 149–185.

13 Baeyens, J.; Zhang, H.; Nie, J.; Appels, L.; Dewil, R.; Ansart, R.; Deng, Y. Reviewing the Potential of Bio-Hydrogen Production by Fermentation. *Renew. Sustain. Energy Rev.* **2020**, *131*.

14 Khanal, S. K. Biohydrogen Production: Fundamentals, Challenges, and Operation Strategies for Enhanced Yield. In *Anaerobic biotechnology for bioenergy production: principles and applications*; Khanal, S. K., Ed.; Wiley-Blackwell, **2008**; pp 189–219.

15 Levin, D. B.; Pitt, L.; Love, M. Biohydrogen Production: Prospects and Limitations to Practical Application. *Int. J. Hydrogen Energy* **2004**, *29* (2). https://doi.org/10.1016/S0360-3199(03)00094-6.

16 Bundhoo, M. A. Z.; Mohee, R. Inhibition of Dark Fermentative Bio-Hydrogen Production: A Review. *Int. J. Hydrogen Energy* **2016**, *41* (16), 6713–6733. https://doi.org/10.1016/j.ijhydene.2016.03.057.

17 Chen, Y.; Yin, Y.; Wang, J. Influence of Butyrate on Fermentative Hydrogen Production and Microbial Community Analysis. *Int. J. Hydrogen Energy* **2021**, *46* (53), 26825–26833.

18 Doelle, H. W. Fermentation. In *Bacterial Metabolism (Second Edition)*; **1975**; pp 559–692.

19 Detman, A.; Mielecki, D.; Chojnacka, A.; Salamon, A.; Błaszczyk, M. K. Cell Factories Converting Lactate and Acetate to Butyrate : Clostridium Butyricum and Microbial Communities from Dark Fermentation Bioreactors. *Microb. Cell Fact.* **2019**, 1–12.

20 Guo-qing, H. E.; Qing, K.; Qi-he, C.; Hui, R. Batch and Fed-Batch Production of Butyric Acid by Clostridium Butyricum ZJUCB. **2005**, No. 11, 1076–1080.

21 Das, D.; Khanna, N.; Dasgupta, C. N. *Biohydrogen Production*; **2014**.

22 Gopalakrishnan, B.; Khanna, N.; Das, D. *Dark-Fermentative Biohydrogen Production*; **2019**.

23 Wang, J.; Yin, Y. Principle and Application of Different Pretreatment Methods for Enriching Hydrogen-Producing Bacteria from Mixed Cultures. *Int. J. Hydrogen Energy* **2017**, *42* (8), 4804–4823.

24 Krupp, M. *Biohydrogen Production from Organic Waste and Wastewater by Dark Fermentation - a Promising Module for Renewable Energy Production*; Shaker Verlag: Aachen, **2007**.

25 Chandrasekhar, K.; Lee, Y. J.; Lee, D. W. Biohydrogen Production: Strategies to Improve Process Efficiency through Microbial Routes. *Int. J. Mol. Sci.* **2015**, *16* (4), 8266–8293.

26 Wang, J.; Yin, Y. Introduction. In *Biohydrogen Production from Organic Wastes*; **2017**; pp 1–17.

27 Sagir, E.; Hallenbeck, P. C. Photofermentative Hydrogen Production. In *Biohydrogen*; **2019**; pp 141–157.

28 Rafa, Ł.; Ho, I.; Kucharska, K.; Glinka, M.; Rybarczyk, P. Hydrogen Production from Biomass Using Dark Fermentation. **2018**, *91* (April), 665–694.

29 Zhang, C.; Yang, H.; Yang, F.; Ma, Y. Current Progress on Butyric Acid Production by Fermentation. *Curr. Microbiol.* **2009**, *59* (6), 656–663.

30 Ahuja, K.; Bayas, S. *Global Butyric Acid Market*, Available at: https://www.gminsights.com/industry-analysis/butyric-acid-market (accessed Jul 22, 2022).

31 Salvachu, D.; Nelson, R. S.; Beckham, G. T.; Karp, E. M.; Linger, J. G.; Saboe, P. O.; Nelson, R. S.; Singer, C.; Mcnamara, I.; Cerro, C.; Chou, Y.; Mohagheghi, A.; Peterson, D. J.; Haugen, S.; Cleveland, N. S.; Monroe, H. R.; Guarnieri, M. T.; Tan, E. C. D.; Beckham, G. T.; Karp, E. M.; Linger, J. G. Process Intensification for the Biological Production of the Fuel Precursor Butyric Acid from Biomass. *Cell Reports Phys. Sci.* **2021**, No. 2, 1–20.

32 Swartz, J. Opportunities toward Hydrogen Production Biotechnologies. *Curr. Opin. Biotechnol.* **2020**, *62*, 248–255.

33 Wang, J.; Yin, Y. Introduction. In *Biohydrogen Production from Organic Wastes*; Wang, J., Yin, Y., Eds.; Springer Nature Singapore Pte Ltd: Singapore, **2017**; pp 1–17.

34 Pachiega, R.; Sakamoto, I. K.; Varesche, M. B.; Hatanaka, R. R.; de Oliveira, J. E.; Maintinguer, S. I. Obtaining and Characterization of Mesophilic Bacterial Consortia from Tropical Sludges Applied on Biohydrogen Production. *Waste and Biomass Valorization* **2019**, *10* (6).

35 Estevam, A.; Arantes, M. K.; Andrigheto, C.; Fiorini, A.; da Silva, E. A.; Alves, H. J. Production of Biohydrogen from Brewery Wastewater Using Klebsiella Pneumoniae Isolated from the Environment. *Int. J. Hydrogen Energy* **2018**, *43* (9).

36 Chu, C. Y.; Tung, L.; Lin, C. Y. Effect of Substrate Concentration and PH on Biohydrogen Production Kinetics from Food Industry Wastewater by Mixed Culture. *Int. J. Hydrogen Energy* **2013**, *38* (35), 15849–15855.

37 Shi, X.; Jin, D.; Sun, Q.; Li, W. Optimization of Conditions for Hydrogen Production from Brewery Wastewater by Anaerobic Sludge Using Desirability Function Approach. *Renew. Energy* **2010**, *35* (7), 1493–1498.

38 Arantes, M. K.; Sequinel, R.; Alves, H. J.; Machado, B.; Fiorini, A.; da Silva, E. A. Improvement of

Biohydrogen Production from Brewery Wastewater: Evaluation of Inocula, Support and Reactor. *Int. J. Hydrogen Energy* **2020**, *45* (8), 5216–5226.

39 Cruz-López, A.; Cruz-Méndez, A.; Suárez-Vázquez, S. I.; Reyna-Gómez, L. M.; Pecina-Chacón, D. E.; de León Gómez, H. Effect of Hydraulic Retention Time on Continuous Biohydrogen Production by the Codigestion of Brewery Wastewater and Cheese Whey. *Bioenergy Res.* **2022**, No. 0123456789.

40 Le, E.; Jacob, G.; Alberto, L. ScienceDirect A Novel Biohydrogen Production Process : Co-Digestion of Vinasse and Nejayote as Complex Raw Substrates Using a Robust Inoculum. **2016**, *2*, 0–11.

41 Xu, S.; Zhu, J.; Meng, Z.; Li, W.; Ren, S.; Wang, T. Bioresource Technology Hydrogen and Methane Production by Co-Digesting Liquid Swine Manure and Brewery Wastewater in a Two-Phase System. *Bioresour. Technol.* **2019**, *293* (July), 122041. https://doi.org/10.1016/j.biortech.2019.122041.

42 Sganzerla, W. G.; Sillero, L.; Forster-Carneiro, T.; Solera, R.; Perez, M. Determination of Anaerobic Co-Fermentation of Brewery Wastewater and Brewer's Spent Grains for Bio-Hydrogen Production. *BioEnergy Res.* **2022**.

43 He, Q. (Sophia); McNutt, J.; Yang, J. Utilization of the Residual Glycerol from Biodiesel Production for Renewable Energy Generation. *Renew. Sustain. Energy Rev.* **2017**, *71*, 63–76.

44 Maru, B. T.; Constanti, M.; Stchigel, A. M.; Medina, F.; Sueiras, J. E. Biohydrogen Production by Dark Fermentation of Glycerol Using Enterobacter and Citrobacter Sp. *Biotechnol. Prog.* **2013**, *29* (1), 31–38.

45 Viana, Q. M.; Viana, M. B.; Vasconcelos, E. A. F.; Santaella, S. T.; Leitão, R. C. Fermentative H2 Production from Residual Glycerol: A Review. *Biotechnol. Lett.* **2014**, *36* (7), 1381–1390.

46 Athanasoulia, E.; Melidis, P.; Aivasidis, A. Co-Digestion of Sewage Sludge and Crude Glycerol from Biodiesel Production. *Renew. Energy* **2014**, *62*, 73–78.

47 Chow, W. L.; Chong, S.; Lim, J. W.; Chan, Y. J.; Chong, M. F. Anaerobic Co-Digestion of Wastewater Sludge : A Review of Potential Co-Substrates and Operating. *Processes* **2020**, *8(1)* (39), 1–21.

48 Silva, F. M. S.; Mahler, C. F.; Oliveira, L. B.; Bassin, J. P. Hydrogen and Methane Production in a Two-Stage Anaerobic Digestion System by Co-Digestion of Food Waste, Sewage Sludge and Glycerol. *Waste Manag.* **2018**, *76*, 339–349.

49 Reiche, A.; Kirkwood, K. M. Comparison of Escherichia Coli and Anaerobic Consortia Derived from Compost as Anodic Biocatalysts in a Glycerol-Oxidizing Microbial Fuel Cell. *Bioresour. Technol.* **2012**, *123*, 318–323.

50 Ghimire, A.; Frunzo, L.; Pontoni, L.; Lens, P. N. L.; Esposito, G.; Pirozzi, F. Dark Fermentation of Complex Waste Biomass for Biohydrogen Production by Pretreated Thermophilic Anaerobic Digestate. **2015**, *152*, 43–48.

51 Wang, J.; Yin, Y. Kinetic Models for Hydrogen Production. In *Biohydrogen Production from Organic Wastes*; **2017**; pp 269–290.

52 Sosa-Hernández, O.; Parameswaran, P.; Alemán-Nava, G. S.; Torres, C. I.; Parra-Saldívar, R. Evaluating Biochemical Methane Production from Brewer's Spent Yeast. *J. Ind. Microbiol. Biotechnol.* **2016**, *43* (9), 1195–1204.

53 Usmanbaha, N.; Jariyaboon, R.; Reungsang, A.; Kongjan, P.; Chu, C.-Y. Optimization of Batch Dark Fermentation of Chlorella Sp. Using Mixed-Cultures for Simultaneous Hydrogen and Butyric Acid Production. *Energies* **2019**, *12*, 2529–2543.

54 Reungsang, A.; Sreela-or, C.; Plangklang, P. Non-Sterile Bio-Hydrogen Fermentation from Food Waste in a Continuous Stirred Tank Reactor (CSTR): Performance and Population Analysis. *Int. J. Hydrogen Energy* **2013**, *38* (35), 15630–15637.

55 Balachandar, G.; Varanasi, J. L.; Singh, V.; Singh, H.; Das, D. Biological Hydrogen Production via Dark Fermentation: A Holistic Approach from Lab-Scale to Pilot-Scale. *Int. J. Hydrogen Energy* **2020**, *45* (8), 5202–5215.

56 Janhom, T.; Wattanachira, S.; Pavasant, P. Characterization of Brewery Wastewater with Spectrofluorometry Analysis. *J. Environ. Manage.* **2009**, *90* (2), 1184–1190.

57 Thiago, R. dos S. M.; Pedro, P. M. de M.; Eliana, F. C. S. Solid Wastes in Brewing Process: A Review. *J. Brew. Distill.* **2014**, *5* (1), 1–9.

58 Coghe, S.; Gheeraert, B.; Michiels, A.; Delvaux, F. R. Development of Maillard Reaction Related Characteristics during Malt Roasting. *J. Inst. Brew.* **2006**, *112* (2).

59 Barbosa-Pereira, L.; Bilbao, A.; Vilches, P.; Angulo, I.; Lluis, J.; Fité, B.; Paseiro-Losada, P.; Cruz, J. M. Brewery Waste as a Potential Source of Phenolic Compounds: Optimisation of the Extraction Process and Evaluation of Antioxidant and Antimicrobial Activities. *Food Chem.* **2014**, *145*.

60 Akunna, J. C. *Anaerobic Treatment of Brewery Wastes*; Elsevier Ltd, **2015**.

61 Elbeshbishy, E.; Dhar, B. R.; Nakhla, G.; Lee, H. S. A Critical Review on Inhibition of Dark Biohydrogen Fermentation. *Renew. Sustain. Energy Rev.* **2017**, *79* (May), 656–668.

62 Gunes, B.; Stokes, J.; Davis, P.; Connolly, C.; Lawler, J. Pre-Treatments to Enhance Biogas Yield and Quality from Anaerobic Digestion of Whiskey Distillery and Brewery Wastes: A Review. *Renew. Sustain. Energy Rev.* **2019**, *113* (July), 109281.

63 David, B.; Federico, B.; Cristina, C.; Marco, G.; Federico, M.; Paolo, P. Biohythane Production From Food Wastes. In *Biohydrogen*; **2019**; pp 347–368.

64 Ren, Y.; Si, B.; Liu, Z.; Jiang, W. Promoting Dark Fermentation for Biohydrogen Production : Potential Roles of Iron-Based Additives. *Int. J. Hydrogen Energy* **2021**, *47* (3), 1499–1515.

65 Patriarca, C.; De Luca, E.; Felici, C.; Lona, L.; Mazzurco Miritana, V.; Massini, G. Bio-Production of Hydrogen and Methane Through Anaerobic Digestion Stages. In *Enriched Methane: The First Step Towards the Hydrogen Economy*; De Falco, M., Basile, A., Eds.; Springer Cham Heidelberg New York Dordrecht London, **2016**; pp 91–109.

66 Lubitz, W.; Ogata, H.; Rüdiger, O.; Reijerse, E. Hydrogenases. *Chem. Rev.* **2014**, *114* (8), 4081–4148.

67 Ruth, J. C.; Milton, R. D.; Gu, W.; Spormann, A. M. Enhanced Electrosynthetic Hydrogen Evolution by Hydrogenases Embedded in a Redox-Active Hydrogel. *Chem. - A Eur. J.* **2020**, *26* (32), 7323–7329.

68 Noguchi, K.; Riggins, D. P.; Eldahan, K. C.; Kitko, R. D.; Slonczewski, J. L. Hydrogenase-3 Contributes to Anaerobic Acid Resistance of Escherichia Coli. **2010**, *5* (4), 27–29.

69 Wongthanate, J.; Chinnacotpong, K. Impacts of PH , Temperature and Pretreatment Method on Biohydrogen Production from Organic Wastes by Sewage Microflora. **2014**.

70 Vijaya Krishna, S.; Kiran Kumar, P.; Chaitanya, N.; Bhagawan, D.; Himabindu, V.; Lakshmi Narasu, M. Biohydrogen Production from Brewery Effluent in a Batch and Continuous Reactor with Anaerobic Mixed Microbial Consortia. *Biofuels* **2017**, *8* (6), 701–707.

71 Veeramalini, J. B.; Selvakumari, I. A. E.; Park, S.; Jayamuthunagai, J.; Bharathiraja, B. Continuous Production of Biohydrogen from Brewery Effluent Using Co-Culture of Mutated Rhodobacter M 19 and Enterobacter Aerogenes. *Bioresour. Technol.* **2019**, *286*.

72 Mohan, S. V.; Rohit, M. V; Amulya, K.; Kumar, A. N.; Modestra, J. A.; Sravan, J. S.; Hemalatha, M.;

Chatterjee, S.; Ranadheer, P.; Swathi, K. *Acidogenic Biohydrogen Production Integrated With Biorefinery Approach*; Elsevier B.V., **2019**.

73 Wicher, E.; Seifert, K.; Zagrodnik, R.; Pietrzyk, B.; Laniecki, M. Hydrogen Gas Production from Distillery Wastewater by Dark Fermentation. *Int. J. Hydrogen Energy* **2013**, *38* (19), 7767–7773.

74 Viana, Q. M.; Viana, M. B.; Vasconcelos, E. A. F.; Santaella, S. T.; Leitão, R. C. Fermentative H2 Production from Residual Glycerol: A Review. *Biotechnology Letters*. **2014**.

75 Bundhoo, Z. M. A. ScienceDirect Coupling Dark Fermentation with Biochemical or Bioelectrochemical Systems for Enhanced Bio-Energy Production : A Review. **2017**, *2*.

76 Yu, H.; Zhu, Z.; Hu, W.; Zhang, H. Hydrogen Production from Rice Winery Wastewater in an Upflow Anaerobic Reactor by Using Mixed Anaerobic Cultures. **2002**, *27*, 1359–1365.

77 García-Depraect, O.; León-Becerril, E. Fermentative Biohydrogen Production from Tequila Vinasse via the Lactate-Acetate Pathway: Operational Performance, Kinetic Analysis and Microbial Ecology. *Fuel* **2018**, *234* (March), 151–160.

78 García-Depraect, O.; Rene, E. R.; Gómez-Romero, J.; López-López, A.; León-Becerril, E. Enhanced Biohydrogen Production from the Dark Co-Fermentation of Tequila Vinasse and Nixtamalization Wastewater: Novel Insights into Ecological Regulation by PH. *Fuel* **2019**, *253* (February), 159–166.

79 Fernandes, B. S.; Peixoto, G.; Albrecht, F. R.; Katia, N.; Zaiat, M. Potential to Produce Biohydrogen from Various Wastewaters. *Energy Sustain. Dev.* **2010**, *14* (2), 143–148.

80 Zhou, P.; Elbeshbishy, E.; Nakhla, G. Optimization of Biological Hydrogen Production for Anaerobic Co-Digestion of Food Waste and Wastewater Biosolids. *Bioresour. Technol.* **2013**, *130*, 710–718.

81 Connaughton, S.; Collins, G.; O'Flaherty, V. Psychrophilic and Mesophilic Anaerobic Digestion of Brewery Effluent: A Comparative Study. *Water Res.* **2006**, *40* (13), 2503–2510.

82 Ince, B. K.; Ince, O.; Anderson, G. K.; Arayici, S. Assessment of Biogas Use As an Energy Source From Anaerobic Digestion of Brewery Wastewater. *Water. Air. Soil Pollut.* **2001**, *126*, 239–251.

83 Chen, R.; Chang, S.; Hong, Y.; Wu, P. Brewery Wastewater Treatment by Anaerobic Membrane Bioreactor. *Proceedings, Annu. Conf. - Can. Soc. Civ. Eng.* **2015**, *1_2015*, 390–399.

84 Borja, R.; Martín, A.; Durán, M. M.; Luque, M.; Alonso, V. Kinetic Study of Anaerobic Digestion of Brewery Wastewater. *Process Biochem.* **1994**, *29* (8), 645–650.

85 Capocelli, M.; De Falco, M. Enriched Methane: A Ready Solution for the Transition Towards the Hydrogen Economy. In *Enriched Methane: The First Step Towards the Hydrogen Economy*; De Falco, M., Basile, A., Eds.; Springer Cham Heidelberg New York Dordrecht London, **2016**; pp 1–21.

86 Middha, P. Explosion Risks of Hydrogen/Methane Blends. In *Enriched Methane: The First Step Towards the Hydrogen Economy*; De Falco, M., Basile, A., Eds., **2016**; pp 235–257.

87 Karim, G. A.; Wierzba, I.; Al-Alousi, Y. Methane-Hydrogen Mixtures as Fuels. *Int. J. Hydrogen Energy* **1996**, *21* (7), 625–631.

88 Cho, S. H.; Kim, J.; Han, J.; Lee, D.; Kim, H. J.; Kim, Y. T.; Cheng, X.; Xu, Y.; Lee, J.; Kwon, E. E. Bioalcohol Production from Acidogenic Products via a Two-Step Process: A Case Study of Butyric Acid to Butanol. *Appl. Energy* **2019**, *252* (June).

Chapter 4. Hydrogen production potential in dark fermentation of a brewery sludge pre-treated with white-rot fungi in submerged culture

Abstract

Numerous strategies integrating a white-rot fungi (WRF) treatment with other microbial fermentations have been explored in the search for a sustainable biofuel production process from lignocellulosic biomass. Little has been reported in the use of liquid residues like brewery wastewaters. The high energy content in these residues can be exploited for biofuels production after a WRF saccharifying pre-treatment, producing fungal biomass, a highly valued by-product, while addressing a wastewater treatment issue. The biomass production of three WRF strains in submerged culture using a high strength brewery waste slurry (BWS) was assessed. *Pleurotus ostreatus* demonstrated better adaptation to the medium, producing 31.2 ± 0.2 g/L of dry weight biomass after 18 days of incubation. COD was reduced 76%, while spectrophotometric analysis showed 78% to 95% removal of the recalcitrant coloured compounds. Hydrogen in dark fermentation (DF) after the fungal pre-treatment (FT) was also assessed. Hydrogen generation reached 495.7 mL ± 6.2 H_2/g COD consumed, and the process exhibited 94.2% of the theoretical molar yield when butyrate is the main end product, which constituted 53% of the total carboxylic acids produced. The combined FT/DF process degraded ~2 times more COD and showed a 25% higher hydrogen yield but 50% lower hydrogen volume compared to DF process without fungal pre-treatment, demonstrating the potential of combining both systems with the aim of producing fungal biomass and hydrogen.

4.1 Introduction

Beer industry's contribution to global trade is so significant that some specialists consider it an effective indicator of the world's economic health[1]. Notwithstanding the commercial relevance, the environmental footprint of the brewing process is also of considerable significance due to the large proportion of residues generated[2,3]. There

are four main solid wastes identified, brewer's spent grain (BSG) and spent yeast (BSY), the hot trub and kieselguhr sludge, each one of them with different characteristics, depending on which part of the brewing process they come from[4]. Brewery wastewaters (BWW), on the other hand, are generated in much larger volumes. The water to beer volume ratio is estimated between 5–15, from which roughly 70% of the water supply is discharged; that is a wastewater to beer volume ratio of 3–10[2,5]. In general, BWW are pre-treated onsite prior to discharge to the sewer system. Compared to other food wastes rich in lipids, BWW has a low biochemical methane potential[6], nevertheless, anaerobic digestion is the most common method applied to manage brewery sludge and wastewaters[5,7].

Given their composition, BSG and BSY attract researchers' attention the most for a myriad of applications[8–11]. However, the composition of BWW, consisting mainly of sugars, soluble starch, ethanol, and volatile fatty acids[12,13], makes them an attractive fermentable substrate for the activity of a wide spectrum of microorganisms. One of the most interesting group of microbiota in this regard is the wood-decaying fungi, in which three types of organisms are identified in accordance to the decomposition they exhibit in woody materials: brown, soft, and white rot fungi[14]. The case of white-rot fungi (WRF) is particularly noteworthy. These are mostly basidiomycetes well known for degrading and mineralizing lignin into CO_2 and H_2O more efficiently than any other microorganism[15] by virtue of an extracellular ligninolytic enzymatic system comprising mainly laccases (*Lac*), lignin (*LiP*) and manganese (*MnP*) peroxidases[16]. Besides being cultured in solid matrix, like woody materials (solid state fermentation, SSF), WRF can also be cultured in submerged fermentation (SmF). Among the most studied WRF in such conditions, there is the well-known genera of *Trametes* spp. and *Bjerkandera* spp.; species such as *Pycnoporus cinnabarinus, Phanerochaete chrysosporium*, and *Ganoderma lucidum*, as well as the edible mushrooms *Flammulina velutipes* (enoki mushroom), *Lentinula edodes* (shiitake mushroom), and the genus *Pleurotus* spp.[17].

WRF exhibit the interesting ability of degrading xenobiotic pollutants including simple aromatic compounds, polychlorinated biphenyls, and polyaromatic hydrocarbons[16].

Therefore, several studied applications in SmF include the bioremediation of pulp and paper mill sludge[18], decolouration of dyes in effluents[19,20], olive mill residues[21,22]; and other wastes similar to BWW, like those from the ethanol industry and distillery wastewaters[23,24]. The type and concentration of organopollutants will depend on the brewing process and stage. Furfuryl alcohol, for instance, is generated mostly during the wort boiling, with significantly more produced in darker beers than in lagers[25].

Melanoidins constitute the main group of organopollutants produced during the brewing process, in part responsible of the colour and taste of beer[26]. The antibacterial activity of melanoidins have a beneficial effect on human health, although releasing them in wastewaters, pose a potential threat to ecosystems by the increased load of recalcitrant organic material, especially to natural water bodies[26,27]. Melanoidins can inhibit microbial growth in biological treatment processes[28]. Physical treatments to remove melanoidins include coagulation, flocculation, electrocoagulation, membrane processes, adsorption, and oxidation[29], nonetheless, the problem of disposal persists, as the melanoidins are not destroyed. According to some studies, notwithstanding the high COD removal yields, conventional aerobic-anaerobic treatment of molasses, distillery, and fermentation industries can reduce only up to 6–7% of melanoidins; consequently, the brown colour remains practically untouched after treatment[30]. Besides chemical degradation and adsorption methods, some acetogenic bacteria can reduce melanoidins in waste streams up to 76% under optimal nutrient conditions[31]. The WRF *P. chrysosporium* and *T. versicolor* can degrade melanoidins by greater than 80%[29,32]. The fungal treatment is attractive for several reasons. Besides the enzymatic system meant to breakdown complex lignin-like molecules, there is the biosorption of pollutants by the mycelium and exopolysaccharides produced, with one study reporting ~17% of the brown colour in molasses and distillery effluents removed by adsorption of the mycelium[27]. Additionally, the fungal strains generate by-products that can be utilized in animal feedstock[29], and in several other potential applications.

Among the by-products of commercial interest, the predominant application exploited is related to the ligninolytic enzymes production with the aim, chiefly, to bioremediate

diverse coloured effluents[33,34]. Although not as extensively reported as the enzymatic production, there are other well-known interesting processes, such as the production of organic alcohols[35]; bioactive compounds with antioxidant activities[36]; and many other functional peptides for medical purposes[37]. In recent years, interest in biomaterials from fungal mycelium has blossomed. Pure mycelium of *Ganoderma* spp., *Trametes* spp., *Pleurotus* spp., and *Pycnoporus* spp., grown in SmF have been exploited to produce a wide variety of biomaterials, like a substitute for conventional leather and textiles[38,39]. The case of the latter have attracted the attention of giants of the fashion industry like Adidas, Lululemon and Hèrmes[40].

Another interesting application is in the field of renewable energy, in which WRF are an attractive option to bio-delignify ligneous materials prior to biofuel production. Thus, there is ethanol being produced after wheat straw pre-treated with *Pleurotus eryngii* and *Irpex lacteus*[41], or even direct ethanol production from different carbon sources by *Trametes hirsuta*[42]. Methane and hydrogen production from pre-treated beech and cedar wood with different WRF strains was markedly improved, with *Phanerochaete sordida* YK-624 more suitable for methane, while *P. chrysosporium* was more suitable for hydrogen production by the pure strain *Clostridium thermocellum*[43]. Another study reported the use of *S. cerevisiae* in co-existence with different white-rot fungi to produce ethanol from sugarcane bagasse obtained between 3.4–6.5 g of sugars per 100 g of solid substrate[44]

In view of the above, the focus of the present study is twofold. Firstly, to evaluate the fungal treatment of a brewery waste slurry (BWS) by WRF and to optimize biomass production in submerged fermentation. From all the known potential applications (production of enzymes, metabolites, etc.), the fungal biomass, including the exopolysaccharides formed along with it, is an attractive by-product in the search for new biomaterials, viz. textiles, electronics, packaging, etc. Three strains were selected: *Pleurotus ostreatus*, *Pleurotus eryngii*, and *Flammulina velutipes*; chosen based on their innocuousness and their use in similar studies, in addition to their commercial value. Oyster mushrooms (*P. ostreatus* and *P. eryngii*) are the second most popular

mushrooms worldwide, easy to cultivate, and grow faster than other species[45]. Enoki mushroom (*F. velutipes*) is among the most appreciated mushrooms, with a cost around $42 USD per kg[46]. Moreover, the biomass produced in submerged fermentation can serve as supplement for human consumption or animal feed. The enzymatic machinery of these mushrooms renders the fruiting bodies safe for consumption[47]. Secondly, it is also sought to assess the potential of the fungal-based treatment as a pre-treatment-step to dark fermentation to generate hydrogen by increasing the fermentable sugars in solution.

4.2 Materials and Methods

4.2.1 Feedstocks, chemicals, and reagents

Czapek Dox is a common medium for the growth of filamentous fungi for enzymatic activity[48]. A modified, 2X concentrated Czapek medium was prepared as follows: 5 g/L yeast extract (Thermo Scientific™), 3 g/L $NaNO_3$ (Sigma-Aldrich™), 1 g/L K_2HPO_4 (Fisher Chemical™), 1 g/L $MnSO_4 \cdot 7H_2O$ (EMD Millipore™), KCl 0.5 g/L (Fisher BioReagents™), 0.01 g/L $FeSO_4 \cdot 7H_2O$ (EMD Millipore™), and 0.10 mL of a trace metal solution (10X) composed of 10 g/100 mL $ZnSO_4$ (Fisher Chemical™) and 5 g/100 mL $CuSO_4$ (Fisher Chemical™). The nitrogen source for all the BWS fermentations was 1 g/L NH_4Cl (Sigma-Aldrich™). The carbon source was D-(+)-glucose anhydrous 99% (Thermo Scientific™). To adjust the pH of the different media KH_2PO_4 and K_2HPO_4 (Fisher Chemical™) as well as sodium acetate (Alfa Aesar™) were used. BD Difco™ Potato-dextrose-agar (PDA), BD Difco™ Malt extract agar (MEA), and pure agar (Neogen™) were employed for the fungal growth in petri dishes. Absolute ethanol, anhydrous (Ricca Chemical) was also employed.

For the analysis of reducing sugars, 250 mL of reactive was prepared mixing the compounds in the following order: 2.5 g 3,5-dinitrosalicylic acid (DNS) 98% (Fisher Scientific™), 0.5 g phenol 99% (Thermo Scientific™), 0.125 g Na_2SO_3 (Fisher Chemical™), 2.5 g NaOH (Fisher Chemical™), 50 g Rochelle salt (Fisher Chemical™). For the total sugars analysis, concentrated sulfuric acid (LabChem™), and 80% w/w

phenol solution were used. Both the DNS and phenol solutions were kept in opaque glass bottles and refrigerated.

The standard solutions for the chromatography analysis were prepared using glacial acetic acid ≥99.5% (Fisher Scientific™), *n*-butyric acid ≥99.0% (Sigma-Aldrich™), lactic acid 98.0% (Sigma-Aldrich™), formic acid 99.0% (Thermo Scientific™), propionic acid ≥99.5% (Sigma-Aldrich™), and the mobile phase was prepared with 0.5 N H_2SO_4 (LabChem™). The gases to obtain the calibration curves for spectrometric analysis (H_2, CO_2, CH_4), as well as argon as the carrier, were compressed pure gases (≥99.9%), all provided by Linde® Canada.

The brewery waste slurry (BWS) was obtained from a regional brewery in eastern Ontario, Canada. It contains slurry from the brewing process in addition to waste beer. The BWS was first filtered through a conventional strainer with a gauze to remove gross solids, and then stored at 4°C for further experiments (**Table 4.1**).

Table 4.1. Characteristics of the brewery sludge after filtration.

COD	68.4 – 74.6 g/L
pH	4.2 – 4.5
Total solids	24.8 – 30.1 g/L
Volatile solids	23.4 – 28.1 g/L
Total sugars	13.8 – 15.3 g/L
Reducing sugars	2.8 – 3.6 g/L
Ammonia	17.3 – 24.7 mg/L

4.2.2 Fungal strains selection

Samples of *Flammulina velutipes*, *Pleurotus ostreatus* and *Pleurotus eryngii* strains were obtained from the collection at the Faculty of Biology of Carleton University. The strains were propagated on plates containing approx. 20 mL PDA and incubated for 10 days at 30°C. After that, circular plugs (diameter 0.8 cm) from the PDA plates served as initial fungal inoculum for the BWS fermentations in solid and liquid state.

After the fungal strains' reactivation growth in PDA, they were adapted first in semisolid media. The three strains were cultured in plates with BWS-agar medium consisted in diluted BWS (50%) and 18 g/L agar. The adaptation to the medium was assessed by measuring the size of the colony from the centre of the Petri dish[49], thus obtaining a specific growth rate for each strain. The growth in the BWS based medium was compared to PDA and malt extract-agar (MEA), a specialized maltose-rich medium for the cultivation of fungi; an important feature since it is known that the main sugar in brewery wastewaters is maltose[12].

4.2.3 Submerged fermentation

Subsequently, small batch liquid fermentations were conducted with 50% diluted BWS. To evaluate the potential of BWS to sustain fungal growth, the effect on the biomass production in SmF of the addition of glucose (10 g/L) as carbon source (CS) and ammonium chloride (1 and 2 g/L), as a nitrogen source (NS) to the BWS was assessed and compared to the 50% BWS medium without these macronutrients. The BWS, and the CS and NS solutions were autoclaved (121°C, 15 psia for 20 min) separately and mixed after the temperature cooled down. Erlenmeyer flasks (125 mL) containing 60 mL of each medium were inoculated in duplicate under aseptic conditions in a biosafety cabinet. Each flask was covered with a sterilized cotton-gauze plug. The pH was adjusted to 5.5 by adding acetic acid and sodium acetate to prepare a 0.025 M pH 5.5 acetate buffer solution (22.4 mM sodium acetate and 2.6 mM acetic acid). The media were fermented initially during 12 days under agitation (120 rpm) at 30°C in a horizontal orbital shaker. Dry weight biomass was determined by drying the filtered mycelium in an oven at 60°C overnight until samples reached a constant weight. The results were compared against fermentation in modified Czapek medium, all expressed in g/L dw. The strain with the best biomass yield was chosen to continue with fermentations on a larger scale and BWS concentration (1L, 60 g/L COD) to produce biomass and the pre-treated (hydrolysate) effluent for the subsequent hydrogen production process by dark fermentation. The operational conditions did not change, only the agitation regime (76 RPM). Reducing and total sugars content after the fungal

fermentation was determined by the Miller's[50] and Dubois's[51] methods, respectively. The concentration of crude exopolysaccharides produced was also determined: the crude extracellular material (EM) was precipitated from the biomass filtrate at a ratio of 1 volume of crude biomass extract with 4 volumes of chilled absolute ethanol, and left for 24 hours at 4˚C, centrifuged (6,000 rpm, 20 min), resuspended in water, and precipitate it again in chilled ethanol, as reported by[52]. The EM, after another 24 h at 4˚C, was dried and weighed after centrifugation.

Fungal biomass growth and COD reduction experimental data were fitted into the Logistic-Monod model according to the following equations[53]:

$$\frac{dX}{dt} = \mu \left(1 - \frac{X}{X_{max}}\right) X \qquad \textbf{(Eq. 4.1)}$$

$$X = \frac{X_{max}}{1 + \left(\frac{X_{max} - X_0}{X_0}\right) e^{-\mu t}} \qquad \textbf{(Eq. 4.2)}$$

$$\mu = k \frac{Y_{X/S}}{X} \cdot \frac{dS}{dt} \qquad \textbf{(Eq. 4.3)}$$

Where, equation (2) relates cell growth X, maximum biomass X_{max} (calculated as the carrying capacity from the experimental data), and X_0 at times $t \to \infty$, and $t = 0$, respectively. Equation (3) relates specific growth rate μ, obtained from the yield biomass/substrate $Y_{X/S}$, which was calculated from experimental data, and substrate consumption S, which in this case was COD concentration.

4.2.4 Dark fermentation

The hydrogen production potential of the BWS treated was analysed in batch fermentations in a 250 mL glass reactor properly sealed but provided with an inlet and outlet for the gas carrier inflow (Argon) to a mass spectrometer to detect the gases of fermentation, and with a sampling port, allowing to collect liquid samples without disrupting the system to determine pH, COD and organic acids produced. The working volume was 120 mL of hydrolysate, inoculated with a 1.3% v/v heat-treated anaerobic

sludge collected from the City of Ottawa's wastewater treatment plant (ROPEC WWTP), and fermented during 30 h (**Chapter 3**). The temperature was kept at 35°C by submerging the reactor in a water bath, and the pH was adjusted to 6.4 by first increasing the alkalinity (addition of 100 mg/L of $CaCO_3$), then kept controlled by adding a 0.03 M pH 6.4 potassium phosphate buffer solution (8.9 mM K_2HPO_4 and 21.1 mM KH_2PO_4). The medium after the fungal treatment were autoclaved (121°C, 15 psia for 20 min) before inoculation.

The final organic acids composition as well as the sugar consumption was determined. The hydrogen production data was processed and modelled using a modified Gompertz function:

$$H(t) = P \times \exp\left\{-\exp\left[\frac{2.71828 \cdot R_m}{P}(\lambda - t) + 1\right]\right\} \qquad \textbf{(Eq. 4.4)}$$

Where $H(t)$ is the cumulative hydrogen (mL) at a given time t, P is the hydrogen production potential, also referred to as the ultimate hydrogen production (mL), λ is the lag phase (h), and R_m is the hydrogen production rate (mL/h). Data processing was carried out in Excel, fitting the RSE of the model versus the data obtained from the Mass-Spectrometer.

4.2.5 Physicochemical analysis

Decolourization of the BWS after the fungal treatment was determined by analyzing diluted samples (1:10) throughout most of the visible spectrum ($380 - 700$ nm), as well as the reduction at the wavelength of 475 nm, in a Varian UV-VIS 50 Spectrophotometer. The percentage of decolourization was calculated by the area under the curve of the spectrophotograms according to the following expression:

$$\%Dec. = \left(1 - \frac{Abs_f}{Abs_0}\right) \times 100 \qquad \textbf{(Eq. 4.5)}$$

where:

Abs_f —absorbance at the end of the fermentation

Abs_0 — initial absorbance

And the area under the curve of each spectrophotogram was calculated as follows:

$$Area = \int_a^b f(x)dx = \lim_{n\to\infty} \sum_{i=1}^{n} f(x_i)\Delta x \qquad \textbf{(Eq. 4.6)}$$

The change in turbidity was measured based on the standard nephelometric method (SM 2130B) using formazin polymer as the standard reference solution, in a HACH® 2100N Laboratory Turbidimeter, reported in nephelometric turbidity units (NTU).

Reducing sugars content was determined by the DNS (Miller's) method[50], colorimetric technique based on the reduction of DNS by glucose or fructose to 3-amino-5-nitrosalicylic acid in an alkaline solution. 0.15 mL of each sample is carefully mixed with 0.45 mL of DNS reactive in 15 mL Hach tubes, properly sealed and heated at 100°C during 15 min. After cooling down, 2.5 mL of distilled water is added to the tubes, thoroughly mixed in vortex. The processed samples are read at the wavelength of 540 nm. Raw samples may be diluted 5 to 10 times before this procedure.

Total sugars concentration was determined by the phenol-sulphuric acid (Dubois's) method[51]. 50 µL of the diluted raw sample (5 to 10 times), is poured in a test tube and distilled water is added to make up to 100 µL. Then, 50 µL of 80% phenol solution is added and carefully vortexed. In a stream, 2.0 mL of concentrated sulfuric acid (95 to 98%) are added and vortexed carefully. After 10 min of digestion at room temperature, the samples are read at the wavelength of 490 nm. The total and reducing sugars samples were read in a HACH® DR6000 UV-VIS Laboratory Spectrophotometer. Both reducing sugars and total sugars are expressed as grams of glucose equivalent per liter.

The production of organic acids was determined by chromatography in an Agilent® HPLC Series 1200, using a Bio-Rad Aminex HPX-87H column and UV at 210 nm. The column was kept at 60°C and the RID at 50°C. Samples from the bottles were taken periodically, centrifuged (10,000 rpm, 10 min), and the supernatant was filtered with a hydrophobic PTFE syringe filter (0.22 µm). Finally, 20 µL of each sample was injected and diluted in H_2SO_4 5 mM as the mobile phase. The elution time of each sample was 25 min. Fermentation gases were monitored continuously through mass spectroscopy

during 30 h in a Dycor Proline Process Mass Spectrometer (Ametek® Instruments), carried by a stream of argon at 100 mL/min, flow rate monitored and controlled by a Horiba® VIA-510 Gas Analyzer. Finally, the COD was determined by the HACH® 8000 Reactor Digestion Method using high range vials (20 – 1,500 mg/L), in which 2 mL of diluted samples (50 – 10 times) were digested in a HACH® DRB200 Dry Thermostat Reactor for 2 hours at 150°C. After cooling, the vials were read in a HACH® DR6000 UV-VIS Laboratory Spectrophotometer to obtain the COD value in mg/L.

4.3 Results and discussion

4.3.1 Screening test of Fungal growth inhibition in BWS

The growth rates of three fungal species in a 50% BWS-agar (BSA) were compared to a malt-extract agar (MEA) and to a standard PDA medium. After nine days of incubation, it was evident that all strains grew at equivalent or higher rates in the BSA than the MEA control, and both showed inhibition compared with PDA (**Table 4.2**). *F. velutipes* demonstrated the fastest growth rate in both the BSA and in the MEA after 9 days (3.9 ± 0.0 mm/day and 2.7 ± 0.1 mm/day, respectively). The same tendency was also observed when the strains were grown in the customary PDA medium. After 9 days of incubation, *F. velutipes* mycelium was fully extended through the entire Petri dish in PDA, whereas *P. ostreatus* and *P. eryngii* were not (see **Appendix**).

Table 4.2. Fungal growth of *F. velutipes*, *P. ostreatus*, and *P. eryngii* after 9 days in three different semisolid media in Petri dishes: 1) Maltose extract agar (MEA), 2) brewery slurry-agar (BSA), 3) potato-dextrose-agar (PDA).

Strain	MEA	BSA	PDA
		diameter in mm	
Pleurotus ostreatus	18.4 ± 0.6	18.9 ± 0.9	71.5 ± 0.9
Pleurotus eryngii	16.7 ± 0.6	25.1 ± 2.5	74.2 ± 0.9
Flammulina velutipes	19.7 ± 0.9	28.6 ± 0.3	86.0 ± 0.0

4.3.2 Fungal growth in submerged fermentation

The growth of the three strains was subsequently assessed in submerged fermentation with and without the addition of a carbon and nitrogen source. Unlike in the agar media, *P. ostreatus* grew slightly more than *P. eryngii*, and *F. velutipes* growth was completely inhibited. Therefore, only the fungal biomass growth exhibited by *P. ostreatus* and *P. eryngii* are presented.

The results clearly demonstrate the potential of BWS as a substrate for the growth of *Pleurotus* spp. in submerged fermentation (**Figure 4.1**). The common oyster mushroom *P. ostreatus* produced the highest biomass yields without carbon addition at 0 and 1 g/L NS of 11.7 ± 5.2 and 11.6 ± 3.5 g/L dw, respectively, compared to 3.1 ± 0.6 g/L dw in the control medium. This yield is similar to that reported by Hultberg *et al.*[54], where the total biomass composed of *P. ostreatus* mycelium, cultured in 200 mL brewery run-off spent grain waste was 13.2 ± 2.2 g/L after 10 days. On the other hand, the highest biomass observed with *P. eryngii* was in the Czapek medium (8.2 ± 0.4 g/L), and for the rest of the conditions, the biomass growth with this strain did not vary significantly (4.5 – 5.7 g/L). *P. eryngii* produced less fungal growth than *P. ostreatus* in all conditions, except in the BWS medium with glucose added and no NS, and more markedly in the Czapek medium, where *P. eryngii* produced twice the biomass as *P. ostreatus*.

The addition of 10 g/L of glucose significantly reduced fungal growth in both strains, while the synergetic effect of both glucose and NS addition significantly reduced fungal growth with 1 g/L NS and had no effect with 2 g/L NS added. The latter is consistent with other reports, where the addition of a carbon source had no impact or even represented a negative impact on WRF growth[55–57]. The reduced growth is explained by the specificity of glucose on the secretion of cellulolytic enzymes in SmF. The secretion of cellulose and hemicellulose degrading enzymes by *P. ostreatus* are naturally induced by ligneous materials in solution, but their expression is repressed by the presence of glucose, whereas other redox enzymes (*e.g.*, laccases) and proteases are not influenced by the type of carbon source in the aqueous medium[58].

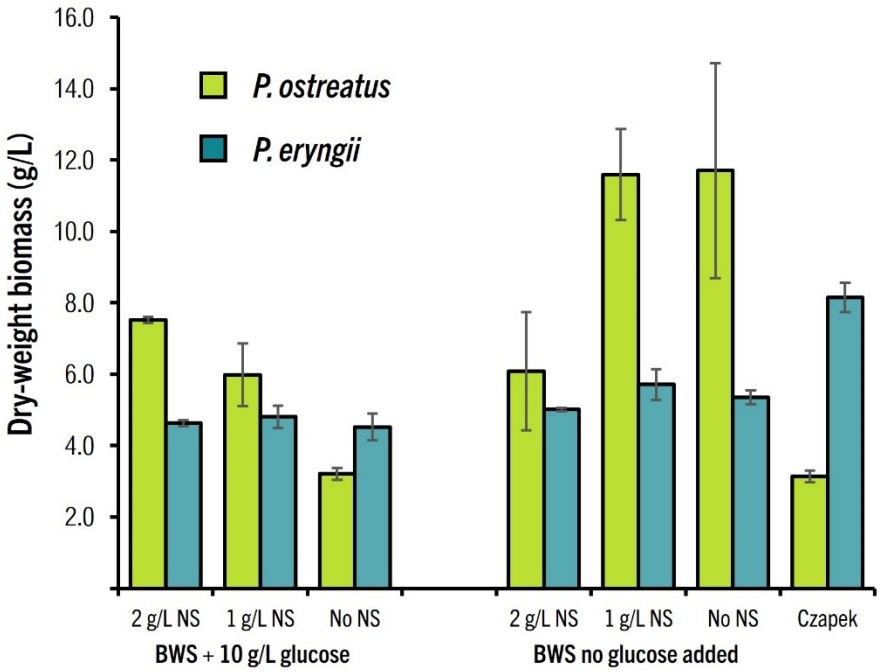

Figure 4.1. *Fungal biomass yield of* P. ostreatus *Eand* P. eryngii *after 12 days in BWS under different conditions. The combined effect of the addition of two different concentrations of NH_4Cl (1 and 2 g/L) as nitrogen source (NS), and the addition of 10 g/L glucose as carbon source, in contrast to BWS without the addition of nutrients and the control medium (Czapek). All the experiments contained 50% BWS, except for the control medium.*

Another interesting material derived from the fungal growth is the extracellular material (EM) binding the mycelium. The enzymes responsible for the degradation of organic matter (*i.e.*, ligninolytic, cellulolytic, etc.) are trapped in the exopolysaccharide matrix formed by WRF, thus helping in the degradation of xenobiotics in aqueous media[59]. Furthermore, the removal of pollutants occurs first by EM absorption, before being degraded by enzymatic activity[60]. Physiologically, there are several roles of the EPS matrix formed by the fungi in response to the environment: from facilitating the diffusion of enzymes in ligneous materials, to storage of a carbon source. One of the main roles though, is to protect the cells against dehydration. The EPS matrix can be several times larger than the cytoplasmic volume, and during adverse conditions, this matrix would retain important amounts of water[61]. Therefore, the moisture content in the crude biomass can provide a good indicator of EPS content.

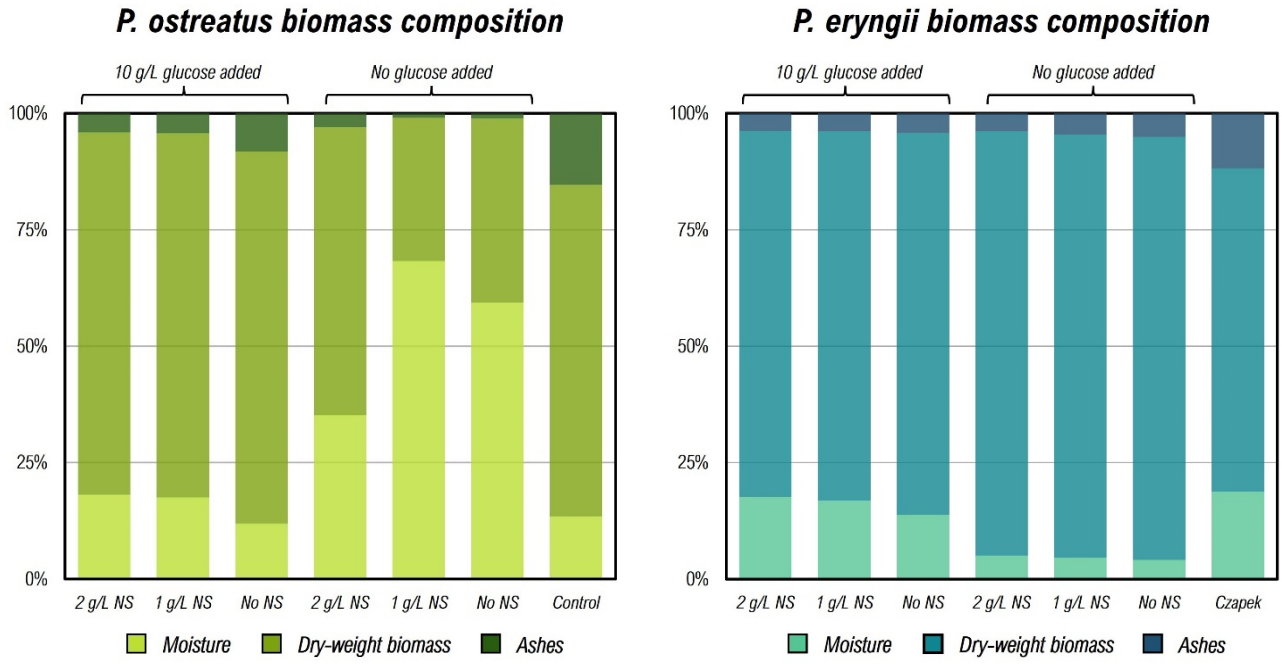

Figure 4.2. *Moisture, dry-weight total biomass, and ashes relative content from the wet biomass of* P. ostreatus *and* P. eryngii *produced in each fermentation condition.*

As seen in **Figure 4.2**, the highest moisture content was observed with *P. ostreatus* under conditions of no carbon addition and either 0 or 1 g/L NS, suggesting higher EPS production than *P. eryngii* under these conditions. Furthermore, the largest dry-weight biomass production with *P. ostreatus* coincided under the same conditions (**Figure 4.1**). The moisture content with glucose addition was similar between *P. ostreatus* and *P. eryngii*, varying between 13.0% and 18.8%, while the moisture content with no glucose addition was much higher with *P. ostreatus*, varying between 36.3% and 68.9% and surprisingly lower with *P. eryngii*, varying between 4.3% and 5.2%. It has been reported that from the WRF dry weight biomass, 40% – 45% account for biopolymers, such as chitin and other exopolysaccharides[62]. This suggests that roughly 5 g/L of crude EPS could be produced by *P. ostreatus* under optimum conditions (1 g/L NS, no glucose added). The formation of an EPS matrix is important in environmental applications since it helps to remove heavy metals by biosorption[63,64], as well as removing COD and other pollutants from food industry effluents[28,65].

4.3.3 Bioremediation of BWS with *P. ostreatus*

In the light of the results obtained, only *P. ostreatus* was cultured for the bioremediation and hydrogen production trials. The BWS strength was diluted to approximately 60 g/L COD and supplemented with 1 g/L NS, based on the optimum conditions for dark fermentative hydrogen production in **Chapter 3**. Furthermore, the working volume was increased to 1 L and the fermentation time increased from 12 to 18 days.

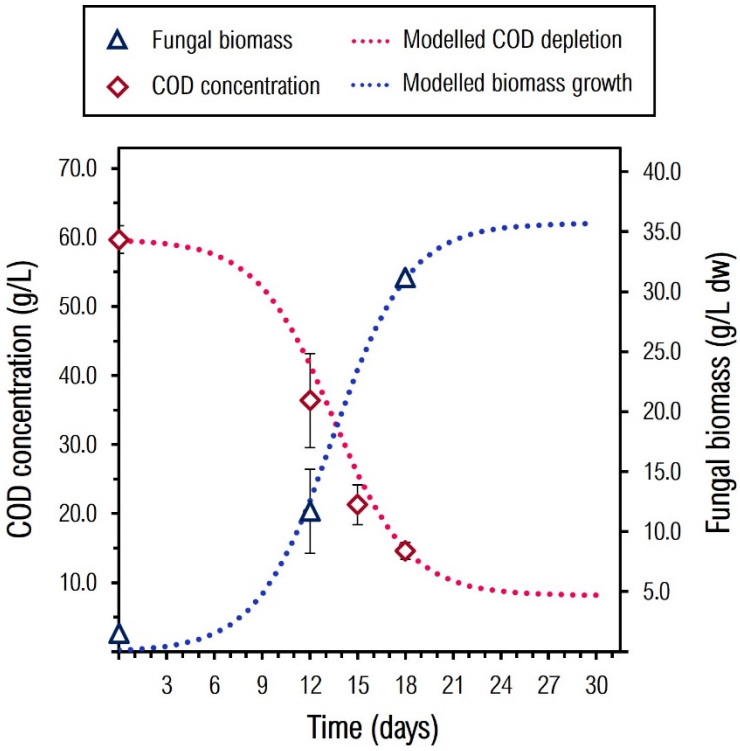

Time	Biomass yield (g/L)	COD removed (%)	Decolouration (%)	Turbidity removal (%)
12 days	11.8 ± 2.3	36.4	77.6	92.8
18 days	31.2 ± 0.2	76.0	>95.0	95.6

Figure 4.3. *Summary of the bioremediation parameters obtained from the small- and large-scale fermentation with* P. ostreatus *in 60 g COD/L BWS (1 g/L N). Modelled fungal biomass growth (g/L dw) and COD consumption (g/L) from experimental data fitted into the Logistic-Monod model.*

The experimental data was fit to the Logistic-Monod model depicted in **Figure 4.3**, with the maximum biomass production (35.5 g/L dw biomass) and an 85.3% COD reduction achieved around 24 days of fermentation. The COD removal by the end of the fermentation

at 18 days was 76% with a biomass yield of 31.2 ± 0.2 g/L dw. This is similar to that reported by Hultberg *et al*.[54], in which *P. ostreatus* in SmF achieved a reduction of 72% and a biomass yield of 22.7 g/L dw from run-off spent grain waste with a similar initial COD (51.5 g/L). The biomass yield can also be compared to other reports of optimized biomass and exopolysaccharides production in different substrates as seen in **Table 4.3**.

The performance of COD removal was also related to biomass growth. Another study reported that *P. ostreatus* achieved higher remediation when vinasses from the tequila industry were inoculated at an initial concentration of 10 g/L of biomass against 5 g/L, reducing the COD more than 86% (initial COD of 75 g/L) after 21 days of fermentation[66]. Therefore, by enabling enough fermentation time under optimal fungal growth conditions, biomass yield can be increased with a commensurate reduction in COD.

Table 4.3. Comparative analysis of studies on the culture of *Pleurotus ostreatus* in submerged fermentation for biomass production.

Strain	Medium	Objective	Biomass yield (g/L)	Working volume (L)	Culture Time (days)	Ref
P. ostreatus	Brewery waste slurry 59.7 g COD/L (12 g/L total sugars)	Biomass production/ bioremediation	31.2 ± 0.2	1.0	18	This study
P. ostreatus M2140	Brewery wastewater (Spent grain run-off) 51.5 g COD/L	Biomass production/ bioremediation	13.2 ± 2.2	0.2	10	[54]
P. ATHUM 4438	57 g/L Corn steep liqueur and 37 g/L xylose	Biomass production	39.2 ± 0.6	20.0	2.8	[67]
P. ostreatus CP-50	Synthetic media: 20 g/L maltose, 10 g/L glucose and 10 g/L yeast extract	Biomass and laccase production	8.6 ± 0.5	10.0	3.5	[68]
P. ostreatus	Milk whey medium supplemented with 20 g/L glucose and nutrients	Biomass and Exo-polysaccharides	9.4 ± 0.2	2.5	10	[69]
P. ostreatus BPPTCC 6017	Synthetic media 20 g/L potato-dextrose and nutrients	Biomass and polysaccharides	32.0 ± 1.3	1.0	7	[70]

Besides reducing COD, *P. ostreatus* was very effective at BWS colour removal with 78% reduction in absorbance in the visible spectrum (380-700 nm) after 12 days of fermentation. This is related to the bioconversion of melanoidins by *P. ostreatus*, measured as a 78% reduction in absorbance at 475 nm[28,71]. Additionally, after mechanically separating the biomass from the medium, the fungal treatment reduced the turbidity by 92.8%, strongly indicating that besides the biological activity, the fungal biomass and the EPS matrix surrounding it, retained most of the macromolecules suspended in the BWS. After 18 days, the final turbidity was 13 NTU (95.6 % reduction) with a colour reduction of greater than 95% (**Figure 4.3**).

4.3.4 Total sugars and crude exopolysaccharides

It was hypothesised that the fungal activity will release sugars from the destruction of lignocellulosic materials in the brewery sludge, which can be exploited to produce hydrogen through dark fermentation after the fungal treatment as observed by[44]. The content of total and reducing sugars in the BWS-based medium before and after the incubation process in the liquid fraction was 11.8 ± 0.5 g/L and 10.9 ± 0.3 g/L, and 2.4 ± 0.1 g/L and 2.7 ± 0.2 g/L, respectively. It is likely that the fungi initially consumed the sugars in the BWS while releasing simple sugars from the breakdown of complex molecules as the fermentation progressed.

Saccharification of lignocellulosic materials occurs by the depolymerization activity of WRF' cellulases and hemicellulases[72]. Some of the simple sugars will be repolymerized into glucans by the intracellular glucanases[73]. Glucans and chitins are the major cell wall components, being found intracellularly, although when WRF are cultured in submerged fermentation, glucans are particularly produced in larger proportions, being released into the media and forming a gel-like matrix around the fungal cells[73,74]. These EPS are mostly hemi-glucans of the (1→3)-β-D-glucosidic type with small branches formed from β-(1→6) linkages[61,75]. However, the constitution of these polysaccharides will vary in accordance to the carbon source[76].

However, sugars were also accumulated in the gel-like matrix surrounding the biomass. These were solubilized by autoclaving the fungal-treated effluent (FT-BWS). As has been mentioned above, thermal processes are part of the physicochemical pre-treatments, widely applied to contribute to the solubilisation of sugars from lignocellulosic biomass. After this step, the final concentration of total sugars in solution increased significantly to 18.8 ± 0.3 g/L and 4.1 ± 0.1 g/L of reducing sugars, a ~60% increase with respect to the concentration before autoclaving the FT-BWS. The sugar content in the raw BWS before and after autoclaving does not vary significantly, thus autoclaving is not a pre-treatment by itself to obtain more soluble sugars, but only a sterilizing step to ensure aseptic conditions before inoculation. Boiling for 10 min was shown to be equivalent to autoclaving, as boiling would be more applicable at large scale (**Table 4.4**).

WRF grow naturally in solid substrates. Therefore, cultures in aqueous media force the cells to clump together, forming pellets as a natural response due to the lack of a solid substrate[77]. A profuse EPS matrix develops to bind the pellets together, to protect the cells in response to the unstable conditions in submerged fermentation[39].

The crude extracellular material precipitated after 18 days accounted for 8.6 ± 0.2 g/L of EPS (dry weight), that is 28% of the total dry biomass. This is higher than that reported by Isikhuemhen *et al*.[52], from different WRF, and EPS extracted by the same methodology. The EPS recovered by ethanol precipitation and centrifugation are those in suspension and binding the pellets only, it must be considered that there are also EPS embedded in the pellets which cannot be separated by coarse physical means[77]. Besides the above-mentioned polysaccharides, crude EPS also contain proteins, nucleic

Table 4.4. Total sugars content (g/L, glucose equivalent) in the BWS-based media before and after the fungal treatment, before and after being autoclaved (121°C, 15 psia for 20 min).

Medium	Before autoclave	After autoclave	Boiled (10 min)
BWS-based medium (80% BWS + 1 g/L NH_4Cl)	11.0 ± 1.5	11.8 ± 0.5	—
BWS-based medium after fungal treatment	10.9 ± 0.3	18.8 ± 0.3	19.0 ± 1.1

acids, humic substances, lipids, and other non-polymeric constituents of low molecular weight, and they exhibit qualities highly appreciated in food and pharmaceutical applications; one of them is their stabilizing property in nano- and microemulsions[78]. Nevertheless, following the purpose of the present work, the extracellular material was subjected to a heat treatment to resolubilize as much sugars as possible from the EPS for the ensuing dark fermentation stage.

4.3.5 Hydrogen production in dark fermentation

The hydrogen production process was conducted at the optimum conditions of pH buffered to 6.4, during 30 h at 35°C, as in Chapter 3. Hydrogen maximum average flow rate attained was 35.9 ± 1.2 mL H_2/h just before the 15th hour. The total cumulative volume of hydrogen produced was 3,793 mL H_2/L. The Gompertz model fit the data very well with the maximum modelled flow rate (R_m) of 35.7 mL H_2/h, and a lag phase 5.9 hours (**Figure 4.4**). The COD reduction by the 18th hour was 34.6%. While the final COD observed at the end of the fungal treatment was 14.7 ± 0.1 g/L, after the autoclave treatment, the COD increased by 43% with the solubilization of the EPS. Hence, the organic load fed to the DF process was 21.0 ± 0.1 g COD/L. Increase in soluble COD has been normally reported in studies on the effect of autoclaving food wastes as substrates for anaerobic digestion[79,80]. Moreover, the non-autoclaved FT-BWS was not successful as a feedstock for DF with inhibition of bacterial growth (**see Appendix**). The extracellular material secreted by WRF not only protects hyphae from physical damage; it also plays the role of protection against pathogens. Many antibiotic compounds are volatile chlorinated aromatic compounds, similar to xenobiotic pollutants[81]. Thus, the purpose of the quick thermal step is twofold: to kill the remaining living fungal cells in the effluent and to destroy the antibiotic compounds that may have a negative impact in the DF inoculum, while contributing to increase solubilized carbon sources in the media, as noted above. At the end of the DF process, the final COD reduction was 36.5%, that is 7.7 ± 0.1 g/L consumed. The overall COD reduction attained was 77.7%, which indicates that all the solubilized compounds after the autoclave step were fully consumed. The reducing sugars were almost completely consumed, and the final

concentration of total sugars was 5.2 ± 0.1 g/L. The concentration for each organic acid analysed by the end of the fermentation was: butyric acid (4.66 ± 0.07 g/L), which accounted for 53% of the total organic acids produced, followed by lactic acid (2.76 ± 0.04 g/L), propionic acid (1.80 ± 0.20 g/L), formic acid (0.84 ± 0.01 g/L), and acetic acid (0.52 ± 0.06 g/L).

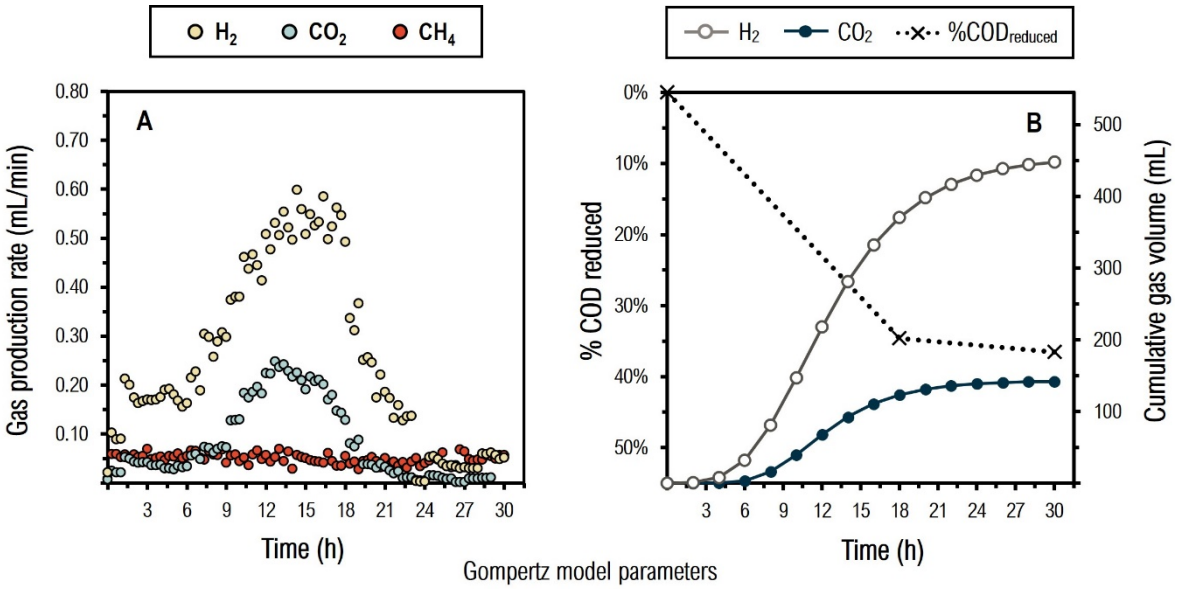

Gompertz model parameters

R_m	λ	P	RSS	RSE	R^2
35.72	5.88	455.11	1.0000	19.60	0.9982

Figure 4.4. *Dark fermentation of the fungal-treated BWS:* ***A)*** *Production rate (mL/min) of hydrogen, carbon dioxide, and methane;* ***B)*** *Hydrogen and carbon dioxide cumulative production, and %COD reduced. Gas production modelled data presented from to the modified Gompertz equation.*

The hydrogen yield based on COD consumed is 495.7 mL ± 6.2 H_2/g COD. In terms of COD fed to the process, it is 181.0 mL ± 1.0 H_2/g COD initial. In relation to the sugars consumed by the bacteria (as glucose equivalents), the process resulted in a generation of 2.26 ± 0.10 mol H_2 per mol of glucose, which in relation to the theoretical molar yield when butyrate is the major end-product (2.4 mol H_2/mol glucose)[82], the yield represents 94.0% conversion. The generation rate of this study is superior to the reported data with similar substrates. Estevam *et al.*[83], obtained a maximum molar yield between 0.80–1.67, and in a similar study it was reported 0.95 ± 0.15 mol H_2/mol

glucose[84], both works using a single-strain culture of *Klebsiella pneumoniae* cultured in diluted brewery wastewaters. Most of the studies regarding hydrogen production after a substrate pre-treatment step are based on the obtention of a hydrolysate from a lignocellulosic biomass. After alkali and enzymatic pre-treated poplar-derived residues, the fermentation carried by *Enterobacter aerogenes* showed 0.6 mol H_2/mol of total released sugars[85]. Regarding a fungal pre-treatment, the majority of works are focus on delignification and saccharification yields in solid-state fermentation, aiming to enhance the production of biofuels, in particular methane[86–88]. To the knowledge of the authors, **t**here is only one study in submerged fermentation reporting the use of a bituminous coal as substrate for *P. chrysosporium* growth, prior to dark fermentation[86]. While several studies in SSF are found, they are related to hydrolysis of various solid lignocellulosic residues. Hydrogen produced in the present project is comparable to those yields obtained after conventional pre-treatment of solid substrates, such as enzymatic and thermo acidic hydrolysis[89,90]. However, the pre-treatment HRT of conventional hydrolysis technologies are unrivalled, from hours to a couple of minutes, in the case of steam explosion[91], against the 18 days of the fungal pre-treatment of the present work. Nonetheless, the relevance of this treatment lies in the generation of highly valued products ranging from the food and pharmaceutical industries to textiles, electronics, bioplastics, and biosensors, as well as in environmental applications.

The fresh biomass produced in submerged fermentation can serve for several purposes. The natural approach is to use the excess of fungal biomass as inoculum for edible mushrooms production, in which case, the brewer's spent grain can be used as solid substrate to sustain the fungal growth. In addition to the mushroom harvesting, there is the widely reported upgrading effect after the SSF over the BSG as livestock feed, providing an enhanced ruminal digestibility, higher protein and minerals content and reduced in lignin, which contributes to a better livestock nutrition[92–94]. The dry biomass can also serve as high-protein fishmeal[95], or simply as a supplement for human consumption. A myriad of benefits from higher mushrooms (including *P. ostreatus*), have been identified; from antidiabetic, antimicrobial and antioxidant activities, in

addition to the rich content of proteins, essential amino acids, functional metabolites, carbohydrates, fats, and minerals[96].

Finally, the pre-treatment of BWS by *P. ostreatus*, has proven to be an efficient step to bioremediate this residue considerably, while discharging an effluent with enough nutrients to sustain a successful ensuing dark fermentative hydrogen producing stage. Compared to the data presented in **Chapter 3,** the combined treatments fungal-dark fermentation (FT-DF), demonstrated an overall COD reduction of 78%; that is a conversion roughly two times higher than DF alone, using the same substrate and process conditions. The fungal treatment helped to reduce the turbidity (above 90% removed), and 78% to 95% removal of coloured compounds, parameters that were not affected by the bacterial treatment in dark fermentation alone, in which turbidity did not change at all, while colour was reduced only by 8%–9% (see **Appendix**). The maximum yield in DF alone was 331.3 mL ± 7.1 H_2/g COD consumed. Under the same conditions, 49.6% more hydrogen per gram of COD consumed were obtained after FT-DF. However, the cumulative hydrogen volume was 34% lower: 3,793 ± 83 mL versus 5,785 ± 72 mL H_2/L in DF alone. Regarding the end-products of the process, the proportion of each organic acid remained similar, except in the case of acetic acid, which was not detected in FT-DF. As seen above, butyric acid is the main end-product, representing ~65% of the carboxylic acids analysed, albeit the concentration is 77% that of DF alone (4.66 ± 0.03 g/L vs 6.09 ± 0.07 g/L). Lastly, the hydrogen molar yield exhibited in the present work represents a 25% increase over the attained in DF alone.

4.4 Conclusions

This study demonstrates the potential of combining a fungal-based treatment aimed to produce biomass, paralleled with the bioremediation of a high strength brewery waste slurry, while providing an effluent with enough nutrients to sustain a successful ensuing dark fermentative hydrogen production stage. Readily available sugars as glucose increased 60%–70% after the fungal treatment. This represented higher rates of energy conversion in the ensuing DF, since while the volume of hydrogen per volume of BWS treated was lower than in DF alone, hydrogen production on the basis of grams of

COD consumed increased by 49%. The total COD and colour removal was 76% and 78% respectively. Moreover, the versatile WRF-based treatment offers a wide variety of potential applications, therefore, more research needs to be done to analyse the revalorisation of other possible by-products from brewery waste slurry treated in a two-staged fungal pre-treatment–dark fermentation process.

References

1 Lindenberger, H. *New Report On Beer's Global Economic Footprint Highlights The Impact The Industry Makes*, Available at: https://www.forbes.com/sites/hudsonlindenberger/2022/02/10/new-report-highlights-the-global-economic-impact-the-beer-industry-makes/?sh=2e748c6b4241 (accessed Jul 29, 2022).

2 Olajire, A. A. The Brewing Industry and Environmental Challenges. *J. Clean. Prod.* **2020**, *256*, 102817.

3 Olivares-Galván, S.; Marina, M. L.; García, M. C. Extraction of Valuable Compounds from Brewing Residues: Malt Rootlets, Spent Hops, and Spent Yeast. *Trends Food Sci. Technol.* **2022**.

4 Thiago, R. dos S. M.; Pedro, P. M. de M.; Eliana, F. C. S. Solid Wastes in Brewing Process: A Review. *J. Brew. Distill.* **2014**, *5* (1), 1–9.

5 Brito, A. G.; Peixoto, J.; Oliveira, J. M.; Oliveira, J. A.; Costa, C.; Nogueira, R.; Rodrigues, A. Brewery and Winery Wastewater Treatment: Some Focal Points of Design and Operation. In *Utilization of By-Products and Treatment of Waste in the Food Industry*; Oreopoulou, V., Russ, W., Eds., **2007**; pp 109–131.

6 Wang, W.; Xu, W.; Collett, J. L.; Liu, D.; Zheng, A.; Dore, A. J.; Liu, X. Chemical Compositions of Fog and Precipitation at Sejila Mountain in the Southeast Tibetan Plateau, China. *Environ. Pollut.* **2019**, *253*.

7 Keenan, J. D.; Kormi, I. Anaerobic Digestion of Brewery By-Products. *Water Pollut. Control Fed.* **1981**, *53* (1), 66–77.

8 Jaeger, A.; Arendt, E. K.; Zannini, E.; Sahin, A. W. Brewer's Spent Yeast (BSY), an Underutilized Brewing By-Product. *Fermentation* **2020**, *6* (4), 1–23.

9 Mussatto, S. I. Brewer's Spent Grain: A Valuable Feedstock for Industrial Applications. *J. Sci. Food Agric.* **2014**, *94* (7), 1264–1275.

10 Marson, G. V.; de Castro, R. J. S.; Belleville, M. P.; Hubinger, M. D. Spent Brewer's Yeast as a Source of High Added Value Molecules: A Systematic Review on Its Characteristics, Processing and Potential Applications. *World J. Microbiol. Biotechnol.* **2020**, *36* (7).

11 Puligundla, P.; Mok, C. Recent Advances in Biotechnological Valorization of Brewers' Spent Grain. *Food Sci. Biotechnol.* **2021**, *30* (3), 341–353.

12 Schneider, T.; Graeff-Hönninger, S.; French, W. T.; Hernandez, R.; Merkt, N.; Claupein, W.; Hetrick, M.; Pham, P. Lipid and Carotenoid Production by Oleaginous Red Yeast Rhodotorula Glutinis Cultivated on Brewery Effluents. *Energy* **2013**, *61*, 34–43.

13 Jia, R.; Sun, D.; Dang, Y.; Meier, D.; Holmes, D. E.; Smith, J. A. Carbon Cloth Enhances Treatment of High-Strength Brewery Wastewater in Anaerobic Dynamic Membrane Bioreactors. *Bioresour. Technol.* **2020**.

14 Schwarze, F. W. M. R. Wood Decay under the Microscope. *Fungal Biol. Rev.* **2007**, *21* (4), 133–170.

15 Kirk, T. K.; Farrell, R. L. Enzymatic "Combustion": The Microbial Degradation of Lignin. *Annu. Rev.*

Microbiol. **1987**, 465–505.

16 Harvey, P. J.; Thurston, C. F. The Biochemistry of Ligninolytic Fungi. *Fungi in Bioremediation* **2009**, 27–51.

17 Knapp, J. S.; Vantoch-Wood, E. J.; Zhang, F. *Use of Wood-Rotting Fungi for the Decolorization of Dyes and Industrial Effluents*; **2009**.

18 Mehdi Dashtban, Y. H. Lignin in Paper Mill Sludge Is Degraded by White-Rot Fungi in Submerged Fermentation. *J. Microb. Biochem. Technol.* **2015**, *07* (04), 177–181. 5948.1000201.

19 Cardona, M.; Osorio, J.; Quintero, J. Degradación de Colorantes Industriales Con Hongos Ligninolíticos. *Rev. Fac. Ing.* **2009**, No. 48, 27–37.

20 Rodríguez, E.; Pickard, M. A.; Vazquez-Duhalt, R. Industrial Dye Decolorization by Laccases from Ligninolytic Fungi. *Curr. Microbiol.* **1999**, *38* (1), 27–32.

21 D'Annibale, A.; Quaratino, D.; Federici, F.; Fenice, M. Effect of Agitation and Aeration on the Reduction of Pollutant Load of Olive Mill Wastewater by the White-Rot Fungus Panus Tigrinus. *Biochem. Eng. J.* **2006**, *29* (3), 243–249.

22 Atila, F. Cultivation of Pleurotus Spp., as an Alternative Solution to Dispose Olive Waste. *J. Agric. Ecol. Res. Int.* **2017**, *12* (4), 1–10.

23 FitzGibbon, F.; Singh, D.; McMullan, G.; Marchant, R. The Effect of Phenolic Acids and Molasses Spent Wash Concentration on Distillery Wastewater Remediation by Fungi. *Process Biochem.* **1998**, *33* (8), 799–803.

24 Strong, P. J. Fungal Remediation of Amarula Distillery Wastewater. *World J. Microbiol. Biotechnol.* **2010**, *26* (1), 133–144.

25 Hernandes, K. C.; Souza-Silva, É. A.; Assumpção, C. F.; Zini, C. A.; Welke, J. E. Carbonyl Compounds and Furan Derivatives with Toxic Potential Evaluated in the Brewing Stages of Craft Beer. *Food Addit. Contam. - Part A Chem. Anal. Control. Expo. Risk Assess.* **2020**, *37* (1), 61–68.

26 Langner, E.; Rzeski, W. Biological Properties of Melanoidins: A Review. *Int. J. Food Prop.* **2014**, *17* (2), 344–353.

27 Chandra, R.; Bharagava, R. N.; Rai, V. Melanoidins as Major Colourant in Sugarcane Molasses Based Distillery Effluent and Its Degradation. *Bioresour. Technol.* **2008**, *99* (11), 4648–4660.

28 Kumar, V.; Chandra, R. Bioremediation of Melanoidins Containing Distillery Waste for Environmental Safety. In *Bioremediation of Industrial Waste for Environmental Safety*; Bharagava, R. N., Saxena, G., Eds.; **2020**; 495–529.

29 Rizvi, S.; Singh, A.; Kushwaha, A.; Gupta, S. K. *Recent Advances in Melanoidin Removal from Wastewater: Sources, Properties, Toxicity, and Remediation Strategies*; Elsevier Inc., **2022**.

30 Liakos, T. I.; Lazaridis, N. K. Melanoidin Removal from Molasses Effluents by Adsorption. *J. Water Process Eng.* **2016**, *10*, 156–164.

31 Sirianuntapiboon, S.; Phothilangka, P.; Ohmomo, S. Decolorization of Molasses Wastewater by a Strain No. BP103 of Acetogenic Bacteria. *Bioresour. Technol.* **2004**, *92*, 31–39.

32 Dahiya, J.; Singh, D.; Nigam, P. Decolourisation of Synthetic and Spentwash Melanoidins Using the White-Rot Fungus Phanerochaete Chrysosporium JAG-40. *Bioresour. Technol.* **2001**, *78* (1), 95–98.

33 Sen, S. K.; Raut, S.; Bandyopadhyay, P.; Raut, S. Fungal Decolouration and Degradation of Azo Dyes: A Review. *Fungal Biol. Rev.* **2016**, *30* (3), 112–133.

34 Gao, D.; Du, L.; Yang, J.; Wu, W. M.; Liang, H. A Critical Review of the Application of White Rot Fungus to Environmental Pollution Control. *Crit. Rev. Biotechnol.* **2010**, *30* (1), 70–77.

35 Nishida, A.; Fukuzumi, T. Formation of Coniferyl Alcohol from Ferulic Acid by the White Rot Fungus

Trametes. *Phytochemistry* **1978**, *17* (3), 417–419.

36 Chandra, P.; Arora, D. S.; Pal, M.; Sharma, R. K. Antioxidant Potential and Extracellular Auxin Production by White Rot Fungi. *Appl. Biochem. Biotechnol.* **2019**, *187* (2), 531–539.

37 Okamoto, K.; Ito, R.; Hayashi, J.; Tagawa, M. Production of the Antihypertensive Peptide Tyr-Pro from Milk Using the White-Rot Fungus Peniophora Sp. in Submerged Fermentation and a Jar Fermentor. *Dairy* **2021**, *2* (3), 452–461.

38 Vasquez, E. S. L.; Vega, K. Myco-Accessories. **2019**, 306–311.

39 Attias, N.; Reid, M.; Mijowska, S. C.; Dobryden, I.; Isaksson, M.; Pokroy, B.; Grobman, Y. J.; Abitbol, T. Biofabrication of Nanocellulose–Mycelium Hybrid Materials. *Adv. Sustain. Syst.* **2021**, *5* (2), 1–12.

40 Vandelook, S.; Elsacker, E.; Van Wylick, A.; De Laet, L.; Peeters, E. Current State and Future Prospects of Pure Mycelium Materials. *Fungal Biol. Biotechnol.* **2021**, *8* (1), 1–10.

41 López-Abelairas, M.; Álvarez Pallín, M.; Salvachúa, D.; Lú-Chau, T.; Martínez, M. J.; Lema, J. M. Optimisation of the Biological Pretreatment of Wheat Straw with White-Rot Fungi for Ethanol Production. *Bioprocess Biosyst. Eng.* **2013**, *36* (9), 1251–1260.

42 Okamoto, K.; Nitta, Y.; Maekawa, N.; Yanase, H. Direct Ethanol Production from Starch, Wheat Bran and Rice Straw by the White Rot Fungus Trametes Hirsuta. *Enzyme Microb. Technol.* **2011**, *48* (3), 273–277.

43 Mori, T.; Iwata, M.; Kimura, H.; Kawagishi, H.; Hirai, H.; Science, G. 木質バイオマスからのメタン発酵前処理に適した 白色腐朽菌の選抜. **2020**, *28* (2), 56–61.

44 Yoon, L. W.; Ngoh, G. C.; Chua, A. S. M.; Abdul Patah, M. F.; Teoh, W. H. Process Intensification of Cellulase and Bioethanol Production from Sugarcane Bagasse via an Integrated Saccharification and Fermentation Process. *Chem. Eng. Process. - Process Intensif.* **2019**, *142* (March), 107528.

45 Barba, M.; Assumpçao, F.; Helayne, A.; Lopes, G.; Ávila, S.; Silveira, P.; Maccari, A.; Hoffman, R. Factors Affecting Mushroom Pleurotus Spp . *Saudi J. Biol. Sci.* **2019**, *26*, 633–646.

46 Goodley, A. 8 Most Expensive Mushrooms on the Market https://rarest.org/nature/expensive-mushrooms.

47 Kulshreshtha, S.; Mathur, N.; Bhatnagar, P. Mushroom as a Product and Their Role in Mycoremediation. *AMB Express* **2014**, *4* (1), 1–7.

48 Górska, E. B.; Jankiewicz, U.; Dobrzyński, J.; Galazka, A.; Sitarek, M.; Gozdowski, D.; Russel, S.; Kowalczyk, P. Production of Ligninolytic Enzymes by Cultures of White Rot Fungi. *Polish J. Microbiol.* **2014**, *63* (4), 461–465.

49 Tomkins, B. R. G. Measuring Growth: The petri dish method. *Transactions of the British Mycological Society*. **1932**, 17 (1-2), 150–153.

50 Miller, G. L. Use of Dinitrosalicylic Acid Reagent for Determination of Reducing Sugar. *Anal. Chem.* **1959**, *31*, 426–428.

51 Dubois, M.; Gilles, K. A.; Hamilton, J. K.; Rebers, P. A.; Smith., F. Colorimetric Method for Determination of Sugars and Related Substances. *Anal. Chem.* **1956**, *28*, 350–356.

52 Isikhuemhen, O. S.; Mikiashvili, N. A.; Senwo, Z. N.; Ohimain, E. I. Biodegradation and Sugar Release from Canola Plant Biomass by Selected White Rot Fungi. *Adv. Biol. Chem.* **2014**, *04* (06), 395–406.

53 Valencia-Hernández, L. J.; Wong-Paz, J. E.; Ascacio-Valdés, J. A.; Contreras-Esquivel, J. C.; Chávez-González, M. L.; Martínez-Pérez, A.; Castillo-Olvera, G.; Aguilar, C. N. Kinetic Study of Fungal Growth of Several Tanninolytic Strains Using Coffee Pulp Procyanidins. *Fermentation* **2022**, *8* (1), 1–18.

54 Bodin, H.; Hultberg, M. Fungi-based Treatment of Real Brewery Waste Streams and Its Effects on Water

Quality. *Bioprocess Biosyst. Eng.* **2019**, *42* (8), 1317–1324.

55 Dekker, R. F.; Vasconcelos, A. D.; Barbosa, A. M.; Giese, E. C.; Paccola-Meirelles, L. A New Role for Veratryl Alcohol: Regulation of Synthesis of Lignocellulose-Degrading Enzymes in the Ligninolytic Ascomyceteous Fungus, Botryosphaeria Sp.; Influence of Carbon Source. *Biotechnol. Lett.* **2001**, *23*, 1987–1993.

56 Brijwani, K.; Rigdon, A.; Vadlani, P. V. Fungal Laccases: Production, Function, and Applications in Food Processing. *Enzyme Res.* **2010**.

57 Strong, P. J. Improved Laccase Production by Trametes Pubescens MB89 in Distillery Wastewaters. **2011**.

58 Alfaro, M.; Majcherczyk, A.; Kües, U.; Ramírez, L.; Pisabarro, A. G. Glucose Counteracts Wood-Dependent Induction of Lignocellulolytic Enzyme Secretion in Monokaryon and Dikaryon Submerged Cultures of the White-Rot Basidiomycete Pleurotus Ostreatus. *Sci. Rep.* **2020**, *10* (1), 1–10.

59 Raghukumar, C.; Shailaja, M. S.; Parameswaran, P. S.; Singh, S. K. Removal of Polycyclic Aromatic Hydrocarbons from Aqueous Media by the Marine Fungus NIOCC # 312: Involvement of Lignin-Degrading Enzymes and Exopolysaccharides. *Indian J. Mar. Sci.* **2006**, *35* (4), 373–379.

60 Zahmatkesh, M.; Spanjers, H.; van Lier, J. B. Fungal Treatment of Humic-Rich Industrial Wastewater: Application of White Rot Fungi in Remediation of Food-Processing Wastewater. *Environ. Technol. (United Kingdom)* **2017**, *38* (21), 2752–2762.

61 Gutiérrez, A.; Martínez, M. J.; Almendros, G.; González-Vila, F. J.; Martínez, A. T. Hyphal-Sheath Polysaccharides in Fungal Deterioration. *Sci. Total Environ.* **1995**, *167* (1–3), 315–328.

62 Hultberg, M.; Bodin, H. Fungi-Based Treatment of Brewery Wastewater — Biomass Production and Nutrient Reduction. *Appl. Microbiol. Biotechnol.* **2017**, 4791–4798. https://doi.org/10.1007/s00253-017-8185-9.

63 Javaid, A.; Bajwa, R.; Shafique, U.; Anwar, J. Removal of Heavy Metals by Adsorption on Pleurotus Ostreatus. *Biomass and Bioenergy* **2011**, *35* (5), 1675–1682.

64 Yang, S.; Sun, X.; Shen, Y.; Chang, C.; Guo, E.; La, G.; Zhao, Y.; Li, X. Tolerance and Removal Mechanisms of Heavy Metals by Fungus Pleurotus Ostreatus Haas. *Water. Air. Soil Pollut.* **2017**, *228* (4).

65 Zhang, X.; Ye, X.; Guo, B.; Finneran, K. T.; Zilles, J. L.; Morgenroth, E. Lignocellulosic Hydrolysates and Extracellular Electron Shuttles for H2 Production Using Co-Culture Fermentation with Clostridium Beijerinckii and Geobacter Metallireducens. *Bioresour. Technol.* **2013**, *147*, 89–95.

66 Retes-Pruneda, J. L.; Davila-Vázquez, G.; Medina-Ramírez, I.; Chavez-Vela, N. A.; Lozano-Álvarez, J. A.; Alatriste-Mondragón, F.; Jáuregui-Rincón, J. High Removal of Chemical and Biochemical Oxygen Demand from Tequila Vinasses by Using Physicochemical and Biological Methods. *Environ. Technol.* **2014**, *35* (14), 1773–1784.

67 Papaspyridi, L. M.; Katapodis, P.; Gonou-Zagou, Z.; Kapsanaki-Gotsi, E.; Christakopoulos, P. Optimization of Biomass Production with Enhanced Glucan and Dietary Fibres Content by Pleurotus Ostreatus ATHUM 4438 under Submerged Culture. *Biochem. Eng. J.* **2010**, *50* (3), 131–138.

68 Tinoco, R.; Acevedo, A.; Galindo, E.; Serrano-Carreón, L. Increasing Pleurotus Ostreatus Laccase Production by Culture Medium Optimization and Copper/Lignin Synergistic Induction. *J. Ind. Microbiol. Biotechnol.* **2011**, *38* (4), 531–540.

69 Silva, S.; Martins, S.; Karmali, A.; Rosa, E. Production, Purification and Characterisation of Polysaccharides from Pleurotus Ostreatus with Antitumour Activity. *J. Sci. Food Agric.* **2012**, *92* (9), 1826–1832.

70 Wahyudi, P.; Mangunwardoyo, W.; Sumaryono, W.; Gandjar, I. Optimization of Submerged Culture for

Biomass and Polysaccaharide of Pleurotus Ostreatus BPPTCC 6017 Using Response Surface Methodology. *Malays. J. Microbiol.* **2015**, *11* (1), 27–39.

71 Majeau, J. A.; Brar, S. K.; Tyagi, R. D. Laccases for Removal of Recalcitrant and Emerging Pollutants. *Bioresour. Technol.* **2010**, *101* (7), 2331–2350.

72 Tri, C. L.; Khuong, L. D.; Kamei, I. Wood Rot Fungi in the Advanced Biofuel Production. *Fungal Biotechnol. Prospect. Ave.* **2022**, 367–382.

73 Dekker, R. F. H.; Queiroz, E. A. I. F.; Cunha, M. A. A.; Barbosa-Dekker, A. M. Botryosphaeran – A Fungal Exopolysaccharide of the (1→3)(1→6)-β-D- Glucan Kind: Structure and Biological Functions. In *Extracellular Sugar-Based Biopolymers Matrices*; Cohen, E., Merzendorfer, H., Eds.; Springer International Publishing, **2019**; pp 433–484.

74 Papaspyridi, L. M.; Zerva, A.; Topakas, E. Biocatalytic Synthesis of Fungal β-Glucans. *Catalysts* **2018**, *8* (7), 1–23.

75 Cunha, M. A. A.; Santos, V. A. Q.; Calegari, G. C.; Sánchez Luna, W. N.; Marin, S. L. A.; Dekker, R. F. H.; Barbosa-Dekker, A. M. Structure and Biological Properties of Lasiodiplodan: An Uncommon Fungal Exopolysaccharide of the (1→6)-β-D-Glucan Type. In *Extracellular Sugar-Based Biopolymers Matrices*; Cohen, E., Merzendorfer, H., Eds.; Springer International Publishing, 2019; pp 409–432.

76 Smiderle, F. R.; Olsen, L. M.; Ruthes, A. C.; Czelusniak, P. A.; Santana-Filho, A. P.; Sassaki, G. L.; Gorin, P. A. J.; Iacomini, M. Exopolysaccharides, Proteins and Lipids in Pleurotus Pulmonarius Submerged Culture Using Different Carbon Sources. *Carbohydr. Polym.* **2012**, *87* (1), 368–376.

77 Maziero, R.; Cavazzoni, V.; Ramos Bononi, V. L. Screening of Basidiomycetes for the Production of Exopolysaccharide and Biomass in Submerged Culture. *Rev. Microbiol.* **1999**, *30*, 77–84.

78 Rahi, D. K.; Rahi, S.; Chaudhary, E. White Rot Fungi in Food and Pharmaceutical Industries. In *Advances In Macrofungi: Pharmaceuticals and Cosmeceuticals*; Sridhar, K. R., Deshmukh, S. K., Eds.; Taylor & Francis Group, LLC, 2021; pp 175–204.

79 Tampio, E.; Ervasti, S.; Paavola, T.; Heaven, S.; Banks, C.; Rintala, J. Anaerobic Digestion of Autoclaved and Untreated Food Waste. *Waste Manag.* **2014**, *34* (2), 370–377.

80 Chang, C. C.; Chen, Y. H.; Lin, Y. S.; Hung, Z. S.; Yuan, M. H.; Chang, C. Y.; Li, Y. S.; Shie, J. L.; Chen, Y. H.; Wang, Y. C.; Ko, C. H.; Lin, F. C.; Ho, C.; Liu, B. L.; Liu, K. W.; Wang, S. G. A Pilot Plant Study on the Autoclaving of Food Wastes for Resource Recovery and Reutilization. *Sustain.* **2018**, *10* (10), 1–14.

81 Schalchli, H.; Hormazábal, E.; Becerra, J.; Briceño, G.; Hernández, V.; Rubilar, O.; Diez, M. C. Volatiles from White-Rot Fungi for Controlling Plant Pathogenic Fungi. *Chem. Ecol.* **2015**, *31* (8), 754–763.

82 Zhang, C.; Yang, H.; Yang, F.; Ma, Y. Current Progress on Butyric Acid Production by Fermentation. *Curr. Microbiol.* **2009**, *59* (6), 656–663.

83 Estevam, A.; Arantes, M. K.; Andrigheto, C.; Fiorini, A.; da Silva, E. A.; Alves, H. J. Production of Biohydrogen from Brewery Wastewater Using Klebsiella Pneumoniae Isolated from the Environment. *Int. J. Hydrogen Energy* **2018**, *43* (9).

84 Arantes, M. K.; Sequinel, R.; Alves, H. J.; Machado, B.; Fiorini, A.; da Silva, E. A. Improvement of Biohydrogen Production from Brewery Wastewater: Evaluation of Inocula, Support and Reactor. *Int. J. Hydrogen Energy* **2020**, *45* (8), 5216–5226.

85 Kucharska, K.; Łukajtis, R.; Słupek, E.; Cieśliński, H.; Rybarczyk, P.; Kamiński, M. Hydrogen Production from Energy Poplar Preceded by MEA Pre-Treatment and Enzymatic Hydrolysis. *Molecules* **2018**, *23* (11).

86 Zhang, H.; Yao, Y.; Deng, J.; Zhang, J. L.; Qiu, Y.; Li, G.; Liu, J. Hydrogen Production via Anaerobic Digestion of Coal Modified by White-Rot Fungi and Its Application Benefits Analysis. *Renew. Sustain. Energy Rev.* **2022**, *157* (February), 112091.

87 Strong, P. J. Fungal Remediation and Subsequent Methanogenic Digestion of Sixteen Winery Wastewaters. *South African J. Enol. Vitic.* **2008**, *29* (2), 85–93.

88 Müller, H. W.; Trösch, W. Screening of White-Rot Fungi for Biological Pretreatment of Wheat Straw for Biogas Production. *Appl. Microbiol. Biotechnol.* **1986**, *24* (2), 180–185.

89 Montiel-Corona, V.; Palomo-Briones, R.; Razo-Flores, E. Continuous Thermophilic Hydrogen Production from an Enzymatic Hydrolysate of Agave Bagasse: Inoculum Origin, Homoacetogenesis and Microbial Community Analysis. *Bioresour. Technol.* **2020**, *306* (February), 123087.

90 Phowan, P.; Danvirutai, P. Hydrogen Production from Cassava Pulp Hydrolysate by Mixed Seed Cultures: Effects of Initial PH, Substrate and Biomass Concentrations. *Biomass and Bioenergy* **2014**, *64*, 1–10.

91 Zhang, S. C.; Lai, Q. H.; Lu, Y.; Liu, Z. D.; Wang, T. M.; Zhang, C.; Xing, X. H. Enhanced Biohydrogen Production from Corn Stover by the Combination of Clostridium Cellulolyticum and Hydrogen Fermentation Bacteria. *J. Biosci. Bioeng.* **2016**, *122* (4), 482–487.

92 Akinfemi, A.; Adu, O. A.; Doherty, F. Conversion of Sorghum Stover into Animal Feed with White-Rot Fungi: Pleurotus Ostreatus and Pleurotus Pulmonarius. *African J. Biotechnol.* **2010**, *9* (11), 1706–1712.

93 Nayan, N.; Sonnenberg, A. S. M.; Hendriks, W. H.; Cone, J. W. Screening of White-Rot Fungi for Bioprocessing of Wheat Straw into Ruminant Feed. *J. Appl. Microbiol.* **2018**, *125* (2), 468–479.

94 Khan, N. A.; Hussain, S.; Ahmad, N.; Alam, S.; Bezabhi, M.; Hendriks, W. H.; Yu, P.; Cone, J. W. Improving the Feeding Value of Straws with Pleurotus Ostreatus. *Anim. Prod. Sci.* **2015**, *55* (2), 241.

95 Karimi, S.; Soofiani, N. M.; Lundh, T.; Mahboubi, A.; Kiessling, A.; Taherzadeh, M. J. Evaluation of Filamentous Fungal Biomass Cultivated on Vinasse as an Alternative Nutrient Source of Fish Feed: Protein, Lipid, and Mineral Composition. *Fermentation* **2019**, *5* (4).

96 Vetter, J. Mushrooms as Functional Foods. In *Advances In Macrofungi: Pharmaceuticals and Cosmeceuticals*; Sridhar, K. R., Deshmukh, S. K., Eds.; Taylor & Francis Group, LLC, 2021; pp 139–174.

Chapter 5. Hydrogen and electricity generation from brewery sludge as primary feedstock using microbial-electrochemical technologies

Abstract

Technologies based on microbial electrocatalysis (METs) applied to wastewater treatment have developed rapidly over the last two decades. However, literature on the combined use of these novel technologies with dark fermentation (DF) using brewery wastewaters is yet scarce. Microbial electrolysis cells (MECs) are presented here as an assistive technology for DF looking to improve hydrogen production from a substrate with high COD concentration (~60 g/L), based on brewery waste slurry and glycerol co-substrate (5 g/L). Microbial fuel cells (MFCs) were also assessed as a proposed supportive technology. Both METs were conditioned with carbon felt electrodes, modified with polyaniline. MFCs failed to sustain bacterial growth after DF due to the lack of fermentable carbohydrates in the effluent, but the direct treatment of fresh medium was successful, converting ~2.0 watts/g of COD destroyed. Similarly, the MEC process after DF did not show the expected behaviour. However, the fermentation simultaneously assisted by electrolysis (DF/MEC) exhibited a hydrogen production above 98% of the theoretical hydrogen-to-substrate molar yield when butyrate is the main end-product. The applied voltage (0.4 V) favoured the growth of hydrogen-producing species, *i.e.*, *Clostridium butyricum*, which constituted almost half of the microbial population. This rendered a production of 17.9 g/L of butyric acid. COD removal efficiencies attained nearly 40% in both METs. Furthermore, the DF/MEC process required 60% less energy input per litter of hydrogen produced compared to an average conventional water electrolysis, reaffirming the potential of these novel technologies as an attractive alternative approach to produce green hydrogen.

5.1 Introduction

Dark fermentation (DF) is generally agreed to be more effective in producing hydrogen than other biocatalytic processes by virtue of the low energy inputs required (optimal conditions are mostly carried out at mesophilic conditions); hydrogen production can

be achieved using a wide variety of substrates; and compared to biophotolysis and photofermentation, DF bioreactors are much smaller, and the process is sunlight-independent[1–6]. In spite of these advantages, hydrogen production in DF is still largely restricted by the microorganisms' metabolism, commonly showing low yields ($2-4$ mol of H_2 per mol of glucose) compared to other conventional technologies[7]. In order to achieve a more practical, energy-efficient DF-based hydrogen production process, various attempts have been studied, such as sequential anaerobic digestion (AD) post-treatment, and two-staged process to generate more hydrogen, like photofermentation or microbial electrochemical technologies (METs)[8,9].

As opposed photofermentation, in which feeds normally are greatly diluted substrates, METs usually accept feeds with higher organic load within the typical DF discharge range ($2-40$ g COD/L). Besides, DF effluents are rich in volatile fatty acids (VFAs), which can serve as suitable carbon source for microorganisms involved in METs[10]. Another advantage is that the dark-fermentative process can be assisted by METs in a single-staged process[11]. The main technologies included in METs are microbial fuel cells (MFCs), and microbial electrolysis cells (MECs). MFCs are devices that convert chemical energy stored in organic matter into electrical energy through electrochemical reactions involving bacteria as catalysts. The working principle is based on the electrons transfer from a reduced substrate to a terminal electron acceptor[12]. In MECs, organic matter is oxidized by electrogenic bacteria in the vicinity of the anode to yield protons and electrons. While in MFCs oxygen is reduced in the cathode to produce water, in MECs, transferred electrons to the cathode reduce H_2O and protons to produce H_2 and OH^-. This coupled redox reaction is thermodynamically unfavourable ($E°_{cell} = -1.23$ V), therefore an external potential must be applied[13]. In theory, however, to produce hydrogen in MECs, electrical energy input could be at around one-tenth of that in conventional water electrolysis[14]. This is possible because the substrate oxidation by microorganisms supplies part of the energy required to split water molecules[15]. Microbial electrolysis is also used to assist methanogenesis in AD, since the potential applied accelerates the synthesis of end products in each stage of

the AD process, and it has been found that above a poised potential of 0.6 V, hydrogen-consuming bacterial communities increased their population in the vicinity of the anode, thus accelerating acetogenesis and reducing HRTs[9,16]. In accordance with the reported data, in general, higher applied potentials (0.6 V–1.8 V) promotes methanogenesis, while hydrogenesis is favoured between 0.4 V–0.6 V[13,15].

Virtually any carbon source can serve as substrate in these technologies. Beyond sludge and municipal wastewaters, METs have been thoroughly studied for the treatment of diverse agro-industrial and lignocellulosic wastes[11]. Among the residues explored are brewery wastewaters (BWW), specially in MFCs[17]. These wastes are an interesting source; rich in carbohydrates and nutrients for microbial growth[18], its chemically stored energy is been estimated around 14 kJ per g of COD[19]. MFCs treating BWW exhibited power outputs from 0.44 W to 24 W per cubic meter[20,21]. In MECs, however, most of the literature reported is related to electrically enhanced anaerobic digestion of BWW[22]. However, methane production from BWW in AD assisted with MECs is still restricted by the activity of methanogens, rather than the organic oxidation rate and the electron transfer in the anode, which is seen by the recent yields reported, 140 – 260 mL CH_4/g COD[23,24], falling within the typical range of conventional AD (150–530 mL CH_4/g COD[25–28]). In contrast, MECs have more potential to enhance hydrogen production. Studies on integrated systems combining DF and MECs, using different food and lignocellulosic wastes, have revealed that microbial electrolysis can increase hydrogen production rates (HPR) up to 400% (with an average of 148%) after DF, and when combined, an average of 225% enhancement was observed[29]. Furthermore, the integration of both METs could also enhance a dark fermentative process, harnessing more energy from wastes. An integrated system combining DF with an MEC post-treatment of a cellulose-based medium, with energy being supplied by MFCs (voltage output of 0.441 ± 0.010 V), demonstrated the potential to enhance HPR by 41% more than in DF alone without energy supply from the grid[30].

The objective of the current work, therefore, is to evaluate the potential of a brewery waste slurry (BWS) with a high concentration of organic matter (COD), supplemented

with 5 g/L glycerol (as has been done in **Chapter 3**), as substrate to produce hydrogen and electricity in METs in two scenarios: 1) after DF process, 2) assisting during the DF process. The performance of a dark fermentative process assisted by simultaneous MEC against microbial electrolysis of a DF effluent as a combined system was evaluated. Similarly, it is sought to compare the MFC post-treatment of the DF effluent versus MFC treatment of fresh BWS-based medium. Since the performance of the electrodes is fundamental for electrocatalytic processes, a polyaniline-modified carbon felt electrode was prepared. Its performance, biocompatibility, and stability with and without ruthenium dioxide nanoparticles was compared to a plain carbon felt electrode using cyclic voltammetry, this with the objective to select the best modified electrode to serve as anode in MFCs and both anode and cathode in MECs.

5.2 Materials and Methods

5.2.1 Feedstocks, chemicals, and reagents

The residue employed was a brewery waste slurry (BWS) obtained from a regional brewery in eastern Ontario, Canada, with characteristics described in **Chapter 3** and **Chapter 4**. It contains slurry from the brewing process in addition to waste beer. The BWS was first filtered through a conventional strainer with a gauze to remove gross solids, and then stored at 4°C for further experiments.

M9 medium (M9M) was used as the control mineral medium. The salts and nutrients employed to prepare it were: KH_2PO_4 (Fisher Chemical™), $Na_2HPO_4{\cdot}7H_2O$ (EMD Millipore™), NaCl (Fisher BioReagents™), NH_4Cl (Sigma-Aldrich™), yeast extract (Thermo Scientific™), glycerol ≥99.5 % (Fisher Chemical™), and the trace salts $MgSO_4$ (Sigma-Aldrich™) and $CaCl_2$ (Fisher Chemical™). Besides KH_2PO_4, other buffer salts include K_2HPO_4 (Fisher Chemical™) and sodium acetate (Alfa Aesar™). M9M was prepared according to the standard procedure shown elsewhere in[31], using a concentration of 5 g/L both of yeast extract and glycerol. Other chemicals used were aniline ACS reagent ≥99.5% (Sigma-Aldrich™), ammonium persulfate ACS (VWR™), 0.5 N sulfuric acid solution (LabChem™) and 36.5 to 38.0% HCl (Fisher Chemical™).

For the analysis of reducing sugars, 250 mL of reactive was prepared mixing the compounds in the following order: 2.5 g 3,5-dinitrosalicylic acid (DNS) 98% (Fisher Scientific™), 0.5 g phenol 99% (Thermo Scientific™), 0.125 g Na_2SO_3 (Fisher Chemical™), 2.5 g NaOH (Fisher Chemical™), 50 g Rochelle salt (Fisher Chemical™). For the total sugars analysis, concentrated sulfuric acid (LabChem™), so as an 80% w/w phenol solution. Both the DNS and phenol solutions were kept in opaque glass bottles and refrigerated for their preservation.

The standard solutions for the chromatography analysis were prepared using glacial acetic acid ≥99.5% (Fisher Scientific™), *n*-butyric acid ≥99.0 % (Sigma-Aldrich™), lactic acid 98.0% (Sigma-Aldrich™), formic acid 99.0 % (Thermo Scientific™), propionic acid ≥99.5% (Sigma-Aldrich™), and the mobile phase was prepared with H_2SO_4 0.5 N (LabChem™). The gases to obtain the calibration curves for spectrometric analysis (H_2, CO_2, CH_4), as well as argon as the carrier, were compressed, pure gases (≥99.9%), all provided by Linde® Canada.

5.2.2 METs configuration

The MFC configuration was a single-chambered cell with a carbon cloth loaded with commercial 0.2 mg/cm^2 of 20% Pt on carbon Vulcan and coated with 30% PTFE (The Fuel Cell Store) as the air cathode. The inner face of the carbon cloth was coated with Nafion (5% wt. solution). The working electrode consisted of rounded pieces of carbon felt (The Fuel Cell Store), eight of them provided with holes to facilitate the flux of liquid through them, and a ninth one fully flat, facing the cathode. Stainless-steel wire served as the current collector between each carbon felt (0.32 cm Ø). Nafion 117 membrane was separating the bulk solution from the air cathode. The electrodes were connected to an external circuit with a 1 kΩ resistor with a Ni-Cu wire. The working volume of the cell is 110 mL. The MEC configuration was a membraneless single-chambered cell with a working volume of 150 mL. Enhanced CF was used as both anode and cathode (5 cm Ø). The cell was provided with a sampling port and outlet and inlet of gas. The potential of the cell was poised at 0.4 V with a potentiostat/galvanostat MSTAT (Arbin Instruments®). As in the MFC, a Ni-Cu wire served as the external circuit between the

electrodes and the potentiostat. For all the experiments, the cells and all their materials were autoclaved (121 °C, 20 min). Once assembled, the cells were purged with nitrogen passed through a 0.22 µm filter to avoid contamination. The experiments were conducted in a controlled environment at 35 °C.

5.2.3 Deposition of polyaniline in carbon-based electrode

The carbon felt was submerged in 0.5 N H_2SO_4 solution overnight, then thoroughly washed with deionized water (DI, 18 MΩ cm) and dried at 60 °C. Aniline polymerization was prepared similarly as the process described elsewhere in[32]. 50 mL of aniline solution in 1M HCl, and 50 mL of ammonium persulfate solution in 1M HCl, were mixed, at a molar proportion of 1:1.25, and constantly agitated. The carbon felt was submerged in the mixing solution. After 15 min, the electrode was washed with 1M HCl solution, then with deionized water, then with acetone. The electrodes were dried overnight at 60 °C in an oven.

5.2.4 Ruthenium dioxide nanoparticles

The electrodes were prepared by submerging the material in a colloidal solution of RuOx nanoparticles (0.5–1.0 nm in diameter) with a concentration of 0.3 mg/mL. When the solution was completely absorbed, the electrodes were dried up at 50 °C in an oven for 24 h. The RuOx nanoparticles colloidal solution synthesis was reported earlier[33–35].

5.2.5 Modified carbon-based electrodes performance

The performance of the carbon-based electrodes was characterised before being used in the electrochemical cells: a plain carbon felt electrode (CF), and a polyaniline-modified carbon felt electrode (PANI-CF), facilely prepared by *in situ* chemical polymerization of aniline. The analysis consisted of first running chronoamperometry (CA), 3.5 A charge during 5 min, then discharge during 20 min, and cyclic voltammetry (CV) using M9M as electrolyte. For the CV tests, two conditions were evaluated: 50 mL of 1) sterile M9M, 2) inoculated M9M with heat-treated anaerobic sludge (see **Chapter 3**). After that, a PANI-modified electrode with ruthenium oxide nano particles (PANI-RO) was also analysed using cyclic voltammetry experiments at 50 mV/s.

5.2.6 Dark fermentation

The hydrogen production potential was analysed in 30 h batch fermentations. The MEC was inoculated with a 1.3% v/v heat-treated anaerobic sludge collected from the City of Ottawa's wastewater treatment plant (ROPEC WWTP). The temperature was kept at 35°C by submerging the reactor in a water bath, and the pH was adjusted at 6.4 by first increasing the alkalinity (addition of 100 mg/L of CaCO3), then kept controlled by adding salts as to prepare a 0.03 M 6.4 pH potassium phosphate buffer solution (8.9 mM K_2HPO_4 and 21.1 mM KH_2PO_4). The final organic acids composition so as the sugar consumption was determined.

5.2.7 Chemical analysis

Reducing sugars content was determined by the DNS (Miller's) method[36], and total sugars concentration was determined by the phenol-sulphuric acid (Dubois's) method[37]. Raw samples may be diluted 5 to 10 times. The processed samples were read in a HACH® DR6000 UV-VIS Laboratory Spectrophotometer at the wavelength of 540 nm in the case of reducing sugars, and 490 nm for total sugars. Both reducing sugars and total sugars are expressed as grams of glucose equivalent per liter. Chemical oxygen demand (COD) was determined by the HACH® 8000 Reactor Digestion Method using high range vials (20 – 1,500 mg/L). Digested samples were read in the same spectrophotometer.

The production of organic acids was determined by chromatography in an Agilent® HPLC Series 1200, using a Bio-Rad Aminex HPX-87H column and UV at 210 nm. The column was kept at 60°C and the RID at 50°C. Samples from the bottles were taken periodically, centrifuged (10,000 rpm, 10 min), and the supernatant was filtered with a hydrophobic PTFE syringe filter (0.22 µm). Finally, 20 µL of each sample was injected and diluted in H_2SO_4 5 mM as the mobile phase. The elution time of each sample was 25 min. Fermentation gases were monitored continuously through mass spectroscopy during 30 h in a Dycor Proline Process Mass Spectrometer (Ametek® Instruments), carried by a stream of argon at 100 mL/min, flow rate monitored and controlled by a Horiba® VIA-510 Gas Analyzer.

5.2.8 Electrochemical measurements

Cyclic voltammetry was carried out in a Bio-Logic SAS potentiostat (model 0474) at a scan rate of 50 mV/s. The three-electrode electrochemical cell consisted of an 18 mm diameter piece of carbon felt (plain CF was the control versus PANI modified CF) as the working electrode (WE); Ag/AgCl (sat. KCl) served as a reference electrode (RE), and a platinum coil (25 cm) as the counter electrode (CE). The initial and final potentials were set to -0.35 V to 1.00 vs Ag/AgCl. The cell was sparged with nitrogen gas continuously, passed through a 0.22 µm filter to avoid contamination. CVs were taken at 0, 6, 9, 12 and 18 hours. Between each run, the cell was poised at 0.4 V. The cell contained 50 mL of electrolyte, pH and temperature were controlled (7.0 pH, 34°C – 36°C). In the case of MFC's, polarization curves were obtained using the same equipment, in which the WE was the anode, and the cathode was both RE and CE.

5.2.9 Hydrogen yield and energy recovery analysis

In addition to overall H_2 recovery, coulombic efficiency (%CE_{COD}), cathodic H_2 recovery (r_{cat}, %), volumetric current density (A/m^3), and energy efficiency relative to electrical input (η_E, %) and substrate input (η_S, %), were the parameters used to evaluate the performance of the electrocatalytic process, in accordance with[38]:

The coulombic hydrogen recovery was calculated as follows:

$$r_{CE} = \frac{\eta_{CE}}{\eta_{th}} \tag{5.1}$$

Where r_{CE} is the coulombic efficiency, and η_{th} and η_{CE} are calculated as follows:

$$\eta_{th} = \frac{b_{H_2/S}\, V_L\, \Delta S}{M_S} \tag{5.2}$$

Where $b_{H_2/S}$ is the maximum theoretical stoichiometric hydrogen production from the substrate (4 mol H_2 per mol of glucose[6], versus 2.4 mol H_2 per mol of glucose when butyrate is the main end product[39]), V_L is the fermentation volume, ΔS is the change in substrate concentration, and M_S is the substrate molecular weight. ΔS can be

substituted by $\Delta\mathrm{COD}$, in which a conversion factor must be used: 1.07 g COD/g glucose, 1.22 g COD/g glycerol, 1.07 g COD/g lactic acid, 1.82 g COD/g butyric acid.

$$\eta_{\mathrm{CE}} = \frac{\int_0^t I\mathrm{d}t}{2F} \tag{5.3}$$

Where, F is Faraday's constant (96,485 $\mathrm{C/mol\ e^-}$), $I = V/R_{ex}$, is the current (A) calculated from the voltage across the external resistor (potentiostat). Whereas $\%\mathrm{CE_{COD}}$ calculated from COD consumption is defined by the following equation:

$$\%\mathrm{CE_{COD}} = \frac{8\int_0^t I\mathrm{d}t}{FV_{an}\Delta\mathrm{COD}} \tag{5.4}$$

Where V_{an} is the volume of the anodic chamber, and 8 is a constant used for COD based on M_{O_2} (32 g/mol) and 4 electrons exchanged per mole of O_2. $\%\mathrm{CE_{COD}}$ in MFCs was calculated using **Eq. 5.4**, while in MECs it was calculated from **Eq. 5.1**.

$$r_{\mathrm{cat}} = \frac{\eta_{\mathrm{H_2}}}{\eta_{\mathrm{CE}}} \tag{5.5}$$

The cathodic hydrogen recovery r_{cat} is the ratio of hydrogen moles recovered relative to that possible based on the measured current, where $\eta_{\mathrm{H_2}}$ is the number of hydrogen moles produced during the process.

$$\eta_{\mathrm{E}} = \frac{W_{\mathrm{H_2}}}{W_{\mathrm{E}}} = \frac{\eta_{\mathrm{H_2}}\Delta H_{\mathrm{H_2}}}{W_{\mathrm{E}}} \tag{5.6}$$

The energy efficiency related to electrical input (η_{E}) is calculated by the energy content of the hydrogen produced, where is $\Delta H_{\mathrm{H_2}} = 285.83$ kJ/mol, and the electrical energy input W_{E}, defined by the following equation:

$$W_{\mathrm{E}} = \sum_1^n \left(I E_{\mathrm{ap}}\Delta t - I^2 R_{ex}\Delta t\right) \tag{5.7}$$

Where E_{ap} is the voltage applied. In this equation is also included the energy applied to heat up the system at 35°C.

$$\eta_S = \frac{W_{H_2}}{W_S} = \frac{W_{H_2}}{\Delta H_i \eta_i} \tag{5.8}$$

The efficiency relative to the added substrate (η_S) is calculated based on the heat of combustion (ΔH_i), and moles (η_i) of each component considered as substrate. Finally, the overall energy recovery based on both the electricity and substrate inputs $\left(\eta_{E+S}\right)$ is given by the following equation:

$$\eta_{E+S} = \frac{W_{H_2}}{W_E + W_S} \tag{5.9}$$

The hydrogen production data was processed and modelled using a modified Gompertz function:

$$H(t) = P \times \exp\left\{-\exp\left[\frac{2.71828 \cdot R_m}{P}(\lambda - t) + 1\right]\right\} \tag{5.10}$$

Where $H(t)$ is the cumulative hydrogen (mL) at a given time t, P is the hydrogen production potential (HPP) in (mL), λ is the lag phase (h), and R_m is the hydrogen production rate (mL/h). Data processing was carried out in Excel, fitting the RSE of the model versus the data obtained from the Mass-Spectrometer.

5.3 Results and discussion

5.3.1 Enhancement of the carbon felt electrode

Deposition of PANI have proven to enhance the performance of carbon-based materials, including carbon felt, specially in METs[40–42]. In the present work, the CA analysis showed a higher cumulative charge of 33.7 A/m^2 by the PANI-CF electrode versus 10.3 A/m^2 of the control. It was also observed a higher stable current density after 10 min of discharge (0.68 A/m^2), while no charge was observed after 50 sec with the bare CF. Moreover, under anaerobic fermentation with the anaerobic heat-treated sludge (closed circuit with 1 kΩ resistor), after 24 h, the PANI-CF also demonstrated to be stable and biocompatible, as seen in the bacterial growth on the carbon fibers in **Figure 5.1 D**. Some researchers have pointed that the internal capacitive features conferred to carbon-based materials by PANI, indicate that the polymer may modify

the anode in such a way that it can function as a bio-capacitor in microbial electrochemical systems. Wang *et al.*[43], described these qualities in modified carbon felt anodes by chemical polymerization of aniline. The authors found a higher average peak current density of the PANI-capacitive *bio*-electrode 2.8 times greater than the control (9.27 mA/cm^2 vs 3.36 mA/cm^2), a similar pattern found in the present work.

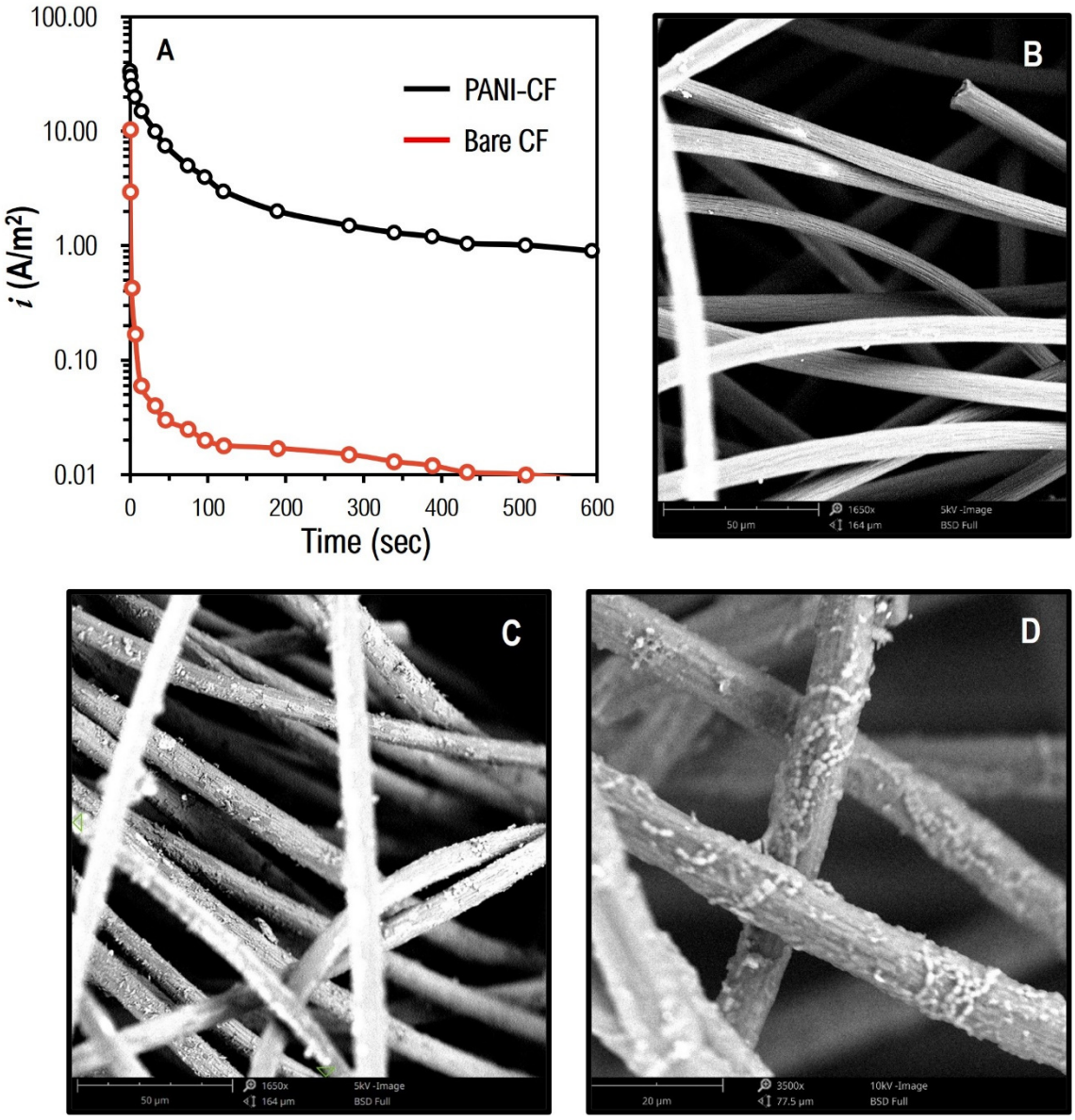

Figure 5.1. *A) Chronoamperometry of PANI-coated carbon felt and bare carbon felt. B) SEM image of bare carbon felt. C) SEM PANI-coated carbon felt after. D) SEM image of bacterial colonies in PANI-coated carbon felt after 24 h of fermentation under anaerobic conditions.*

Beyond the conductivity and capacitive enhancement of the electrode, the most important factor is biocompatibility. In this regard, PANI has demonstrated not only to be biologically stable, but also to perform as mediator, assisting in the electron transfer chain between bacteria's outer cell wall and electrodes. As seen in **Figure 5.2 A**, the

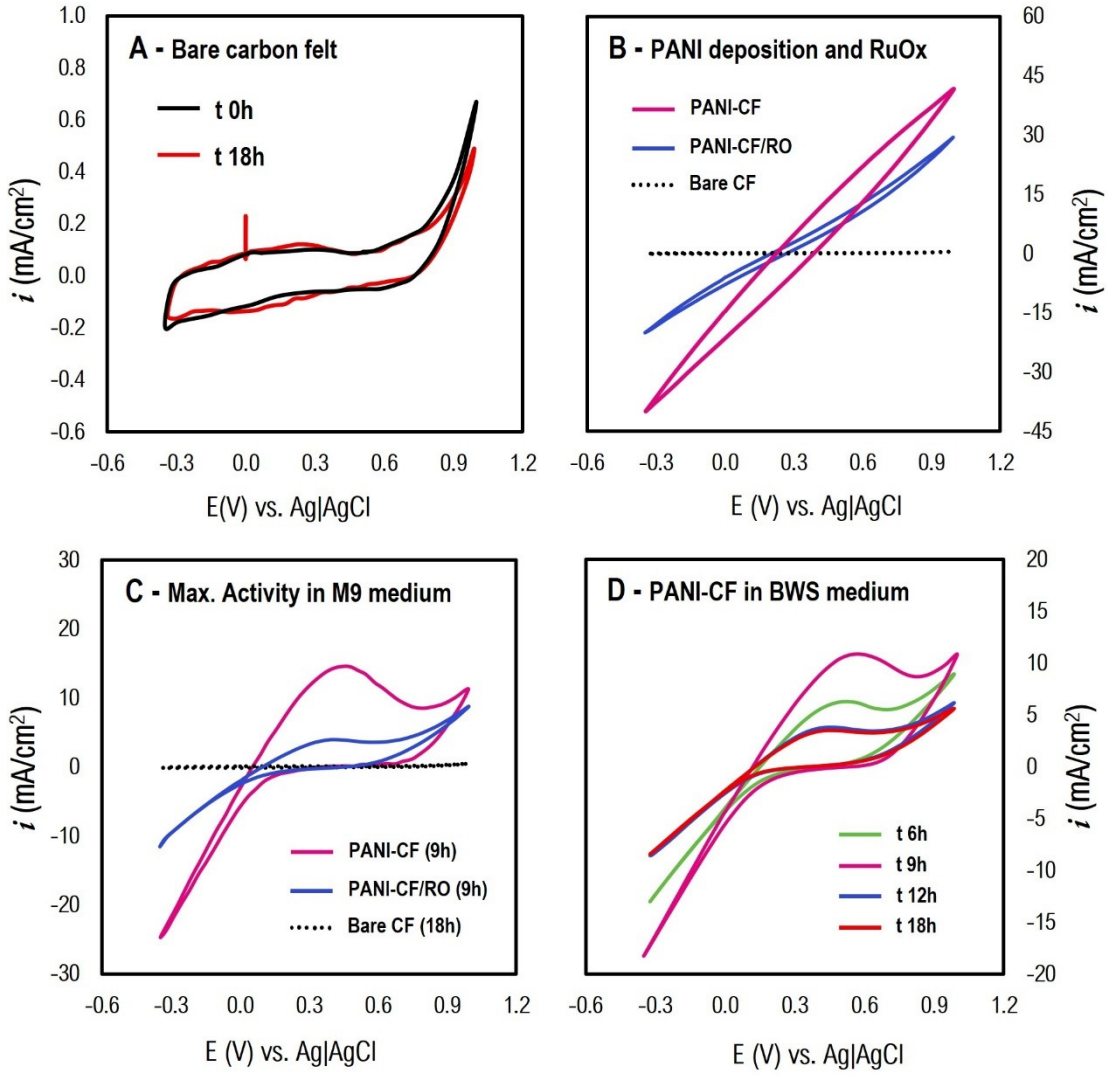

Figure 5.2. *Cyclic voltammetry (50 mV/s, pH 6.4). A) Plain carbon felt in M9 medium from t = 0 h to t = 18 h. B) Effect of polyaniline deposition on the carbon felt, with and without RuOx nanoparticles in M9 medium (no inoculum). C) CF, PANI-CF with and without RuOx nanoparticles. D) Polyaniline modified carbon felt in inoculated brewery waste slurry and 5 g/L glycerol as a function of time (pH 6.4, adjusted with 0.03 M potassium phosphate buffer).*

bare CF does not exhibit any activity over time when using the sterile M9M, nor when the medium was inoculated (**Figure 5.2 C**). On the contrary, PANI coating renders electrochemical activity over the medium when this is inoculated. More importantly, this activity is directly related to biological growth, since there was no electrochemical activity whatsoever observed over time in the sterile M9M (**Figure 5.2 B**). PANI-modified electrode with ruthenium nanoparticles was also analysed using CV. The deposition of RuOx nanoparticles demonstrated biocompatibility, and it was expected to enhance the MFCs performance by accumulating charge in the anode as has been proposed[44]. Nevertheless, this PANI/RuOx composite electrode did not demonstrate an enhanced behaviour when compared to the simple PANI-modified material. This could have been due to the fact that the RuOx nanoparticles might be more efficient at alkaline pH, while the CV tests were performed at pH 6.4.

In M9M, an irreversible oxidation activity was observed in both PANI-modified electrodes, being more notorious with PANI-CF alone (**Figure 5.2 C**). Electrocatalytic activity of PANI-CF in inoculated BWS-based medium shows max. oxidation peaks between 0.48 V and 0.57 V, the highest attained at 9 h of incubation. The behaviour shown in **Figure 5.2 D** resembles the electrocatalytic profile of glucose oxidation on PANI and glucose oxidase nanocomposite electrodes[45], indicating the link between the modified electrode and the biological activity over the substrate in the BWS medium.

5.3.2 Microbial fuel cells

All MFCs devices, (including the MECs), were conditioned for 3 days running in M9M, closed circuited at a fixed 1 kΩ resistor, room temperature, and inoculated with the heat-treated sludge under anaerobic conditions. The three MFCs were evaluated according to each different anode employed: 1) plain CF (MFC-CF); 2) PANI coated CF (MFC-PA); and 3) PANI-CF/RuOx composite electrode (MFC-PR). Towards the end of the conditioning period, all MFCs began to show a stable closed-circuit voltage (CCV) between 60 – 65 mV. At this point preliminary tests were conducted to treat 80% BWS and glycerol co-substrate (5 g/L) with an initial COD of 58.9 g/L, at 35 °C. After 12 hours of incubation, the highest open-circuit voltage (OCV) measured was 420 mV in the

MFC-PA, whereas the lowest was observed in the MFC-CF (144 mV). According to the CV results, it was expected a higher voltage by the 18th hour, however, the OCV showed a drop between 11% to 13% in all three cells (196, 375, and 315 mV, respectively). After 24 hours, the OCV upsurged, showing a steady voltage for few hours (223 ± 13 mV MFC-CF; 480 ± 30 mV MFC-PA; 372 ± 26 mV MFC-PR), before dramatically drop below 50 mV after the 30th hour. This clearly indicates the suitable HRT for a fed-batch, or continuous MFC process. The polarization curves depicted in **Figure 5.3** were taken at the highest peak of activity, between 24 to 30 hours.

The COD consumption at the end of the process was also determined. As seen previously in **Chapter 3**, by the end of the fermentation, the bacteria would have depleted the readily fermentable sugars. This can be related to the similar percentage of COD consumed: 35.3% after 30 h of dark fermentation versus: 1) 36.5% in MFC-CF; 2) 38.3% in MFC-PA; 3) 33.4% in MFC-PR. In this regard, the coulombic efficiency (%CE) was higher in the MFC with the PANI/RO composite electrode (75.1%), followed by MFC-PA with 69.7%, while the MFC with the bare CF attained a 57.1%.

Polarization curves of each cell are depicted in **Figure 5.3**. The highest maximum power density observed was in the MFC with the PANI modified electrode, 57.0 mW/m^2, followed by the PANI/RO composite anode, 32.6 mW/m^2, and 21.9 mW/m^2 obtained by the MFC-CF. However, the current density exhibited by the MFCs with the bare CF and the PANI-CF was similar (291 and 290 mA/m^2, respectively), while the MFC-PR reached 360 mA/m^2. This demonstrates that, even though the RuOx nanoparticles did not exhibit a big impact in this particular biological process reflected in the CVs (**Figure 5.2 C**), the capacity of the electrode to collect more current was increased by 24%, enhancement shown in the higher $\%CE_{COD}$ as well. In accordance with the CV tests, it would be expected a higher current density by the MFC with the PANI-modified electrode than at least the MFC with the plain CF. But these curves demonstrate that the limiting factor is still the oxygen reduction reaction (ORR) in the cathode and the projected area of the proton exchange membrane (PEM), which is the same as that of the cathode.

It is common practice to report power densities calculated on the basis of anodic chamber volume as well[46]. The maximum volumetric power density calculated was 410.5 mW/m^3 for the MFC-PA, which is superior to some similar works, although is lower to the majority of the reported literature, as seen in **Table 5.1**. In the case of MFCs, several factors affect their performance, from the nature of the inoculum to the characteristics of each material and even the cell configuration. The size of the proton exchange membrane and the cathode are the limiting factors to scale these devices, for instance. The larger the projected surface area of these two components, the higher power output delivered[47]. However, PEMs and active cathodes for ORR are expensive materials. Therefore, smaller working volumes are often sought. To illustrate this, Feng *et al*.[48], reported the performance of an MFC treating a highly diluted brewery wastewater (2.24 g/L COD) calculating 5.1 W/m^3, or 205 mW/m^2 power density, with a OCV of 362 mV. Although the projected surface area of their device is similar to the one of the present work (7 cm^2 against 7.9 cm^2), the working volume of the anode chamber was 28 mL, 4 times lower, a proportional difference that can be related by comparing the power densities.

In this vein, increasing the size of MFC's PEM surface area is not ideal, but the use of small stacked units instead[49]. Zhuang *et al*.[50] designed a serpentine-like reactor with a 10 L working volume in which 40 small sequential MFC units were placed, attaining 4.1 W/m^3 and an overall OCV of 23 V. In agreement with this, a case scenario of a microbrewery with annual production of 15,000 hL, the electricity that could be generated is less than 0.05 kWh per cubic meter treated on a daily basis, using an MFC with a PANI modified electrode. However, the same volume of BWS distributed in 30 to 40 MFC-PA units would represent 1.2 - 1.6 kWh/m^3-day, energy output comparable to the 1.44 kWh daily output of a conventional 1.6 m^2 solar panel[51]. This also would represent an energy conversion of 1/3 of the total energy chemically stored in the BWS, in accordance with the estimations presented in[19].

Table 5.1. Comparative analysis of studies on energy conversion in MFCs from brewery wastewaters

Seed sludge	Electrodes		Membrane		Vol.	COD initial	COD removed	OCV	Current density		$\%CE_{COD}$	Ref.
	Anode	Cathode		(cm^2)	(mL)	(g/L)	(%)	(mV)	(mW/m^2)	(mW/L)	(%)	
Anaerobic sludge	PANI/ carbon felt	Carbon cloth Pt (0.2 mg/cm^2)	Nafion 117	7.9	110	59.0 ± 2.1	38.3	480	57.0	0.41	69.7	This study
Brewery wastewater	Carbon cloth	Carbon cloth Pt (0.35 mg/cm^2)	E-TEK®	7.0	28	2.25	87	362	205	5.10	10	48
Anaerobic mixed consortium from the brewery	Carbon fibre (TC35-12K)	Stainless steel Pt load	Nafion 117	36.0	100	1.5	20.7	560	669	24.10	—	52
Activated sludge	Graphite felt/ Carbon cloth	Carbon cloth PTFE/Pt load	PP fabric	12.0	225	0.51	—	656	552	2.94	41	53
MFC adapted inoculum	Graphite felt	GORE-TEX® cloth Ni-based layer	—	NA [a]	250 [b]	2.1	87.1	580 [c]	65.4	4.10	6.3	54
Sludge from lagoon sediment	Carbon fibre Cloth (Zoltek)	Carbon fibre Cloth (Zoltek)	NFM	25,900	18,800	3.2	94.5	—	2.76	0.44	5.5	20
Anaerobic mixed consortium from the brewery	Carbon felt Graphite rods	Carbon felt biocathode	Nafion 117	36.0	100	1.2	95.7	434	7.5	0.83	—	55
Anaerobic sludge from the brewery	Tin-coated copper mesh	Tin-coated copper mesh	Nafion 117	7.0	275	2.3	82	—	80	—	—	56
Anaerobic sludge	Carbon fibre brushes	PFSA AC (0.5 mg/cm^2)	PFSA	113	1,000	3.3	13	—	31	0.31	—	57
Anaerobic sludge from the brewery	Carbon brushes	Carbon brushes	CT/PMC	24.1	650	3.3	72	—	120	3.49	—	58
Anaerobic mixed consortium from the brewery	Carbon fibres Graphite rods	Nafion/AC/PTFE Pt (0.8 mg/cm^2)	Nafion 117	36	100	1.7	41.7	578	264	9.52	19.8	59

[a] Membraneless (155 cm2, projected surface area between anode and cathode); [b] Individual cell volume, 10 L total volume; [c] Individual OCV, overall OCV 20.1 V

PFSA – Persulfonic acid membrane; NFM – nano filtration membrane; PTFE – Polytetrafluoroethylene; AC – Activated carbon; CT/PMC – Chitosan/copolymer membrane

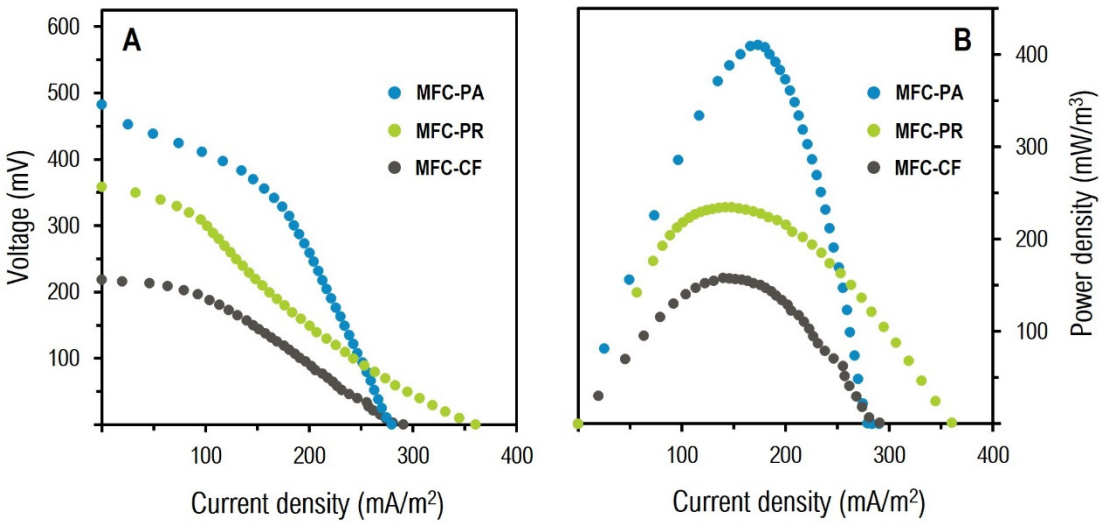

Figure 5.3. *A) Polarization curves of each MFC at the highest activity. B) Power density for each MFC expressed in mW/m³.*

Regarding the treatment of a DF effluent in MFCs, it was not observed a considerable electricity generation, as in all readings, the CCV hardly exceeded the 20 mV. The performance was far below the optimum conditions when the fresh BWS is supplied to the cells (see **Appendix**). This low performance is presumably related to the lack of enough nutrients in the DF effluent. The residual fermentable sugars after dark fermentation was 1.50 ± 0.1 g/L. After 20 hours of MFC process of this effluent, the remaining total carbohydrates were determined around 0.61 g/L. In the following section this matter will be further discussed.

5.3.3 Hydrogen production

In view of the previous results, in this section it is only presented the hydrogen production potential (HPP) of the MEC with the PANI-modified carbon felt, performance compared to the HPP in dark fermentation from **Chapter 3**, as the PANI-CF/RO composite electrode did not exhibit a positive response during the conditioning steps, but rather proved counterproductive, thus it will not be discussed in this section (see **Appendix**). Therefore, hereafter, MEC will only refer to the membraneless, single-chambered electrolysis cell with PANI-modified electrodes, *i.e.*, both anode and cathode. Furthermore, two conditions were tested: 1) BWS (80%, supplemented with

5 g/L glycerol) treated in a dark fermentative microbial electrolysis process (DF/MEC); 2) microbial electrolysis treatment of a DF effluent. Both treatments were conducted at the optimum conditions of pH buffered to 6.4, during 30 h at 35°C, while the potential was poised at 0.4 V.

Hydrogen maximum production rate (HPR) attained in the DF/MEC was 1.63 ± 0.06 mL H_2/min after 17 hours, that is more than 2 times the maximum HPR registered in DF alone. The total cumulative volume of hydrogen produced per litter of BWS was 9.95 L H_2/L, which is 1.6 times more hydrogen, or a 56.7% increase with respect to DF alone. The Gompertz model fit the data very well with the maximum modelled flow rate (R_m) of 70.9 mL H_2/h, and a there is a longer lag phase of 7.9 hours, 3 hours more than in DF alone (**Figure 5.4**). The final COD was 22.8 ± 0.1 g/L (38.7% reduction).

On the contrary, treating the effluent from the dark fermentation in MEC did not produce a considerable amount of hydrogen, in fact, the data collected suggests as if the bacterial activity were stuck in a loop of consuming and re-forming end products. Butyric acid concentration dropped from 6.00 g/L to 4.04 g/L by the 18Th hour, but the final concentration determined was 4.42 g/L at 30 hours, for instance. The HPR exhibited a rather erratic behaviour in contrast with all previous experiments as well (**see Appendix**), neither could be modelled. Notwithstanding, the final cumulative volume measured was 0.86 L H_2 per L of DF-treated BWS effluent, albeit around 12 times lower than the yield in the MEC treating the raw BWS. The final COD did not vary much either; it was reduced only 4.8 ± 0.2 g/L, which added to the COD reduction during the 1st stage (DF), represents a 44% overall removal after the 2nd stage. This low performance can be related to the following factors.

The microbial background of the inoculum is an important factor to consider. The major organic compounds in the DF effluent are volatile fatty acids (VFAs), end products from the metabolic pathway of the same inoculum in the MEC processes. Since the major end products detected are butyric, lactic, and propionic acids, different sources of inoculum should be explored in further experiments, or even the use of pure strain

cultures that can consume these organic acids. Another strategy is the direct electrolysis of these VFAs in solution, under low acidic conditions[60].

Though several works report the successful application of MECs as 2nd stage after DF, there are some other considerations hindering the feasibility of the coupled system that must be addressed first. Some authors have mentioned that DF effluent may not be directly applicable in MEC; dilution and certain amendments might be necessary, such as balancing the availability of nutrients, or maintaining an adequate feedstock concentration[61]. In this vein, the residual concentration of reducing sugars determined after the DF process was less than 1 g/L glucose equivalent (0.61 ± 0.1). Hence, the lack of readily fermentable sugars in addition to the nature of the inoculum, can be a good explanation to why the 2nd stage, failed to exhibit a further considerable reduction of COD while producing more hydrogen, so as in the MFCs.

In the case of the DF/MEC process, the major end product was butyric acid (HBu), making up to the 92% of the total organic acids detected (17.92 ± 0.85 g/L), followed by propionic acid (1.01 ± 0.01 g/L), and the rest were found below 0.22 g/L. Glycerol could not be detected, assuming therefore that it was depleted. In the beginning of the process, lactic acid (HLc) dominated the composition in the effluent (85% at 9 h). As seen in **Figure 5.4 A**, around the 12th hour of incubation there was an important upsurge in hydrogen production, reaching its maximum peak at the 17th hour. Samples at 18 h of incubation confirmed a decline in lactic acid concentration (71% of the total composition), and the appearance of HBu in the solution. By the end of the fermentation, HLc was barely detected (0.20 g/L). This behaviour indicates that during the first 7 – 9 hours, hydrogen production was dominated by the acetate metabolic route. After that, there is a sudden increase in hydrogen production governed by butyrate metabolic route. However, it is yet unclear if lactate was used to form butyrate, thus producing more hydrogen, or if it was fully oxidized. Final gas total composition may suggest the latter, since 58% more CO_2 was generated compared to the DF alone, although this matter will be furtherly discussed in the following sections.

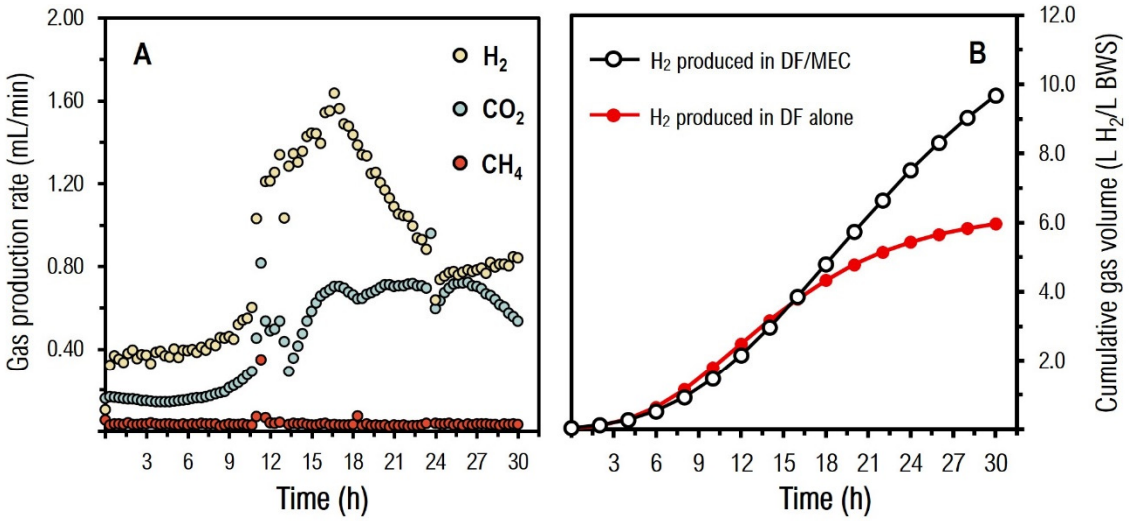

Gompertz model parameters

Treatment	R_m	λ	P	RSS	RSE	R^2
DF alone	41.95	4.90	762.86	1.0243	17.63	0.9994
DF-MEC	70.92	7.86	2,010.25	1.0000	19.61	0.9997

Figure 5.4. *A) Production rate (mL/min) of hydrogen (○), carbon dioxide (○), and methane (●) during dark fermentative microbial electrolysis process (DF/MEC); B), Modelled cumulative hydrogen volume from DF/MEC versus dark fermentation alone.*

The end products profile clearly reflects an impact by the poised potential applied to the electrolysis over the microbial community, since it hasn't been seen something similar in other fermentations. This conclusion is reinforced by the volume of methane produced in MEC against DF alone. The poised potential helped to control methane producers' activity more efficiently since there was 57% less methane detected. In this regard, a population analysis was conducted to compare the inoculum population before and after the MEC process.

5.3.4 Microbial population analysis

The main microbial species detected before and after each electrochemical process are listed, according to their order, in **Figure 5.5**. It is also depicted the abundance of the main species by genus after both DF/MEC and MFC processes. Sequencing analysis of the 16s rRNA gene was conducted and analysed in accordance to the methodology

shown elsewhere in[62]. The effect of the applied voltage over the population is clearly evident, showing the suppression of methanogens, and promoting the growth of hydrogen-producing bacteria in the MEC process. The population analysis reflects and confirms the behaviour already observed by the end-products profile determined at the end of the fermentation in DF/MEC. The main genus observed was *Clostridium*, followed by *Pseudomonas*. *Clostridium butyricum* alone constituted ~45% of the total population, undoubtedly the responsible of the over production of butyrate at the end of the process. Electric pre-treatment of dark-fermentative seed sludges has been used to suppress methanogens by applying 3.0 to 4.5 V[63], and at higher voltages (10 V – 20 V), 95% *Clostridium* spp. abundance was observed[64]. In contrast, the low voltage applied in the current research was 0.4 V during the 30 hours of fermentation, in which methanogens suppression was attained and a high yield of butyrate production.

Two different unclassified *Pseudomonas* species were identified[65,66], together making up 33% of the total population in DF/MEC. These organisms are known to secrete aromatic secondary metabolites (*i.e.*, phenazines and pyocyanin), serving as electron shuttles fulfilling diverse functions, which include antibiotic activities that elicit competitive advantages over other bacterial and fungi species[21]. These compounds not only are involved in the extracellular electron transfer by *Pseudomonas* in bioelectrochemical systems, but also in enabling it for gram-positive bacteria in co-culture[69], such as *Clostridiales*. The characteristic benzenoid-ringed skeleton of *Pseudomonas*' secreted metabolites is also found in oligomers formed during polymerization of aniline[70]. Notwithstanding, *Pseudomonas* might not be directly involved in the catalytic process. As seen above from voltammograms in **Figure 5.2 D**, the maximum peak of the irreversible electrocatalytic activity occurs between 0.48 and 0.57 V, but it has been reported the electrocatalytic activity of *Pseudomonas*, using different carbon sources, between −0.40 to −0.01 V vs Ag|AgCl[71]. Thus, the abundance of *Pseudomonas* shows the important role in the DF/MEC process played by these bacteria, acting as the intermediate entity between the electrodes and the *hydrogenogenic* activity of the *Clostridiales*.

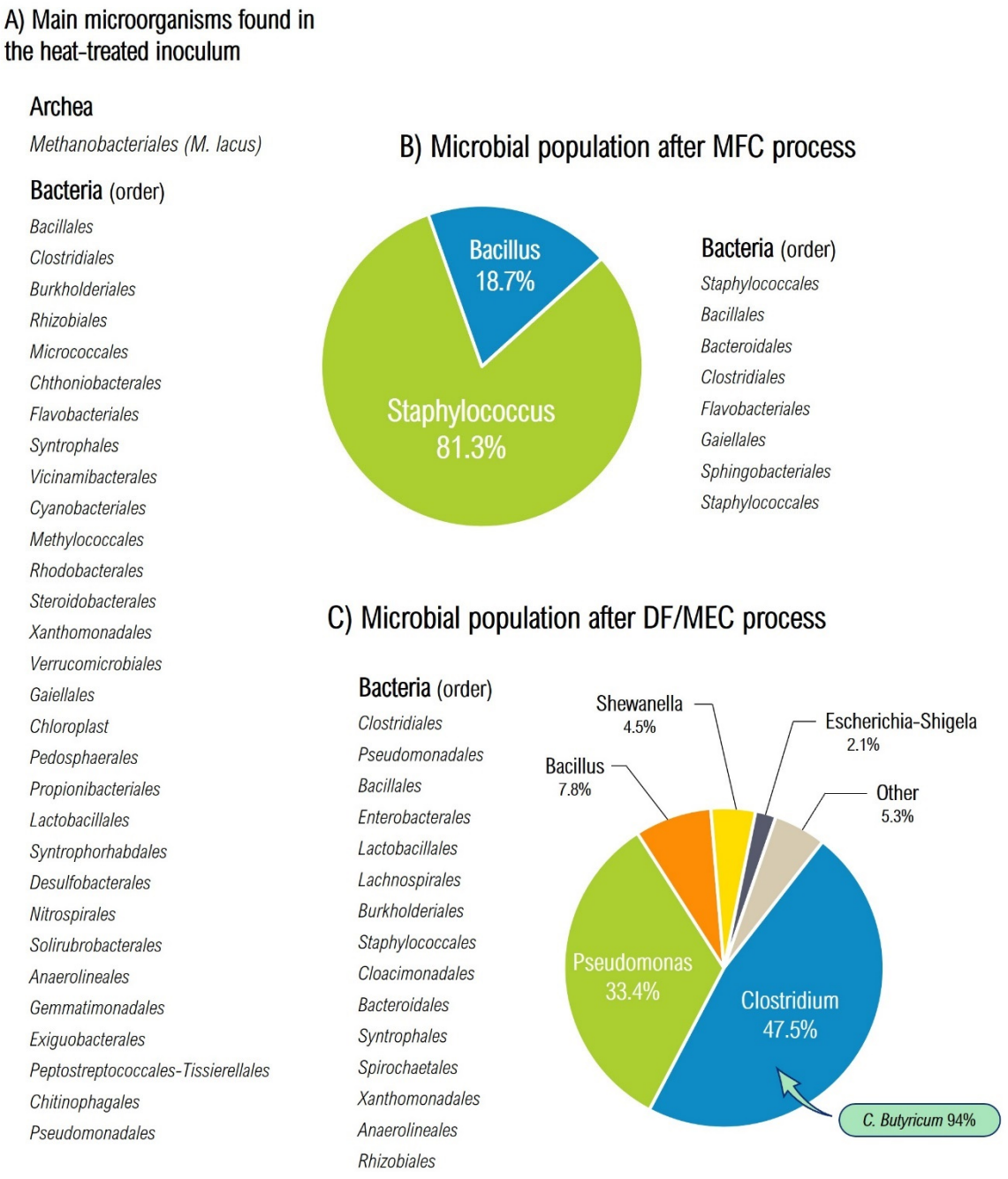

Figure 5.5. *Microbial population analysis of A) the heat-treated inoculum; B) after the MFC process; and C) after the dark fermentative MEC assisted processes (DF/MEC).*

Regarding the MFCs, the population was not as varied as in the MEC, since it was dominated by the genus *Staphylococcus*, followed by *Bacillus* only. *Staphylococci*, considered opportunistic pathogens, are facultative bacteria. At a first glance, the

dominant presence of this genus may indicate a substantial oxygen transfer through the air-cathode and the PEM in the MFC during the fermentation. Although these organisms grow better in the presence of oxygen, it has been noted that under anaerobic conditions *Staphylococcus aureus* and *Staphylococcus epidermidis* produced more polysaccharide intercellular adhesin involved in the formation of biofilms, enhancing the virulence of these pathogens[72]. In this regard, the ability to form an electrocatalytic active biofilm by *Staphylococcus* spp. in bioelectrochemical applications has been studied. It was demonstrated that *S. aureus* can form an electrochemical active biofilm on the surface of carbon felt electrodes depleting substrates such as cellulose[73]. *S. aureus* has also been studied in direct electron transfer with carbon nanotubes for their use in MFCs[74]. *S. warneri* demonstrated to produce electricity metabolizing lactic acid in lactate-rich human skin[75]. But perhaps the most remarkable thing to note, is that the dominant bacteria found after the MFC process in the current study is related to *S. epidermidis*, a species found in human skin, which has shown electrogenic activity in MFCs by fermenting glycerol[76].

5.3.5 Hydrogen yield and energy efficiency

In dark fermentation, hydrogen yield (HY) on the basis of COD consumed is typically reported around 100 mL H_2/g COD[77]. In this study, the applied potential during the DF/MEC process rendered 436.4 ± 2.4 mL H_2/g COD consumed, or 169.0 ± 5.9 mL H_2 per gram of COD initial, which means 32% and 44% more hydrogen than in DF alone, respectively, whereas in the MEC treatment of DF effluent, the yield observed was 24.4 ± 0.6 mL H_2/g COD initial. Compared to similar reports using MECs to treat brewery wastewaters, Lu *et al*.[78], obtained a HY of 1.76 L H_2/L BWW, using a Pt/Nickel foam cathode, applying a voltage of 0.8 V, that is 5.7 times less than in the present work, however, since the effluent used in that study was a low strength BWW (1.01 g/L COD initial), the rate of H_2/g COD fed was 10 times higher (1.64 L H_2/g of COD initial).

The molar yield cannot be determined directly from glucose or glycerol consumption. since it is not clear the contribution of each substrate in the final volume of hydrogen produced, but it is possible to relate the molar yield to the theoretical maximum yield

based on butyrate formed when the fermentation is dominated by this compound as the end product[39]. 95.8% of the maximum theoretical H_2 yield was attained by the DF/MEC process, and 7.9% from the DF effluent treated in the second stage. In contrast, the DF alone showed 72.4% in this regard.

Continuing with the energy recovery analysis of the DF/MEC process only, the $\%CE_{COD}$ was 38.5%, whereas the theoretical coulombic hydrogen recovery was estimated around 93.2% – 94.8%. However, the cathodic hydrogen recovery (r_{Cat}) was 81.7%, reflecting the efficiency of hydrogen conversion with respect to the current collected from the solution. The energy efficiency calculated (η_E) was 121.6%, indicating that the energy recovered is more than the energy applied, including the temperature control, which constitutes 60% of the electric input. After 30 hours of DF/MEC process, 79.7% of total sugars were depleted (9.34 g of glucose equivalents consumed). However, to calculate the energy efficiency relative to the added substate (η_S), it must be considered not only the share of glucose, but also lactate and glycerol consumption too, in relation to COD removal. As mentioned before, it is not clear exactly how HLc consumption could be involved in HBu formation. The necessary moles of glucose to form the amount of butyrate obtained at the end of the process exceeds the glucose present in the process. The surplus of HBu was produced from other sources, besides glucose and glycerol. It is known that *Clostridium* spp. can synthetize butyrate from lactate and acetate[79]. Hence, the share of HLc consumption (12.3 g/L), is also included in the COD balance. Considering the latter, therefore, the η_S is 14.9%, and the net energy recovery (η_{E+S}), based on both the electricity and substrate inputs is 13.2%. From these calculations, it can be observed that the fresh BWS-based medium fed to the cell accounted for 89.1% of the gross energy supply converted into hydrogen, rendering a yield equivalent to 2.37 mol H_2/mol substrate. On the other hand, from the net energy balance it is estimated 1.8 kWh supplied per m^3 of H_2 produced, which is around ~2.5 times less energy compared to average water electrolysis energy inputs (4.1 – 4.9 kWh/m^3 H_2[80]). In **Figure 5.6**, it is summarized the energy recovery analysis of the two systems DF/MEC and DF followed by MEC.

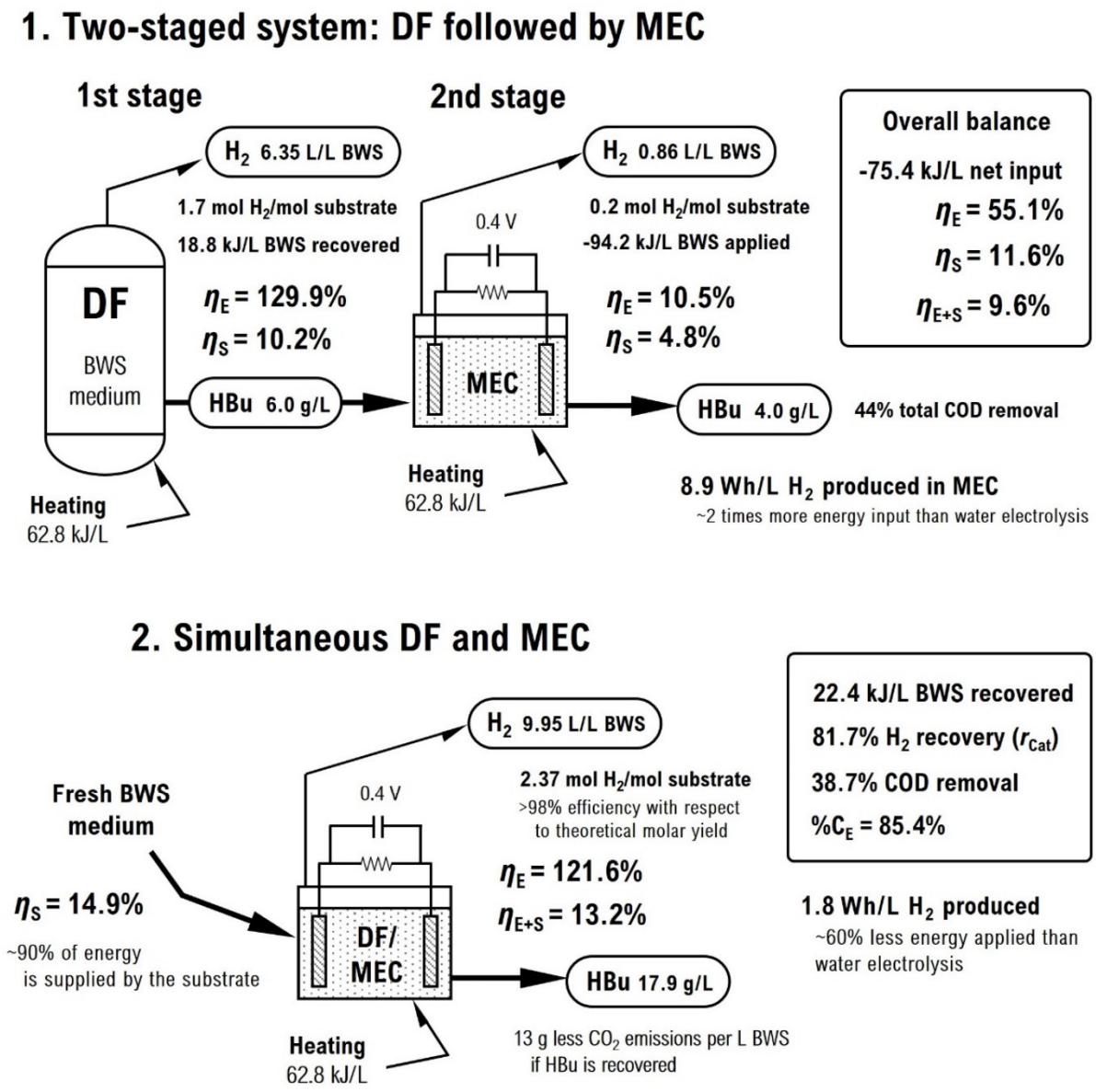

Figure 5.6. *Energy balance of the two proposed systems to produce hydrogen from a medium based on high strength brewery waste slurry: 1. Two-staged combined system showing dark fermentation followed by microbial electrolysis cells; 2. Simultaneous DF/MEC treatment.*

The gross energy output on the basis of hydrogen produced in DF alone in **Chapter 3** was reported around 81.6 kJ/L BWS treated. This yield was 1.6 times higher in DF process assisted by MEC. Comparing this process against the biochemical methane potential (BMP) of the BWS, as in **Chapter 3**, considering a 90% of COD removal

efficiency in anaerobic digestion, and an average conversion rate of 283 mL CH_4/g COD removed (NTP values of both CH_4 and H_2, collected in[81]), the BMP of the effluent from the DF/MEC process would account for roughly 330 kJ/L BWS in a subsequent AD stage, which in addition to the ~128 kJ/L BWS from the energy content of hydrogen produced in the first stage, together would represent 85% of the gross bioconversion into methane if the BWS were to be fully digested. However, the high yield of butyrate observed at the end, confers a great significance to the DF/MEC process, beyond comparison with anaerobic digestion. Its extraction alone (considering an 88% recovery efficiency as described in[82]) represents a reduction of 13 kg of CO_2 emissions per cubic meter of BWS treated, without considering the great opportunities as a raw material for the manufacture of bioplastics or its conversion to butanol. Alone, the potential value of butyric acid from this process is around $28 USD/$m^3$ BWS treated, which is 3 times the estimated benefits in DF alone.

5.4 Conclusions

The proposed coupled system based on a subsequent stage after DF, under the conditions here presented, did not show any advantage on hydrogen production, nor electricity generation. However, the simultaneous DF/MEC approach demonstrated promising results, attained a hydrogen yield 1.6 higher than DF alone. Moreover, this improved performance was attained with 56%–63% less energy input to produce hydrogen as per unit volume than conventional water electrolysis. The required power input could be supplied by a series of MFCs operating continuously. The treatment of the BWS-based medium directly in MFCs, showed a maximum voltage output within the range of the optimum potential to elicit hydrogenesis in a microbial electrolysis process (0.4 V). However, the overall current density calculated from the data set was ~32.6 A/m^3 for the entire MEC process (30 h), which is 80 times higher than the power output exhibited by the MFCs at the highest activity. Therefore, there is still the challenge to increase and sustain a constant power output to meet the MECs energy requirements, which has to do more with improving the oxygen reduction reaction efficiency in the air-cathode.

On the other hand, the production of butyric acid exceeded by 3 times that of DF alone, which makes the recovery of this compound even more attractive. The increase in production of this acid was directly linked to the effect of the applied voltage over the microbial population, leading to the proliferation of *Clostridium butyricum*. Furthermore, the molar ratio H_2/substrate showed above 98% of the theoretical when butyrate is the major end-product in dark fermentations. Hence, in the light of the results presented here, assisting a DF process with microbial electrolysis is an efficient alternative to produce green hydrogen, exploiting the potential energy content of residues like brewery wastewaters by using lower energy inputs than conventional approaches, reaffirming the attractiveness of these novel technologies in the pursuit of substituting fossil fuel sources to produce hydrogen.

References

1 Krupp, M. *Biohydrogen Production from Organic Waste and Wastewater by Dark Fermentation - a Promising Module for Renewable Energy Production*; Shaker Verlag: Aachen, **2007**.

2 Chandrasekhar, K.; Lee, Y. J.; Lee, D. W. Biohydrogen Production: Strategies to Improve Process Efficiency through Microbial Routes. *Int. J. Mol. Sci.* **2015**, *16* (4), 8266–8293.

3 Wang, J.; Yin, Y. Introduction. In *Biohydrogen Production from Organic Wastes*; **2017**; pp 1–17.

4 Sagir, E.; Hallenbeck, P. C. Photofermentative Hydrogen Production. In *Biohydrogen*; **2019**; pp 141–157.

5 Rafa, Ł.; Ho, I.; Kucharska, K.; Glinka, M.; Rybarczyk, P. Hydrogen Production from Biomass Using Dark Fermentation. **2018**, *91* (April), 665–694.

6 Ntaikou, I.; Antonopoulou, G.; Lyberatos, G. Biohydrogen Production from Biomass and Wastes via Dark Fermentation: A Review. *Waste and Biomass Valorization* **2010**, *1* (1), 21–39.

7 Swartz, J. Opportunities toward Hydrogen Production Biotechnologies. *Curr. Opin. Biotechnol.* **2020**, *62*, 248–255.

8 Bakonyi, P.; Kumar, G.; Koók, L.; Tóth, G.; Rózsenberszki, T. Bioresource Technology Microbial Electrohydrogenesis Linked to Dark Fermentation as Integrated Application for Enhanced Biohydrogen Production : A Review on Process Characteristics , Experiences and Lessons. **2018**, *251* (November 2017), 381–389.

9 Premier, G. C.; Kim, J. R.; Massanet-nicolau, J.; Kyazze, G.; Esteves, S. R. R. Integration of Biohydrogen , Biomethane and Bioelectrochemical Systems. *Renew. Energy* **2013**, *49*, 188–192.

10 Guwy, A. J.; Dinsdale, R. M.; Kim, J. R.; Massanet-nicolau, J.; Premier, G. Bioresource Technology Fermentative Biohydrogen Production Systems Integration. *Bioresour. Technol.* **2011**, *102* (18), 8534–8542.

11 Sadhukhan, J.; Lloyd, J. R.; Scott, K.; Premier, G. C.; Yu, E. H.; Curtis, T.; Head, I. M. A Critical Review of Integration Analysis of Microbial Electrosynthesis (MES) Systems with Waste Biore Fi Neries for the Production of Biofuel and Chemical from Reuse of CO_2. **2016**, *56*, 116–132.

12 Scott, K. *An Introduction to Microbial Fuel Cells*; Elsevier Ltd., **2016**.

13 Zhou, M.; Wang, H.; Hassett, D. J.; Gu, T. Recent Advances in Microbial Fuel Cells (MFCs) and Microbial Electrolysis Cells (MECs) for Wastewater Treatment, Bioenergy and Bioproducts. *J. Chem. Technol. Biotechnol.* **2013**, *88* (4), 508–518.

14 Cotterill, S.; Heidrich, E.; Curtis, T. *Microbial Electrolysis Cells for Hydrogen Production*; Elsevier Ltd., **2016**.

15 Logan, B. E.; Rabaey, K. Conversion of Wastes into Bioelectricity and Chemicals by Using Microbial Electrochemical Technologies. *Science (80-.).* **2012**, *337* (6095), 686–690.

16 Wang, X. T.; Zhang, Y. F.; Wang, B.; Wang, S.; Xing, X.; Xu, X. J.; Liu, W. Z.; Ren, N. Q.; Lee, D. J.; Chen, C. Enhancement of Methane Production from Waste Activated Sludge Using Hybrid Microbial Electrolysis Cells-Anaerobic Digestion (MEC-AD) Process – A Review. *Bioresour. Technol.* **2022**, *346* (December 2021),

17 Simate, G. S. *Water Treatment and Reuse in Breweries*; Elsevier Ltd, **2015**.

18 Schneider, T.; Graeff-Hönninger, S.; French, W. T.; Hernandez, R.; Merkt, N.; Claupein, W.; Hetrick, M.; Pham, P. Lipid and Carotenoid Production by Oleaginous Red Yeast Rhodotorula Glutinis Cultivated on Brewery Effluents. *Energy* **2013**, *61*, 34–43.

19 Ojong, E. T.; Brunschweiger, S.; Glas, K.; Haseneder, R. Brewery Wastewater as Source of Raw Material for Electrical Energy Generation and Hydrogen Production. *Chemie Ing. Tech.* **2020**, *92* (9), 1278–1278.

20 Lu, M.; Chen, S.; Babanova, S.; Phadke, S.; Salvacion, M.; Mirhosseini, A.; Chan, S.; Carpenter, K.; Cortese,

R.; Bretschger, O. Long-Term Performance of a 20-L Continuous Flow Microbial Fuel Cell for Treatment of Brewery Wastewater. *J. Power Sources* **2017**, *356*, 274–287.

21 Wen, Q.; Wu, Y.; Zhao, L.; Sun, Q. Production of Electricity from the Treatment of Continuous Brewery Wastewater Using a Microbial Fuel Cell. *Fuel* **2010**, *89* (7), 1381–1385.

22 Jia, R.; Sun, D.; Dang, Y.; Meier, D.; Holmes, D. E.; Smith, J. A. Carbon Cloth Enhances Treatment of High-Strength Brewery Wastewater in Anaerobic Dynamic Membrane Bioreactors. *Bioresour. Technol.* **2020**, *298* (December 2019), 122547.

23 Guo, Z.; Thangavel, S.; Wang, L.; He, Z.; Cai, W.; Wang, A.; Liu, W. Efficient Methane Production from Beer Wastewater in a Membraneless Microbial Electrolysis Cell with a Stacked Cathode: The Effect of the Cathode/Anode Ratio on Bioenergy Recovery. *Energy and Fuels* **2017**, *31* (1), 615–620.

24 Sangeetha, T.; Guo, Z.; Liu, W.; Cui, M.; Yang, C.; Wang, L.; Wang, A. Cathode Material as an Influencing Factor on Beer Wastewater Treatment and Methane Production in a Novel Integrated Upflow Microbial Electrolysis Cell (Upflow-MEC). *Int. J. Hydrogen Energy* **2016**, *41* (4), 2189–2196.

25 Connaughton, S.; Collins, G.; O'Flaherty, V. Psychrophilic and Mesophilic Anaerobic Digestion of Brewery Effluent: A Comparative Study. *Water Res.* **2006**, *40* (13), 2503–2510.

26 Ince, B. K.; Ince, O.; Anderson, G. K.; Arayici, S. Assessment of Biogas Use As an Energy Source From Anaerobic Digestion of Brewery Wastewater. *Water. Air. Soil Pollut.* **2001**, *126*, 239–251.

27 Chen, R.; Chang, S.; Hong, Y.; Wu, P. Brewery Wastewater Treatment by Anaerobic Membrane Bioreactor. *Proceedings, Annu. Conf. - Can. Soc. Civ. Eng.* **2015**, *1_2015*, 390–399.

28 Borja, R.; Martín, A.; Durán, M. M.; Luque, M.; Alonso, V. Kinetic Study of Anaerobic Digestion of Brewery Wastewater. *Process Biochem.* **1994**, *29* (8), 645–650.

29 Lu, L.; Ren, Z. J. Microbial Electrolysis Cells for Waste Biorefinery: A State of the Art Review. *Bioresour. Technol.* **2016**, *215*, 254–264.

30 Wang, A.; Sun, D.; Cao, G.; Wang, H.; Ren, N.; Wu, W. M.; Logan, B. E. Integrated Hydrogen Production Process from Cellulose by Combining Dark Fermentation, Microbial Fuel Cells, and a Microbial Electrolysis Cell. *Bioresour. Technol.* **2011**, *102* (5), 4137–4143.

31 Reiche, A.; Kirkwood, K. M. Comparison of Escherichia Coli and Anaerobic Consortia Derived from Compost as Anodic Biocatalysts in a Glycerol-Oxidizing Microbial Fuel Cell. *Bioresour. Technol.* **2012**, *123*, 318–323.

32 Abu-thabit, N. Y. Chemical Oxidative Polymerization of Polyaniline: A Practical Approach for Preparation of Smart Conductive Textiles. **2016**.

33 Dole, H. A. E.; Safady, L. F.; Ntais, S.; Couillard, M.; Baranova, E. A. Electrochemically Enhanced Metal-Support Interaction of Highly Dispersed Ru Nanoparticles with a CeO 2 Support. *J. Catal.* **2014**, *318*, 85–94.

34 Baranova, E. A.; Page, Y. Le; Ilin, D.; Bock, C.; Macdougall, B.; Mercier, P. H. J. Size and Composition for 1 – 5 Nm Ø PtRu Alloy Nano-Particles from Cu K ⎵ X-Ray Patterns. **2009**, *471*, 387–394.

35 Panaritis, C.; Michel, C.; Baranova, E. A.; Steinmann, S. Unraveling the Origin of Electrochemical Promotion for the CO2 Hydrogenation Reaction over Ru Nanoparticles. *Electrochim. Acta* **2020**, *350* (136405).

36 Miller, G. L. Use of Dinitrosalicylic Acid Reagent for Determination of Reducing Sugar. *Anal. Chem.* **1959**, *31*, 426–428.

37 Dubois, M.; Gilles, K. A.; Hamilton, J. K.; Rebers, P. A.; Smith., F. Colorimetric Method for Determination of Sugars and Related Substances. *Anal. Chem.* **1956**, *28*, 350–356.

38 Call, D.; Logan, B. E. Hydrogen Production in a Single Chamber Microbial Electrolysis Cell Lacking a Membrane. *Environ. Sci. Technol.* **2008**, *42* (9), 3401–3406.

39 Zhang, C.; Yang, H.; Yang, F.; Ma, Y. Current Progress on Butyric Acid Production by Fermentation. *Curr. Microbiol.* **2009**, *59* (6), 656–663.

40 Hidalgo, D.; Tommasi, T.; Bocchini, S.; Chiolerio, A.; Chiodoni, A.; Mazzarino, I.; Ruggeri, B. Surface Modification of Commercial Carbon Felt Used as Anode for Microbial Fuel Cells. *Energy* **2016**, *99*, 193–201.

41 Schröder, U.; Nießen, J.; Scholz, F. A Generation of Microbial Fuel Cells with Current Outputs Boosted by More than One Order of Magnitude. *Angew. Chemie - Int. Ed.* **2003**, *42* (25), 2880–2883.

42 Lai, B.; Tang, X.; Li, H.; Du, Z.; Liu, X.; Zhang, Q. Biosensors and Bioelectronics Power Production Enhancement with a Polyaniline Modified Anode in Microbial Fuel Cells. *Biosens. Bioelectron.* **2011**, *28* (1), 373–377.

43 Wang, Y.; Chen, Y.; Wen, Q. Microbial Fuel Cells: Enhancement with a Polyaniline/Carbon Felt Capacitive Bioanode and Reduction of Cr(VI) Using the Intermittent Operation. *Environ. Chem. Lett.* **2018**, *16* (1), 319–326.

44 Lv, Z.; Xie, D.; Li, F.; Hu, Y.; Wei, C. Microbial Fuel Cell as a Biocapacitor by Using Pseudo-Capacitive Anode Materials. *J. Power Sources* **2014**, *246*, 642–649.

45 German, N.; Ramanaviciene, A.; Ramanavicius, A. Formation and Electrochemical Evaluation of Polyaniline and Polypyrrole Nanocomposites Based on Glucose Oxidase and Gold Nanostructures. *Polymers (Basel).* **2020**, *12* (12), 1–20.

46 Wang, H.; Wang, G.; Ling, Y.; Qian, F.; Song, Y.; Lu, X.; Chen, S.; Tong, Y.; Li, Y. High Power Density Microbial Fuel Cell with Flexible 3D Graphene-Nickel Foam as Anode. *Nanoscale* **2013**, *5* (21), 10283–10290.

47 Oh, S. E.; Logan, B. E. Proton Exchange Membrane and Electrode Surface Areas as Factors That Affect Power Generation in Microbial Fuel Cells. *Appl. Microbiol. Biotechnol.* **2006**, *70* (2), 162–169.

48 Feng, Y.; Wang, X.; Logan, B. E.; Lee, H. Brewery Wastewater Treatment Using Air-Cathode Microbial Fuel Cells. *Appl. Microbiol. Biotechnol.* **2008**, *78* (5), 873–880.

49 Zhang, Q.; Hu, J.; Lee, D. Bioresource Technology Microbial Fuel Cells as Pollutant Treatment Units : Research Updates. *Bioresour. Technol.* **2016**, *217*, 121–128.

50 Zhuang, L.; Yuan, Y.; Wang, Y.; Zhou, S. Long-Term Evaluation of a 10-Liter Serpentine-Type Microbial Fuel Cell Stack Treating Brewery Wastewater. *Bioresour. Technol.* **2012**, *123*, 406–412.

51 Lavaa, A. A *Complete Guide To Solar Panel Output*, **2021**. Available at: https://www.linquip.com/blog/a-complete-guide-to-solar-panel-output/ (accessed Apr 25, 2022).

52 Wen, Q.; Wu, Y.; Zhao, L.; Sun, Q. Production of Electricity from the Treatment of Continuous Brewery Wastewater Using a Microbial Fuel Cell. *Fuel* **2010**, *89* (7), 1381–1385.

53 Yu, J.; Park, Y.; Kim, B.; Lee, T. Power Densities and Microbial Communities of Brewery Wastewater-Fed Microbial Fuel Cells According to the Initial Substrates. *Bioprocess Biosyst. Eng.* **2015**, *38* (1), 85–92.

54 Zhuang, L.; Yuan, Y.; Wang, Y.; Zhou, S. Long-Term Evaluation of a 10-Liter Serpentine-Type Microbial Fuel Cell Stack Treating Brewery Wastewater. *Bioresour. Technol.* **2012**, *123*, 406–412.

55 Wen, Q.; Wu, Y.; Zhao, L. X.; Sun, Q.; Kong, F. Y. Electricity Generation and Brewery Wastewater Treatment from Sequential Anode-Cathode Microbial Fuel Cell. *J. Zhejiang Univ. Sci. B* **2010**, *11* (2), 87–93.

56 Çetinkaya, A. Y.; Köroğlu, E. O.; Demir, N. M.; Baysoy, D. Y.; Özkaya, B.; Çakmakçi, M. Electricity Production by a Microbial Fuel Cell Fueled by Brewery Wastewater and the Factors in Its Membrane Deterioration. *Cuihua Xuebao/Chinese J. Catal.* **2015**, *36* (7), 1068–1076.

57 Brunschweiger, S.; Ojong, E. T.; Weisser, J.; Schwaferts, C.; Elsner, M.; Ivleva, N. P.; Haseneder, R.; Hofmann, T.; Glas, K. The Effect of Clogging on the Long-Term Stability of Different Carbon Fiber Brushes in Microbial Fuel Cells for Brewery Wastewater Treatment. *Bioresour. Technol. Reports* **2020**, *11* (March), 100420.

58 Harewood, A. J. T.; Popuri, S. R.; Cadogan, E. I.; Lee, C. H.; Wang, C. C. Bioelectricity Generation from Brewery Wastewater in a Microbial Fuel Cell Using Chitosan/Biodegradable Copolymer Membrane. *Int. J. Environ. Sci. Technol.* **2017**, *14* (7), 1535–1550.

59 Wen, Q.; Wu, Y.; Cao, D.; Zhao, L.; Sun, Q. Electricity Generation and Modeling of Microbial Fuel Cell from Continuous Beer Brewery Wastewater. *Bioresour. Technol.* **2009**, *100* (18), 4171–4175.

60 Tuna, E.; Kargi, F.; Argun, H. Hydrogen Gas Production by Electrohydrolysis of Volatile Fatty Acid (VFA) Containing Dark Fermentation Effluent. *Int. J. Hydrogen Energy* **2009**, *34* (1), 262–269.

61 Bakonyi, P.; Kumar, G.; Koók, L.; Tóth, G.; Rózsenberszki, T.; Bélafi-Bakó, K.; Nemestóthy, N. Microbial Electrohydrogenesis Linked to Dark Fermentation as Integrated Application for Enhanced Biohydrogen Production: A Review on Process Characteristics, Experiences and Lessons. *Bioresour. Technol.* **2018**, *251* (November 2017), 381–389.

62 Tsitouras, A.; Butcher, J.; Li, J.; Stintzi, A.; Delatolla, R. Biofilm Morphology and Microbiome of Sequencing Batch Moving Bed Biofilm Reactors Treating Cheese Production Wastewater. *Bioresour. Technol. Reports* **2022**, *17* (August 2021), 100898.

63 Khanal, S. K. Biohydrogen Production: Fundamentals, Challenges, and Operation Strategies for Enhanced Yield. In *Anaerobic biotechnology for bioenergy production: principles and applications*; Khanal, S. K., Ed.; Wiley-Blackwell, 2008; pp 189–219.

64 Jeong, D. Y.; Cho, S. K.; Shin, H. S.; Jung, K. W. Application of an Electric Field for Pretreatment of a Seeding Source for Dark Fermentative Hydrogen Production. *Bioresour. Technol.* **2013**, *139*, 393–396.

65 Dueholm, M. K. D.; Nierychlo, M.; Andersen, K. S.; Rudkjøbing, V.; Knutsson, S.; Arriaga, S.; Bakke, R.; Boon, N.; Bux, F.; Christensson, M.; Chua, A. S. M.; Curtis, T. P.; Cytryn, E.; Erijman, L.; Etchebehere, C.; Fatta-Kassinos, D.; Frigon, D.; Garcia-Chaves, M. C.; Gu, A. Z.; Horn, H.; Jenkins, D.; Kreuzinger, N.; Kumari, S.; Lanham, A.; Law, Y.; Leiknes, T.; Morgenroth, E.; Muszyński, A.; Petrovski, S.; Pijuan, M.; Pillai, S. B.; Reis, M. A. M.; Rong, Q.; Rossetti, S.; Seviour, R.; Tooker, N.; Vainio, P.; van Loosdrecht, M.; Vikraman, R.; Wanner, J.; Weissbrodt, D.; Wen, X.; Zhang, T.; Nielsen, P. H.; Albertsen, M.; Nielsen, P. H. MiDAS 4: A Global Catalogue of Full-Length 16S RRNA Gene Sequences and Taxonomy for Studies of Bacterial Communities in Wastewater Treatment Plants. *Nat. Commun.* **2022**, *13* (1), 1908.

66 Nierychlo, M.; Andersen, K. S.; Xu, Y.; Green, N.; Jiang, C.; Albertsen, M.; Dueholm, M. S.; Nielsen, P. H. MiDAS 3: An Ecosystem-Specific Reference Database, Taxonomy and Knowledge Platform for Activated Sludge and Anaerobic Digesters Reveals Species-Level Microbiome Composition of Activated Sludge. *Water Res.* **2020**, *182*, 115955.

67 Hadla, M.; Halabi, M. A. Effect of Quorum Sensing; 2018; pp 95–116.

68 Blankenfeldt, W.; Kuzin, A. P.; Skarina, T.; Korniyenko, Y.; Tong, L.; Bayer, P.; Janning, P.; Thomashow, L. S.; Mavrodi, D. V. Structure and Function of the Phenazine Biosynthetic Protein PhzF from Pseudomonas Fluorescens. *Proc. Natl. Acad. Sci. U. S. A.* **2004**, *101* (47), 16431–16436.

69 Pham, T. H.; Boon, N.; Aelterman, P.; Clauwaert, P.; De Schamphelaire, L.; Vanhaecke, L.; De Maeyer, K.; Höfte, M.; Verstraete, W.; Rabaey, K. Metabolites Produced by Pseudomonas Sp. Enable a Gram-Positive Bacterium to

Achieve Extracellular Electron Transfer. *Appl. Microbiol. Biotechnol.* **2008**, *77* (5), 1119–1129.

70 Sapurina, I.; Stejskal, J. The Mechanism of the Oxidative Polymerization of Aniline and the Formation of Supramolecular Polyaniline Structures. **2008**, *1325* (August), 1295–1325. https://doi.org/10.1002/pi.

71 Bosire, E. M.; Blank, L. M.; Rosenbaum, M. A. Strain- and Substrate-Dependent Redox Mediator and Electricity Production by Pseudomonas Aeruginosa. *Appl. Environ. Microbiol.* **2016**, *82* (16), 5026–5038.

72 Cramton, S. E.; Ulrich, M.; Götz, F.; Döring, G. Anaerobic Conditions Induce Expression of Polysaccharide Intercellular Adhesin in Staphylococcus Aureus and Staphylococcus Epidermidis. *Infect. Immun.* **2001**, *69* (6), 4079–4085.

73 Bhuvaneswari, A.; Navanietha, K. R.; Berchmans, S. Metamorphosis of Pathogen to Electrigen at the Electrode/Electrolyte Interface: Direct Electron Transfer of Staphylococcus Aureus Leading to Superior Electrocatalytic Activity. *Electrochem. commun.* **2013**, *34*, 25–28.

74 Morozan, A.; Stamatin, L.; Nastase, F.; Dumitru, A.; Vulpe, S.; Nastase, C.; Stamatin, I.; Scott, K. The Biocompatibility Microorganisms-Carbon Nanostructures for Applications in Microbial Fuel Cells. *Phys. Status Solidi Appl. Mater. Sci.* **2007**, *204* (6), 1797–1803.

75 Huang, T. Y.; Lim, H. L. Electrogenic Staphylococcus Warneri in Lactate-Rich Skin. *Biochem. Biophys. Res. Commun.* **2022**, *618*, 67–72.

76 Balasubramaniam, A.; Adi, P.; Thi, T. M. Do; Yang, J. H.; Labibah, A. S.; Huang, C. M. Skin Bacteria Mediate Glycerol Fermentation to Produce Electricity and Resist Uv-B. *Microorganisms* **2020**, *8* (7), 1–11.

77 Bundhoo, Z. M. A. ScienceDirect Coupling Dark Fermentation with Biochemical or Bioelectrochemical Systems for Enhanced Bio-Energy Production : A Review. **2017**, *2*.

78 Lu, L.; Hou, D.; Fang, Y.; Huang, Y.; Ren, Z. J. Nickel Based Catalysts for Highly Efficient H2 Evolution from Wastewater in Microbial Electrolysis Cells. *Electrochim. Acta* **2016**, *206*, 381–387.

79 Detman, A.; Mielecki, D.; Chojnacka, A.; Salamon, A.; Błaszczyk, M. K. Cell Factories Converting Lactate and Acetate to Butyrate : Clostridium Butyricum and Microbial Communities from Dark Fermentation Bioreactors. *Microb. Cell Fact.* **2019**, 1–12.

80 Grigoriev, S. A.; Fateev, V. N. Hydrogen Production by Water Electrolysis. In *Hydrogen Production Technologies*; Sankir, M., Sankir, N. D., Eds.; **2017** Scrivener Publishing LLC, 2017; pp 231–276.

81 Capocelli, M.; De Falco, M. Enriched Methane: A Ready Solution for the Transition Towards the Hydrogen Economy. In *Enriched Methane: The First Step Towards the Hydrogen Economy*; De Falco, M., Basile, A., Eds.; Springer Cham Heidelberg New York Dordrecht London, **2016**; pp 1–21.

82 Salvachu, D.; Nelson, R. S.; Beckham, G. T.; Karp, E. M.; Linger, J. G.; Saboe, P. O.; Nelson, R. S.; Singer, C.; Mcnamara, I.; Cerro, C.; Chou, Y.; Mohagheghi, A.; Peterson, D. J.; Haugen, S.; Cleveland, N. S.; Monroe, H. R.; Guarnieri, M. T.; Tan, E. C. D.; Beckham, G. T.; Karp, E. M.; Linger, J. G. Process Intensification for the Biological Production of the Fuel Precursor Butyric Acid from Biomass. *Cell Reports Phys. Sci.* **2021**, No. 2, 1–20.

Chapter 6. Conclusions

6.1 Summary

Throughout this doctoral research work, different biotechnological approaches to exploit the organic-rich wastewaters from the brewing industry were studied, all of them with the main goal in mind of producing hydrogen, without losing sight of the revalorisation of these wastes in the most complete way possible. The simple approach of dark fermentation alone was first presented. It was demonstrated that it is possible to anaerobically ferment a brewery waste slurry with high COD content of between 50 to 60 g COD per L of BWS, producing more hydrogen per g COD than the few reported studies using brewery wastewaters, which only treated 6 to 7 g COD per L. The performance observed in the present study is comparable to other reports using residues with similar characteristics and high organic content. Nonetheless, the maximum net energy recovered from the single DF process, based on the chemically stored energy in the substrate was 10.2% (**Table 6.1**). This low conversion rate is due to metabolic limitations, something repeatedly stressed by both detractors and supporters of dark fermentation. With that in mind, then, the exploration of different techniques to assist or complement the dark fermentative process emerges as a strategy to overcome the limiting barriers imposed by the nature of metabolic pathways.

Firstly, a fungal pre-treatment was proposed with the aim of degrading the BWS organic component by the biological activity of a white-rot fungi strain, leading to the production of an effluent rich in readily fermentable sugars for the dark fermentative bacteria. Secondly, a series of several experiments were devised in an attempt to improve the energy conversion from the BWS by the use of microbial electrochemical devices. On the one hand, the feasibility of coupling microbial fuel cells to generate electricity from the biodegradation of a dark fermentation effluent was evaluated. Similarly, microbial electrolysis was incorporated to continue with the biodegradation of a DF effluent with a view to producing more hydrogen. For comparison, experiments were carried out, treating the BWS directly on MFCs and MECs, the latter being in fact

Table 6.1. COD reduction and energy conversion efficiencies exhibited by each treatment studied in the present research work.

Treatment	COD removed	Hydrogen yield	Energy conversion		Efficiency		
					η_E	η_S	η_{E+S}
	(%)	(mL H_2/g COD)[d]	(kJ/L BWS)	(kJ/g COD)[d]	(%)	(%)	(%)
1. DF*	35.3	331.3 ± 7.1	81.6	4.3	129.9	10.2	9.5
2. FT→DF[a]	36.5[a]	495.7 ± 6.2	48.7[a]	6.3[a]	77.6[a]	15.8[a]	13.1[a]
3. DF*→MFC	36.5	—	—	—	—	—	—
4. DF*→MEC	44.0	24.4 ± 0.6	92.6	3.6	40.1	11.6	9.0
5. MFC	38.3	—	44.3[b]	2.0[c]	1.2	5.1	5.1
6. DF/MEC	38.7	436.4 ± 2.4	127.8	5.6	121.6	15.0	13.3

* Dark fermented BWS + 5g/L glycerol; [a] considering only the data from the dark fermentative process after the fungal treatment; [b] Joules/L BWS; [c] Joules/g COD; [d] COD consumed; η_E – efficiency related to electrical input, including heating. η_S – efficiency related to the substrate added. η_{E+S} – overall energy efficiency based on both the electricity and substrate inputs.

a simultaneous DF/MEC process, or rather and *electrolysis-assisted dark fermentation*, harnessing anaerobic bacteria in the medium as catalysts to improve hydrogen production.

The two different biotechnologies were tested separately given their nature: the fungal treatment is a longer aerobic process, highly susceptible to contamination in the early stages, while METs work with bacteria as catalysts under anaerobic conditions, and whose replication rate can be up to 20 times faster than that of white rot fungi. Initially, the final objective of the study was to test all technologies as a single combined system, degrading BWS in sequential steps from fungal treatment through dark fermentation all the way to METs, however, this hypothesis was soon discarded as the rates of substrate degradation as well as the metabolism of the microorganisms impeded the concatenation of more than two stages at best. The highlighted outcomes of each of the proposed techniques are discussed below.

Fungal treatment

The fungal treatment was effective at considerably reducing the organic content of the brewery slurry, while the dark fermentative process of the effluent from this process exhibited higher energy conversion rates per gram of substrate than any of other

treatments evaluated. The COD reduced after this process was about 2 times higher than the other treatments, with the FT alone able to reduce COD of BWS by up to 76%. Moreover, decolouration and turbidity were both highly reduced by greater than 90%, indicating that this treatment is very efficient in removing recalcitrant compounds hard to destroy by other means. In contrast, the anaerobic DF treatment is able to reduce only 9% of the colour, while turbidity was not affected. However, a disadvantage is the lengthy retention time. It took 18 days to reach such organic matter reduction, and according to the Logistic-Monod model from the experimental data, biomass production as well as COD consumption, could have reached their maximum around 24 days of fermentation with 36 g/L dw biomass and 85% COD reduction.

Longer fermentation periods imply higher energy inputs; in this case, to control the temperature (30°C) and the stirring regime. Nevertheless, the by-products that can be obtained from fungal fermentations can be marketed as valuable feedstock for various applications. In this project, the primary focus was on optimizing fungal biomass production for two main reasons: it is a simpler approach and more importantly, COD reduction is closely related to biomass growth. Although this proposed process is not limited to biomass production only, for as has been widely documented over the last decades, the metabolites generated by these fungi are used in different industrial applications such as in pharmaceuticals, food, biomaterials, as biosensors and also in bioremediation.

The natural choice for economically exploiting the fungal biomass is for human consumption. The fresh biomass produced in submerged fermentation can serve as inoculum for edible mushrooms production, in which case, the brewer's spent grain from the same brewery would be used as the solid substrate to sustain the fungal growth. Once the mushrooms are harvested, the residual BSG can be sold as livestock feed, because compared to the raw BSG disposed without any fungal treatment, it will have an enhanced digestibility and a higher protein and minerals content, contributing to a better livestock nutrition. Another strategy is to simply obtain a dry powder that can served as supplements and nutraceutical products for human consumption, as well

as for animal food. Likewise, fungal biomass can be the feedstock for the production of various biomaterials, like a substitute to animal leather, biodegradable packaging, or textiles with electrically conductive properties.

Microbial electrolysis and fuel cells

Technologies based on microbial catalysis applied to wastewater treatment have developed rapidly over the last two decades. In this regard, brewery wastewaters have been treated while generating electricity in MFCs, as well as in MECs, mostly to enhance methane production. But little has been documented on the combined use of these novel technologies with dark fermentation to produce hydrogen from brewery waste slurries. The rationale for combining these technologies is that METs can increase the biodegradation of substrates after they have been treated by dark fermentation, obtaining additional energy. Hereof, however, the data showed that the combined two-staged system DF followed by MFCs and MECs does not represent any improvement, nor any advantage. On the contrary, the two-staged system is counterproductive in the overall energy balance, at least under the operational conditions of this study.

Firstly, in the case of MFCs, the cells failed to sustain bacterial processes such that it was not possible to measure a significant energy generation. However, the direct treatment of BWS in MFCs was successful. Among the three electrodes analysed, the polyaniline-carbon felt electrode demonstrated the best MFC performance, with an average energy generated of 44.3 J/L BWS, that is 12.3 mWh per cell, in which roughly 2.0 W are produced per gram of COD destroyed. Although the energy conversion is the lowest exhibited (5.1% with respect to the substrate added), this balance comes from the energy conversion by a single cell only with a small working volume (110 mL). What is important about this technology is the use of multiple small units simultaneously to increase energy conversion rates, rather than design a single larger cell. For the sake of illustration, it will take 9 days to treat 1 L of BWS using just one MFC unit alone, recovering 1.6 W/g COD per day. However, 9 MFCs together would generate over 14 W per g COD consumed on a daily basis from the simultaneous treatment of 1 L of BWS

per day, also representing an energy conversion of 30.7% based on the substrate added. Hence, considering the wastewater discharge of an average small brewery in Canada (1,500 m^3 annually), the use of 30 to 40 MFC units, like the ones presented here, would harness approx. 1/3 of the chemically stored energy in the waste slurry, generating 1.2−1.6 kWh/m^3 per day, which is an energy output comparable to that of a conventional solar panel, although with the advantage that MFCs can still generating electricity regardless the daytime and the weather.

Similarly, in the MEC process fed with the dark fermentation effluent, although microbial activity was observed, the hydrogen yield was not as high as hypothesized. This is clearly depicted by the energy efficiency calculated on the basis of both energy and substrate supplied, which was the same as by DF alone. By treating the BWS directly into the electrolysis cell, the simultaneous process DF/MEC showed better results. In this modality, it was observed the highest energy recovery per L of BWS, producing 1.6 more hydrogen than in DF alone. Moreover, compared to conventional water electrolysis, the process consumes around 60% less energy, that is 1.8 Wh/L of hydrogen produced. However, the efficiency based on energy input was slightly lower than DF alone, due to the combined effect of heating the cell and the voltage input. The necessary energy to maintain the temperature of the medium accounts for 60% of the total electrical energy supplied to the process. In the case of the voltage input, if this is to be supplied by one MFC unit simultaneously degrading BWS, it will be necessary to process 115 L per day to generate the power output to supply the DF/MEC process. Considering 30 MFC units combined, it will be necessary to optimize each cell to process 4 L of BWS per day in order to supply the electrolysis.

Furthermore, the effect of the applied voltage on the microbial population is a remarkable finding, as the poised potential enabled the conditions to greatly improve the fermentative performance. At the end of the fermentation, half of the microbial population was found to be *Clostridium butyricum* (44.7%), followed by *Pseudomonas* spp. (33.4%). Moreover, poising the cell potential at 400 mV improved hydrogen production not only by promoting the proliferation of hydrogen-producing bacteria, but

also by 1) inhibiting the growth of hydrogen-consuming bacteria, since no methanogens were detected; and 2) by redirecting the metabolism during the process, as it was observed that in the first 18 hours the major end-product was lactic acid, and in the last 12 hours this acid was totally consumed resulting in the highest butyric acid production exhibited in this research work. Butyric acid was found as the major end-product in all dark fermentative processes. In DF alone, 53% of the end-products composition was butyric acid, (6.1 g/L), while in the DF after the fungal treatment, 4.7 g/L were measured, comprising 65% of the total end-products. In the DF/MEC process, up to 17.9 g/L of butyric acid was produced, comprising 92% of the total end-products. Hence, besides an enhanced hydrogen production, the electrolysis assisting the fermentative process can also increase the amount of butyric acid which, at such concentrations, could be economically profitable to extract it as a feedstock for bioplastics production, or to convert it into butanol, thereby increasing the energy conversion potential of brewery waste slurries.

Finally, it is important to mention that, as in the case of the MFCs, these performances were obtained using PANI-modified carbon felt electrodes (both anode and cathode), furnished in a single chamber MEC. The results obtained, both in MFCs and MECs, can be largely attributed to the use of PANI-modified electrodes, which in addition to conferring higher conductivity, promote the direct interaction of bacteria with the electrode surface. This is decisive for the functioning of the cells, since hydrogen-producing bacteria are not *electrogenic*, which means that these microorganisms require external mediators in order to use the electrodes as electron acceptors/donors. Moreover, these modified electrodes are not electrochemically active towards the organic component in the BWS, as evidenced by cyclic voltammetry, demonstrating that the bacteria are effectively the catalysts of these processes. The use of RuOx nanoparticles deposited on the PANI-modified electrodes was also evaluated with a view to increasing the conductivity, although the results were not favourable.

In summary, as seen in Table 6.1, the dark fermentative process after the fungal treatment and the one assisted electrochemically (DF/MEC), demonstrated the highest

energy conversion efficiencies, based on both the energy and substrate supplied. Although the total amount of hydrogen produced per L of BWS in the DF after the fungal treatment was lower compared to DF alone and DF/MEC (1.6 and 2.6 times lower, respectively), the energy conversion per grams of COD consumed exhibited by this approach was the highest. Hence, the fungal treatment was effective at breaking down lignocellulosic materials into simple sugars, increasing the energy conversion per g COD, while reducing the total gas production as feedstock was consumed in the production of fungal biomass. The COD in the effluent from the WRF treatment was 21.0 g/L, 2.5 to 3 times lower than the organic load fed to the DF alone (54.2 g/L) and the DF/MEC (59.0 g/L). However, in all DF treatments a similar rate of COD consumption was observed, between 35% to 39%, regardless of the initial COD, demonstrating the metabolic limitations of the DF process.

Regarding the valorisation of the BWS beyond hydrogen production, it is in the fungal pre-treatment where a wide variety of by-products in several industrial applications can be exploited, although in this project the focus was placed only on biomass production, which was considerable, with a yield comparable to other optimized processes reported. Moreover, by the end of the fungal treatment, the COD was reduced up to 76%, and the colour and turbidity removal efficiencies were above 90%, indicating the degradation of recalcitrant compounds which are not easy to remove by other means, including DF and METs.

Given the fermentative metabolic limitations, it was not possible to extract more energy by linking the DF process to a second stage using METs. However, the direct treatment of fresh BWS in MFCs, showed an energy conversion of 2.0 W/g COD, reducing the organic content by 38.3%, a similar performance to that of the DF/MEC. Although apparently with a low energy recovery, these numbers represent the efficiency per one MFC single unit. Several small MFC units, simultaneously degrading the BWS, would considerably increase the energy conversion, with the attractive advantage of not being affected by the weather nor limited by the availability of daylight.

6.2 Recommendations for future research

First and foremost, it is strongly suggested to optimise the dark fermentation process alone to operate in continuous regime, either in a CSTR or a UASB prototype reactor, in order to obtain the appropriate operating parameters, aiming to reduce the HRT. According to the data obtained in this study, an optimal HRT could be found between 9 to 12 hours. It is suggested to evaluate hydrogen yields at lower temperatures, with the objective of eliminating the power supply to control the temperature, or at least reducing it as much as possible. This with the aim of optimizing the fermentative process as a starting point for other biotechnologies, as is suggested below.

6.2.1 Dark fermentation and anaerobic digestion

As has been proposed already in **Chapter 3**, if it is intended to go down the path of dark fermentation alone, without any pre-treatment or electrochemical assistance, it is therefore suggested to continue the biodegradation process towards anaerobic digestion to reduce more organic matter while recovering more energy in the form of methane. It is known that a gas mixture ratio of 4:1 parts of methane to hydrogen can significantly reduce NOx emissions, as well as making combustion more efficient, limiting the generation of CO, while harnessing more energy from conventional engines working on methane.

This suggested path is based on the pre-existing situation of many breweries and small agro-industries that are already equipped with reactors and engines to generate electricity from the combustion of methane obtained from their own wastes. Separating hydrogen from a first stage is not new, but as has been mentioned before, little has been reported regarding hydrogen production from brewery wastewaters. Custom case studies can be made either to 1), enhance methane production through the separation of hydrogen in a first stage, reincorporating it through a by-pass to the methanogenic phase; or 2), to incorporate hydrogen in the gas mixture fed to the already installed engines, seeking to make the energy conversion process more efficient. It is also suggested to assess the economic potential of butyric acid extraction from the first acidogenic stage.

6.2.2 Dark fermentation and microbial electrochemical technologies

Firstly, from an optimized continuous process, the input and output of organic load can be varied, hence it is suggested to reduce the retention time in DF to supply more COD to fuel cells and electrolysis as a second stage. By increasing the organic load fed to the METs after DF, it may be possible to achieve a sustained yield in the latter, seeking to prove the feasibility of a combined DF-MET system, since the observed problem during this research work in this regard was associated to the lack of available organic matter after the fermentative process. However, the main recommendations revolve around improving the performance of each MET.

– *MFCs*

Improving the MFCs to generate more energy will require the development of better electrodes, testing different cultures and reduce HRTs. It is suggested to try different nano particles to enhance the PANI-modified electrode:

- Study different seed cultures better adapted to the MFC environment.
- Reduce HRT to 9 – 12 hours, stablishing the conditions to operate continuously.
- Characterise the performance of the PANI-carbon felt anode with the deposition of other nanoparticles based on nickel and/or iron.

– *MECs*

As well as in previous suggestions, it is important to optimise the process by reducing the HRT. As this process (DF/MEC) showed good production of butyric acid, it is also suggested to assess the feasibility and economic potential this organic acid extraction. And, as well as in MFC, improving the electrodes with different nanoparticles is also strongly suggested, like iron, extensively studied since iron is an important redox species in hydrogenases:

- Develop and maintain the adapted seed culture to keep the optimal performance.
- Reduce HRT to 9 – 12 hours, stablishing the conditions to operate continuously.
- Characterise the performance of the PANI-carbon felt anode with the deposition of other nanoparticles, based on nickel and/or iron.

6.2.3 Fungal treatment

The fungal treatment was demonstrated to be an attractive alternative by itself. Besides biomass production, it can be envisioned the optimization of this process to obtain other value-added by products. Nevertheless, In view of the results, it is suggested to deepen the research on the development of this treatment in the following areas:

Characterisation of exopolysaccharides

The formation of EPS is profuse in submerged fermentation. It will be important to characterise the functional groups and properties to evaluate their importance as isolated by-products worth separating from the fungal culture.

- Apply a more efficient methodology for EPS extraction and purification.
- Determine the functional groups by Fourier transform infrared (FTIR) spectroscopy.
- Elucidate elements composition and linkages in the EPS by nuclear magnetic resonance (NMR) spectroscopy.

Saccharification associated with enzymatic activity

To fully understand the saccharification process during the fermentation, it is important to analyse cellulose and hemicellulose content, as well as determining lignin degradation. It is suggested to follow the activities of all enzymes involved in de decaying of the lignocellulosic substrate:

- carboxymethyl cellulases, glucanases, xylanases, β-glucosidases, etc.
- ligninolytic enzymes (laccases, manganese, and lignin peroxidases).

Fermentation kinetics

It is important to elucidate the kinetic parameters governing the fungal growth. In this research, the Logistic-Monod model was shown to fit to the experimental data, albeit with limited data, so it is suggested to explore other models such as the Han-Levenspiel and Yamani models, which consider the inhibition of substrate over fungal growth, as well as non inhibitory models like the Moser model.

Logistic-Monod model

$$\mu = k\frac{Y_{X/S}}{X}\cdot\frac{dS}{dt} \tag{1}$$

Han-Levenspiel model

$$\mu = \frac{\mu_m S\cdot(1-S/K_2)^n}{S+K_1\cdot(1-S/K_2)^m} \tag{2}$$

Yamani model

$$\mu = \frac{\mu_m S}{K_s+S+(S/K_I)^n} \tag{3}$$

Moser model

$$\mu = \frac{\mu_m S^n}{(K_s+S^n)};\quad n>0 \tag{3}$$

K_1, K_2, μ_m – constants; K_s – saturation constant; K_I – inhibition constant; μ – specific growth rate; S – substrate concentration; X – biomass concentration; $Y_{X/S}$ – yield biomass/substrate

These models will provide a deeper insight into the process not only in terms of biomass production, but also in the substrate consumption, saccharification, and enzymatic activity, which will allow optimizing the process to find the right conditions to produce the highest amount of biomass in the shortest possible time. It is also suggested to try different fungal species. Given the main purpose of this research, only one species was selected to demonstrate the hypothesis, but the process is not limited to *P. ostreatus*. Other white-rot fungi species can perform as good as this strain (*e.g.*, *Trametes* spp., *Ganoderma* spp., even other species among the genus *Pleurotus*).

As a final note, the use of glycerol is optional. It was found that in DF alone it increases hydrogen production by 10%, but its effect is not yet clear, and the DF after the fungal treatment was not fed with glycerol. Its use, hence, is not mandatory to enhance hydrogen production in future research.

Appendix

A.1 Efficiencies calculations

Hydrogen properties

density H_2	0.0000899	*g/mL*
M.W. H_2	2.00	*g/mol*
ΔH H_2 (HHV)	285.83	*kJ/mol*
ΔH H_2 (HHV)	142.915	*kJ/g*

Substrates properties

ΔH Glc	2,840.00	*kJ/mol*
ΔH Gro	1,654.30	*kJ/mol*
ΔH HLc	1,343.98	*kJ/mol*
ΔH HBu		*kJ/mol*

M.W. Glc	180.16	*g/mol*
M.W. Gro	92.1	*g/mol*
M.W. HLc	90.08	*g/mol*
M.W. HBu	88.11	*g/mol*

Glc → COD	1.07	*g COD/g glucose*
Gro → COD	1.22	*g COD/g glycerol*
HLc → COD	1.07	*g COD/g lactic acid*
HBu → COD	1.82	*g COD/g butyric acid*

Microbial electrolysis operation parameters

Current based on external circuit	0.165	*A*
Current measured (30 h)	0.147	*A*
Poised potential	0.400	*V*
Faraday's constant	96,485	*C/mol e–*
Time	30	*h*
Working Volume	0.150	*L*

Summary of energy conversion efficiencies exhibited by each treatment

	DF/MEC	DF (alone)	MEC after DF	DF after FT	MFC-PA*
η_{CE}	0.082 mol H_2	—	—	—	—
η_{TH}	0.087 mol H_2	—	—	—	—
$\%r_{CE}$	93.2 %	—	—	—	—
$\%CE_{COD}$	38.5 %	—	—	—	69.7 %
$\%r_{cat}$	81.7 %	—	—	—	—
η_{E} (%)	121.6 %	129.9 %	40.1 %	77.6 %	1.2 %
η_{S} (%)	15.0 %	10.2 %	11.6 %	15.8 %	5.1 %
η_{E+S} (%)	13.3 %	9.5 %	9.0 %	13.1 %	5.1 %

** Data presented here corresponds only to the MFCs with polyaniline-modified carbon felt anode (MFC-PA), without RuOx nanoparticles.*

1. η_{CE} represents the moles of H_2 that can be recovered based on the measured current (0.147 A), and it is calculated as follows:

$$\eta_{\mathrm{CE}} = \frac{\int_0^t I\mathrm{d}t}{2F}$$

2. η_{TH} is the theoretical number of moles (H_2) that can be recovered based on substrate consumption. It is considered the removal of every substrate, (i.e., glycerol, lactate) and the remaining COD is considered as glucose:

$$\eta_{\mathrm{TH}} = \frac{b_{\mathrm{H_2/S}} V_{\mathrm{L}}\ \Delta \mathrm{S}}{M_{\mathrm{S}}}$$

3. The hydrogen coulombic recovery $\%r_{CE}$ or simply the coulombic efficiency of the MEC, is the relation of moles of electrons recovered as current versus the total amount of electrons consumed as substrate. It is calculated by the ratio between η_{CE} and η_{TH}:

$$\%r_{\mathrm{CE}} = \frac{\eta_{\mathrm{CE}}}{\eta_{\mathrm{TH}}}$$

4. Whereas the coulombic efficiency based on COD consumption was calculated according to the following expression for both MECs and MFCs:

$$\%\mathrm{CE}_{\mathrm{COD}} = \frac{8\int_0^t I\mathrm{d}t}{FV_{an}\Delta\mathrm{COD}}$$

5. The cathodic hydrogen recovery $\%r_{cat}$ is the ratio of hydrogen moles recovered relative to that possible based on the measured current:

$$\%r_{\mathrm{cat}} = \frac{\eta_{\mathrm{H_2}}}{\eta_{\mathrm{CE}}}$$

6. The energy efficiency related to electrical input η_E is calculated by the energy content of the hydrogen produced, where is ΔH_{H_2} = 285.83 kJ/mol:

$$\eta_{\mathrm{E}} = \frac{W_{\mathrm{H_2}}}{W_{\mathrm{E}}} = \frac{\eta_{\mathrm{H_2}}\Delta H_{\mathrm{H_2}}}{W_{\mathrm{E}}}$$

and the electrical energy input W_E, is defined by the following equation:

$$W_{\mathrm{E}} = \sum_1^n \left(I E_{\mathrm{ap}}\Delta t - I^2 R_{ex}\Delta t\right)$$

Where E_{ap} is the voltage applied, which also includes the energy supplied to heat up the system at 35°C during the fermentation time.

7. The efficiency relative to the added substrate (η_S) is calculated based on the heat of combustion (ΔH_i), and moles (η_i) of each component considered as substrate:

$$\eta_{\mathrm{S}} = \frac{W_{\mathrm{H_2}}}{W_{\mathrm{S}}} = \frac{W_{\mathrm{H_2}}}{\Delta H_i \eta_i}$$

8. The overall energy recovery based on both the electricity and substrate inputs (η_{E+S}) is given by the following equation:

$$\eta_{\mathrm{E+S}} = \frac{W_{\mathrm{H_2}}}{W_{\mathrm{E}} + W_{\mathrm{S}}}$$

A.2 Summary of hydrogen and energy data obtained in each process

Dark fermentation alone (BWS + Gro) followed by MEC

		①	②	Total	
Vol. H_2 produced	*(mL/L BWS)*	6,351	858	7,209	*mL/L BWS*
n H_2	*(mol/L BWS)*	0.285	0.039	0.324	*mol/L BWS*
COD initial	*(g/L BWS)*	54.2	35.1	54.2	*g/L BWS*
COD consumed	*(g/L BWS)*	19.1	4.8	23.9	*g/L BWS*
n glucose (initial)*	*(mol/L BWS)*	0.250	0.160	0.250	*mol/L BWS*
n glycerol (initial)	*(mol/L BWS)*	0.054	0.031	0.054	*mol/L BWS*
$W_S = \Sigma\, \Delta H_i \cdot \eta_i$	*(kJ/L BWS)*	798.46	505.43	798.46	*kJ/L BWS*
$W_{H2} = \Delta H_{H2} \cdot \eta_{H2}$	*(kJ/L BWS)*	81.58	11.02	92.60	*kJ/L BWS*
W_E	*(kJ/L BWS)*	—	42.34	42.34	*kJ/L BWS*
$W_E + W_{Heat}$	*(kJ/L BWS)*	62.8	105.14	167.94	*kJ/L BWS*

**Assuming COD initial as glucose equivalent, less the initial COD equivalent to glycerol concentration (5.0 g/L initial in DF, equivalent to 6.1 g COD/L, and 3.45 g/L initial in MEC, equivalent to 4.2 g COD/L)*

Simultaneous DF/MEC

Vol. H_2 produced	9,950	*mL/L BWS*
n H_2	0.447	*mol/L BWS*
COD initial	59.0	*g/L BWS*
COD consumed	22.8	*g/L BWS*
Glucose consumed	9.34	*g/L BWS*
HLc consumed	12.30	*g/L BWS*
n glucose (initial)*	0.274	*mol/L BWS*
n glycerol (initial)	0.054	*mol/L BWS*
$W_S = \Sigma\, \Delta H_i \cdot \eta_i$	852.33	*kJ/L BWS*
$W_{H2} = \Delta H_{H2} \cdot \eta_{H2}$	127.81	*kJ/L BWS*
W_E	42.34	*kJ/L BWS*
$W_E + W_{Heat}$	105.14	*kJ/L BWS*

**Assuming COD initial as glucose equivalent, less the initial 5 g/L of glycerol equivalent to 6.1 g COD/L*

DF after fungal treatment

Vol. H_2 produced	3,794	*mL/L BWS*
n H_2	0.171	*mol/L BWS*
COD initial	21.00	*g/L BWS*
COD consumed	7.7	*g/L BWS*
Glucose consumed	13.60	*g/L BWS*
n Glc (initial)*	0.109	*mol/L BWS*
n Glc (consumed)	0.109	*mol/L BWS*
$W_S = \Sigma\, \Delta H_i \cdot \eta_i$	309.39	*kJ/L BWS*
$W_{H2} = \Delta H_{H2} \cdot \eta_{H2}$	48.73	*kJ/L BWS*
W_E	—	*kJ/L BWS*
$W_E + W_{Heat}$	62.8	*kJ/L BWS*

**Assuming total COD initial as glucose equivalent*

MFC alone

COD initial	59.0	*g/L BWS*
COD consumed	22.6	*g/L BWS*
Glucose consumed	9.34	*g/L BWS*
n glucose (initial)*	0.274	*mol/L BWS*
n glycerol (initial)	0.054	*mol/L BWS*
$W_S = \Sigma\, \Delta H_i \cdot \eta_i$	869.11	*kJ/L BWS*
W_E	—	*kJ/L BWS*
$W_E + W_{Heat}$	—	*kJ/L BWS*

**Assuming COD initial as glucose equivalent, less the initial 5 g/L of glycerol equivalent to 6.1 g COD/L*

A.3 Fungal treatment

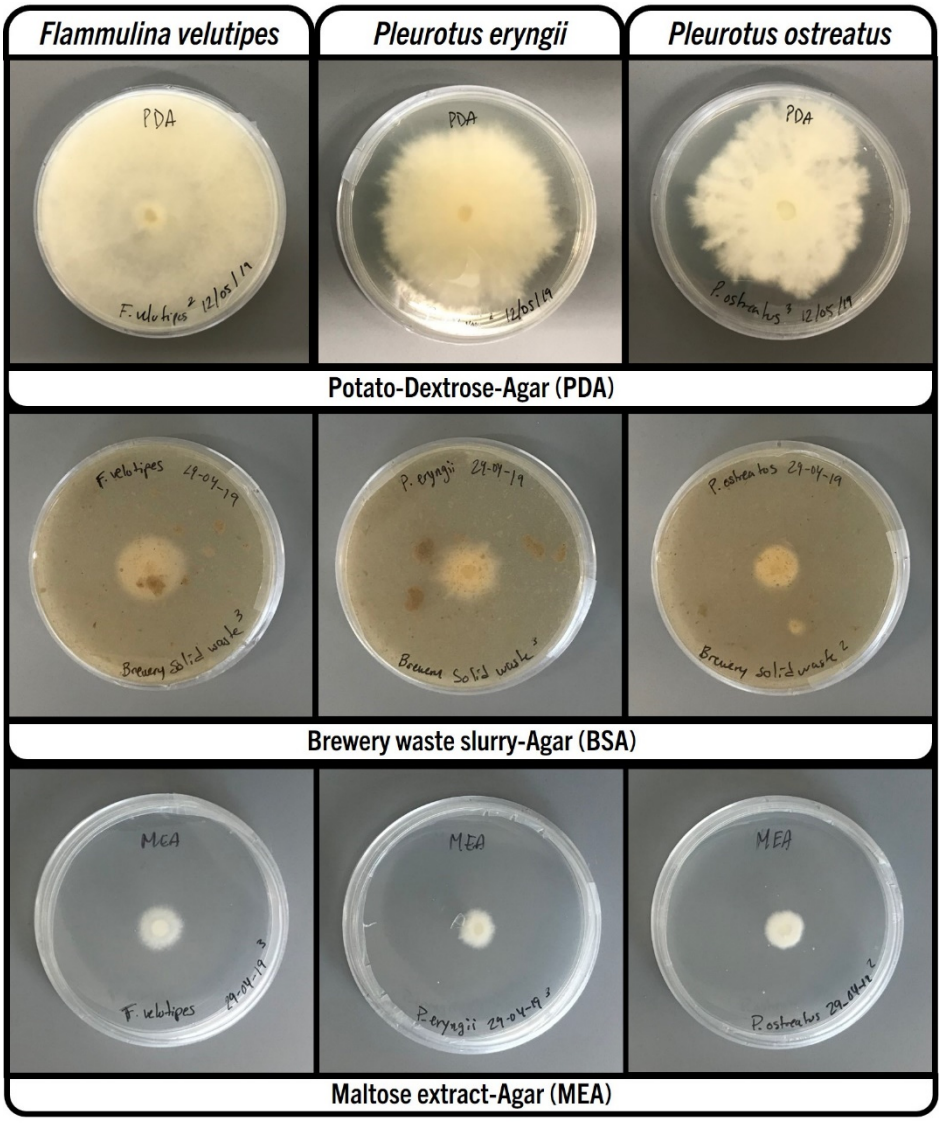

Figure A1. *Radial mycelial growth in Petri dishes on different semisolid media after 9 days of incubation at 30°C. 1) PDA – Potato-dextrose-agar; 2) BSA, medium prepared with brewery waste slurry, diluted 1:2, and agar (18 g/L); 3) MEA – Maltose extract-agar.*

Figure A2. *Preliminary growth tests of the three fungal strains in submerged fermentation. Effect of the addition of 10 g/L glucose as a carbon source (CS) alone and combined with two different concentrations of ammonium chloride (1 and 2 g/L) as a nitrogen source (NS) to the brewery waste slurry, in contrast to the control medium (Czapek). 1) CS+2 g/L NS; 2) CS+1 g/L NS; 3) CS alone; 4) Czapek medium.*

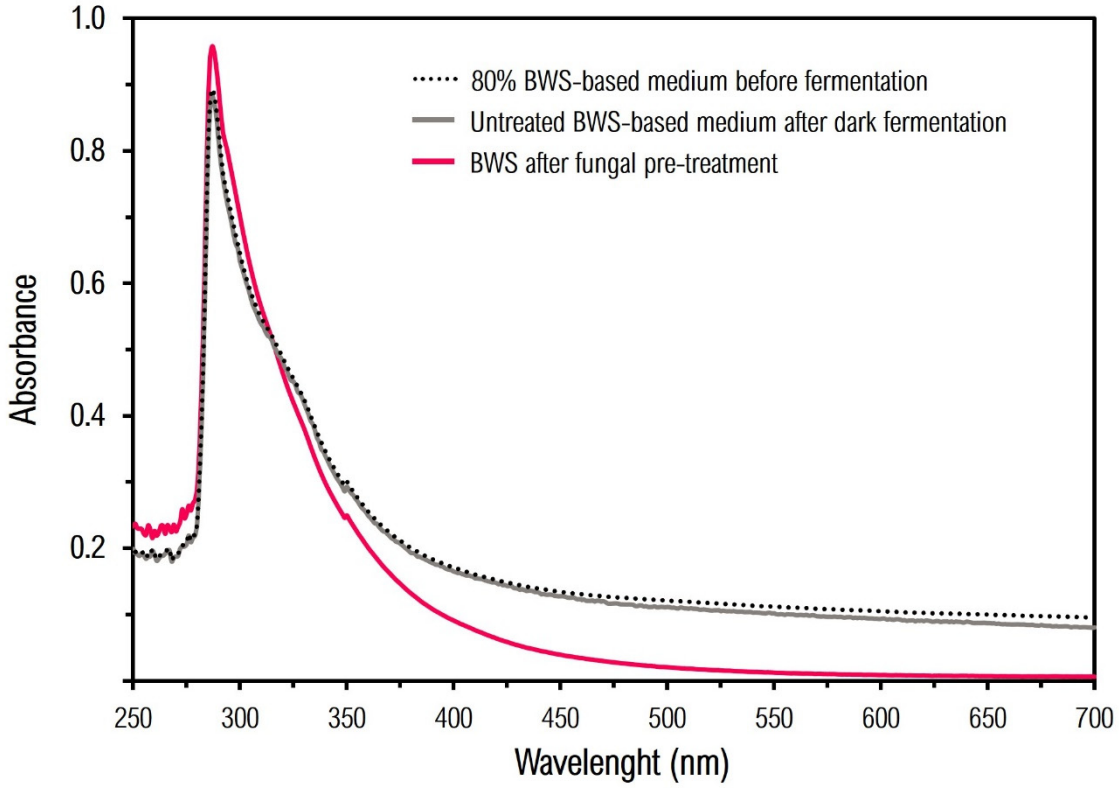

	BWS-based medium: 80% BWS + 1 g/L NH_4Cl Autoclaved (121°C, 20 min)	**BWS-based medium** after dark fermentation (no fungal pre-treatment)	**BWS-based medium** FT-BWS after *P. ostreatus* incubation (12 days)
$A = \sum_{i=380}^{700} f(x_i)\Delta x$	38.88346932	35.4712103	8.70116268
A_{475}	0.126212716	0.11628347	0.027677186

Figure A3. *Spectrophotogram of brewery waste slurry based medium (80% BWS + 1 g/L NH_4Cl, autoclaved: 121°C, 15 psia, 20 min), before any treatment (····), against (—) the BWS-based medium after dark fermentation (no fungal pre-treatment), and (—) BWS-based medium after the fungal treatment inoculated with* P. ostreatus *(12 days). Area under the curve within the visible spectrum wavelengths (380 nm – 700 nm), and at the punctual wavelength of 475 nm, calculated for each treatment.*

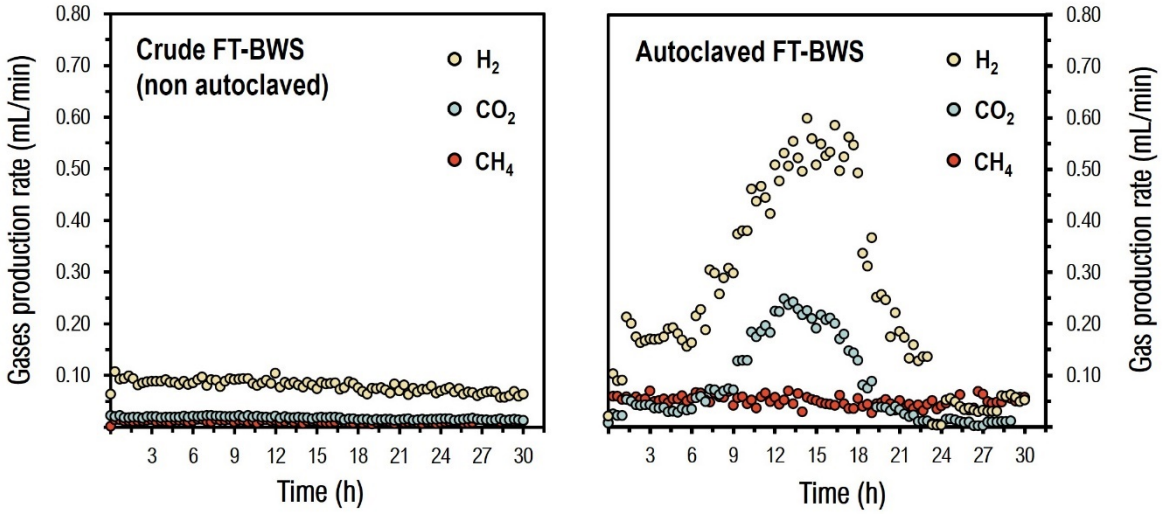

Figure A4. *Production rate (mL/min) of hydrogen (○), carbon dioxide (○), and methane (●) during the dark fermentation treatment of non autoclaved and autoclaved, fungal-treated BWS effluent.*

A.4 Microbial electrocatalysis

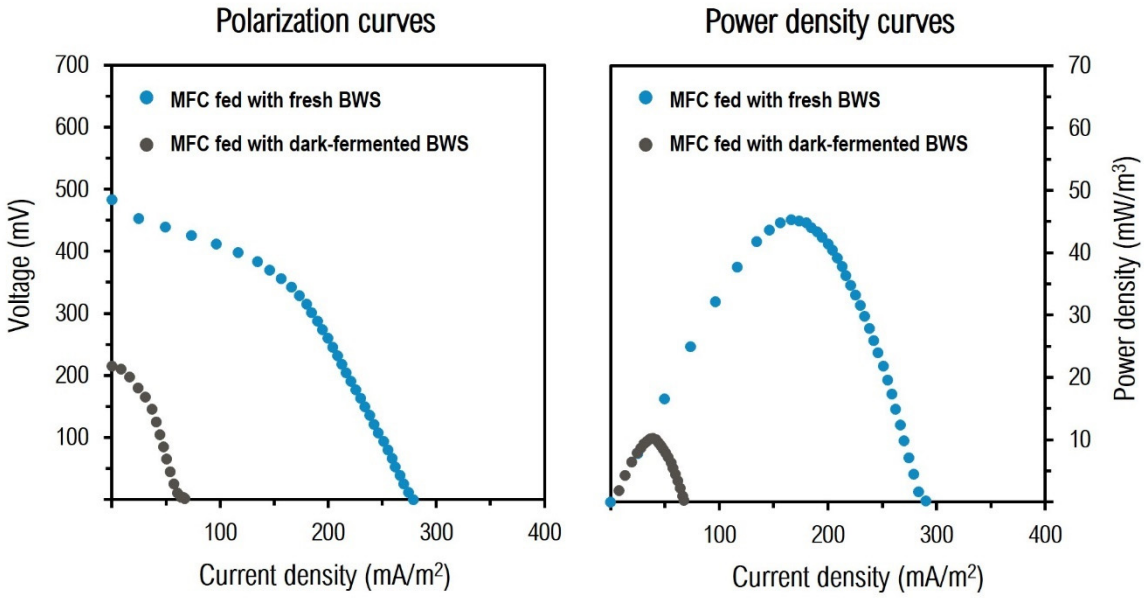

Figure A5. *Polarization and power density curves of the MFCs fed with fresh BWS compared to the MFCs fed with the effluent from the dark fermentation process. Both devices used PANI/CF electrodes.*

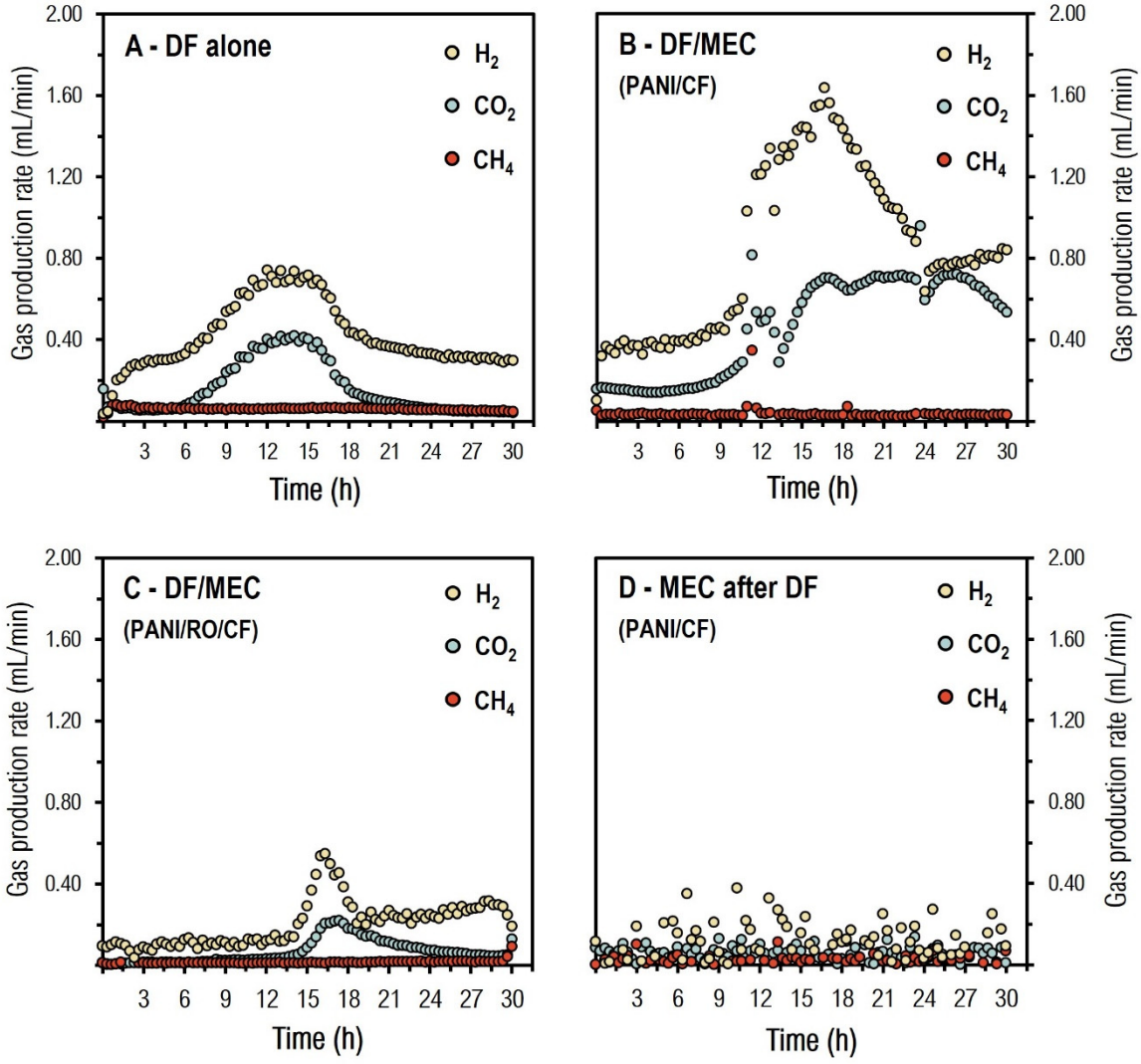

Figure A6. *Gas production rates using the same substrate conditions (BWS+5 g/L glycerol) in different treatments, comparing:* ***A*** *– DF alone, and* ***B*** *– simultaneous DF and MEC using PANI-modified carbon felt electrode, against* ***C*** *– simultaneous DF and MEC using a PANI/RuOx composite carbon felt electrode, and* ***D*** *– subsequent MEC after DF, using PANI-modified carbon felt electrode.*

A.5 Reactor and Microbial Electrochemical Cells designs

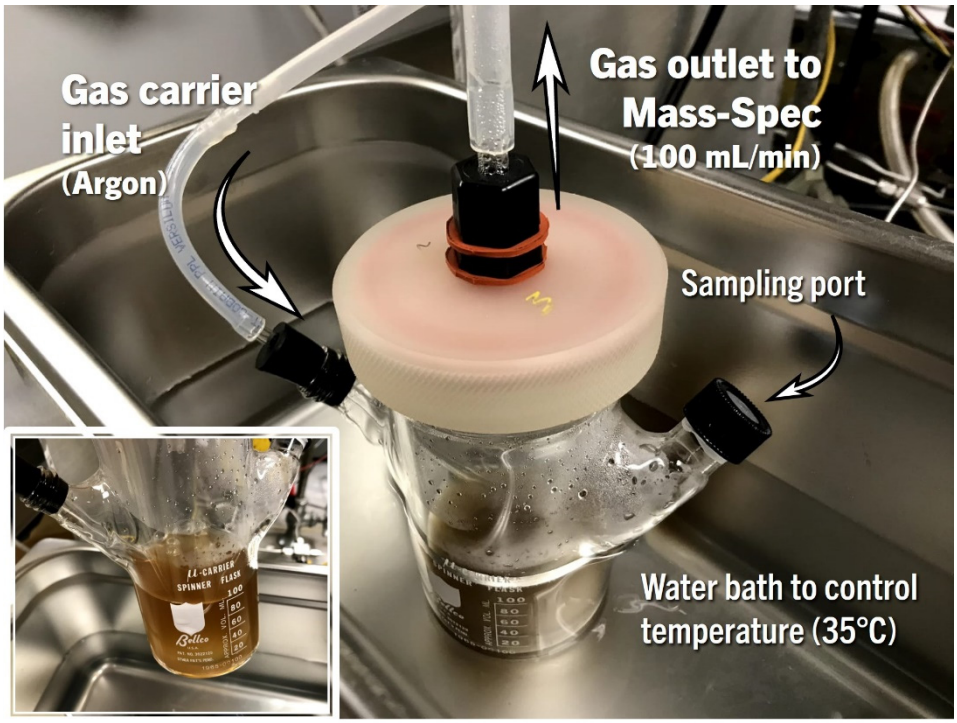

Figure A7. *Reactor used for dark fermentation with continuous measurement of hydrogen production*

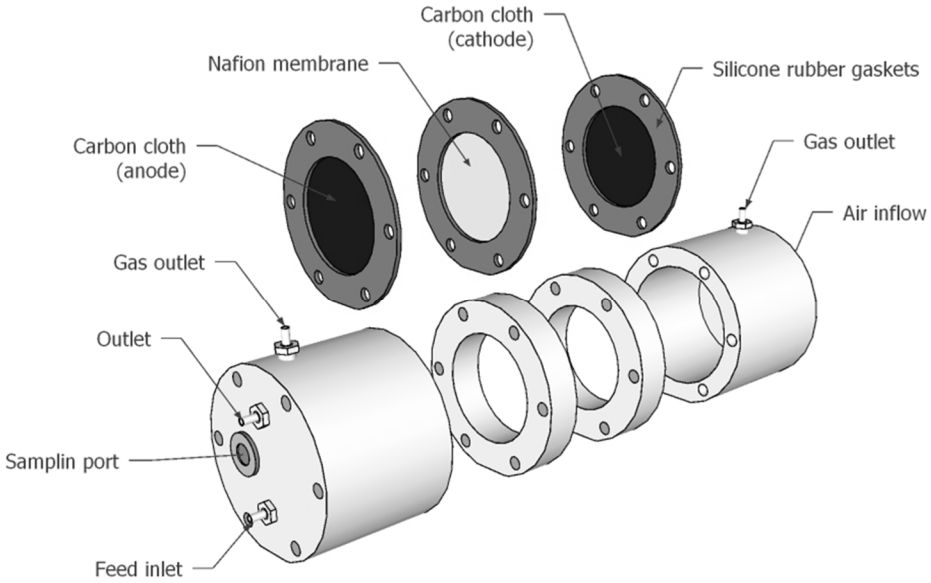

Figure A8. *Double chamber cylindrical cell design*

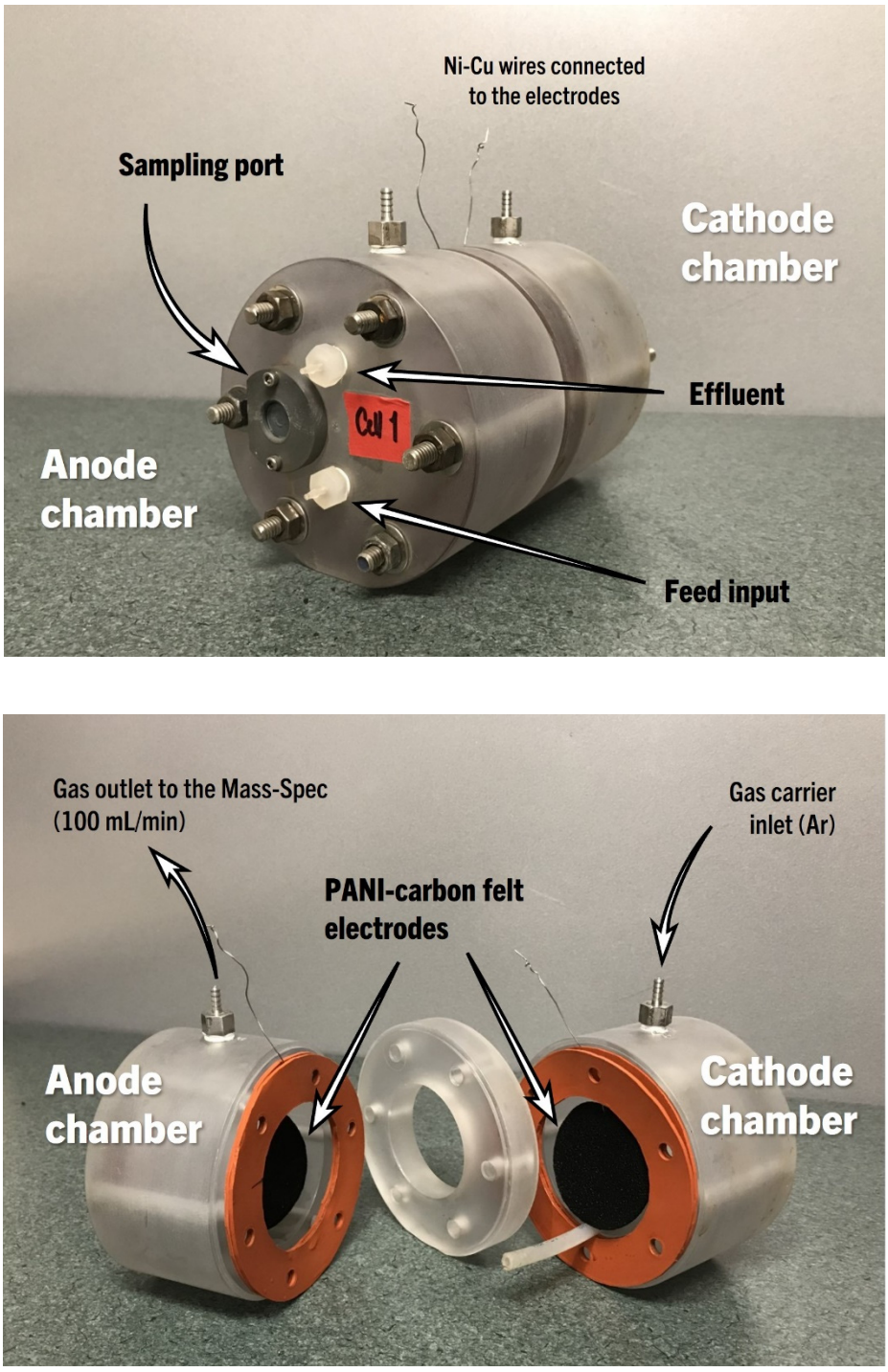

Figure A9. *Membraneless, single-chambered microbial electrolysis cell used in this project*

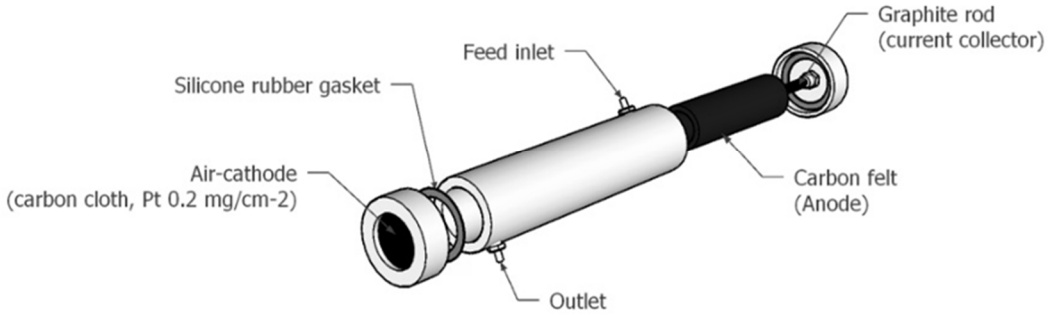

Figure A10. *Single chamber tubular cell design*

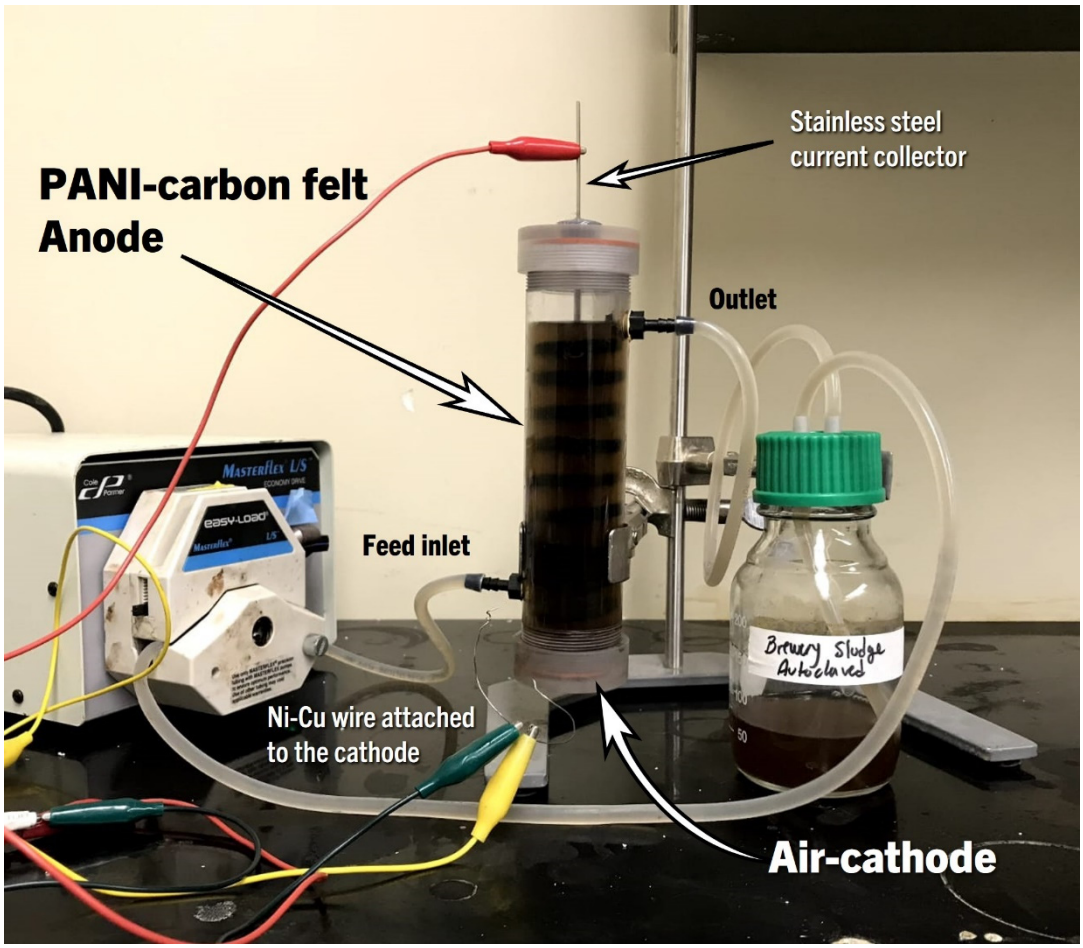

Figure A11. *Single-chambered microbial fuel cell used in this project*